

**Geochemistry in the Critical Zone: Limestone-Shale and Kimberlite weathering in the
Flint Hills, Kansas, USA**

by

Colleen Marie Gura

B.S., Kansas State University, 2004

A THESIS

submitted in partial fulfillment of the requirements for the degree

MASTER OF SCIENCE

Department of Geology
College of Arts and Sciences

KANSAS STATE UNIVERSITY
Manhattan, Kansas

Graduation Year
2017

Approved by:

Co-Major Professor
Dr. Pamela Kempton

Approved by:

Co-Major Professor
Dr. Saugata Datta

Copyright

© Colleen M. Gura 2017.

Abstract

The Critical Zone is the realm where rocks meet life. This study examines the physicochemical interactions that occur when interbedded limestone-shale systems and kimberlitic rocks weather to form soils. Fast weathering processes with extensive soil loss have been a major environmental concern in the Flint Hills for decades. Knowledge of soil formation processes, rates of formation and subsequent loss, and understanding how these processes differ in different systems are critical for managing soil as a resource. Kimberlites are CO₂-rich igneous rocks that are high in Mg and Fe; they are compositionally distinct from the Paleozoic limestones and shales found throughout the rest of the region. This study will compare the geochemistry and mineralogy of the Stockdale Kimberlite in Riley county to that of interbedded limestone-shale system typical of the Flint Hills as sampled from Konza Prairie LTER. Bulk composition and mineralogy of the soils overlying these different bedrock types have been analyzed using X-Ray Fluorescence (XRF), X-Ray Diffraction (XRD), bulk elemental extractions, and particle size analyses. Results show that the kimberlitic soils have higher concentrations of Fe, Mg, Ca, K and some trace elements in greater proportions (e.g. Ti, Ni, Cu).

The weathering products differ mineralogically as well, e.g. lizardite is abundant in kimberlitic soils and absent from the limestone terranes. Kimberlite derived soils also contain minerals as well such as kleberite (an alteration product of illminite), phlogopite, and magnetite. Kimberlite-sourced soils have different physical properties than the thin limestone-sourced soils surrounding them. Particle size analysis shows that the limestone-shale soils have different proportions of the clay size fraction in different core locations (~47% in highlands, ~51% at watershed base, ~41% in lowlands) whereas kimberlitic soils have a larger sand fraction than Konza (~19% vs. 10%). Clay minerals from the limestone-shale system reveals clay micas, kaolinite, and some expandable 2:1 layer silicates. Clay minerals from kimberlite-sourced soils are identified as primarily smectites with clay micas and kaolinites. Similarities between the kimberlite and limestone-shale soils are primarily seen in the shallower portions of the soil profile, suggesting that loess/wind-blown dust make a significant contribution to the soils in both areas. It could be concluded that kimberlite-sourced and limestone-shale-sourced soils produce weathering products that differ both chemically and mineralogically and could potentially have agricultural significance in terms of water retention as well as ionic and nutrient mobilities in these soils.

Table of Contents

List of Figures	vi
List of Tables	ix
Acknowledgements	x
Dedication	xi
Chapter 1 - Introduction.....	1
Chapter 2 - Background	3
2.1-The Flint Hills.....	3
2.2 – Previous Studies.....	7
Chapter 3 - Methods and Materials.....	10
3.1 - Sample Collection and Processing	10
3.2 – Bulk Sediment X-Ray Fluorescence Analysis	12
3.3 – Particle Size Analysis	13
3.4 – X-Ray Powder Diffraction Analysis.....	14
3.5 – Clay Fraction X-Ray Diffraction Analysis	14
3.6 – Bulk Digestion and ICP-OES Analysis	18
3.7 – ATP Analysis.....	20
Chapter 4 - Results.....	22
4.1 – Field observations made during coring at Stockdale Kimberlite.....	22
4.2 – Results from X-ray fluorescence	25
4.2.1 – Konza Prairie	25
4.2.2 – Stockdale Kimberlite	28
4.3 – Results from Particle Size Analysis with SANDY	31
4.4 – Results of X-Ray Powder Diffraction Analysis.....	36
4.5 – Clay Fraction X-Ray Diffraction	42
4.6 – Results of bulk extraction by aqua regia and ICP-OES analysis	43
4.6.1- Results of bulk extraction by aqua regia.....	43
4.6.2-Chemical Index of Alteration (CIA).....	47
4.7 – ATP Analysis.....	49
Chapter 5 - Discussion	50

5.1-Konza Geochemistry and Mineralogy	50
5.1.1 – Geochemistry	50
5.1.2 - Mineralogy.....	52
5.1.3 – Clay Mineralogy, Weathering, and Particle Size Analysis	54
5.2-Stockdale Kimberlite Geochemistry and Mineralogy	56
5.2.1-Stream Transects.....	57
5.2.2-Uphill Transect	58
5.2.3-Clay mineralogy and weathering	60
5.3-Chemical Index of Alteration (CIA) and Weathering in the Flint Hills	62
5.3.1 - CIA	62
5.3.2 – Element Ratios and Weathering.....	64
5.4-Variations in microbial activity in Konza and Stockdale soils.....	72
Chapter 6 - Conclusion	73
Chapter 7 - References.....	77
Appendix A - General Sample Location Descriptions	83
Appendix B - X-Ray Fluorescence (XRF) Data	84
B.1 – Accuracy Table	84
B.2 – XRF Raw Data	85
B.3 – XRF Processed Data per Core Location (wt %)	94
Appendix C - Particle Size (PSA) Data	111
C.1 – Raw Data.....	111
C.2 – Particle Size Data, Graphed Data and Summarized.....	114
Appendix D - Bulk Powder X-Ray Diffraction (XRD) Data	123
D.1-Konza Diffraction Analyses	123
D.2-Stockdale Diffraction Analyses	148
Appendix E - ICP-OES Data	198
Appendix F - Clay Fraction XRD Data	200
Appendix G - ATP Analysis Data	209

List of Figures

Figure 2.1-Terraced erosion of the Flint Hills. a. Diagram of underlying geology (NPS, 2016). b. Photo taken in Aug. 2016 at Konza Prairie LTER showing flat top limestone bench, shale slope and lower limestone bench.	3
Figure 2.2-Konza Prairie limestone-shale core sample map. N4D watershed is shaded.....	4
Figure 2.3-Konza and Stockdale area location maps.....	8
Figure 3.1-Konza Core location map.....	10
Figure 3.2-Stockdale Kimberlite core location map	12
Figure 3.3-XRD diffractogram of interlayer expansion and collapse after various treatments for smectite (SDK 1), expandable 2:1 layer silicates (Konza 6, 0-10cm) and vermiculite (Konza 6, 70-80cm)	18
Figure 4.1. Stockdale Kimberlite core location map. The gray area in the center of the map is the surface exposure of the kimberlite diatreme	22
Figure 4.2. Stockdale Kimberlite Upstream Transect core location map. Blue arrow indicates the approximate stream path and direction of flow.	23
Figure 4.3-Stockdale Kimberlite Downstream Transect core location map. Blue arrow indicates the approximate stream path and direction of flow	24
Figure 4.4- Stockdale Kimberlite Uphill Transect core location map. The purple arrow indicates the direction moving upslope from the surface exposure. Bright blue diamonds mark the core locations along this transect	25
Figure 4.5-Konza cores: Elemental concentrations as determined by HHXRF. Concentrations are reported in element weight % (unless otherwise stated).....	27
Figure 4.6-Stockdale kimberlite Cores: Elemental concentrations as determined by HHXRF. Concentrations are reported in element weight % (unless otherwise stated).....	30
Figure 4.7-Particle size analysis graph of Konza core 9.....	31
Figure 4.8- Particle size analysis graph of Konza core 6 (a) and core 5 (b)	32
Figure 4.9-Particle size analysis of Stockdale Kimberlite Core 2, upstream transect	33
Figure 4.10- Particle size analysis of Stockdale Kimberlite Core 4A, downstream transect	33
Figure 4.11-Particle size analysis of Stockdale Kimberlite cores 2B and 1B, uphill transect.....	35

Figure 4.12-Average of particle size measurements for each sample taken from within cores in both Konza Prairie and at the Stockdale Kimberlite	36
Figure 4.13-XRD peak intensities for quartz and calcite for Konza Core 5 (left) and Konza Core 6 (right)	38
Figure 4.14 - XRD Peak intensity of quartz and lizardite for core SDK 1B	41
Figure 4.15-Element concentrations in mg/kg as determined ICP-OES analyses via bulk extractions by aqua regia. Inset shows data rescales without Konza core 6 to show greater detail for other cores	45
Figure 4.16- Element concentrations in mg/kg of major and trace metals as determined ICP-OES analysis via bulk extractions by aqua regi	46
Figure 4.17 – ATP as measured by relative light units.....	49
Figure 5.1-Adapted from the Jackson Weathering Stages of Clay-Sized Minerals. Identifies weathering range of Konza clay minerals (Essington, 2004).	55
Figure 5.2-Identifies weathering range of clay minerals in cores SDK 1 and SDK 2 in the upstream transect, core SDK 2A in the downstream transect and cores SDK 1B and SDK 2B in the uphill transect at the Stockdale kimberlite. Adapted from The Jackson Weathering Stages of Clay Sized Minerals (Essington, 2004).....	61
Figure 5.3-CIA calculated for Konza core 6 and select cores surrounding the Stockdale kimberlite. **CIA for Stockdale kimberlite bedrock surface exposure is 28.....	63
Figure 5.4-Molar ratios of K/Na compared to K/Ca. Konza and Stockdale (SDK) data were determined by ICP-OES. KS Shale is average of published data from grey shales in central KS (Cullers, 1994). World Loess data points from loess samples from 3 different countries (Yang et al., 2004; Gallet et al., 1998). UCC from published data (Taylor and McLennan, 1985).	65
Figure 5.5- a. Co-variance graph of Sr and Ca. Konza and Stockdale (SDK) data were determined by ICP-OES. b. K/Na molar ratio compared to CIA. Konza and Stockdale (SDK) data were determined by ICP-OES. KS Shale is average of published data from grey shales in central KS (Cullers, 1994). World Loess data points from loess samples from 5 different countries (Yang et al., 2004; Gallet et al., 1998). UCC from published data (Taylor and McLennan, 1985).	66

Figure 5.7-Plot of element ratios Ti/Nb vs. K/Rb. Loess values in northern Kansas fall within the red circle. Loess values in eastern Colorado fall within the green circle. (Muhs et al., 2008)	67
Figure 5.8-Ratios of conservative elements commonly found in wind-blown dust. Konza cores are red and Stockdale cores are purple. Elemental concentrations used were those determined by HHXRF. (a) Major element wt%/Zr wt% ratios (b) Major element wt%/Si wt%	69
Figure 5.9-Relative amount of ATP in Konza and Stockdale cores. Results are measured in relative light units (RLU).	72

List of Tables

Table 2.1 -Mineralogy of Stockdale Kimberlite, Riley County limestones, and Riley County shales. (1) Brookins (1970). (2) Runnels and Schleicher (1956). (3) Dulekoz (1969) and Pecchioni (1981).	5
Table 2.2-Major element oxide weight percent. ND = no data. (1) Stockdale kimberlite (Cullers et al., 2006). (2) Average of Eskridge, Cottonwood and Ft. Riley Limestones (Runnels and Schleicher, 1956). (3) Average of post-Archean shales (Taylor and McLennan, 1985).	6
Table 4.1 – Konza Prairie core mineralogy. Numbers refer to site locations (see Figure 3.1) Note: Oligoclase is identified as “Albite, calcian” in Highscore PLUS® during analysis and is listed as such on individual sample scans in Appendix D. A blank cell indicates mineral was not identified in the core	37
Table 4.2-Stockdale Kimberlite core mineralogy. A blank cell indicates mineral was not identified in the core	40
Table 4.3-Mineralogy of <2µm clay fraction. Proportion key: T = Trace (<5%), L = Low (5-20%), M = Medium (20-50%), H = High (>50%)	43
Table 4.4- Elemental concentrations as determined by ICP-OES. Concentrations are reported in element oxide wt % unless.....	48
Table 5.1-Chemical Indices of Alteration (CIAs) of common rocks and minerals (Nesbitt and Young, 1982)	62
Table 5.2-Element ratio data for Konza LTER core average, Stockdale kimberlite core average, source rock, and various loess samples. *Data from Konza cores 5 & 6 not included. **Data from core SDK not included. ***Data determined by XRF from Shales rock chips collected 20km of both study sites. (1) Cullers et al., 2006. (2) Cullers, 1994. (3) Gallet et al., 1998.	70

Acknowledgements

I would first and foremost like to thank Pamela and Saugata for their infinite patience with me and their unending support. You took a chance on someone who had been out of school for a decade and helped me navigate through life as a student again. I enjoyed all the time we spent over the last few years both personally and professionally. You let me pitch an idea for a project and run with it, but I know this research would not have been possible without your ideas and guidance. Your thoughtful suggestions helped flesh out some unexpected findings. Thank you for your time and for your insightful edits through this process.

I also would like to thank Micky Ransom and Ganga Hettiarachchi for being on my committee and for also being so generous with your time. Both your classes were incredibly interesting and valuable in working through this project. I very much appreciated your willingness to help anytime I had a question. And Micky thank you for your help with interpreting my clay slides which underwent XRD analysis. I learned so much through our conversations.

Additionally, I want to acknowledge the help I received from so many other professors and post-docs I worked with. Sometimes it was quite a lot, sometimes it was just a little, but it was all needed and appreciated. Every bit of it contributed to the completion of this project. So, thank you Matt Kirk, Brice Le Croix, Matt Totten, Kendra McLauchlan, Berangere Leys, Sara Vero, Keith Miller, Sambhudas Chaudhuri, Karen Goldberg, and Matt Brueseke.

As for all the other graduate students in the department and to a few in other departments, there is absolutely no way I would have made it through this without all of you! There are a few however, that really made my time here special, Katie, Michelle, Beth, Ian, Megan, Tyler, and David, I simply cannot thank you enough.

And of course, a huge thank you to my family, Mom and Dad first for love and support. My girls for patience and giggles. Thank you for believing in me and for coming along on this crazy adventure! I love you so much!

Dedication

To Maggie and Pia for whom I do all things.....you are the lights of my life

Chapter 1 - Introduction

“A heterogeneous, near surface environment in which complex interactions involving rock, soil, water, air and living organisms regulate the natural habitat and determine availability of life sustaining resources.” --- a definition by The National Research Council about the Critical Zone of planet Earth (NRC 2001). Understanding how soils are generated is crucial to developing a thorough knowledge of the complex interactions that occur in the Critical Zone. Part of the goal of studying the Critical Zone is to answer the following question: “How do the physical, chemical and biological components of Earth’s weathering engine transform mineral and organic matter to nourish and sustain ecosystems, regulate the migration and fate of toxins, sculpt terrestrial landscapes, and control the exchange of greenhouse gases and dust with the global atmosphere?” (NRC 2001). This work provides information that will help answer that question.

This work examines some of the physical, chemical and biological interactions that occur when kimberlite eruptive products breakdown and form soils. Soils do not mix components easily, nor do they readily separate. They do not rush along the surface, as does water, but rather stay put, mostly, and undergo changes and transformations in place, acting as a sort of environmental record for that area (Ma, 2010). Soils can, however, be lost due to erosion, exhaustion or when human development covers over them. Therefore, knowledge of soil formation processes is critical if we are to manage this vital resource for human use—and the many economies that depend heavily on soils. In Kansas alone, agriculture accounts for 43% of the state’s Gross Regional Product (GRP). In 2015, this translated into \$62.8 billion, involved 88.9% of the acreage of the state and employed nearly 215, 000 people (KS Ag Dept., 2015). Riley County alone, nestled in the heart of the Flint Hills and home to both Konza Prairie LTER and the Stockdale kimberlite, saw \$158 million contribution to the county GRP from agricultural activities in 2015 (KS Ag Dept. Riley Co., 2015).

Soil surveys have been conducted in Kansas since the early 1900s. The most recent published surveys for counties in the Flint Hills cover a period from 1975-1991. The bedrock for most of the Flint Hills consists of alternating beds of Permian limestones and shales. Most of the limestone beds vary in thickness from 2-6 m and many are fossiliferous and contain a large proportion of microcrystalline flint nodules. The interbedded shales range in thickness from 1-5 m and are sometimes fossiliferous. They also appear in various colors such as red, bluish grey,

purple, grey, and nearly black (Jewett, 1941). The soils derived from these rocks are described as silty loams and silty clay loams. They are well drained and range in thickness from a few centimeters in upland areas to several meters in lower areas and in river valleys, which cut through the eastern edge of the county (Jantz et al., 1975). However, for the approximately 66.8 acres (0.017%) of Riley County that are directly underlain by kimberlites, no mention of these rocks, or their contribution to the local soils, is made in the soil surveys.

Since soil is primarily composed of mineral matter and the alteration products of weathering of the parent rock, studying the extent to which this has occurred is critical to understanding soil formation processes. Even though kimberlite outcrops are relatively rare, knowing how they impact soils and how their constituent ions behave is important for a complete understanding of the soil formation processes in the region. The Flint Hills of Kansas is a well-suited area to study this. There is an unmanaged expanse of prairie land called Konza Prairie Long-Term Ecological Research (LTER) site, which is underlain by alternating beds of shale and chert or flint laced limestone. This is representative of the geology and weathering pattern seen throughout the Flint Hills and serves as a natural analog for this area. There is also an outcrop of an exposed kimberlite easily accessible for study called the Stockdale kimberlite. It has previously been characterized geologically and has been classified as a micaceous kimberlite (Brookins, 1970). These two areas are near each other (43km) and thus serve as a natural laboratory in which to examine the extent to which the contributions of the kimberlite weathering can be detected.

Chapter 2 - Background

2.1-The Flint Hills

The Flint Hills of east central Kansas stretch from the Nebraska border in the north to just across the border south into Oklahoma. Outcropping lithologies are predominantly Permian-age alternating layers of shale and limestone containing microcrystalline quartz in the form of chert or flint. The chert- or flint-bearing limestones are more resistant to erosion than the shale layers, leading to differential weathering, which results in a terraced appearance for weathering outcrops that is characteristic of the Flint Hills (Tallgrass Prairie, 2014). The Florence limestone, which forms the highest benches in Konza, is capped with a loess layer that is less than 1 m thick and was deposited during Pleistocene glaciation, though aeolian-dust deposition continues today and makes for a significant input of mass to the Konza area (Oviatt, 1998). This can be found on other formations as well.

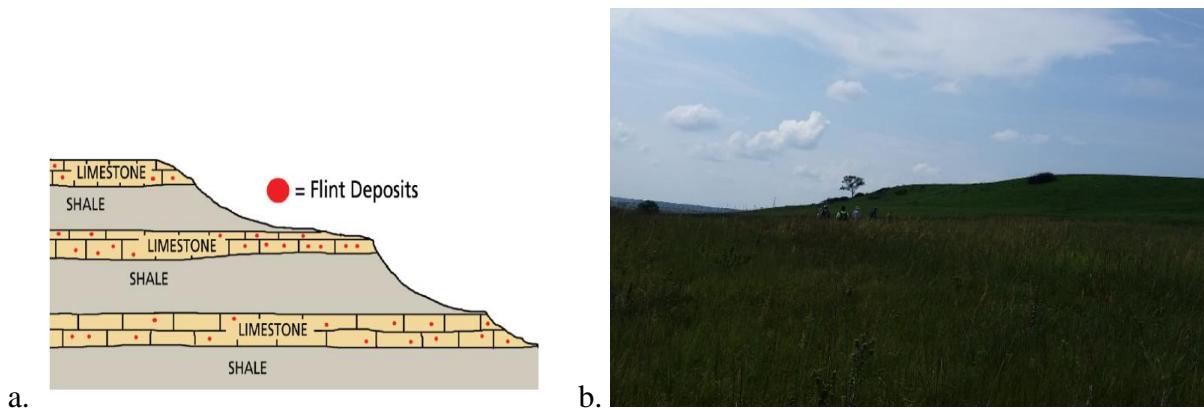


Figure 2.1-Terraced erosion of the Flint Hills. a. Diagram of underlying geology (NPS, 2016). b. Photo taken in Aug. 2016 at Konza Prairie LTER showing flat top limestone bench, shale slope and lower limestone bench.

Konza Prairie LTER is a tallgrass prairie preserve and research facility, roughly 35 km² in size. This area is being used in this study as an analog for the wider Flint Hills, due to the classic Flint Hills geology found here. It is an area of alternating limestone laced with chert and shale with the terraced erosional features. The limestones range in thickness from ~0.5m to ~26m, though most units are between 3m and 6m in thickness. Because the chert-bearing varieties are relatively resistant to erosion, they tend to form flat hilltops and benches. In contrast, the shales, which range from ~3m to ~17m thick, are more commonly 4m to 6m in thickness. The rocks in these layers are not all fissile and so are a mixture of shales and

mudstones; however, for the reader's convenience these layers will be referred to as shale throughout the rest of this thesis. These shales erode more easily than the limestone and form slopes between the limestone benches.

The Konza samples used for this study were collected by a previous Kansas State University graduate student (Eke, 2012), in and around a well-studied watershed in Konza, watershed N4D, shown in the shaded area of the map in Figure 2.2 below. The six sites are located near intermittent stream beds in highland areas near the top of the slopes in and near the uplands of the N4D watershed (elevation 397m), at the base of the N4D watershed where the streams converge (elevation 382m) and near King's creek which runs by (elevation 345m) as seen in Figure 2.2. This gives a difference in the elevation of all the sample sites at Konza of just over 52m (Appendix A).

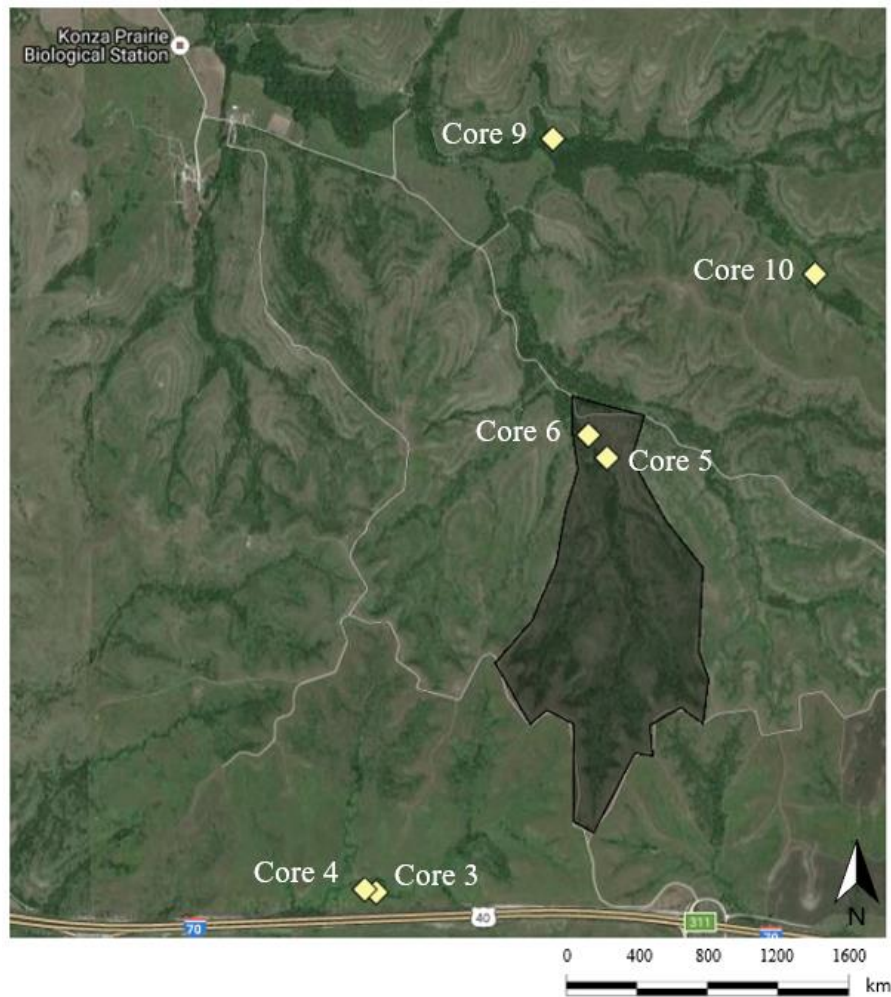


Figure 2.2-Konza Prairie limestone-shale core sample map. N4D watershed is shaded

The Stockdale kimberlite has a surface exposure of approximately 0.024 km² in size and is located at 39°20'30" N latitude and 96°43'26" W longitude (Cullers et al., 2006), based on magnetic surveys. It has a surface exposure on the edge of a stream valley near a fence on a parcel of range land (Figure 2.3). Stream flow is intermittent, and upstream from the kimberlite outcrop, a pond has been created in recent years by damming of the stream. However, when the stream has water in it, it flows past the exposed face of the kimberlite. The source of the water is primarily runoff from the surrounding watershed, though during periods of heavy rain overflow from the stock pond may contribute as well.

Kimberlites are CO₂-rich ultrabasic igneous rocks that originate deep within the Earth's mantle (ca. 150km or more). Compared to most igneous rocks, they are low in SiO₂, but enriched in incompatible major elements, such as K₂O and Na₂O, as well as a range of trace elements. As such, they contrast markedly in composition with the limestone and shale country rock into which they are intruded here in Kansas.

Table 2.1 -Mineralogy of Stockdale Kimberlite, Riley County limestones, and Riley County shales. (1) Brookins (1970). (2) Runnels and Schleicher (1956). (3) Dulekoz (1969) and Pecchioni (1981).

Kimberlite Mineralogy (1)	Generalized Riley County Limestone Mineralogy (2)	Flint Hills Shale Mineralogy (3)
Pyrope Garnet	Calcite	Quartz
Ilmenite	Dolomite	Calcite
Phlogopite (some Chloritized)	Chert	Gypsum
Magnetite		Kaolinite
Perovskite		Illite
Olivine (some Serpentinized)		Chlorite
Orthopyroxene		Rutile
Clinopyroxene		Zircon
Melilite		

They cut through the overlying upper mantle and crust on their way to the surface, ripping off pieces of crust and mantle rocks that are referred to as xenoliths. The intrusions, called diatremes, tend to be conic in shape, with the widest dimensions at the surface; they form

sharp contacts with the country rock through which they erupt (PIC 16, 2000). In the Flint Hills, the kimberlites range up to 0.07 km² and, as noted by Brookins (1970), kimberlites tend to occur in swarms, which is what we see here in the Flint Hills.

There are 13 identified kimberlite intrusions in this area, each with a slightly different composition, though there are several similarities. The rocks tend to be highly porphyritic and exhibit brecciated textures. They are usually highly altered, containing abundant serpentine (~35%) and calcite, but also retaining significant amounts of primary olivine, pyrope garnet, phlogopite, ilmenite, and magnetite (Brookins, 1970). Alteration tends to begin almost immediately after the eruption because most of the primary igneous minerals are not stable at surface temperatures and pressures. Therefore, nearly all olivine phenocrysts found in the kimberlite have been completely serpentinized. U-Th/He geochronology indicates that the kimberlites were emplaced between 85 and 110 Ma (Blackburn et al., 2008).

Table 2.2-Major element oxide weight percent. ND = no data. (1) Stockdale kimberlite (Cullers et al., 2006). (2) Average of Eskridge, Cottonwood and Ft. Riley Limestones (Runnels and Schleicher, 1956). (3) Average of post-Archean shales (Taylor and McLennan, 1985).

	Stockdale Kimberlite Surface (1)	Riley Co. Kimberlites (Range all) (1)	Limestone (2)	Shale (3)
SiO ₂	31.8	22.2-31.8	1.12	62.8
TiO ₂	1.98	1.5-4.4	0.026	1.0
Al ₂ O ₃	2.18	2.0-4.6	0.45	18.9
FeO _{Total}	8.54	8.5-11.6	0.17	6.5
CaO	5.69	5.69-16.7	54.59	1.3
MgO	33.52	20.4-33.5	0.33	2.2
K ₂ O	0.04	0.02-0.3	ND	3.7
Na ₂ O	0.01	0.01-0.51	ND	1.2
MnO	0.14	0.08-0.24	ND	0.11
P ₂ O ₅	ND	0.91-1.37	ND	0.16
LOI	16.7	15.4-21.4	43.13	6.0
Total	100.6	~100	99.82	99.9

As seen in Table 2.2 above, the generalized geochemistry of the rock types involved in this study differ significantly. The kimberlites in general, and Stockdale specifically, are low in silica and aluminum, whereas the shales are much higher in these elements; in contrast, the limestones are much lower. Magnesium, and to a lesser extent iron and titanium, are high in the kimberlites compared to the shales and limestones. Limestone has nearly 10 times more calcium than the kimberlite and 50 times more than shales.

Soils from the interbedded limestone-shale system were sampled at Konza Prairie Biological Station, southeast of Manhattan, Kansas. Kimberlite-sourced soil samples were obtained from the vicinity of the Stockdale kimberlite outcrop (Figure 2.3). The two sites are 43km apart and experience similar temperatures and precipitation rates since they are in the same climatic region. Temperatures range from an average high of 33.3°C in summer to an average low of -8.1°C in winter, with an annual average of 12.7°C. Average annual precipitation is 904 mm, with most falling in late spring/early summer and the winter months being drier (US Climate Data, 2017). Due to their proximity, both Konza and Stockdale have similar climate patterns, unmanaged open prairie lands and shared geologic history from the time the kimberlites erupted to present day. Because of this, isolating products that are due solely to differences in source material will be clearer.

2.2 – Previous Studies

Konza Prairie Long-Term Ecological Research (LTER) Site is utilized by researchers from many fields studying a multitude of different aspects of the Critical Zone. A list of past and ongoing projects can be found on the Konza LTER website (Konza Research, 2016). This body of work includes investigations of the underlying geology, geomorphology and the weathering processes at work in this area. The geomorphological processes that have given Konza its signature terraced erosion pattern have been extensively studied, along with the significant influences of fluvial processes in shaping the history of this area (Oviatt, 1998). Most weathering studies have focused on the relationships with key aquifers in the region. These studies have shown that these aquifers weather because of belowground CO₂ coupled with rapid water movement through the subsurface in these areas, and weathering rates have increased over the last 15 years (Macpherson et al., 2008). The soils have also been extensively studied at Konza. The soils derived from the interbedded limestones and shales tend to be extremely thin to nearly

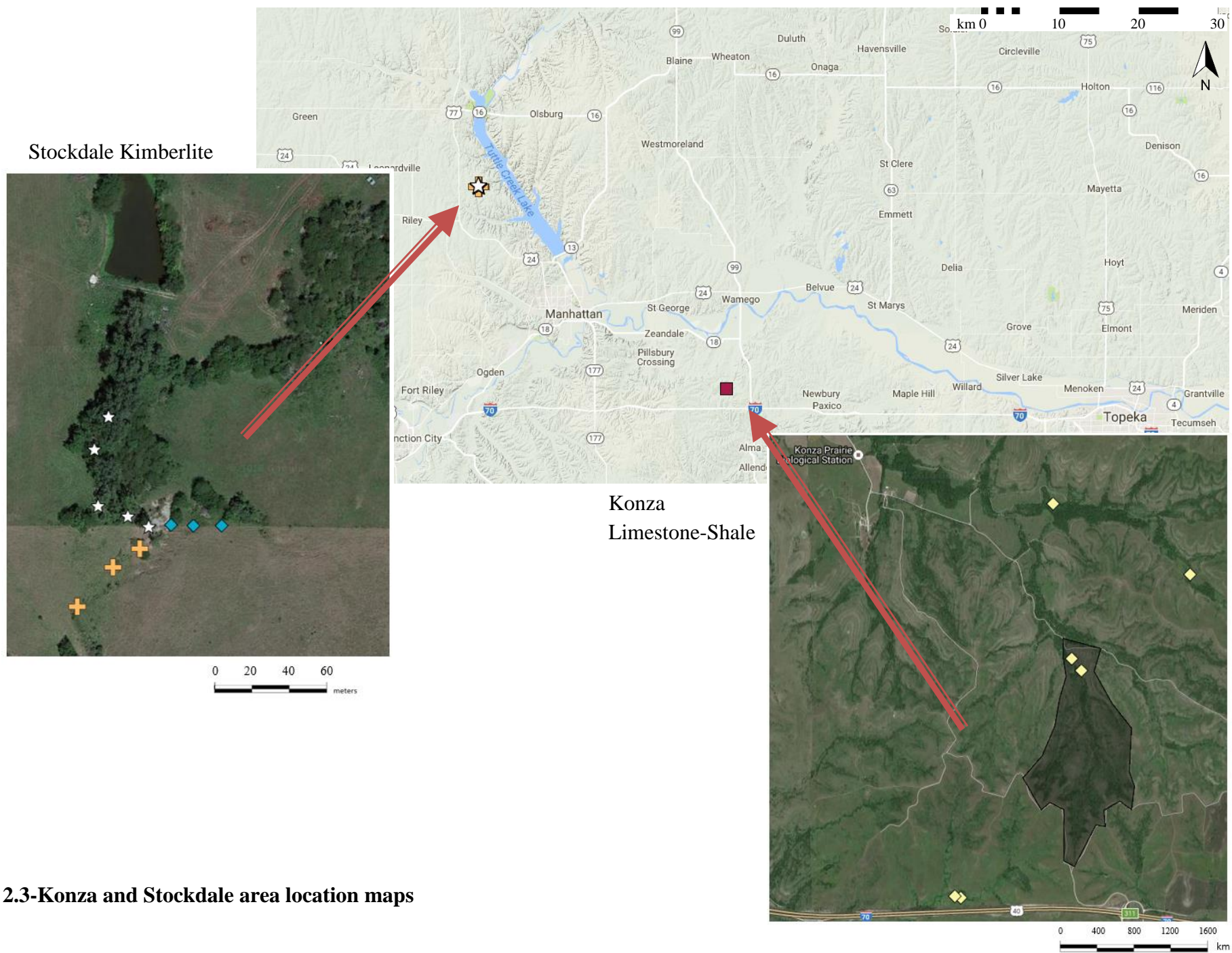


Figure 2.3-Konza and Stockdale area location maps

absent in upland areas and near the tops of hillslopes. At the base of hillslopes soils are thicker, 1-2 m on average. Soils at Konza Prairie LTER generally have low carbonate contents, under 35% of observed soil minerals, and have moderate to low cation exchange capacities (Ransom et al., 1998).

Most of the kimberlite outcrops in the Flint Hills have been mapped and had their mineralogy characterized, beginning in the 1940's shortly after the first outcrops were identified (Brookins, 1970). Some investigations have been conducted into dating the timing of intrusion (Blackburn et al., 2008), the geochemistry of a few specific minerals (Meyer and Brookins, 1976 and Rost et al., 1975), and trace element contents in the kimberlites (Cullers et al., 1982). However, in total, this body of work is rather limited and there has been no study of the weathering of, or the soils associated with, these kimberlites. Other work investigating weathering processes on other kimberlites is limited as well. One study investigated susceptibility of kimberlites to anthropogenic weathering as a method of ore processing. This study found those with higher percentages of smectite were more weatherable (Morkel and Vermaak, 2006). Since studies investigating the soils produced from kimberlite parent rock are extremely limited, a look at studies of parent rocks with similar minerals may provide some information relevant to this study. For example, studies involving the weathering products of and soils from ultramafic rocks, such as ophiolites, center on the formation of smectites and the impact of higher levels of trace metals. While the soils formed at kimberlites aren't "serpentine" soils, kimberlites do have high levels of serpentine and chlorite. Serpentinic soils ultimately generate smectites as an alteration product. The serpentine weathers into high-Mg, low-charge smectite, whereas the chlorite weathers to high-charge smectite (Lee et al., 2003, Estrade et al., 2015).

Chapter 3 - Methods and Materials

3.1 - Sample Collection and Processing

The Konza samples were collected in the summer of 2010 over a one-week period using a hydraulic geoprobe, which recovered cores to from the surface to a maximum depth of 2m. Core locations are mapped below in Figure 3.1 and more detailed location data are in Appendix A. The cores were stored in 24-inch clear plastic tubes under nitrogen at -4°C in the Department of Geology since the time of collection. Cores were thawed for 24 hours at room temperature before sampling. The top end of the tube was then opened and 10cm (~60g) of sediment was removed. Samples were taken from the ends of the tubes to leave as much of the core undisturbed as possible. Sediment was scooped out with a scupula, which was cleaned with deionized water and wiped dry between each tube. Sediment was placed onto a clean paper plate and loosely covered with another to avoid cross contamination. The tube was then flushed with nitrogen, resealed and returned to cold storage. For Konza localities 4, 6 and 9, samples were taken from both the top and bottom ends of the uppermost tube from the profile, because there was a change in color from the top of the tube to the bottom (4 and 9 were lighter in color at the bottom) and/or there was a change in texture (4 and 6 appeared to have an increased clay content).

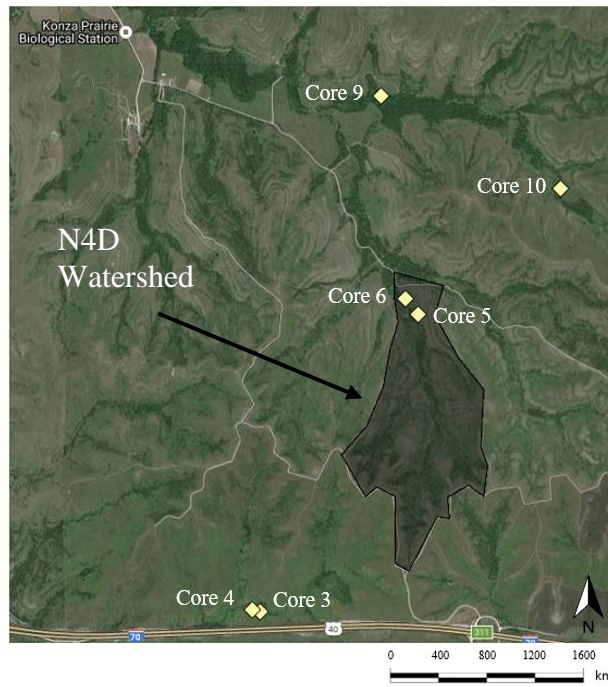


Figure 3.1-Konza Core location map

Sampling of the Stockdale kimberlite area started where the intermittent stream intersected with the surface exposure of the outcrop at the base of the stream gully. Samples were collected along three transects: upstream, downstream, and uphill, as shown in Figure 3.2. GPS locations are found in Appendix A. Five different sites in the streambed were cored north-northwest of the kimberlite outcrop at intervals of 16m – 37m. The variability in distance was to avoid tree roots while sampling along this route. A hand-turned auger was used to sample as deep as possible or until I struck the kimberlite bedrock. Samples were taken from the surface, at periodic intervals of 10-20cm and from the lower most core available; core length was limited by striking bedrock in several locations (cores SKD 1, 2, 3, 5, and 1B). Additional samples were collected when upon visual inspection as the core was pulled up the color of the sediment appeared darker or lighter, or where the sediment appeared grittier or more clay-rich. Cores downstream from the kimberlite outcrop were taken using the same sampling methodology. Three locations were sampled on this transect to the south-southwest of the intersection of the surface exposure and the stream. Maximum depths for these were limited to the intersection with the water table. At this depth cores slid off the auger blade and were too wet to be retrieved. The uphill transect started at the east edge of the kimberlite surface exposure and three localities were selected uphill from the kimberlite outcrop at a 7% gradient due east away from the stream. Cores were taken following the same methodology as used for the other two transects. Core depths were limited by the depth of the kimberlite bedrock and the maximum depth at which the auger could still be turned by hand.

Sixty-eight samples in total were collected for this study, 22 from Konza and 46 from Stockdale. All samples were stored in a cooler at ~5°C for 2-3 days until they could be air dried. Approximately 30g of each sample was placed on a paper plate and covered loosely with another plate and allowed to dry on a lab counter for a period of 2-4 days until completely dry. Samples were spread out on a large sheet of brown paper and large clumps of soil were disaggregated with a wooden roller by slowly applying pressure until it broke apart, being careful to not break large chips of rock. The disaggregated sediment was then sifted with a brass, U.S. Standard size No. 10 sieve to remove all particles > 2mm. The <2mm fraction was used for all analyses described below, except for the ATP (Adenosine Triphosphate) analysis.

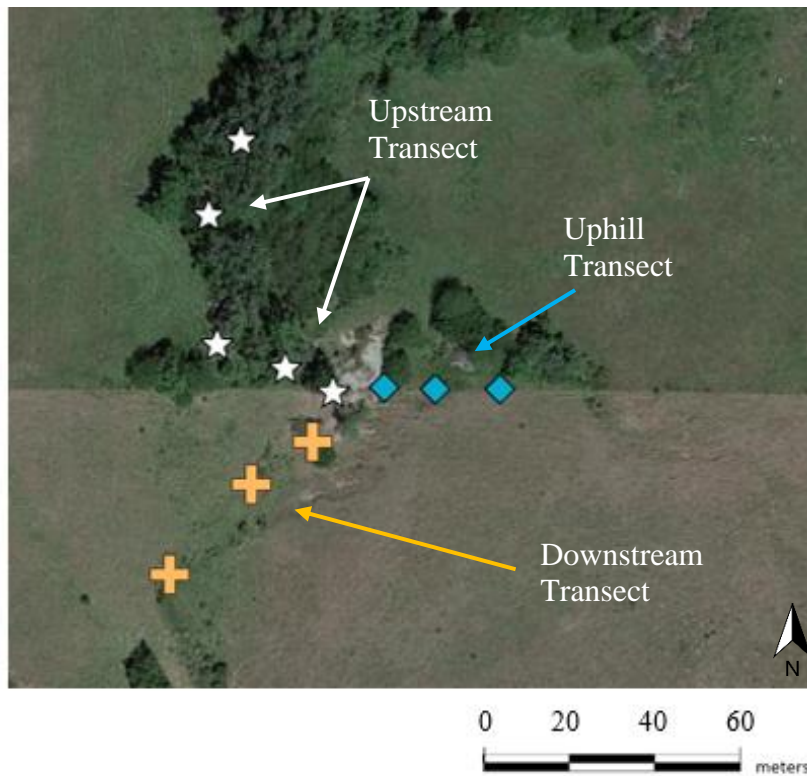


Figure 3.2-Stockdale Kimberlite core location map

3.2 – Bulk Sediment X-Ray Fluorescence Analysis

X-Ray Fluorescence (XRF) analysis was conducted on all sediment to determine the bulk elemental composition. Analyses were conducted using a Bruker Tracer III Handheld XRF and composition was determined using the Bruker mudrock calibration (Rowe, 2012), which was refined with the addition of chemical data from shales located in Kansas and Oklahoma (Rowe, per coms, 2015). Samples were prepared by grinding ~3-4g of the <2mm fraction of previously sieved sediment. Using an agate mortar and pestle, samples were ground to a fine powder (~50µm) and put into a small plastic Chemex® XRF sample cup. One end was covered with a plastic cap and the other end was covered with 4µm thick Prolene® film. Each sample was analyzed twice, once for trace elements (Co, Ni, Cu, Zn, Ga, As, Rb, Sr, Y, Zr, Nb, Mo, Ba, Pb, Th and U) and once for major elements (Mg, Al, Si, P, S, K, Ca, Ti, V, Cr, Mn and Fe).

Trace elements were analyzed with the following settings and procedure:

- yellow filter (12 mil Al + 1 mil Ti)
- 40kV and 12.4µA for 120 seconds

Each sample was analyzed 6 times. To ensure homogenization between individual analyses, the sample cup was agitated, then tapped on a table to compact the powder.

The mudrock calibration converts the photon intensity peaks generated from the XRF to elemental concentration data, which it reports in weight percent. These values were averaged and reported on a plot vs. depth per sample spot.

Major elements were analyzed with the following settings and procedure:

- no filter
- 15kV and 25 μ A for 180 seconds
- vacuum pump was attached to create a vacuum in the interior of the gun. This improves the intensity of the analysis for lighter mass elements

To ensure homogenization between individual analyses, the sample cup was agitated then tapped on a table to compact the powder.

Initially analyses were made six times per sample. However, part way through the analysis period, it was discovered that the XRF had an intermittent malfunction that skewed the data. The malfunction was resolved and all samples were reanalyzed in the same way as before, but in the interest of time, each sample was analyzed only three times. Standard RTC-WS-220 (Rowe, 2012) was analyzed between every third and fourth samples to ensure quality control. Again, the mudrock calibration was used to generate elemental weight percent. These values were averaged and reported on a plot vs. depth per sample spot.

3.3 – Particle Size Analysis

Particle sizes analysis (PSA) was conducted on each sample using a Malvern Mastersizer 3000 laser diffraction particle size analyzer with a Hydro EV wet dispersion accessory. Samples were pretreated with hydrogen peroxide to remove any organic material that could cause clumping. Approximately 0.5g of air-dried sample was put into a 50mL centrifuge tube to which was added 1mL 30% hydrogen peroxide and 5mL deionized water. Tubes were left to react until the rapid effervescing stopped, approximately 5 minutes, and were then filled up to 30mL with deionized water. The tubes were then placed in an 80°C water bath until all bubbling stopped, approximately 12 hours. Samples were removed and cooled to room temperature, then washed with deionized water and centrifuged at 6000 rpm for 2 minutes, after which the supernatant liquid was carefully poured off to avoid disturbing the solid particulates at the bottom of the

centrifuge tube. This process was repeated twice. Deionized water was then added to the tubes to return the volume to 30 mL. The propeller on the wet dispersion accessory of the particle size analyzer, affectionately nicknamed “Sandy”, was set for 1500rpm. The tube was agitated for 15 seconds then a pipette was used to extract a 1-2mL representative sample which was then analyzed by “Sandy”. Particle size data are reported as % by volume.

3.4 – X-Ray Powder Diffraction Analysis

X-Ray Diffraction (XRD) analysis was conducted on each sample to determine the bulk mineralogy. Analyses were conducted using a PANalytical Empyrean X-Ray Diffractometer, using a PIXcel 3D scanning line detector. X-rays were generated with a Cu tube and Ni-filter at a setting of 45kV, 40mA through a range of 2.5° to 70°(2 θ). Approximately 3-4g of the <2mm fraction of the air dried, sieved sediment was ground to a fine powder (~ 50 μ m) with an agate mortar and pestle. The sediment was then frontloaded and packed firmly into a 27mm sample holder mounted into a spinning sample stage and rotated at 4 rpm. Peak data for each sample were analyzed using Highscore Plus® software and compared to International Center for Diffraction Data (ICDD) reference data cards to determine the mineralogy of the sample. A mineral was determined to be included in sample when the top three to four most intense peaks as determined by I/I₀ on the ICDD reference card matched peaks in the sample XRD spectra. Software generated matches were manually verified before a mineral was included in the assemblage for that sample.

3.5 – Clay Fraction X-Ray Diffraction Analysis

After studying the mineralogy as determined by XRD, chemical data as determined by XRF and particle size data as determined by PSA analysis, eight of the 68 samples were selected for further analysis to determine the mineralogy of the clay fraction. The samples chosen had either a mineral or mineral assemblage which was unique compared to other samples and had a high enough clay proportion that sufficient clay could be collected for analysis. The < 2 μ m clay fraction was separated by centrifugation.

Samples were pretreated in accordance with USGS standard protocol (Poppe et al., 2001). Approximately 20g of each dry sample were first added to a beaker and combined with

50mL of a 20% acetic acid solution to remove excess carbonates. Once effervescence subsided, ~5-7 minutes, another 50mL of the same solution was added and samples sat overnight in a fume hood. Samples were transferred to polypropylene wash bottles then washed with deionized water in and centrifuged at 6000 rpm for 2 minutes, after which the supernatant liquid was carefully poured off. When more deionized water was added, the bottles were capped and shaken vigorously for one minute. This process was repeated twice. Sediments were then treated with hydrogen peroxide to remove organic material; 50mL of a 3% hydrogen peroxide solution was added to each sample and stirred. After effervescence slowed, another 50mL of the peroxide solution was added to the sample and allowed to sit until all effervescence stopped, ~4 hours. The suspension was again washed three times with deionized water by centrifugation at the same setting with the supernatant liquid poured off after each wash.

Samples were then put into 50mL centrifuge tubes. Approximately 0.25g of Na hexametaphosphate, a dispersant, was added to each tube, which was then agitated and centrifuged for 87 seconds at 1000rpm. This setting was calculated using the method outlined in the USGS's Laboratory Manual for X-Ray Powder Diffraction (Poppe et al., 2001). This processing time left the $< 2 \mu\text{m}$ clay fraction suspended in the supernatant liquid, which was then removed with a syringe and collected in a beaker. The above process was repeated four times to ensure an adequate amount of clay-sized sediment was collected to be able to conduct all desired analyses.

The clay fraction suspension for each sample was divided into three different 50 mL centrifuge tubes. For each sample the following treatments and slide preparations were performed.

- Tube 1 – Mg treatment, to hydrate interlayers of clay minerals:
 - Add 30 mL 0.5M MgCl_2 to sediment and agitate vigorously for 30 seconds; centrifuge the tube at 1800 rpm for 5 min and discard the supernatant fluid
 - Repeat step 1 twice
 - Wash sediment with 30 mL deionized water to remove superfluous salt and agitate vigorously for 30 seconds, the centrifuge at 2500 rpm for 5 minutes
 - Repeat step 3 until the sample is fully dispersed (~3 times)
- Tube 2 – Glycerol treatment, to expand interlayer spacing of expandable clay minerals:

- Add 30 mL 0.5M MgCl₂ to sediment and agitate vigorously for 30 seconds; centrifuge tube at 1800 rpm for 5 min and discard the supernatant fluid
- Repeat step 1 twice
- Wash sediment with 30 mL 1% (v/v) glycerol and agitate vigorously for 30 seconds, then centrifuge at 2500 rpm for 5 minutes
- Repeat step 3 twice to ensure all excess salt had been removed
- Tube 3 – K treatment, to dehydrate interlayers of clay minerals:
 - Add 30 mL 1M KCl to sediment and agitate vigorously for 30 seconds; centrifuge tube at 1800 rpm for 5 min and discard the supernatant fluid
 - Repeat step 1 twice
 - Wash sediment with 30 mL deionized water to remove superfluous salt and agitate vigorously for 30 seconds, then centrifuge at 2500 rpm for 5 minutes
 - Repeat step 3 until the sample is fully dispersed (~3 times)

For each sample six frosted petrographic glass slides were labeled as follows: Mg-25, Mg-EG, Mg-GLY, K-25, K-350, K-550. For each slide, 2 mL of clay suspension from the centrifuge tube was measured out using a volumetric pipette and distributed evenly over the glass slide. Slides were then left to air dry for 48 hours, at which time any further treatments were performed. Below is the description of the clay treatment used and any post-drying treatments that were performed:

- Mg-25 – 2mL clay from tube 1, no treatment after drying
- Mg-EG – 2mL clay from tube 1, after drying slide was placed in a sealed desiccator with ethylene glycol in the bottom and baked in an oven for 12 hours at 60°C; slides were left inside the sealed desiccator to cool to room temperature
- Mg-GLY – 2mL clay from tube 2, baked in oven for 4 hours at 60°C
- K-25 – 1mL clay from tube 3, no treatment after drying
- K-350 – 1mL clay from tube 3, after drying slide was baked in a high temperature oven for 4 hours at 350°C then allowed to cool to room temperature in a covered desiccator
- K-550 – 1mL clay from tube 3, after drying slide was baked in a high temperature oven for 4 hours at 550°C then allowed to cool to room temperature in a covered desiccator

Because of the layered structure of phyllosilicates, when they are mounted in a parallel orientation on the glass slide several different types of clay can have the same d-spacing.

However, these clays behave differently under different conditions, so by creating these conditions with the treatments described above, the differential d-spacing of the clays can be compared to more accurately determine the type of clay present. Once all treatments were complete, all six slides for each sample underwent XRD analysis with the same instrument described above. The slides were mounted on the flat sample holder and analyzed with the Ni-filtered Cu tube set to 35kV and 20mA. The Mg-25 slide for each sample was scanned through a range of 2° - 35° (2θ) to allow for the identification of non-clay minerals that appear in the clay size fraction. All other slides for all samples were scanned through a range of 2° - 15° (2θ) to determine if any peaks had shifted due to the clays expanding from the treatments listed above. Peaks for each treatment for a sample were then compared to determine the clay mineralogy for that sample.

The identification of smectites and expandable 2:1 layer silicates can be difficult. This is accomplished by comparing the d-spacing in the d_{001} orientation of these minerals after the various treatments detailed in section 3.5 had been undertaken. If vermiculite is present in the sample, all Mg-saturated treatments will remain at 14 Å and all K-saturated treatments will remain collapsed at 10 Å at all temperatures (25°C, 350°C and 550°C). If chlorite is present in the sample, the d_{001} -spacing will remain at 14 Å under all treatment conditions. When smectite is present in the sample, Mg-saturated air-dried smectite will have a d-spacing of 14 Å and this will expand to around 17 Å when baked with ethylene glycol. In Mg-saturated glycerol washed smectites, the interlayer will expand to around 18 Å. K-saturated air-dried smectites will measure 12 Å then will collapse to 10 Å with heat treatment. Expandable 2:1 layer silicates will have a d-spacing of 14 Å when Mg-saturated and air dried. After treatment with ethylene glycol, they will expand to approximately 17 Å like smectite. However, these clays show little to no measurable change from the Mg-saturated air dried treatment. If the vermiculite and smectite are regularly interstratified, a sharp peak will be seen at 28 Å, whereas if they are randomly interstratified the peak will be more broad and rounded. It is only when overlying the diffractograms from all treatments that a minor change in the shape of the line may be detected in the 17-18 Å range, but this change is not enough to be considered a peak or qualify as peak shift (Moore and Reynolds, 1989).

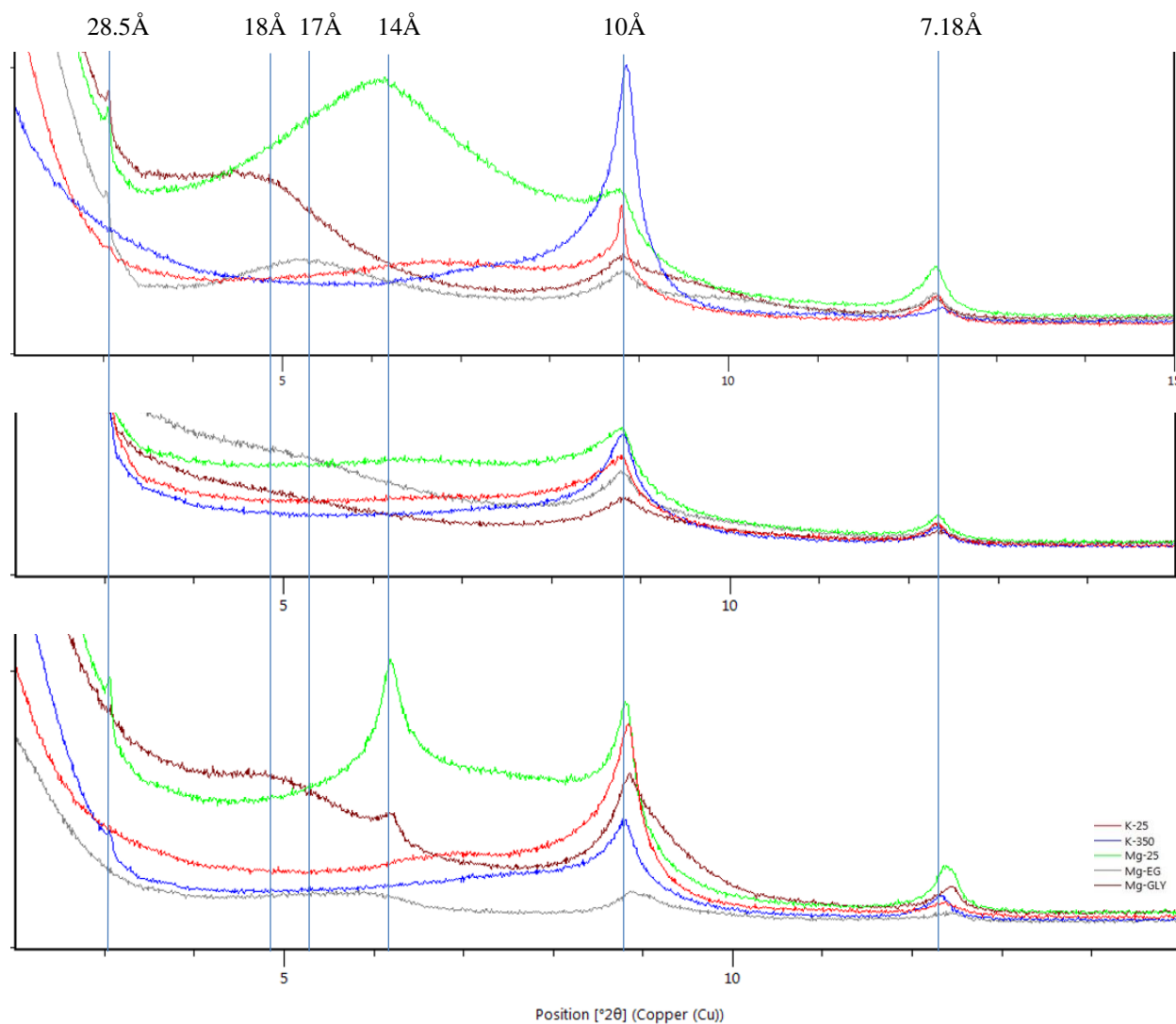


Figure 3.3-XRD diffractogram of interlayer expansion and collapse after various treatments for smectite (SDK 1), expandable 2:1 layer silicates (Konza 6, 0-10cm) and vermiculite (Konza 6, 70-80cm)

3.6 – Bulk Digestion and ICP-OES Analysis

A bulk elemental extraction was conducted by digesting the sediments in aqua regia. Twenty-one samples were chosen for this analysis based on major and trace element compositional data, as determined by XRF, and particle size data, as determined by PSA analysis. Based on these data, the Konza samples chosen were those from the N4D watershed deemed to warrant further analysis due to their differing Ca content and mineralogy as compared to the rest of the Konza cores. Samples from the Stockdale area were chosen to encompass (i) a

wide spatial distribution; (ii) a range of depths; (iii) a range of compositions, particularly where differences with Konza sediments were apparent; and (iv) a range of clay contents, particularly those with higher clay contents. This was done to ensure a more complete snapshot of what is occurring in this area. This “spatial snapshot” was not possible at Konza, since I was working with samples retrieved from existing core. The procedure used for these analyses is the standard aqua regia bulk chemical extraction procedure used at the Soil Chemistry Laboratory of the Agronomy Department at Kansas State University, which has been adapted from Methods of Soil Analysis, Part 3, Soil Science Society of America (Swift and Sparks, 1996).

For this analysis 0.5g of the < 2mm fraction of sample, which had been air dried and sieved as previously described in Section 3.2, was put into a glass digestion tube. The mass was recorded to 2 significant digits for future dilution calculations. To this 0.5mL of 30% hydrogen peroxide was added and allowed to react for 10 minutes. Then 2.5mL more was added and allowed to react for 12 hours at room temperature. 5mL of 1:3 ratio of concentrated HNO₃: HCl, mixed immediately before use, was added to each tube and allowed to react in a fume hood overnight, approximately 10 hours. In the morning, each tube was swirled with a vortex mixer to ensure all sediment had reacted with the acid. Tubes containing the sediment-acid mixture were placed into a digestion block for heating. Tubes were swirled every 10-15 minutes with the vortex mixer during the full duration of the following time and temperature regimen: 75°C for 30 minutes, 100°C for 30 minutes, 110°C for 30 minutes, 140°C until ~1mL material remained in the tube. The time for the last step varied per tube. As they approached the 1mL mark, tubes were closely watched so as not to overshoot this mark and dry out. Once all tubes were reduced to 1mL of liquid, they were cooled to room temperature, being swirled every 15-30 minutes. Each tube was then brought up a total volume of 25mL with 0.1% HNO₃ and mixed well with the vortex mixer. Samples were then filtered through Whatman No. 42 filter paper into clean Falcon® tubes and refrigerated at 5°C until the time of analysis.

Inductively Coupled Plasma Optical Emission Spectroscopy (ICP-OES, Varian, Inc.) analysis was conducted on the filtered digestate to more accurately quantify the concentrations of certain elements present in the selected sediment samples. Analyses were conducted with a Varian 720-ES Inductively Coupled Plasma-Optical Emission Spectrometer. This instrument is capable of quantifying multiple elements simultaneously down to concentrations as low as 1 mgL⁻¹ (ppm). Each sample was analyzed for Al, Ca, Cr, Cu, Fe, K, Mg, Mn, Na, Ni, P, S, Si, Ti

and Zn concentrations. Samples were grouped into four suites based on the dilutions necessary to fall within the maximum detection limits of the instrument: Al, Ca, Fe, Mg at 50X dilution, K, Na, Si at 4X dilution, Mn, P, S, Ti at 3X dilution and Cr, Cu, Ni, Zn undiluted. Five multi-element standards of varying concentrations were custom made for each suite with standard stock solution using the sample addition method, except for the undiluted suite as this would have brought the standards over the detection limits of the instrument for the elements of interest. During analysis, three to four samples were randomly selected for a duplicate measurement and three to four more samples were spiked with a known amount of one of the standards so that when calculations were run, quality control issues could be constrained.

3.7 – ATP Analysis

ATP analysis was conducted at sample sites 3, 4, 5, and 6 at Konza and 1, 2, 5, 2A, 4A, 1B and 3B at Stockdale to determine the amount of microbial activity. Because the Konza soil samples had been in cold storage for so long, it was determined that fresh samples would yield a more accurate measure of microbial activity. Since Konza and the Stockdale kimberlite localities are only 43 km apart, all samples for this analysis were collected on the same day. This ensures that any measurable differences are due to the soil components and not other factors, such as temperature or rainfall in the days leading up to sampling. Samples were collected at a depth at 6-10 cm using sterile techniques. The scoop was rinsed with deionized water and sterilized by flame between each collection and placed into sterile 15mL centrifuge tubes, which were immediately sealed. It was unnecessary to preserve the samples with dry ice, because they were analyzed on the same day as collection. However, they were kept in a cooler during travel between sites and on the return trip to the laboratory.

Once in the lab, 2g of sediment was placed into a sterile 50mL centrifuge tube and agitated via vortex mixer for 1 min with 20mL deionized water which had sterilized in an autoclave (120°C for 30min in a closed glass jar). Samples were centrifuged for 2 minutes at 6500 rpm. The supernatant liquid remained cloudy for samples Konza 3, Konza 4, SDK 5 and SDK 3B. For all other samples, supernatant liquid was clear, although pale / medium brown in color. The solution was filtered with 0.45µm Whatman filter attached to a sterile syringe. A 100µL sample was removed with a sterile pipette and placed into an Aquasnap ATP testing pen.

The reagent reacted for 5 seconds while the pen was shaken, then the pen was put into a Hygenia SuperSURE Plus® and the relative light units (RLU) were recorded.

Chapter 4 - Results

4.1 – Field observations made during coring at Stockdale Kimberlite

In the Stockdale locality, sediment was collected in October 2015. The exposed surface of the kimberlite is in an agricultural field used for cattle grazing. It is approximately 400 m from a dirt access road and is located at the bottom of a small hill. At the bottom of the hill is an intermittent creek with an uphill slope on the other side. Approximately 60m upstream from the kimberlite is a dam and stock pond used to water cattle. Cores were collected along three different transects and were numbered according to their proximity to the exposed surfaces of the kimberlite. Core location distance intervals vary due to the presence of tree roots in the creek bed. Where this occurred, offsets of between 2 and 17 m from the intended sampling site were made in the upstream direction. Cores 1 and 1B are within 2 m of the exposed kimberlite surface. For each transect, the core number goes up as distance from the kimberlite increases. The three transects are upstream, downstream, and uphill. Detailed core location data are found in Appendix A.

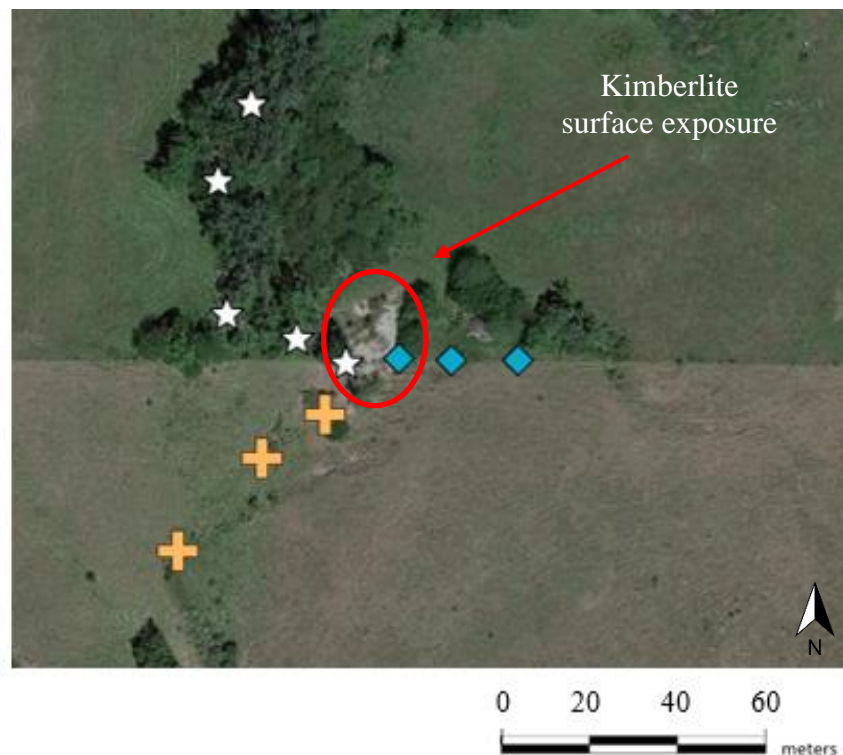


Figure 4.1. Stockdale Kimberlite core location map. The gray area in the center of the map is the surface exposure of the kimberlite diatreme

The upstream transect has five cores, as seen in Figure 4.2. Core 1 was taken from the streambed where the stream crosses over the west edge of the exposed surface of the kimberlite at the bottom of a hill, and subsequent cores were taken moving upstream from this location. Exact distances between cores (for all 3 transects) can be found in Appendix A. All cores along this transect were taken from the dry creek bed. Cores range from 12 to 52cm in length, with maximum depth limited in all cases by intersecting kimberlite bedrock. The sediment contained in these cores was very dark brown to black. It was sticky and appeared to be clay-rich. Rock chips, 2 - 5 mm in size, were distributed throughout the sediment, especially in the lower part of the core.

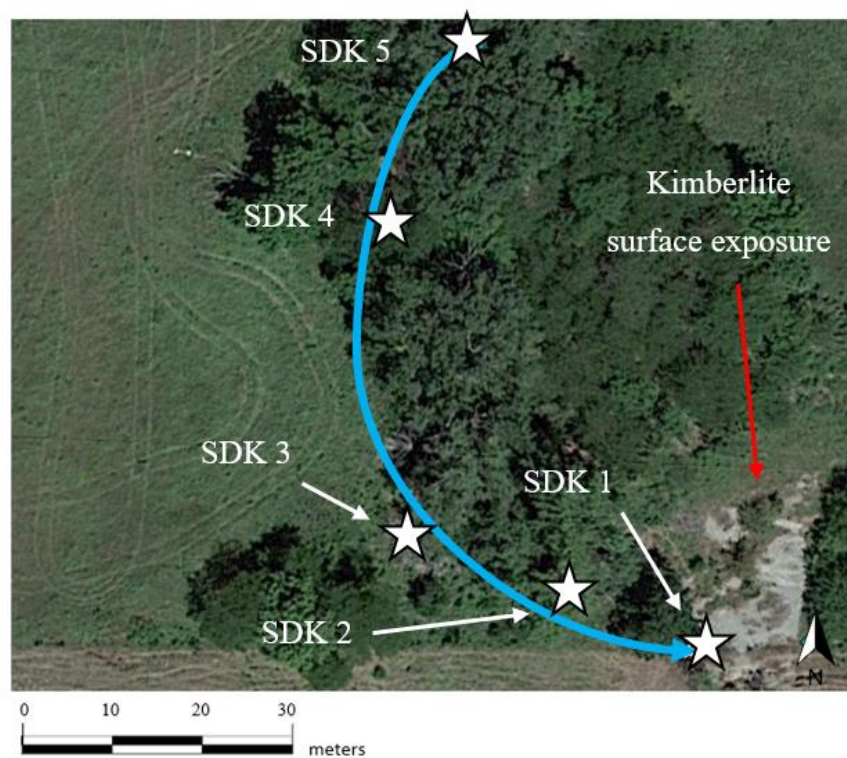


Figure 4.2. Stockdale Kimberlite Upstream Transect core location map. Blue arrow indicates the approximate stream path and direction of flow.

The downstream transect (Figure 4.3) has three cores and are all designated with the letter A after the core number. The first core along this transect, core 2A, was augered 20 m downstream of the edge of the kimberlite exposure in the same dry creek bed. The sediment contained in these cores was also a very dark brown to black, sticky and appeared to be clay-rich. These cores intersected the shallow water table, resulting in collection of wet sediment at the

bottom of each. For cores 3A and 4A this limited the depths to which sediment could be collected. The depth for core 2A was limited by the ability to turn the auger in such thick sticky soil.

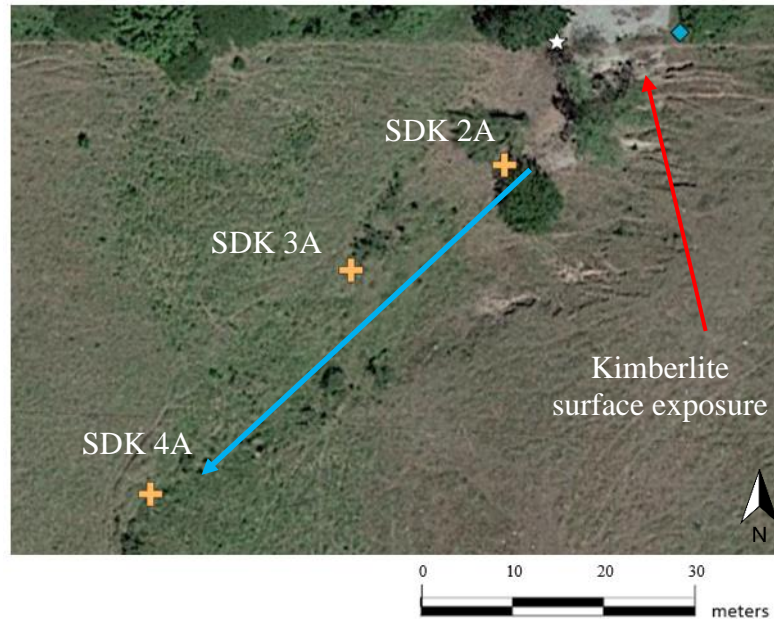


Figure 4.3-Stockdale Kimberlite Downstream Transect core location map. Blue arrow indicates the approximate stream path and direction of flow

The uphill transect has three cores and all are designated with letter “B” and moved up the hill slope as they were located further from the exposed kimberlite surface. Core 1 B was taken approximately 2m uphill from core 1 on the east side of the exposed kimberlite surface. Sediment contained in these cores was orange- brown in color. It was drier than other two transects and not as sticky. For all three of the cores along this transect the number of rock fragments increased with depth.

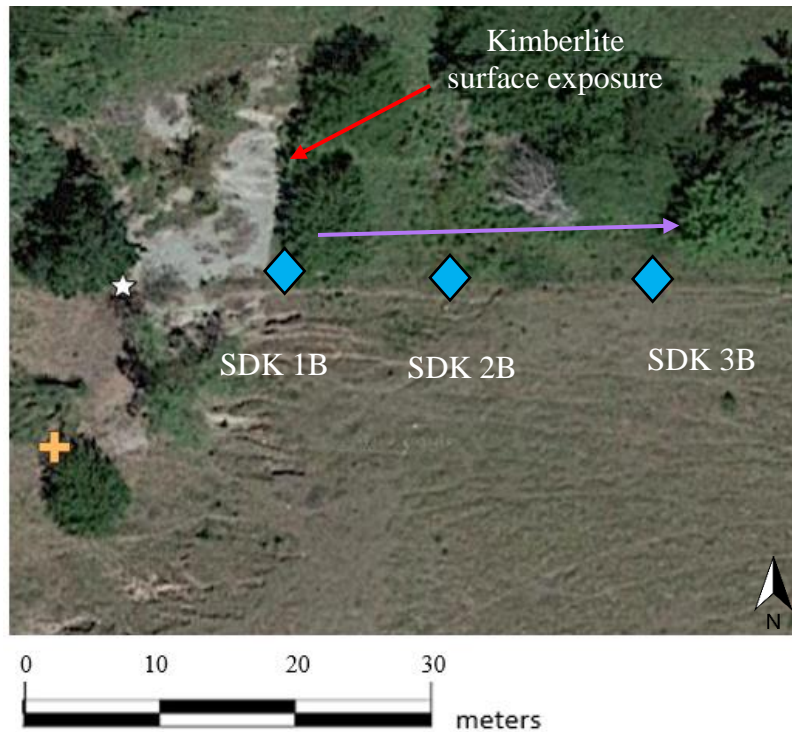


Figure 4.4- Stockdale Kimberlite Uphill Transect core location map. The purple arrow indicates the direction moving upslope from the surface exposure. Bright blue diamonds mark the core locations along this transect

4.2 – Results from X-ray fluorescence

Hand held XRF (HHXRF) analysis was performed on 68 samples in total. All data are provided in Appendix B. Appendix B.1 contains a table demonstrating the analytical uncertainty of the instrument by comparing the data collected on standard RC-W-220 (which was analyzed at the same time as the cores) to published values for this standard. All raw data from the analyses of all cores are also found in this section.

4.2.1 – Konza Prairie

Hand held XRF analyses of Konza cores show wide variability in elemental concentrations with depth over the 140 – 200 cm sampled. The variations with depth are similar for cores 3, 4, 5, 9 and 10; core 6 is more extreme in its variations (Figure 4.5). The description of trends which follows is for all Konza cores except core 6, which will be reported separately. Silicon (Si) concentrations range from 17wt % to 24.1wt % through the 200 cm of sampled core (Figure 4.5). However, Konza core 6 exhibits the greatest variability in Si from 9.5wt % to

20.6wt %. Aluminum concentrations tend to be at a maximum at a depth of 30-38cm, decreasing both above and below this depth. Cores show variation, ranging from 4wt % to 5.3wt %. Cores 3, 4, 9 and 10 indicate a slight decrease (~0.8-1wt % reduction) in Al in the upper 10 cm of the core. Core 6 exhibits the largest drop in concentrations, with an overall range of 3wt % to 6wt %. Cores 5 and 6 show an increase in Al with depth. For all cores, there is little change in Ti concentration through the full depth of the cores, as seen in Figure 4.5. This range is from 0.22wt% to 0.42wt%.

Concentrations of Ca and Mg exhibit similar patterns of variation with depth. In cores 3, 4, 9 and 10 the Ca concentration detected ranges from 0.4 wt% to 3.5wt % and Mg ranges from 0.15% to concentrations below detection limits of the HHXRF. In cores 5 and 6 the range for both elements is from 0.5wt % up to 17wt % for Ca and from below detection limits to a high of 0.43wt % for Mg.

Concentrations of Zn and Cu also change similarly to each other with depth in the Konza cores. Zn ranges from 68ppm to 201ppm (ppm = mg/kg), whereas Cu ranges from 28ppm to 68ppm through a depth of 200cm. Concentrations of Zn and Cu for all cores, except core 6, have a slight decreasing trend over a total range of 38ppm and 13ppm, respectively. For both elements in core 6, there is an overall decreasing trend moving from the deepest part of the core at 120 cm up to the surface. Zinc in core 6 decreases by a total of 111ppm, from 200ppm to 89ppm, whereas Cu decreases by a total of 19 ppm, from 54ppm to 35ppm.

The trends seen in the concentrations of both Fe and Ni are also similar to each other. Iron concentrations for cores 3, 4, 5, 9 and 10 ranges from 2wt % to just over 3wt % with core 6 extending that range up to 4.6wt% at a depth of 30 cm, but otherwise falling within the same range as the other cores. Ni for all cores except 6, ranges from 27ppm to 48ppm. Core 6 broadens that range up to 65ppm, with the maximum concentration again being measured at 30cm depth as seen in Figure 4.5.

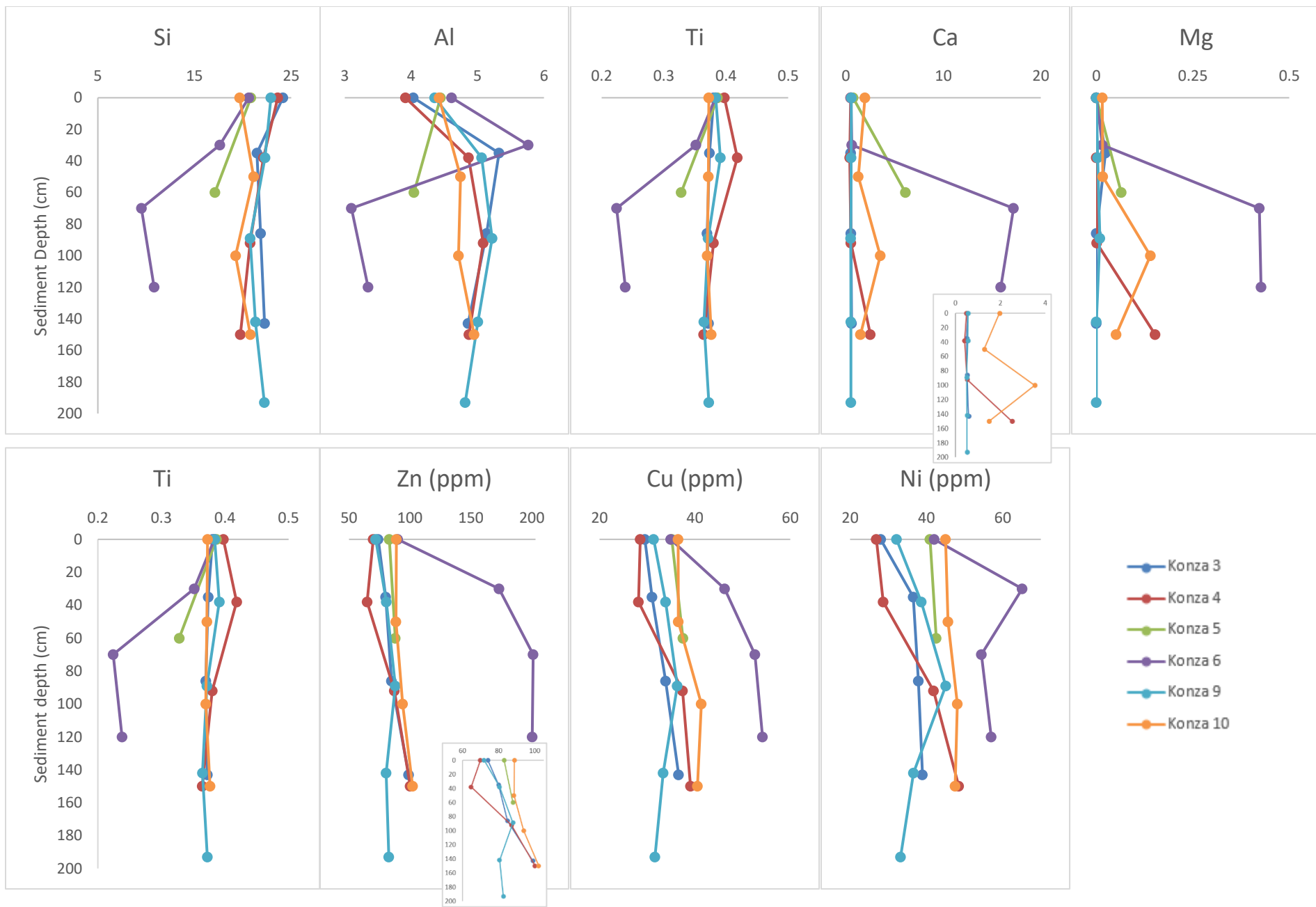


Figure 4.5-Konza cores: Elemental concentrations as determined by HHXRF. Concentrations are reported in element weight % (unless otherwise stated).

4.2.2 – Stockdale Kimberlite

HHXRF analyses of the Stockdale kimberlite cores show a high degree of variability in concentrations for many elements and a few apparently systematic trends in concentration with depth. Silicon in cores SDK 3, 3A and 1B exhibit greater variability in concentration than all other cores. SDK cores 3, 3A and 1B range from 8.3wt % to 20.2wt %, and show an increasing concentration of Si from the bottom of the core to the surface. All other cores have an Si concentration between 18.4wt % and 22.6wt % as seen in Figure 4.6. Al concentrations for cores SDK 3, 3A and 1B are like those seen in Si, in that they increase in concentration from the deepest part of the core up to the surface and have a broader concentration range: from less than 1wt % to 4.5wt %. Al for all other cores ranges from 4wt % to approximately 5.5wt % and exhibits no clear trend with depth.

The following description of data trends is for all cores excluding SDK 1B, which will be described separately. Iron concentrations show some variability, ranging from 2.7wt % to 3.8wt % with no systematic variation. However, cores SDK 2B and 3B see an initial increase in concentration moving from depth up to 28-30cm at which point concentrations decrease up to the surface. Concentrations of Mg vary from below detection limits to just over 1wt %. Titanium concentrations show minor variations with depth amongst the remaining cores, ranging from a concentration of 0.35wt % to about 0.46wt %. Trends in Ni and Cu concentrations for the kimberlite cores are similar to each other as well. Nickel concentrations for all cores except SDK 1, 3A and 4A 44ppm to 166ppm and exhibit no trend with depth. The addition of these cores extends that range up to 384 ppm. Copper concentrations, excluding cores SDK 1, 3A and 4A, also show no clear trend and range from 33ppm to 56ppm, including these cores brings the upper limit of the range to 95ppm. Concentrations of K range from 1.2wt % up to about 1.9wt % with no systemic variation. Calcium concentrations, including core SDK 1B, range from 0.4wt % to about 2.6wt % with only cores SDK 5 and 2A exhibiting a concentration above 1.5wt %. Calcium exhibits no apparent trends with depth.

Core SDK 1B has a range on concentrations markedly different from those in other cores for many of the analyzed elements, as seen in the graphs in Figure 4.6. Potassium increases with decreasing depth in core SDK 1B from 0.3wt % at the bottom of the core to 1.5wt % at the surface. Iron and Mg have much higher concentrations in this core than any other and concentrations decrease from the base of the core up to the surface. Iron decreases from 5.2wt %

to 3wt % at the surface and Mg decreases from 7.5wt % to 0.2wt % at the surface. Mn, Ti, Zn, Cu and Ni all occur in much higher concentrations in core 1B than in others as well. Manganese concentrations in core 1B extend the maximum up to 0.26wt %, Ti to 0.58wt % and Zn to 107ppm. In all three cases concentrations initially increase, reaching a maximum at 20-28cm depth and then decreasing with shallower depths. Nickle and Cu concentrations decrease from the bottom of the core to the surface. Nickle decreases from 753ppm to 158ppm and Cu from 237 to 47ppm.

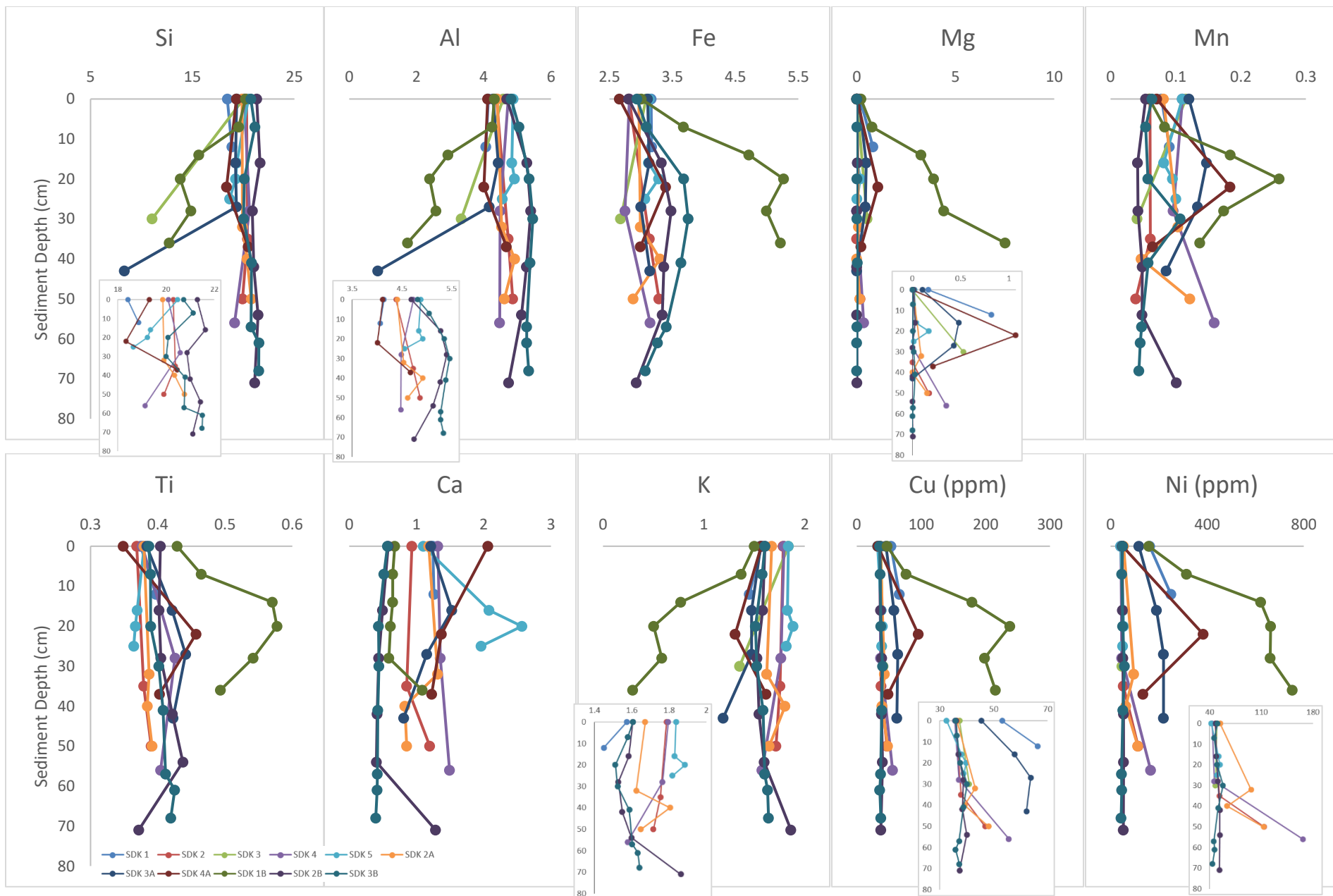


Figure 4.6-Stockdale kimberlite Cores: Elemental concentrations as determined by HHXRF. Concentrations are reported in element weight % (unless otherwise stated)

4.3 – Results from Particle Size Analysis with SANDY

Particle size analyses results as determined by the Malvern Mastersizer 3000™ are reported as percent by volume. The US Department of Agriculture (USDA) soil particle size ranges were used in defining the size of sand, silt and clay. Sand-sized particles range from 0.05mm to 2mm, silt from 0.002 to 0.05mm and clay is anything smaller than 0.002mm. However, for analysis the clay/silt boundary has been adjusted to 0.008mm. This adjustment compensates for the tendency of laser methods to underestimate the amount of clay. Particles are measured as larger than they are because of their shape. This adjustment is consistent with the findings of Konert and Vandenburghe (1997).

Konza cores 3, 4, 9 and 10 all showed similar trends in the results of the particle size analysis. In all four of these cores the deepest sample from the core contains the lowest proportion of clay. In each, the highest clay contents occur from a depth of 86 to 100 cm: core 3 at 86-96cm, core 4 at 91-102cm, core 9 at 89-99cm, core 10 at 100-110cm. Samples from these depths also had the largest proportion of fine silt, whereas the uppermost sample from 0 to 10 cm depth had the largest amount of coarse silt. Figure 4.7 below illustrates these trends.

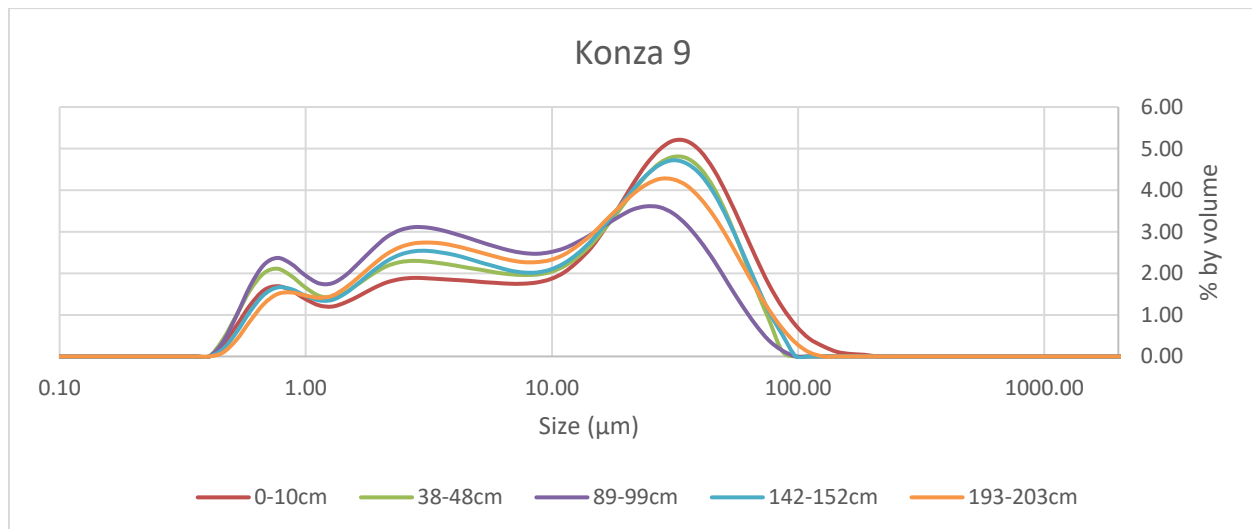
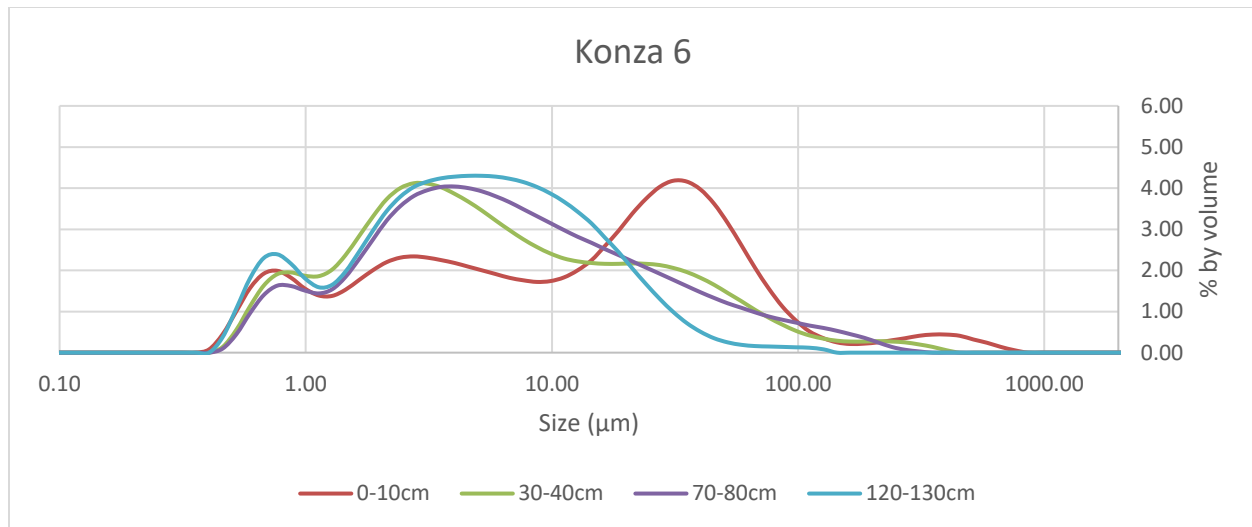
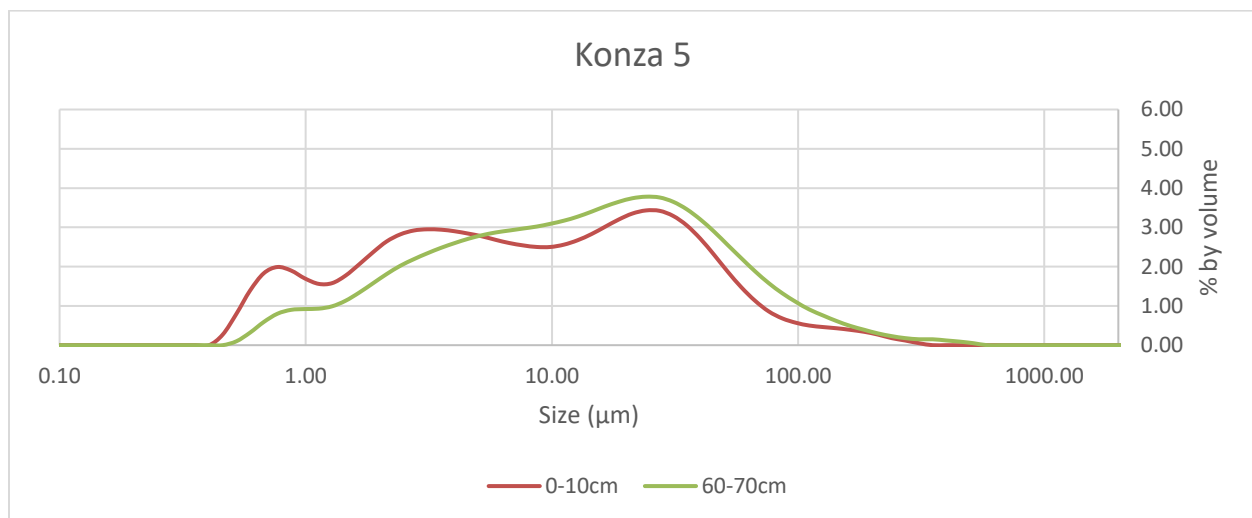


Figure 4.7-Particle size analysis graph of Konza core 9

For Konza core 6, the trend is like that described above except that the highest proportion of clay is found deeper in the core at a depth of 120-130 cm. The uppermost sample in the core has the largest amount of coarse silt and sand, as seen in Figure 4.8. This figure also shows that Konza core 5 does not follow this trend, nor does it have a trend with depth. Bedrock was reached at a depth of 60 cm, which terminated the coring.



a.



b.

Figure 4.8- Particle size analysis graph of Konza core 6 (a) and core 5 (b)

Many of the cores at the Stockdale kimberlite exhibit similar trends in particle size to those seen at Konza. More of the larger sediments are seen in the upper portions of the core. However, there is more variability in this generalized trend and there is some variation amongst the various transects sampled at Stockdale. For the upstream transect, core 1, which is at the base of the exposed portion of the kimberlite as seen in Figure 4.2, there is more sand in the uppermost part of the core from 0-11 cm. Cores 2, 3 and 5 show this as well, whereas core 4 has its highest proportion of sand at 28-40 cm. Cores 2 and 4 had most of the clay and fine silt proportion located in the sample at a depth of 50-60 cm. This can be seen clearly in Figure 4.9.

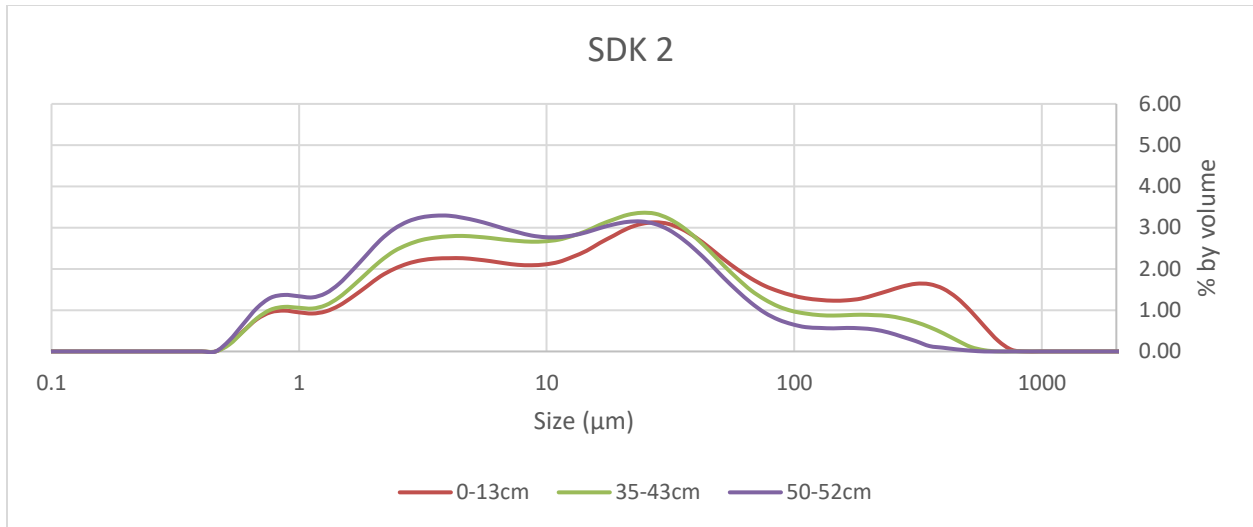


Figure 4.9-Particle size analysis of Stockdale Kimberlite Core 2, upstream transect

In the downstream transect at the Stockdale kimberlite the trend of fine silt and sand in the uppermost sample from the core is seen more strongly. This occurred in all three cores along this transect. And for each of these cores the highest proportion of clay and fine silt occurred between 40 and 56 cm of depths. This is illustrated in the particle size analysis graph for core 4A shown in the figure below.

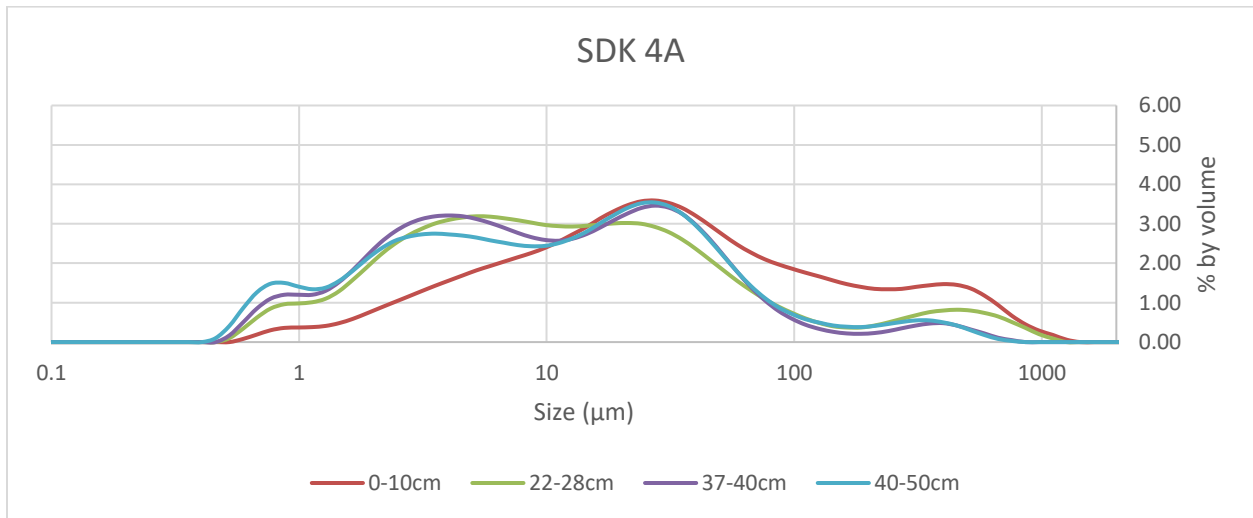


Figure 4.10- Particle size analysis of Stockdale Kimberlite Core 4A, downstream transect

Along the uphill transect (see

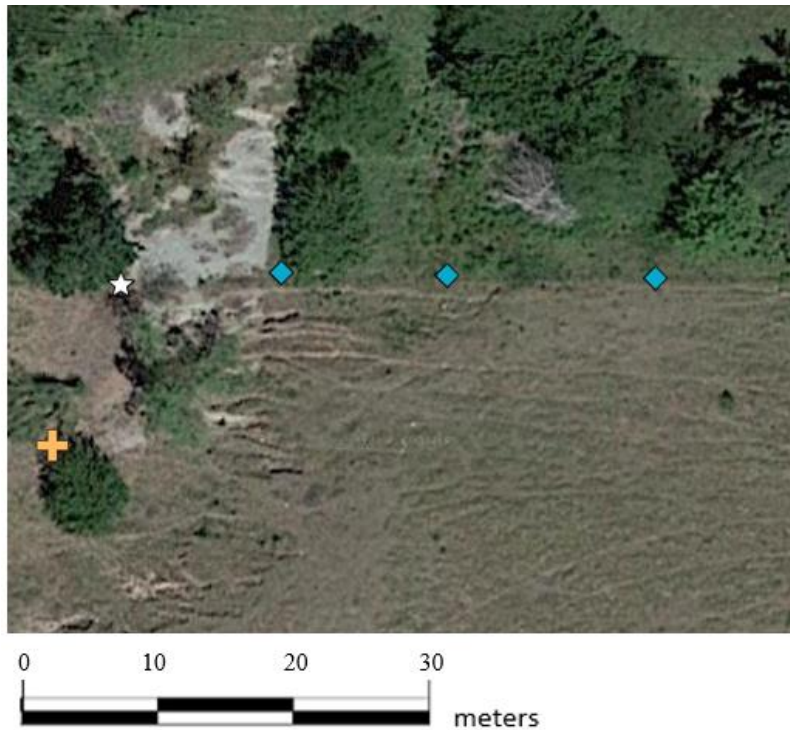
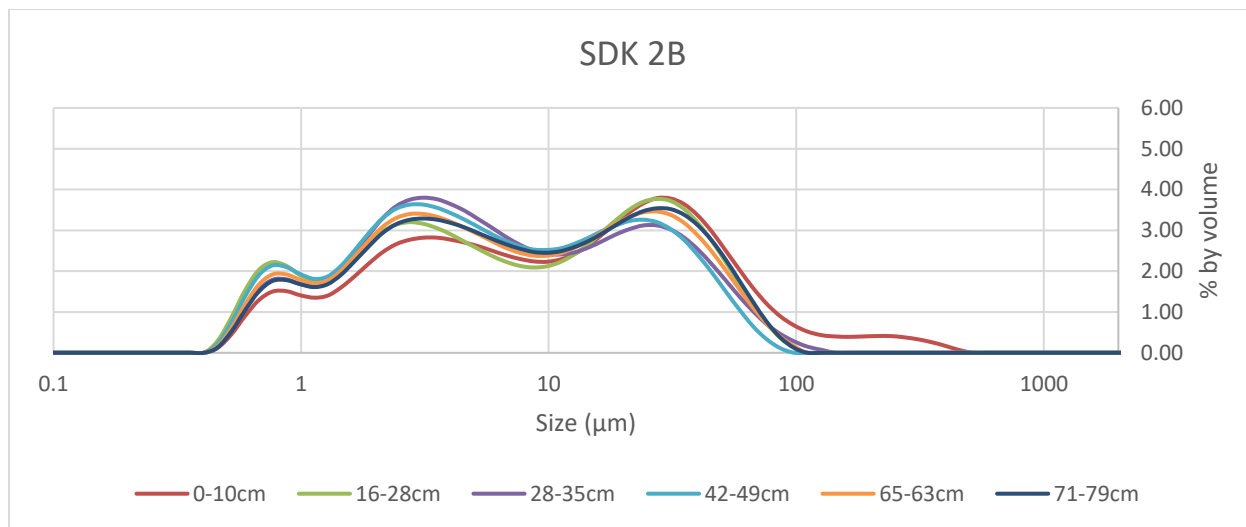
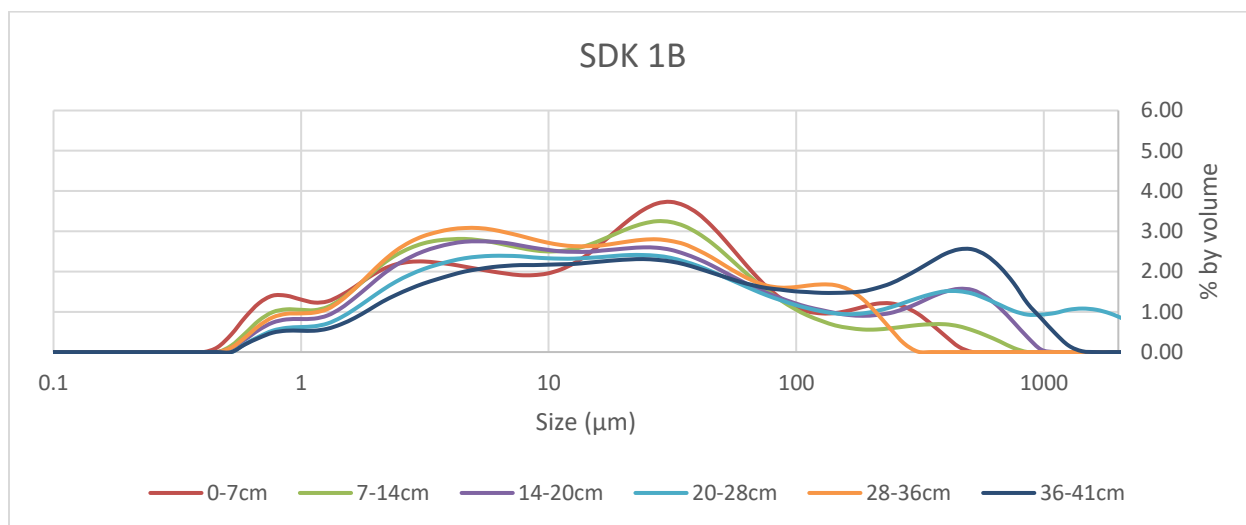


Figure 4.4), the two cores further up the hill exhibit a trend that resembles those already described, though not as strongly. The core that is closest to the kimberlite, core 1B, has a trend that is different from the others. Cores 2B and 3B have the most clay at a depth of 40 to 60 cm and in 2B it also has a higher proportion of clay slightly shallower from 16 to 28 cm. In both cores, the upper samples from 0 to 25 cm have higher proportion of coarse silt as seen in the top graph of Figure 4.11. Core 1B has a very different trend. The highest proportion of clay and fine silt here is seen at the top of the core and decreases with depth. A higher proportion of coarse silt and clay is seen deeper along the core profile. One sample, from 28 to 36 cm, does not follow this trend and has more sand than the deepest sample. This is seen in graph b of Figure 4.11.



a.



b.

Figure 4.11-Particle size analysis of Stockdale Kimberlite cores 2B and 1B, uphill transect

When looking at the overall trends in each area, Konza cores 5 and 6—which are both located at the base of the N4D watershed—have a higher proportion of clay than the other cores. Cores 3 and 4 are in upland area near the top of the watershed and cores 9 and 10 are located along the creek away from the base of the hill. At Stockdale, both the upstream and downstream transect average a lower clay content, approximately 30% by volume, than the uphill transect. The uphill transect has a lower sand proportion than the stream transects by approximately the

same amount as seen in Figure 4.12. In both areas, the dominant particle size is silt (0.008-0.05mm).

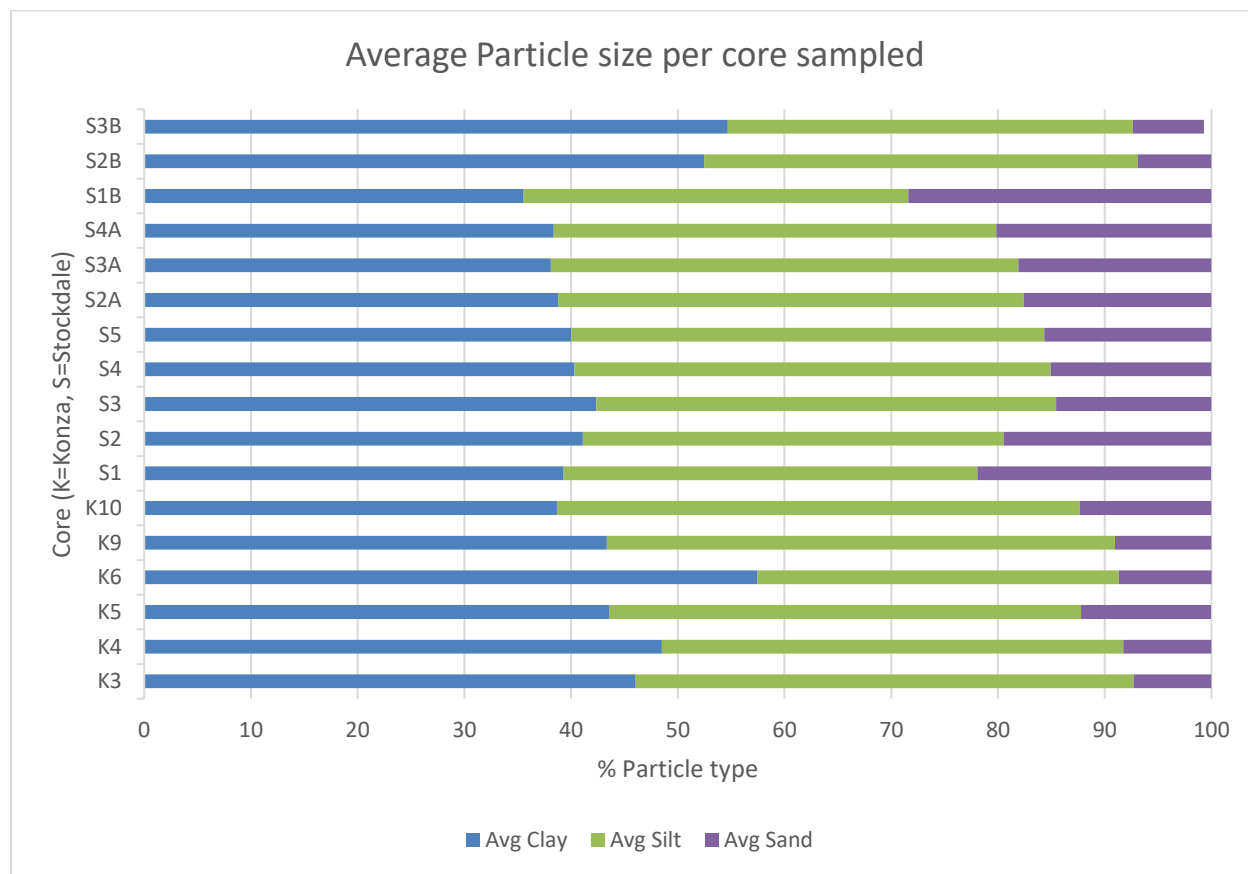


Figure 4.12-Average of particle size measurements for each sample taken from within cores in both Konza Prairie and at the Stockdale Kimberlite

4.4 – Results of X-Ray Powder Diffraction Analysis

XRD analysis was performed on 68 samples in total, 22 from Konza Prairie LTER and 46 from the area surrounding the Stockdale Kimberlite. All X-ray spectra are provided in Appendix D. Summaries of the collective mineralogy for each site are provided in Table 4.1 (Konza) and

Table 4.2 (Stockdale). Summaries of the mineralogy of individual samples within each core are provided in the Appendix at the beginning of Section D.1 (Konza) and D.2 (Stockdale). It should be noted that with bulk powder X-Ray diffraction vermiculite, smectite, interlayered vermiculite, interlayered smectite, and expandable 2:1 layer silicates are nearly impossible to distinguish from each other without applying treatments to see potential expansion of the interlayer spaces. For this reason, all clay minerals identified in this section as vermiculite by Highscore PLUS ® could actually be any of the aforementioned clay types. From this point forward clays in this category will be referred to as 2:1 layer silicates. Clay mineral identification was performed on selected samples to determine possible occurrences of any of these clay types. X-ray diffraction (XRD) analysis of sediment retrieved from Konza cores reveals similarities in mineralogy, with some variation amongst core locations, as shown in Table 4.1.

Table 4.1 – Konza Prairie core mineralogy. Numbers refer to site locations (see Figure 3.1)
Note: Oligoclase is identified as “Albite, calcian” in Highscore PLUS® during analysis and is listed as such on individual sample scans in Appendix D. A blank cell indicates mineral was not identified in the core

Mineral	Konza 3	Konza 4	Konza 5	Konza 6	Konza 9	Konza 10
Albite	X	X		X	X	X
Oligoclase	X		X		X	
Calcite		X	X	X		X
Dolomite		X			X	
Microcline		X	X		X	X
Muscovite		X	X	X	X	X
Quartz	X	X	X	X	X	X
2:1 layer silicate	X				X	X
Zeolite	X	X			X	X

The sediments from all six Konza locations contain quartz and albite, and oligoclase being identified in core 3, 5 and 9. Calcite, microcline, muscovite, zeolite and 2:1 layer silicates are also detected in at least half the cores: calcite in Konza cores 4, 5, 6 and 10; microcline in Konza cores 4, 5, 9 and 10; muscovite in all Konza cores except core 3; zeolite in Konza cores 3, 4, 9 and 10; 2:1 layer silicates in Konza cores 3, 9 and 10. Dolomite and anorthoclase occurs in Konza cores 4 and 9. A variety of other minerals were detected in only one core: alunite and

unnamed mica in Konza core 3, cristobalite, nontronite and illite in core Konza 6, Mg silicate in Konza core 10, nepheline in Konza core 9, orthoclase in Konza core 4.

There is little variability in mineral assemblage with depth in the cores (see Appendix D.1). The exception are cores 5 and 6, taken near the base of the N4D watershed in Konza; these cores are also not as deep as the other cores from Konza, because the geoprobe could not penetrate further into bedrock and encountered only within shallower depths. In both cores, the appearance of calcite in the mineral assemblage alters the proportion of quartz markedly with depth as shown in (Figure 4.13). For core 5, at 0-10cm depth, peak intensities for the primary quartz and primary calcite peaks are 100% and 0%, respectively; whereas at 60-70cm depth these proportions change to 100% and 25.83%, respectively. Core 6 exhibits a similar variation with depth. At 30-40cm depth the peak intensities for quartz and calcite are 100% and 0%, respectively; whereas at 70-80cm calcite is the 100% peak and quartz is the next most prominent peak at 35.83 %. This illustrates that samples taken from right near the bedrock still have a high proportion of those minerals contained in the soil, in this case calcite. But as the calcite disappears quartz dominates the soil mineralogy.

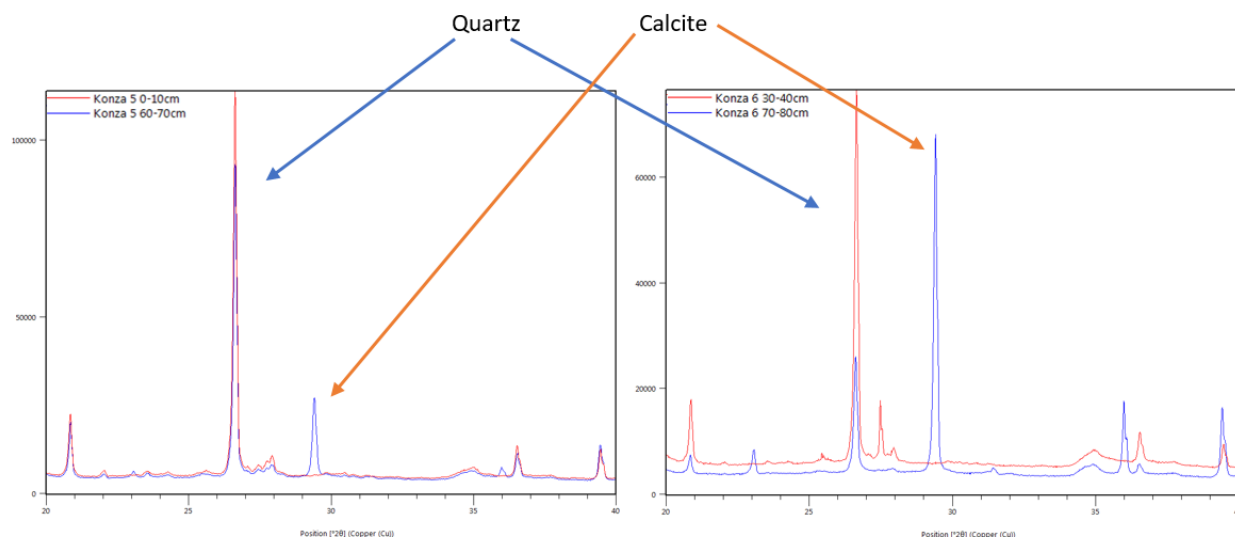


Figure 4.13-XRD peak intensities for quartz and calcite for Konza Core 5 (left) and Konza Core 6 (right)

The cores taken adjacent to the Stockdale kimberlite are mineralogically more varied than those seen in the Konza prairie cores. Like Konza, quartz and albite are found in every core, and microcline, muscovite and 2:1 layer silicates are found in 90% or more of the cores as shown in

Table 4.2. Also common is the presence of biotite, calcite, dolomite, kleberite (an alteration product of ilmenite), magnetite and lizardite. Less than 30% of cores contain the following minerals: anorthite, anorthoclase, chrysotile (primarily in the uphill transect), enstatite (upstream transect only, two cores closest to the surface exposure), magnesioferrite (uphill transect only), unnamed mica (primarily downstream), olivine, phlogopite (primarily in the uphill transect) and an unidentified zeolite (downhill transect only). Other minerals that were detected in just a single core include: clinocllore in SDK 3A; unnamed feldspar in SDK 1B; Na-feldspar, clinopyroxene and diopside in SDK 3B; perovskite in SDK 4A and siderophyllite in SDK 4. The appearance of primary minerals in the samples is most likely due to the presence of small chips of kimberlite rock in the soil cores.

Table 4.2-Stockdale Kimberlite core mineralogy. A blank cell indicates mineral was not identified in the core

Core Transect →	Upstream					Downstream			Uphill		
Mineral	SDK 1	SDK 2	SDK 3	SDK 4	SDK 5	SDK 2A	SDK 3A	SDK 4A	SDK 1B	SDK 2B	SDK 3B
Albite	X	X	X	X	X	X	X	X	X	X	X
Anorthite		X							X		
Anorthoclase					X	X					
Biotite				X	X					X	X
Calcite		X	X	X	X	X	X				
Chrysotile						X			X	X	
Dolomite	X		X		X		X				X
Enstatite	X	X									X
Kleberite		X		X	X		X				
Lizardite	X						X		X	X	
Magnesioferrite									X	X	
Magnetite	X							X		X	X
Mica, unnamed				X			X	X			
Microcline	X		X	X	X		X		X	X	X
Muscovite		X	X	X	X	X	X	X	X	X	X
Muscovite, phengitic										X	X
Olivine				X		X					
Phlogopite			X						X	X	
Quartz	X	X	X	X	X	X	X	X	X	X	X
2:1 layer silicates		X	X		X	X	X	X	X	X	X
Zeolite						X	X				

In the upstream transect (SDK1 – SDK5, Figure 4.2), samples from core SDK 1 (maximum depth 15 cm) show the greatest resemblance to the kimberlite whole rock mineralogy. The soils in this core include albite, dolomite, enstatite, lizardite, magnetite, microcline and quartz. The other cores in this transect include some mixture of these minerals; however, all lack lizardite and magnetite, which have been found only in core SDK 1 on this transect. Cores SDK 2-5 also include calcite, kleberite and muscovite, but these minerals are not observed in core

SDK 1. Dolomite, enstatite and phlogopite only appear at depths below 20 cm, otherwise there are no other trends in mineralogy with depth.

In the downstream transect (SDK2A – SDK4A, Figure 4.3), all cores contain albite, muscovite, quartz, and 2:1 layer silicates; SDK2A and SDK3A also contain calcite, mica and an unidentified zeolite. Anorthoclase and chrysotile appear in core SDK 2A only below a depth of 32 cm, dolomite and lizardite are in core SDK 3A below a depth of 27 cm, kleberite also in core SDK 3A below a depth of 16 cm, magnetite and olivine are also seen in at least one of the cores. Olivine is observed in the top 10 cm of core SDK 2A. Kleberite is found in all samples in core SDK 3A below a depth of 16 cm.

In the uphill transect (SDK1B – SDK3B, Figure 4.4), all cores contain albite, microcline, muscovite, quartz and 2:1 layer silicates. Biotite appears beneath 71 cm in core SDK 2B, phlogopite and chrysotile are both seen below a depth of 16 cm 36 cm respectively in cores SDK 1B and 2B, magnesioferrite is seen in cores SDK 1B and 2B, magnetite and phengitic muscovite are found in cores SDK 2B and 2B below a depth of 20 cm, and kleberite is in core SDK 3B below a depth of 20 cm.

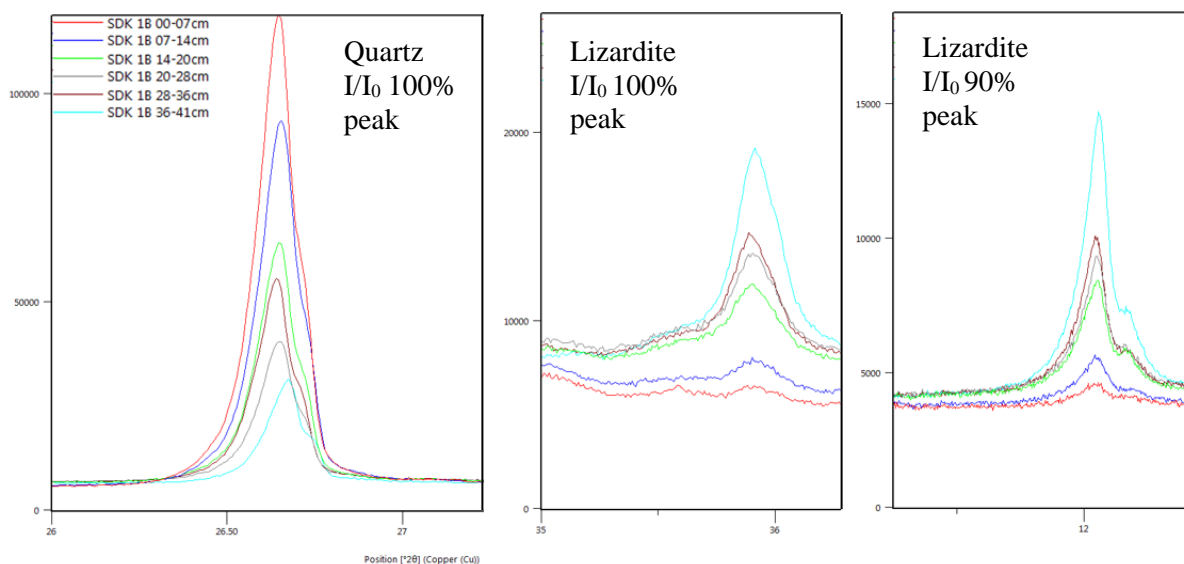


Figure 4.14 - XRD Peak intensity of quartz and lizardite for core SDK 1B

Core SDK1B exhibits an inverse relationship between the abundance of quartz and lizardite. Figure 4.14 indicates the 100% intensity peak for quartz is highest at the surface and decreases with depth, whereas the lizardite peak is most intense at the deepest part of the core

and decreases as it approaches the surface. During initial mineral identification, lizardite was not identified in the top two samples from this core (red and blue line at the bottom of the lizardite intensity peaks). When looking at the overlay of all analyses from this core, what appeared to be background noise in the top two samples may be a very weak lizardite signal (see Appendix D Section 2)

4.5 – Clay Fraction X-Ray Diffraction

Eight samples were selected for specific clay mineral identification. Three samples were taken from Konza, two from core 6 and one from core 9 (Figure 3.1). Of the two samples from core 6, one was from 0-10 cm, where it resembles much of the rest of the Konza cores, and one from a depth of 70 to 80 cm, where the sample has a high proportion of calcite. The sample from core 9 was taken from depth of 193 to 203 cm, deeper than any other sample taken from a Konza core. At this depth, while the bulk mineralogy resembles the rest of the cores in Konza, it shows some clay mineralogy that is indicative of the transition between soils with a high proportion of calcite and those with essentially no calcite at all, This could indicate the depth at which partially weathered parent rock is no longer incorporated into the soil as rock chips.

Five samples were taken from Stockdale, two from the upstream transect (SDK 1 and 2, Figure 4.2), one from the downstream transect (SDK 2A, Figure 4.3), and two from the uphill transect (SDK 1B and 2B, Figure 4.4). The three samples taken from cores in the streambed are the three cores nearest the kimberlite. This was to see how the clay mineralogy changed as the water passed through the kimberlite exposure and carried soil downstream. The two uphill samples were taken from core at different distances from the kimberlite to assess the differing mineralogy with distance and elevation from the kimberlite exposure.

X-ray diffraction of oriented clay slides measures the d-spacing of the d_{001} orientation of the mineral, showing the first order peak for each treatment and may also show second order peak most commonly for quartz and kaolinite. Table 4.3 shows the mineral content of each clay sample analyzed and a semi-quantitative analysis of mineral proportion. Mineral proportions were determined by comparing peak intensities on the Mg-25 diffraction spectra and by overlaying the spectra of all treatments for the same sample to assess peaks shift with different treatments. Quartz, kaolinite and clay mica are present in all samples from both locations. Dolomite appears in the deeper Konza 6 core (70-80cm), in the upstream Stockdale core SKD 2

and the closest uphill core to the kimberlite, SDK 1B. Potassium feldspar is seen in the surface Konza 6 core, Konza 9, SDK 1, 2 and 2B. Vermiculite is only found in the deeper Konza 6 core. Expandable 2:1 layer silicates are found in all three Konza cores and in SDK 1B and 2B, the uphill transect. Interstratified mica-smectite is found in all Stockdale cores. A trace amount of smectite is found in the deeper Konza 6 core and core 9, with a medium to high amount found in SDK 1, 2, 2A and 1B.

Table 4.3-Mineralogy of <2µm clay fraction. Proportion key: T = Trace (<5%), L = Low (5-20%), M = Medium (20-50%), H = High (>50%)

Core & Depth (cm)→	Konza 6 (0-10cm)	Konza 6 (70-80cm)	Konza 9	SDK 1	SDK 2	SDK 2A	SDK 1B	SDK 2B
Quartz	L/T	L/T	L	L	T	T	L	L
Dolomite		T			T		L	
K-feldspar	T		L		M	L		T
Kaolinite	L/M	L	M	L	M	L	M/L	M/L
Clay Mica	M	H	M	L	L	L	L	M
Interstratified Mica-Smectite				L	M	M	L	L
Smectite		T	T	H	M	H/M	M	
Vermiculite		L						
Expandable 2:1-layer silicate	L/M	L	T				L	L

4.6 – Results of bulk extraction by aqua regia and ICP-OES analysis

4.6.1- Results of bulk extraction by aqua regia

Bulk element analyses by bulk extractions via aqua regia digestion and subsequent ICP-OES analysis revealed variability in elemental concentrations with depth in all cores, both in Konza and Stockdale. All data are provided in Appendix E. It also contains a table demonstrating the analytical uncertainty of the instrument by comparing the data collected on

NIST standard 2711a, Montana II (which was digested at the same time as the core samples) to published values for this standard.

Variations in Ca concentrations in Konza core 6 are much higher than in the Stockdale kimberlite cores. Calcium concentrations for the Konza core decrease from the bottom of the core up to the surface from 175 to 5 (10^3 mg/kg) as seen in Figure 4.15, whereas at Stockdale the range is much narrower going from 3.8 to 25.2 (10^3 mg/kg) and exhibit no apparent trend. Potassium concentrations at Konza also decrease from 13.1 to 6.4 (10^2 mg/kg). The range for Stockdale cores is a little broader, from 1.7 to 7.9 (10^2 mg/kg), with no apparent trend. Sodium concentrations of all samples range from 3.9 to 1.4 (10^2 mg/kg); except for Stockdale core 3A, all cores decrease in Na concentration moving up from depth to the surface. Phosphorus concentrations for all cores range from 12.6 to 1.6 (10^2 mg/kg), exhibiting no systemic variation with depth. Konza core 6 contains very low concentration of P and it changes very little moving from depth to the surface ranging from 2.3 to 3.3 (10^2 mg/kg). Most Stockdale cores are in the middle to upper limit of this range (Figure 4.15).

Graphical representation of the variations in major metals Fe, Mg and Mn and for trace metals Ti, Cr, Ni, Cu and Zn is reported in Figure 4.16. For each of these elements, except Zn, the concentrations found in Konza core 6 stay at the extreme low end of their respective concentration ranges, whereas Stockdale core 1B is at the upper limit of each concentration range. Iron concentrations for Konza core 6 exhibit the highest variability for any of the elements listed above, ranging from 2.9 to 4.4 (10^4 mg/kg). Stockdale kimberlite cores range in concentration from 2.7 to 6.1 (10^4 mg/kg). Magnesium concentrations range from about 5.2 to 120 (10^3 mg/kg). Konza core 6 shows little variation with depth and stays at the lower end of the range with a maximum concentration of 12.5 (10^3 mg/kg). Manganese concentrations range from 3.6 to 14.2 (10^2 mg/kg). The trends observed with other metals are seen less strongly with Mn. Konza core 6 is still at the low end of the range and exhibits little variability. However, Stockdale core 1B is at the upper end of the range and does not lay far beyond the concentration seen in other cores as it did with the other elements reported above. In fact, it is Stockdale core 5 that has the highest concentration of Mn.

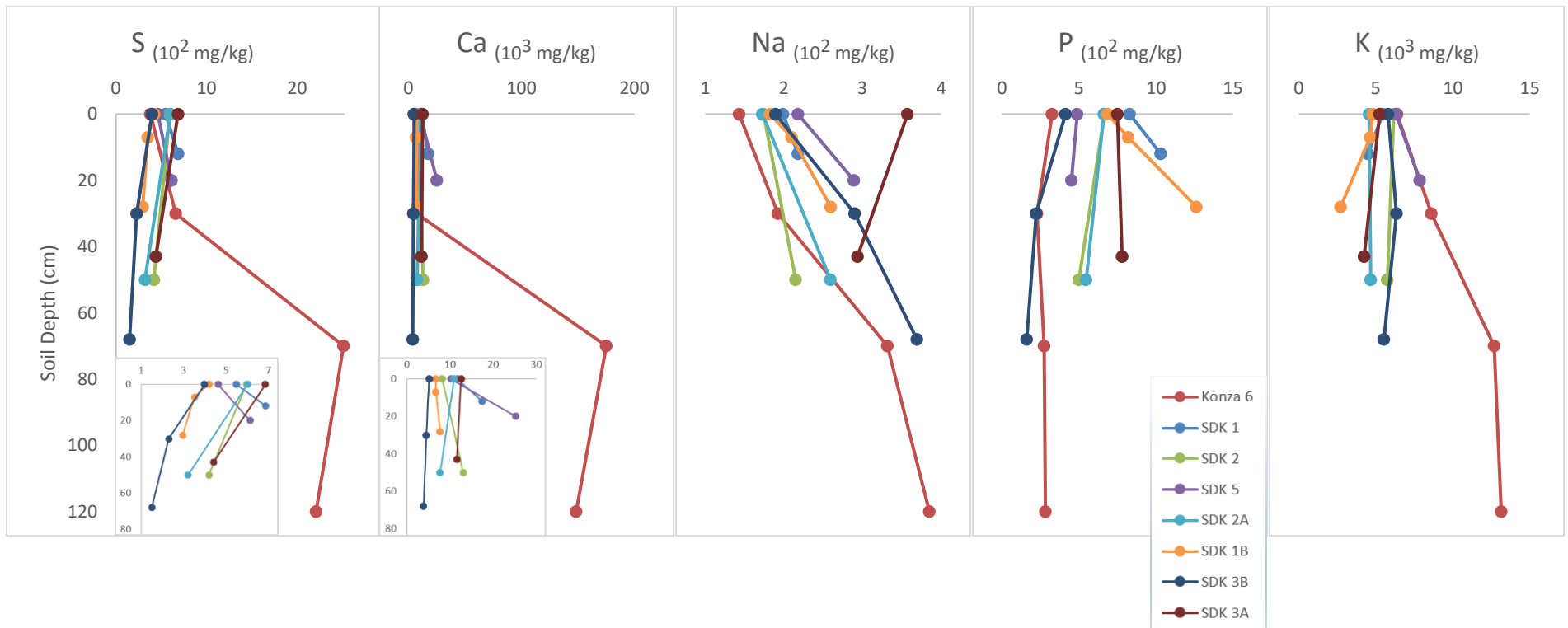


Figure 4.15-Element concentrations in mg/kg as determined ICP-OES analyses via bulk extractions by aqua regia. Inset shows data rescales without Konza core 6 to show greater detail for other cores

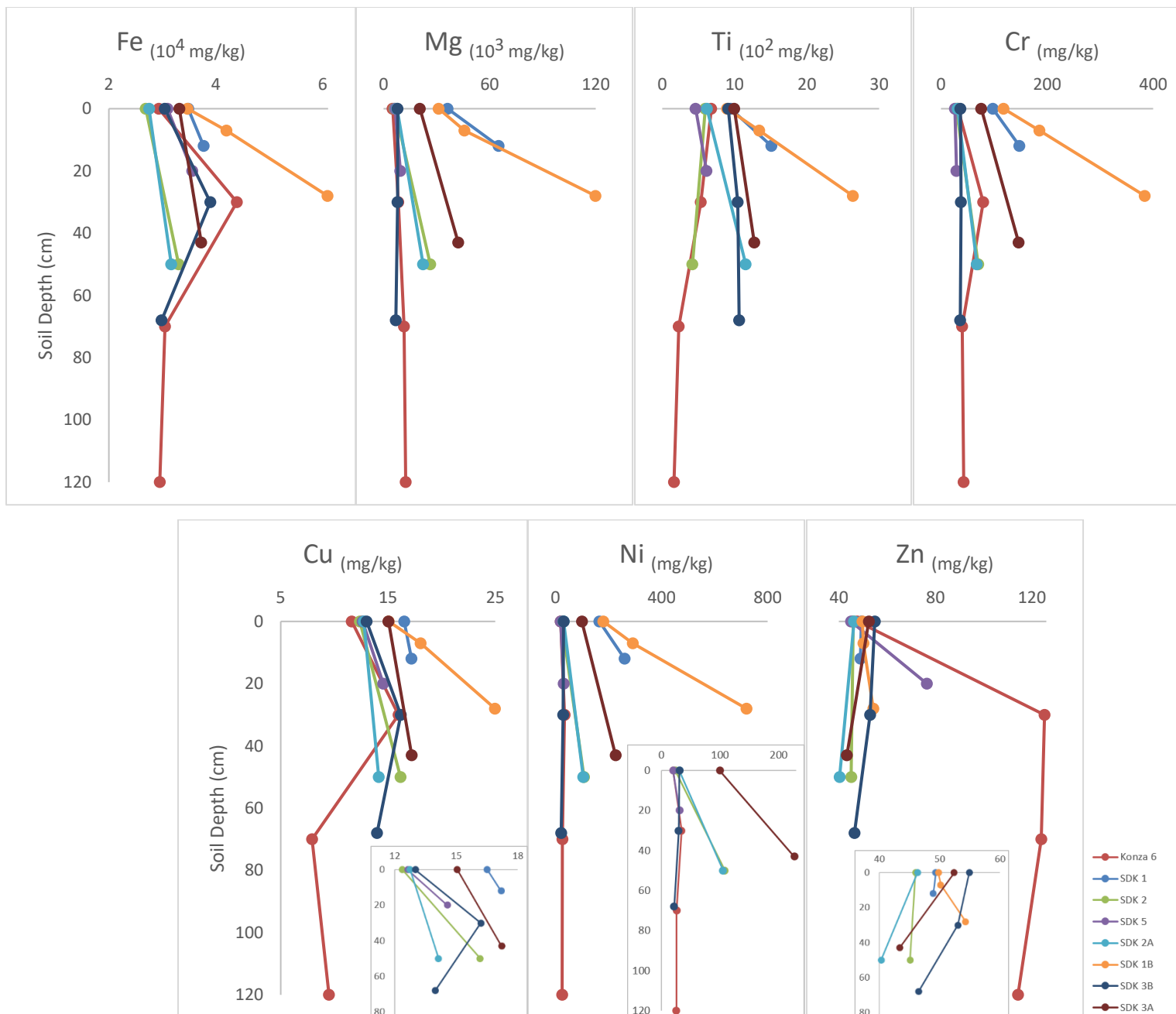


Figure 4.16- Element concentrations in mg/kg of major and trace metals as determined ICP-OES analysis via bulk extractions by aqua regi

Titanium concentrations range from 1.6 to 26.4 (10^2 mg/kg) with Konza core 6 reaching a maximum concentration of 6.8 (10^2 mg/kg) in the uppermost 10 cm of the core. Chromium concentrations range from 26.3 up to 148.1 mg/kg not including Stockdale core 1B, which goes up to 425.8 mg/kg. Similarly, Ni concentrations range from 20.1 up to 260.9 mg/kg not including Stockdale core 1B which goes up to 784 mg/kg. Copper concentrations show some variation in concentrations along the depth of Konza core 6 from 7.9 to 16 mg/kg whereas the Stockdale cores range from 12.4 mg/kg up to a high of 25 mg/kg in core 1B. Zinc concentrations for Stockdale range from 39.3 to 76.5 mg/kg. Konza core 6 Zn concentrations are much higher and push the range up to a high of 125.3 mg/kg.

4.6.2-Chemical Index of Alteration (CIA)

The chemical index of alteration is a numerical measure of the extent of weathering of a rock, calculated by comparing the ratio of Al to certain other cations in the rock or soil. A lower value indicates less weathering whereas a higher number indicates more extensive weathering with a value of 100 indicating pure kaolinite which is assumed to be the terminal mineral in weathering processes. The chemical data used in these calculations were the data generated by the ICP-OES analysis of the soils. The equation used to calculate CIA is from Nesbitt and Young (1982).

$$\text{CIA} = [\text{Al}_2\text{O}_3 / (\text{Al}_2\text{O}_3 + \text{CaO}^* + \text{Na}_2\text{O} + \text{K}_2\text{O})] \times 100$$

CaO* is the total concentration of calcium oxide less the contribution from apatite and from carbonates. The lower two samples from Konza core 6, from depths 70-80cm and 120-130cm, possess a high proportion of calcite. The inorganic carbon chemical data needed to calculate the calcium contribution from calcite to remove it from the total CaO concentration was unavailable. Because of this, the CIA for these samples is not included in these results.

Table 4.4- Elemental concentrations as determined by ICP-OES. Concentrations are reported in element oxide wt % unless.

Sample Labels	Depth		Al ₂ O ₃	CaO	Na ₂ O	K ₂ O	CIA
	in cm						
Konza 6-1T	0		7.905	0.697	0.019	0.769	84.186
Konza 6-1B	30		12.993	1.000	0.026	1.038	86.291
Konza 6-2	70		7.791	24.514	0.045	1.530	22.996
Konza 6-3	120		6.708	20.780	0.052	1.584	23.033
SDK 1 0-11	0		6.419	1.637	0.027	0.656	73.451
SDK1 12-15	12		5.754	2.444	0.029	0.542	65.616
SDK 2 0-13	0		6.717	1.147	0.023	0.743	77.823
SDK 2 50-52	50		7.551	1.826	0.029	0.694	74.761
SDK 5 0-12	0		7.379	1.428	0.029	0.760	76.888
SDK 5 20-25	20		7.826	3.532	0.039	0.948	63.394
SDK 2A 0-10	0		6.206	1.527	0.023	0.550	74.710
SDK 2A 50-60	50		6.413	1.080	0.035	0.563	79.257
SDK 3A 0-9	0		7.034	1.764	0.048	0.633	74.203
SDK 3A 43-49	43		5.738	1.620	0.040	0.511	72.557
SDK 1B 0-7	0		6.633	0.939	0.025	0.580	81.114
SDK 1B 7-14	7		6.777	0.938	0.028	0.559	81.634
SDK 1B 28-36	28		5.099	1.074	0.035	0.328	78.014
SDK 1B 36-41 *	36		3.275	1.600	0.036	0.201	64.053
SDK 3B 0-7	0		7.928	0.722	0.026	0.699	84.564
SDK 3B 30-40	30		10.889	0.629	0.039	0.764	88.377
SDK 3B 68-76	68		8.880	0.539	0.050	0.667	87.614

4.7 – ATP Analysis

ATP analysis, which measures the amount of microbial activity, was conducted on samples of soil at a depth of 6-10cm. Results are reported in relative light units (RLU) which directly correlates to the amount of ATP present.

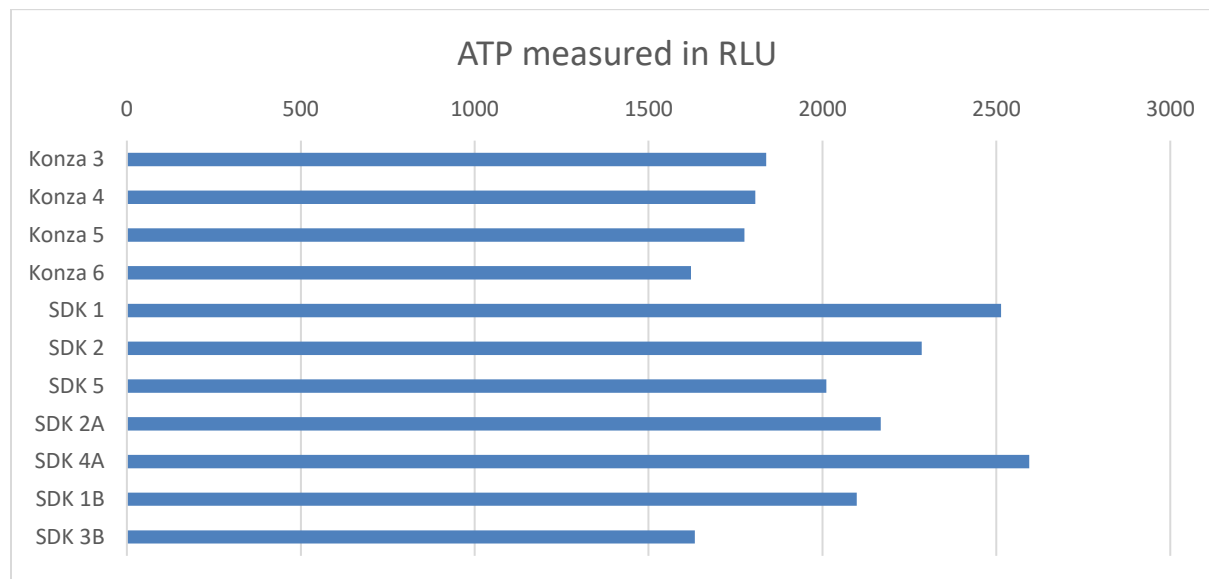


Figure 4.17 – ATP as measured by relative light units

The ATP measured in Konza varies from the upland area near the top of the N4D watershed to the down slope area at the base of the N4 D watershed. ATP measured at the base of the watershed is lower than at the top. ATP measurements at the Stockdale kimberlite vary along each of the samples in the transects. Starting at the outcrop moving upstream, ATP measurements decrease as you move away from the outcrop. Moving downstream from this same point, ATP measurements increase. Along the entire path of the stream, ATP is lowest furthest upstream and then increases downstream. Along the uphill transect, the ATP measurement is highest near the kimberlite and decreases moving uphill.

Chapter 5 - Discussion

5.1-Konza Geochemistry and Mineralogy

Konza Prairie LTER is underlain by interbedded limestones and shales that are characteristic of the Flint Hills. Though the limestone mineralogy is dominated by calcium carbonate, soils at Konza tend to be carbonate poor. They are generally ~1 m thick with thicker deposits at the base of hill slopes (Schaefer et al., 2007; Eke, 2012). For this study, four of the six cores used were thicker than the average Konza soil, with core 9 measuring 2m in depth. While these soil thicknesses are atypical for the region, they potentially give us a better picture of the processes occurring with depth in the soils in this area than we otherwise would have from sampling of thinner soils.

Konza cores 5 and 6, that are located at the base of the steep hillslope in the N4D watershed (Figure 3.1), should extend deeper than the other cores. However, they are shallower and at the bottom of each core bedrock was visible. The probable reason for this is unknown, but may be related to the proximity of King's Creek. As it travels down the relatively steep slope of the watershed, the creek periodically washes away some soil and sediment. Konza cores 3 and 4 were taken from the bench that forms the highest elevation in Konza, referred to here as upland cores. Konza cores 9 and 10 were collected from a lower elevation alongside a tributary of King's creek, referred to here as lowland cores. Although these cores were also collected near a stream, like cores 5 and 6, they extend much deeper. This area does not have the same high relief as the area where cores 5 and 6 were collected (see Figure 3.1) so there is not the same issue with the sediment being washed away and thinning the soil beds.

5.1.1 – Geochemistry

The limestone bedrock in these areas weathers to form shallow aquifers whereas the shales form aquitards (Tsypin and Macpherson, 2012). After a precipitation event, water levels in the underlying aquifers increase within just a few hours. Studies of the waters in these aquifers show increasing Mg^{++} and Ca^{++} concentrations indicating chemical weathering of these limestones is active and may be increasing since 1998 (Macpherson, 2008). As limestones in the system weather chemically, the Ca released is highly mobile and is quickly leached out of the soil, as evidenced by the chemical and mineralogical composition of the soils. Since calcite, and to a lesser extent dolomite, are the primary minerals in these limestones, when they dissolve

during chemical weathering, the remaining minerals in the soil are primarily sourced from the shale layers of the system. This part of the Flint Hills also receives a significant influx of wind-blown dust that becomes incorporated into these soils. Konza cores 5 and especially 6 exemplify this in the differing chemistry (Figure 4.5) and mineralogy (Appendix D.1) seen with depth, as compared to the other Konza cores. The influence of the limestone is detected in the samples from the deepest part of the core where the limestone was reached, thus incorporating chips into the sample. In the shallower samples (0-30cm) for these cores the mineralogy and chemistry change drastically from depth due to the weathering of the limestone and the incorporation of windblown dust. This highlights the heavy influence of windblown material on the chemistry and mineralogy of these soils.

The geochemistry of the Konza cores was analyzed using two different methodologies, HHXRF of bulk powders and ICP-OES analysis of extractions via aqua regia. HHXRF was used initially to evaluate all samples, because this can be done rapidly, the method is nondestructive, and differences amongst samples can be compared easily. Based on these data, cores 5 and 6 are distinct, compared to the other Konza cores. When evaluating the other four cores from the upland and lowland areas as the group, the concentration ranges and trends in concentration among them are consistent for the elements analyzed. Trace metal concentrations (Ti, Zn, Cu, and Ni) show minor variations with depth. Core 4 exhibits more variation with Fe and these trace metals except Ti (Figure 4.5). Concentrations of Zn, Cu, Fe and Ni all increase with increasing depth in core 4. There is no mineralogical evidence suggesting minerals such as metal oxides with increasing depth in this core. However, it is possible for these oxides to reside in the clay-size fraction, which was not analyzed for this core. It is also possible that these metals were incorporated into clays during weathering. Compared to the source bedrock, concentrations of Ca and Mg are extremely low in the four upland and lowland cores, with a slight increase in concentration at the lower part of cores 4 and 10. These low concentrations were expected, given that during chemical weathering, the major cations in limestones, Ca and to a lesser extent Mg, go into solution and are mobilized out of the system. Aluminum and Fe occur in slightly higher concentrations deeper in these cores (i.e. depths great than 40cm) than at the surface. The opposite is seen for Si, which occurs in higher concentrations at the surface of the cores. This could possibly be due to the eluviation of clay particles, which then concentrate below 40 cm depth. Another explanation would be the addition of silica-enriched wind-blown dust, or

possibly the combination of both these processes. Core 5 and 6 show much lower concentrations of Si, Al and Ti deeper in the core, but concentrations for the surface sample are consistent with all the other cores collected at Konza. The limestone bedrock chips, which were incorporated into the deeper samples for these two cores, would be depleted in these three elements as they tend to occur preferentially in clays. Zinc, Cu, Ni, and Mg concentrations in core 5 are similar to those in other Konza cores, but Ca concentrations are much higher primarily due to the limestone rock chips observed in this portion of the core during sampling. In contrast, these elements in core 6 occur in higher concentrations than in any other Konza cores at all depths other than the surface sample. Rock chips were also observed mixed in with the soil in the deeper samples taken from core 6. This accounts for the markedly higher concentrations of Ca and Mg below a depth of 40 cm. The same rock chips may account for the higher concentrations of Zn, Cu, and Ni if some of those chips were unweathered parent shale bedrock rather than limestone.

Because core 6 appeared to be different from the other cores, bulk elemental extraction via aqua regia was performed and ICP-OES analysis was conducted on the digestate. This analysis confirmed the similar trends in element concentration variation as seen with HHXRF for this core, except for Mg. In this analysis, Mg has a slightly higher concentration deeper in the core rather than the large increase exhibited in the HHXRF analysis. The reason for this is not completely known. It is possible that the HHXRF analysis hit on a high Mg mineral in the sample, however further analysis would be required to know for certain. Additionally, Na concentrations were analyzed, which is not possible with HHXRF. Sodium concentrations are higher deeper in the core and decrease toward the surface, which could indicate silicate dissolution (Yang et al., 2004) or the influx and mixing of loess.

5.1.2 - Mineralogy

Understanding soil mineralogy is critical to understanding the behavior of a soil's past, present, and future. Generally speaking, minerals make up about 45% of the volume of soils, with the remainder being comprised of ~25% air, ~25% water, and ~5% organic matter (UH Manoa, 2007). Soil mineralogy dictates much of what happens chemically in soil. Minerals regulate the chemical composition through precipitation and dissolution. Their reactive surfaces, particularly those of phyllosilicates, strongly influence the soil's physical and chemical

characteristics. They govern a soil's ability to mobilize and exchange anions and cations, to retain water by swelling, and affect reactions with organic matter.

Mineralogy as determined by bulk powder XRD of the soils at Konza reveals that carbonate minerals, which are a chief component of the bedrock at Konza, are a small component of the overall mineral assemblage. This reinforces the notion that shale and, to an unknown extent, loess deposits are the source of most parent material which then undergo alteration due to weathering in soil profiles. Weathering-resistant silicate minerals dominate the mineralogy in the Konza cores. However, in some cores the influence of the limestone can still be detected. Core 3 and 4, from the upland area (Figure 3.1), have the least varied mineralogy. Every sample in cores 3 and 4 is dominated by quartz and albite. The albite, for which the dominant cation outside the silicate tetrahedral structure is Na, is identified by XRD as calcian albite. More correctly, this is the mineral oligoclase and is found in the deepest part of core 3 at a depth of 143 cm, meaning that this site in the crystal structure, typically occupied by Na, is instead occupied by Ca more than 10% of the time. Vermiculite was also identified in this core. However, as stated in Results Section 4.3, clay minerals identified as vermiculite by bulk powder diffraction may actually be one of several different varieties of interlayered vermiculite, interlayered smectite, or an unnamed expanding 2:1 layer silicate. In addition to the quartz and albite found in core 3, core 4 also has microcline, muscovite, zeolite and at a depth of 150cm calcite was identified. These minerals are consistent with the geochemistry of these cores in that these are primarily silicate and aluminosilicate minerals with cations of Na, K and to a lesser extent Ca, Mg and Fe. This also accounts for the low concentrations of trace metals found in these cores. The minerals present here are low in concentrations of metals for which the trace metals could easily substitute. However, some trace metals will always be found in soil minerals, as some readily substitute for more common elements such as Rb substituting for K or Sr substituting for Ca.

Samples taken from the surface to a depth of 40 cm in cores 5 and 6, located at the base of the slope in the N4D watershed (Figure 3.1), have similar mineralogy to upland cores 3 and 4 described above. The only difference is the addition of muscovite, which is seen in both core 5 and 6. However, the mineralogy in the deeper part of both cores is quite different. The deep part of core 5 shows no evidence of microcline or muscovite but rather contains calcite instead. The two deeper samples in core 6, taken from depths below 70 cm, contain no identifiable albite, and

contain illite rather than muscovite. Both samples also have a high proportion of calcite, more than core 5, which is most likely due to the inclusion of partially weathered parent material from the bedrock below and thus the deeper samples from core 5 and 6 are mineralogically different from the shallow samples from both cores. The shallow samples from cores 5 and 6 (0-70 cm) had element concentrations consistent with all other cores.

5.1.3 – Clay Mineralogy, Weathering, and Particle Size Analysis

Clay mineral identification performed on two samples from core 6 at depths of 0-10cm and 70-80cm, also show differing mineralogy with depth. Kaolinite, clay mica and an expandable 2:1 layer silicate were identified in both samples, but the deeper sample had more clay mica and less of both the expandable 2:1 layer silicate and kaolinite. The deeper sample also contains a low proportion of vermiculite and trace amounts of smectite. The higher proportion of expandable clays in the shallower soils samples is suggestive of more weathering of the minerals contained here. Both samples had low to trace amounts of non-clay minerals in the clay-size fraction as well. Both contained low to trace amounts of quartz. Echoing the mineralogy of the bulk samples, the deep clay sample contained a trace amount (< 5%) of dolomite and the surface sample contained trace amounts of K-feldspar, which could also be plagioclase feldspar or be mixed with plagioclase feldspar. Feldspars in the clay-size fraction are difficult to distinguish from each other. Peaks for orthoclase, microcline and albite/anorthite are very close together, measuring 3.31 Å, 3.25 Å, and 3.19 Å, respectively. Compositions of these minerals are variable, which often causes these peaks to shift (Moore and Reynolds, 1989). To further complicate identification, the peak at 3.34 Å, which is the second order peak for quartz and the third order peak for clay mica, obscures the feldspar peak(s) and makes them indistinguishable from each other. The Jackson weathering stages of clay-sized minerals (Essington, 2004) uses clay mineral assemblages and the relative amounts of each in a soil to estimate the extent of the weathering occurring in a soil. During the early stages of weathering, young soils have yet to weather out dolomite; therefore, its presence in a soil indicates it has not been weathered much. Feldspars and quartz are also present in young soils before much chemical weathering occurs. If a soil contains muscovite, vermiculite, or smectite, it is in the intermediate stages of weathering. Highly weathered soils will contain kaolinite. These stages of clay mineral weathering can, at best, give a general sense of the weathering conditions experienced by the soil. At Konza,

minerals from both ends of the spectrum are found in the soils, so their relative abundances help determine the extent of weathering experienced. In Figure 5.1, the bar representing the mineralogy extends up to or past the mineral of interest, based on the abundance of that mineral. The appearance of extensively altered weathering products in the same profile with early and intermediate stage weathering products could indicate some type of erosion or a depositional mixing of materials weathered in differing areas (Jackson and Sherman, 1953). According to these stages, the surface sample from Konza core 6 seems to have experienced slightly more advanced weathering than that of the deeper sample. Core 6, 0 to 10cm also shows potential evidence of the influx of material from other areas.

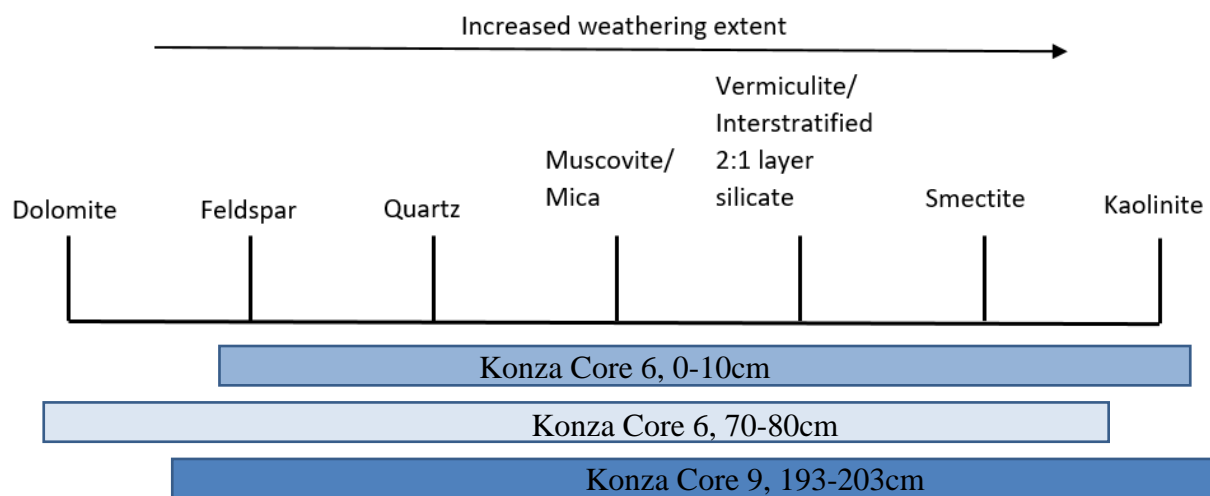


Figure 5.1-Adapted from the Jackson Weathering Stages of Clay-Sized Minerals. Identifies weathering range of Konza clay minerals (Essington, 2004).

Konza lowland cores 9 and 10 are located at a lower elevation than the others along the stream running along the base of several whole slopes, Figure 3.1. Like most of the other cores in Konza, quartz and albite are seen through the entire depth of both cores. However, there are key differences in their mineralogy. In core 9, the albite is calcian. Muscovite is present through the entire depth of core 10 and core 9 until a depth of 193 cm; at this depth, vermiculite is detected. Core 9 also contains anorthoclase throughout, and dolomite above a depth of 48 cm. In core 10, microcline is present from 0 to 60 cm, vermiculite is present below 100 cm, and calcite is identified throughout the entire depths of the core. It appears that the soils minerals

contained in core 9 have more calcium than core 10, and it also still has detectable dolomite which may indicate that the soils in core 9 are not as weathered as core 10.

Clay mineral identification was conducted on the deepest sample in core 9 (193 to 203 cm) from the upland area. Kaolinite and clay mica comprise most of the clay in the sample. There was also a low amount of quartz and K-feldspar, along with trace amounts of smectite and an expandable 2:1 layer silicate. The clay mineral content of this sample indicates that the weathering extent is like that of Konza core 6, 0-10cm. The complete mineral assemblage for core 9 is consistent with the elemental analysis of this core. Like cores 3 and 4, most minerals here are silicate and aluminosilicate minerals with cations of Na, K and small amounts of Ca, Mg and Fe. In core 10, the concentrations of most elements follow the same trend as cores 3, 4, and 9, with the exceptions being Si, Al, Ca and Mg. Silicon concentrations stay consistent throughout the depth of this core as do Al concentrations, both of which are lower than in core 3, 4, and 9. Calcium and Mg concentrations for core 10 are higher than in core 3, 4, and 9 and increase below a depth of 100 cm. The differences in the concentrations of these four elements for this core can somewhat be explained by the presence of calcite through the entire depth. The addition of loess may also partially explain the changes in these concentration, however

Particle size analysis shows that, except for core 10, all Konza cores possess a greater than 14% clay proportion by volume with core 6 approaching 20%. The samples with the largest clay proportion in each core tend to be located at depths of 86 to 100 cm. Within this clay proportion, the dominant clay minerals appear to be clay mica and kaolinite with lesser amounts of vermiculite and expandable 2:1 layer silicates. Clay micas and kaolinite do not readily exchange cations, nor do they swell (Essington, 2004), and their prevalence in these cores is a contributing factor as to why the soils have low cation exchange capacity (CEC) (Macpherson, 2008) and are thus undesirable for agriculture.

5.2-Stockdale Kimberlite Geochemistry and Mineralogy

The Stockdale kimberlite diatreme is an ultramafic igneous intrusion that erupted from the deep mantle at 85 to 110 Ma (Blackburn et al 2008). Because of the origin of the material and the chemical composition of the magma, the minerals contained within the diatreme are very different from the surrounding country rock. The most prevalent mineral found in the kimberlite is serpentine (~39%), followed by carbonates (both primary and secondary calcite and dolomite,

~24%). The rest of the kimberlite is composed of many other iron- and magnesium-rich minerals such as olivine (serpentinized), pyroxene (serpentinized), perovskite, magnetite, ilmenite, and phlogopite (Rosa and Brookins, 1966). Thus, the weathering of this outcrop will produce different weathering products than those seen in the surrounding country rock. Because serpentine (and serpentinized olivine and pyroxene) is the dominant mineral in the kimberlite, the dissolution of serpentine will drive the production of weathering products (Essington, 2004). As serpentine weathers, Mg and Si are released into the soil environment. These dissolution products allow for the neoformation of smectite. Since it forms from serpentine parent material, the resulting smectite will be a Mg-rich, low-charge, dioctahedral smectite (Lee et al., 2003). Cores were taken along three different transects in relation to the location of the kimberlite to investigate any local influences on the products that form because of the chemical weathering of the kimberlite and to examine the mobility of the weathering products.

5.2.1-Stream Transects

The first and second transects cored were along a stream bed, which ran past the western edge of the exposed surface of the kimberlite. Farthest upstream toward the stock pond is core SDK 5. Core numbers decrease traveling downstream toward the kimberlite exposure such that the lowest number (SDK 1) is closest to the exposed edge of the kimberlite (~2m from the outcrop surface) at which point core numbers increase and are designated with the letter A as they get further from the kimberlite (see Figure 4.2).

Chemical analysis reveals that K and Si concentrations are slightly lower than those seen in Konza. However, the reverse of this is exhibited by some major and trace metal concentrations. Iron, Ca, Al, and Cu concentrations are all slightly higher along the stream bed transects compared to Konza soils. At the furthest core downstream, SDK 4A, Mg and Ti concentrations are higher than anywhere else along a transect. This is most probably due to sediments or soils containing minerals enriched in these elements being washed downstream. Nickle concentrations along the stream are roughly double those seen in Konza. Magnesium concentrations are roughly 2 to 3 times as much as seen in Konza. Core SDK 1 is 2 m from the kimberlite exposure and is the most influenced chemically by it as compare to the other cores in this transect. The concentrations of Mg, Ca, Ni and Cu are higher in this core than in the rest of

the transect due to the impact of the Kimberlite. The influence of the Kimberlite's chemistry is seen in all cores along this transect.

Bulk powder X-ray diffraction analysis of the cores on the stream transects reveal highly varied mineralogy. All samples of all cores contain albite and quartz, just like most of Konza. Calcite was identified in both the shallow and deeper portions of these cores, but was seen more frequently in deeper samples. From XRD it is impossible to tell the origin of the calcite. It is possible that the calcite is primarily from the kimberlite, or forms as a secondary mineral from the dissolution of nearby limestones during weathering, or is due to the mixing in of rock chips eroded into the stream channel, or some combination thereof. Mg-rich and Fe-rich minerals such as magnetite, phlogopite, kleberite, olivine, lizardite, and chrysotile occur randomly with regard to depth in these cores. Chrysotile is found in the shallow part of core SDK 2A, whereas kleberite is found deeper in portions core SDK 3A and magnetite occurs in deeper portions of core SDK 4A. The lack of trend in mineralogy is most likely due to stream action. As the stream travels the channel, it is moving material and eroding minerals from the streambed further upstream and picking up pieces of minerals that have dropped directly off of the kimberlite. This would explain how primary minerals like olivine are being identified in in core 2A, 20 m from the kimberlite surface. Coring did not extend far enough downstream to determine the extent to which this mineral movement might be seen. Specific trends in mineralogy neither along the transects, nor with depth were detected.

5.2.2-Uphill Transect

The last transect cored was uphill away from the stream (Figure 4.4). This transect starts on the upslope eastern edge of the Kimberlite exposure with core SDK 1B located 2m from the edge of the surface exposure and continues uphill; thus, elevation increases as core number increases. The surface sample of core SDK 3B is 3m higher in elevation over just a 40m lateral distance from SDK 1B which is near the edge of the Kimberlite Exposure (Figure 4.4). This transect demonstrates how the weathering process progresses without the influence of a stream. Additionally, it shows the impact (if any) of elevation on these processes.

Elemental analysis as determined by HHXRF in this transect reveals a few differences in trend between this transect and the stream transects. For all cores in this transect Mg, Fe, Ti, Ni, and Cu all have their lowest elemental concentrations in the surface sample of each core from 0

to 10 cm and increase concentration with increasing depth. The lowest Mg concentrations in all of Stockdale are found in this transect (except for SDK 1B), and this is the same for Ca, and K. Cores SDK 2B and 3B make up the bottom of the concentration range for Stockdale. These concentrations are consistent with those seen in Konza. This is most likely due to a greater influence of country rock in these cores. As the surrounding bedrock weathers both physically and chemically, the products mix with the kimberlite's weathering products, thus diluting the high concentrations of these elements seen closer to the kimberlite outcrop. Hence, the Kimberlite signal disappears quickly with increasing distance in this direction. Core SDK 1B exhibits similar trends in elemental concentrations as the other cores, both in this and the stream transects, but is also the extreme example of trends seen in major and trace metal concentration. Magnesium concentrations in core SDK 1B are 10 to 20 times that seen in other cores and other transects. Iron concentrations for this core are almost twice what is seen in the rest of this transect; Ni is up to 20 times more and Cu is 6 times more reflecting proximity to the kimberlite as a source for these elements. While also seen in other cores, the chemistry of core SDK 1B is the most complete example of the progression of the dilution of the Kimberlite signal by the surrounding country rock and by windblown dust.

Mineral identification by XRD analyses reveal a trend with the depth wise location of Mg- and Fe-bearing minerals. This trend can most strongly be exemplified in core SDK 1B but is also present in the other two cores in this transect. As with the stream transects and most of Konza, albite and quartz are present in every sample of every core. Microcline was found in the shallow samples only for each core. In core SDK 1B, moving down from the surface deeper in the core, the dominant cations of the minerals change. Primarily K and Na are present in minerals near the surface due to the presence of minerals like albite and microcline. As depth increases, and distance to the kimberlite decreases, dominant mineral cations shift to reflect a larger proportion of Fe and Mg bearing minerals. These minerals contain more trace metals which can more readily be substituted these elements in such minerals. At 7 cm depth, one such mineral makes an appearance, lizardite. Moving deeper into the core, lizardite continues to be seen all the way to the bottom of the core and at a depth of 28 cm is joined by phlogopite, magnesioferrite and chrysotile. This same increase in the appearance of Mg- and Fe-rich minerals with increasing depth also occurs in the other two cores for this transect. In core SDK 2B, the surface sample has no such minerals, but rather contains microcline, muscovite, and

vermiculite. At a depth of 16 cm, phlogopite and lizardite were identified, and in deeper samples chrysotile, biotite and magnetite are present. SDK 1B can be treated as an analog for what is occurring farther from the kimberlite. It is essentially a compressed version of the full weathering profile; it shows the full transition from kimberlite-dominated, high-Mg, high-Fe soil mineralogy at the base of the core up to the surface where these mineral phases are diluted with the incorporation of country rock and wind-blown material.

5.2.3-Clay mineralogy and weathering

Clay mineral identification was performed on 5 cores from Stockdale. There is some overlapping mineralogy with the clay minerals seen in Konza, though there are differing proportions. Stockdale clays contain a lower proportion of clay mica and only two of the five cores contained an expandable 2:1 layer silicate. All Stockdale cores contain interstratified mica-smectite, which was not present in the Konza cores, and Stockdale cores contain a much higher proportion of smectite than Konza. Four of the five Stockdale cores contain medium (20-50%) to high (> 50%) amounts of smectite, whereas two Konza cores contained a trace (<5%) amount.

Using the Jackson Weathering Stages of Clay Sized Minerals to compare the extent to which the soil has been weathered, is a first step in getting a general sense of the extent of weathering. Dolomite is one of the first clay-size minerals to weather and if detected indicates that the soil is in the early stages of chemical weathering. Muscovite, vermiculite, interstratified 2:1 layer silicates, and smectites are present during intermediate stages of chemical weathering. The presence of kaolinite indicates the soil is heavily weathered. In Figure 5.2 below, the bar length in the figure for each core is adjusted to not just indicate the minerals present but also the amount observed. This allows for the comparison of the extent of weathering for these two cores based on clay mineralogy. Based on the mineralogy, SDK 2 appears to be slightly more weathered than SDK 1 due to a higher proportion of kaolinite. However, the presence of dolomite and feldspar also indicate some minerals are still in the early stages of weathering. The wide breadth of weathering extents for the minerals in this core makes it difficult to say conclusively the extent of weathering using this metric. An additional method of assessing weathering extent will be necessary.

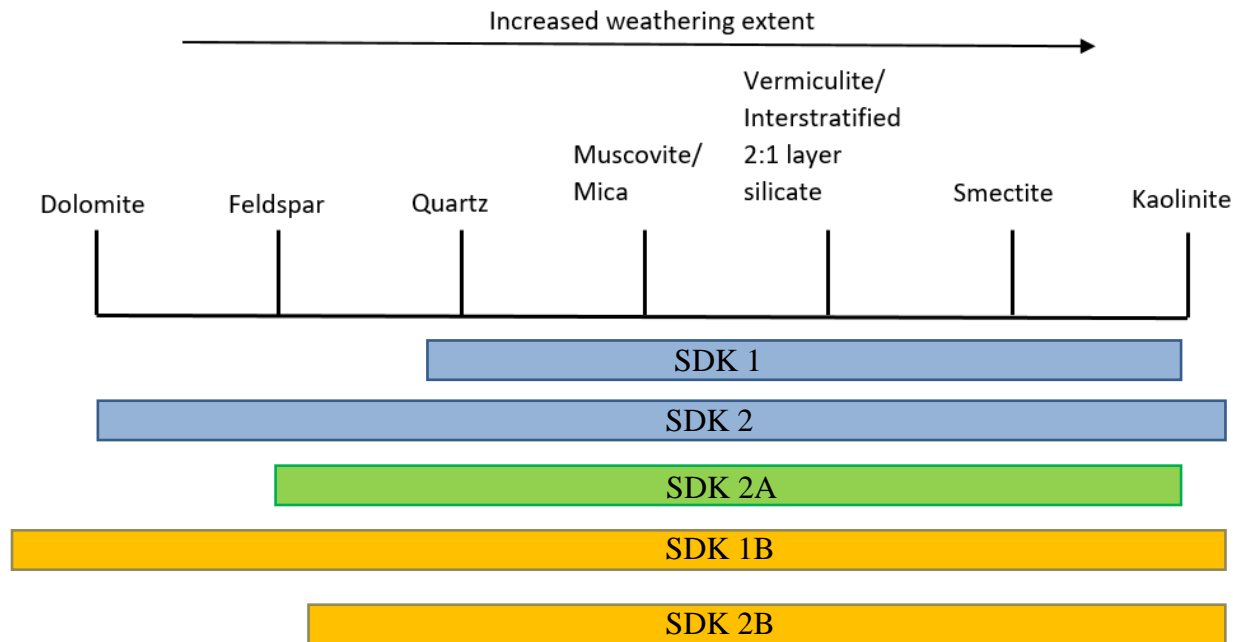


Figure 5.2-Identifies weathering range of clay minerals in cores SDK 1 and SDK 2 in the upstream transect, core SDK 2A in the downstream transect and cores SDK 1B and SDK 2B in the uphill transect at the Stockdale kimberlite. Adapted from The Jackson Weathering Stages of Clay Sized Minerals (Essington, 2004).

Particle size analysis measured the proportion of clay sized minerals in cores along this transect to consistently fall between 38% and 43% by volume. Since smectite is the dominant clay mineral in these cores, it will play a role in how the soils retain water and plays a role in soil fertility, increasing both. During the transformation from mica to smectite, K is released into the soil and can be taken up by plants. Smectite also has a high cation exchange capacity (CEC), which aids in soil fertility. Because of this, smectites can hold and make available to plants fertilizers, macronutrients like Ca and Mg, and micronutrients such as Zn. Because of the swelling property of smectite, if the amount found in the soil is too high, soils drain poorly and could negatively impact plant growth (Brochart, 1989). All SDK cores contained a medium to high proportion of smectite in the clay size fraction. The presence of smectite in soils near kimberlites will be characteristic of these soils. However, this “signal” becomes diluted quickly with distance from the kimberlite along the uphill transect by the chemical influences of country rock and of loess. Core SDK 2B mineralogy is such that it may not retain water as well as the

other Stockdale cores, because of the differing clay mineralogy—specifically lack of detectable smectite.

5.3-Chemical Index of Alteration (CIA) and Weathering in the Flint Hills

5.3.1 - CIA

The chemical index of alteration (CIA) is a quantification of the extent to which a rock or soil bed has been weathered. As Ca, Na and K are weathered from minerals during the weathering process, the proportion of Al remaining in the soil will increase. Ideally, the closer the number is to 100, the more weathered the soil is. Realistically, in assessing the weathering extent using CIA, the value of the weathered rock or soil should be compared to the value of the ratio of the same elements for the fresh or parent rock. The calculation for this index is described in Section 4.6.2. Reference indices for the calculated CIA or ratio value of some common rocks and minerals are provided in Table 5.1 below.

Table 5.1-Chemical Indices of Alteration (CIAs) of common rocks and minerals (Nesbitt and Young, 1982)

Rock/Mineral	CIA/Ratio of same elements
Diopside	0
Fresh basalt	30-40
Unaltered albite, anorthite and K-feldspar	50
Granites	45-55
Shale (worldwide avg.)	70-75
Muscovite (idealized)	75
Illite and montmorillonite	75-85
Kaolinite and chlorite	Near 100

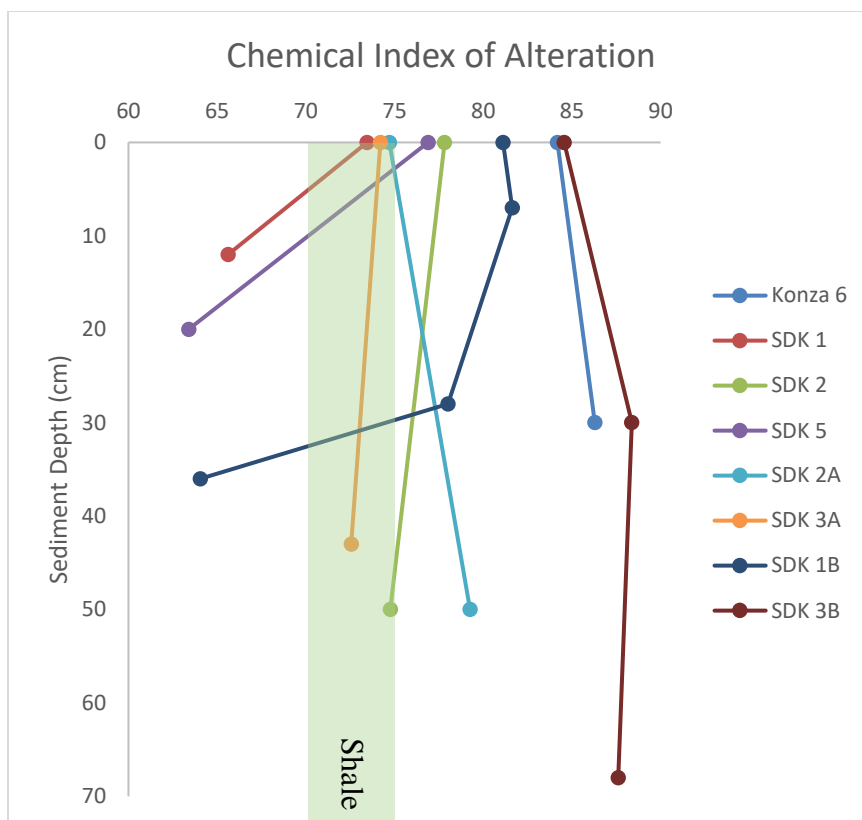


Figure 5.3-CIA calculated for Konza core 6 and select cores surrounding the Stockdale kimberlite. **CIA for Stockdale kimberlite bedrock surface exposure is 28

Two samples from Konza core 6, one at the surface and the other at 30 cm depth, have calculated CIA values of 84 and 86, respectively. Given that the parent material for these soils is primarily shale (\pm loess), the calculated CIA suggests that they represent a more weathered product than the original source material. It is possible that the CIA values for surface and shallower soils are skewed slightly higher if loess deposited in these areas has a higher Al content. However, without chemical data for the loess it is impossible to know if, or to what extent, this is the case. The CIA values for cores SDK 1, 2, 5, 2A, 3A, 1B and 3B are displayed with depth in Figure 5.3. The CIA calculated for the Stockdale kimberlite is 28, based on published chemical data (Cullers et al., 2006) for the exposed kimberlite. Mineralogical and geochemical data indicate that the exposed kimberlite has been modified by weathering since the time of eruption roughly 85 to 110 Ma (Blackburn, 2008). The extent of weathering is unknown due to the inability to drill a core in the outcrop and obtain an unweathered sample for

comparison. However, it is reasonable to assume that the CIA for the unweathered Kimberlite is lower than 28.

The higher CIA values for the deeper samples from core SDK 1, 5 and 1B all indicate that these soils have higher Al relative to Ca (in silicate minerals, not in carbonates), Na, and K suggesting that they represent a higher degree of weathering than the kimberlite parent rock. However, the CIA value of the surface soil sample for each of these cores is higher than that of soils deeper in the section and may indicate a higher proportion of clay minerals due to more extensive weathering. Except for core SDK 3B, the soils around the kimberlite, while they have been weathered, have not been weathered as extensively as those seen at Konza core 6. Since measured CaO located in silicates cannot be separated from that which is in carbonates, in this study, a CIA cannot be calculated for the other soils collected at Konza. Hence, it is uncertain if the CIA values for core 6 are truly representative of all collected Konza soils.

5.3.2 – Element Ratios and Weathering

Certain elemental relationships can also indicate the type of weathering, not just that it has occurred, as with CIA. Calculating the ratio of K to Ca in soil can help determine the extent of carbonate dissolution during weathering, as Ca is often leached out of the soils during weathering, whereas the K may be retained in some clays. A high K/Ca ratio, therefore, indicates strong carbonate dissolution. Calculating the ratio of K to Na will give similar information for silicate dissolution, since these elements are often leached from soils during silicate weathering, specifically mica and feldspar. A high K/Na ratio indicates strong silicate dissolution (Yang et al., 2004). Figure 5.4 shows that Konza core 6 soils have higher K/Na ratios than most soils from Stockdale, suggesting that they experienced stronger carbonate and silicate dissolution. Konza core 6 soils exhibiting stronger silicate dissolution than Stockdale could possibly be due to more extensive albite weathering. This is possible if the water chemistry is different in the two areas; however, this was not tested. Since relative proportions of albite were not determined for the two areas, it is also possible that loess incorporated into the soil here is being weathered and could thus impact this result.

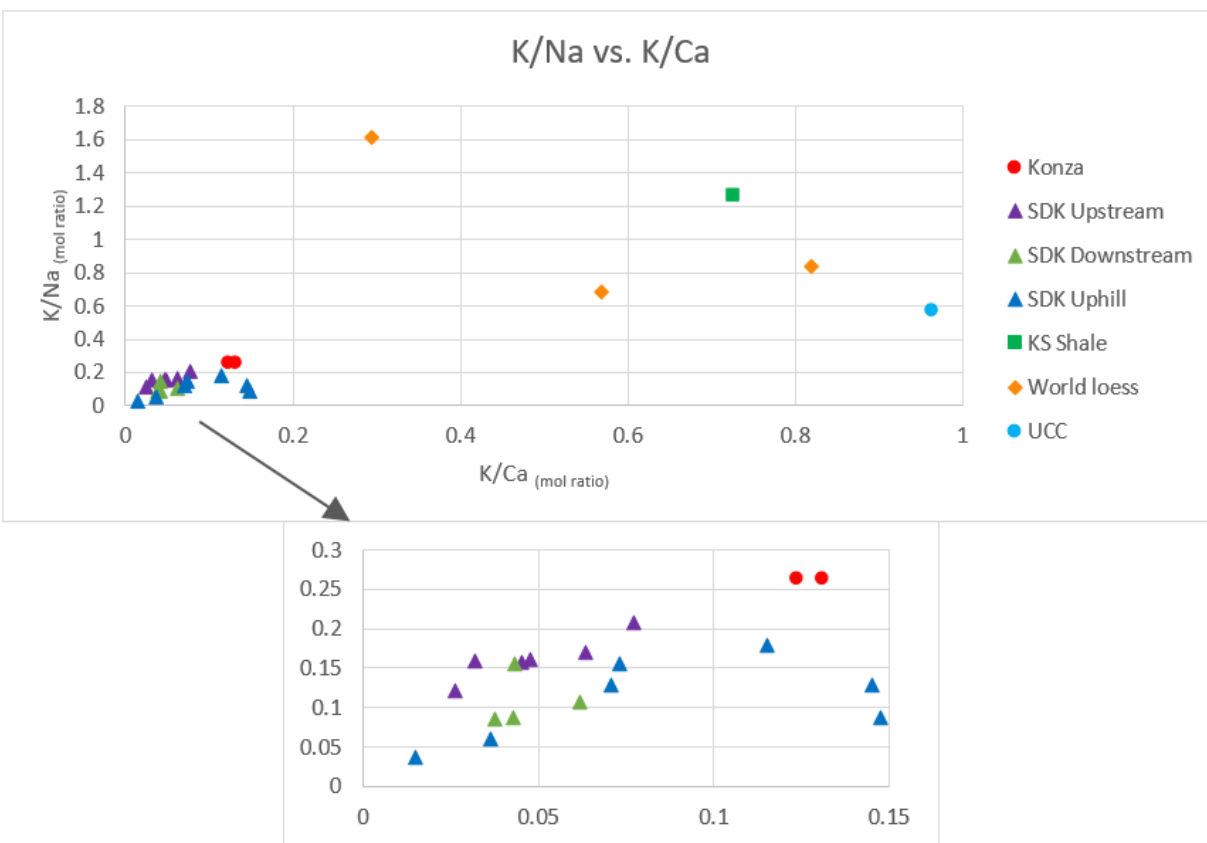


Figure 5.4-Molar ratios of K/Na compared to K/Ca. Konza and Stockdale (SDK) data were determined by ICP-OES. KS Shale is average of published data from grey shales in central KS (Cullers, 1994). World Loess data points from loess samples from 3 different countries (Yang et al., 2004; Gallet et al., 1998). UCC from published data (Taylor and McLennan, 1985).

The trace element Sr readily substitutes for Ca in carbonate rocks and minerals. If the concentrations of these two elements are plotted against each other, it is possible to assess whether one is leached preferentially during carbonate dissolution. The co-variance of Sr and Ca is shown in Figure 5.5a. The data show a broad positive correlation for the Stockdale soils; with only two data points for Konza, the relationship between these two elements, and the role of carbonate dissolution, cannot be assessed unambiguously. While studying Sr isotopes in groundwater at Konza LTER, Wood and Macpherson (2005) found a strong co-variance between these two elements both in soil and limestone weathering. More data are needed to clearly assess the relationship between strontium and calcium in these specific soil cores.

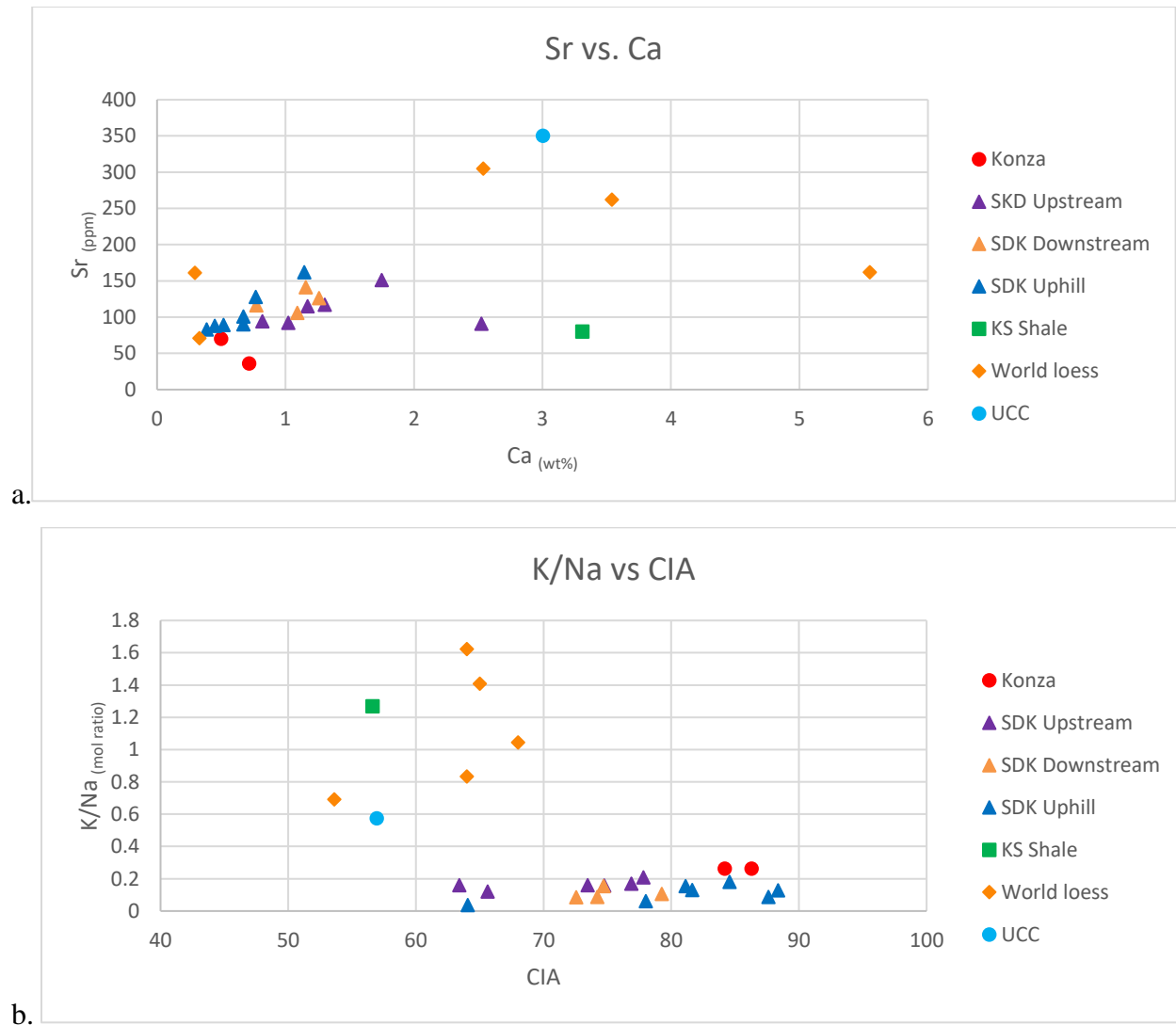


Figure 5.5- a. Co-variance graph of Sr and Ca. Konza and Stockdale (SDK) data were determined by ICP-OES. b. K/Na molar ratio compared to CIA. Konza and Stockdale (SDK) data were determined by ICP-OES. KS Shale is average of published data from grey shales in central KS (Cullers, 1994). World Loess data points from loess samples from 5 different countries (Yang et al., 2004; Gallet et al., 1998). UCC from published data (Taylor and McLennan, 1985).

Aside from a CIA calculation, comparing this metric to the K/Na molar ratio can help determine whether one rock or soil type has undergone enhanced silicate weathering. Figure 5.5b shows that for both Konza and Stockdale there is very little variation in the K/Na ratio across a broad range of CIA's. This could indicate that the control on CIA is not weathering, i.e. increasing silicate weathering and proportional increase in the clay component of the soils, but rather some other process. One possible explanation for this is the inclusion of already

extensively weathered wind-blown dust. The K/Na ratio for both Stockdale and Konza soils is lower than the starting values for each rock type and for loess which suggests that in both areas K is being removed preferentially to Na during weathering.

While the CIA demonstrates that surface samples from cores from both Konza and Stockdale contain material more weathered compared to soil deeper in the core, the question remains: To what extent is this due to the incorporation of wind-blown material? Charles G. (Jack) Oviatt stated that dust deposition was “a significant input of mass to the Konza geomorphic system” (1998). The influx of wind-blown dust in the 1960s was calculated at 50kg/ha/month near Manhattan, Kansas, the municipality located directly between the two sites for this study (Smith et al., 1970).

Looking at element ratio behavior in the cores for this study compared to trends seen by others for the same element ratios in wind-blown sediments, it is difficult to determine exactly how the loess is impacting the chemistry of the soil without chemical data for the actual loess component in Kansas. Without knowing the source of the loess (local, far flung, or a mixture), and / or its composition, quantification of the contribution of loess to the soil profiles cannot be done. However, using data from previous studies general trends can still be assessed.

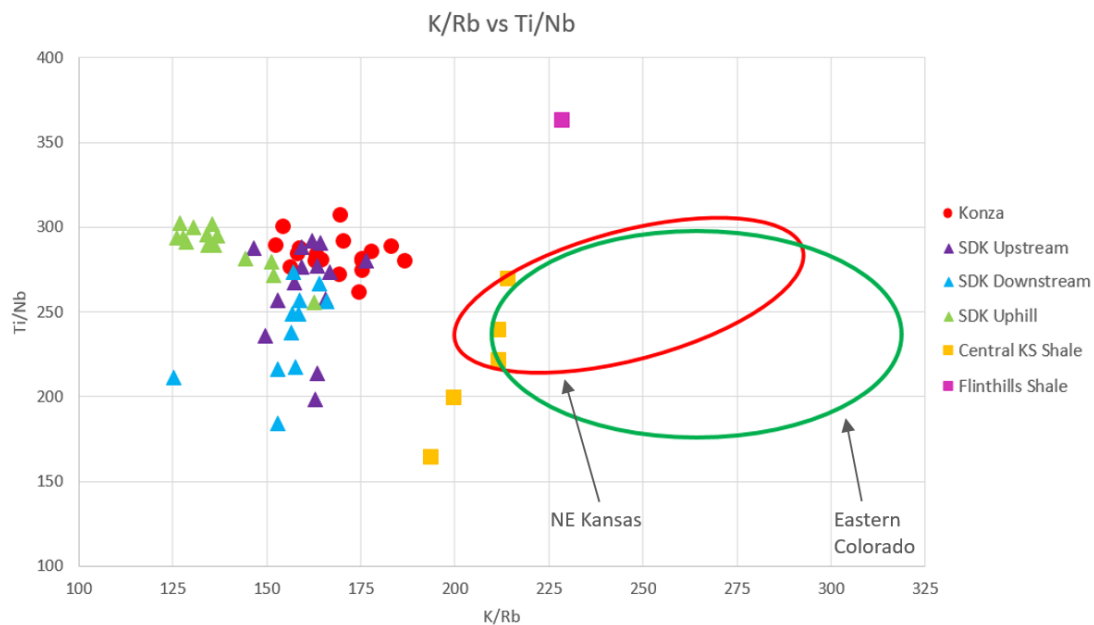


Figure 5.6-Plot of element ratios Ti/Nb vs. K/Rb. Loess values in northern Kansas fall within the red circle. Loess values in eastern Colorado fall within the green circle. (Muhs et al., 2008)

In a 2008 study of the origin of loess in Nebraska, Muhs et al. used the ratio of K/Rb compared to Ti/Nb as a method for characterizing loess from specific locations and as an aid in determining the provenance of the loess in their study. These two ratios are useful because Nb will readily substitute for Ti in minerals, and as conservative elements the ratio will be reflective of the parent rock (Muhs et al., 2008). The K/Rb ratio was used because Rb substitutes for K in micas and K-feldspar, though it does so more easily in micas (Lange et al., 1966). Hence, more mica in the soil or loess will result in a lower K/Rb ratio. In Figure 5.6, The K/Rb vs. Ti/Nb ratios for the soils in this study show that despite the large amount of loess deposition in the Flint Hills reported by Smith et al. (1970) (50 kg/ha/mo.), these soils are not purely loess derived. It is possible that the Smith et al. calculation is a bit high. If the loess which is deposited in the Flint Hills is from one or both areas on the graph, then the mixing in with parent material and in situ weathering are changing the resulting chemistry. However, there is no evidence yet of the origin of the loess being blown into the Flint Hills.

Zircon content of loess tends to decrease with distance from the source (Ebens and Connor, 1980). Mason and Jacobs, in their 1998 study (1998), found loess that was a mixture of local and distant sources had major element/Zr ratios two to four times higher (Reheis and Kihl, 1995) than the locally derived loess in their study site in Wisconsin. The graphs in **Error! Reference source not found.** (a) show significantly lower ratios of Al/Zr and Fe/Zr, and slightly lower Ti/Zr ratios in the shallower sediments of both Konza and Stockdale cores. Table 5.2 below shows averages of these ratios for both study sites as well as for the average composition of rock chips collected from shales local to both sites. Also included in the table are the ratio data for several different types of loess from around the world. Loess from Spitsbergen, an island in northern Norway, is a near-sourced periglacial dust. Loess sampled in Argentina is glacial with some volcanic glass included, most likely sourced from Patagonia. Loess sampled from the UK and from France are both near-sourced and most likely marine or paleoestuary in origin (Gallet et al., 1998). These data demonstrate the highly-varied nature of the geochemistries of loess and show how the incorporation of any one of these could alter element ratios push element ratios higher or lower from what would be seen purely from bedrock weathering based on type, source, and relative amount.

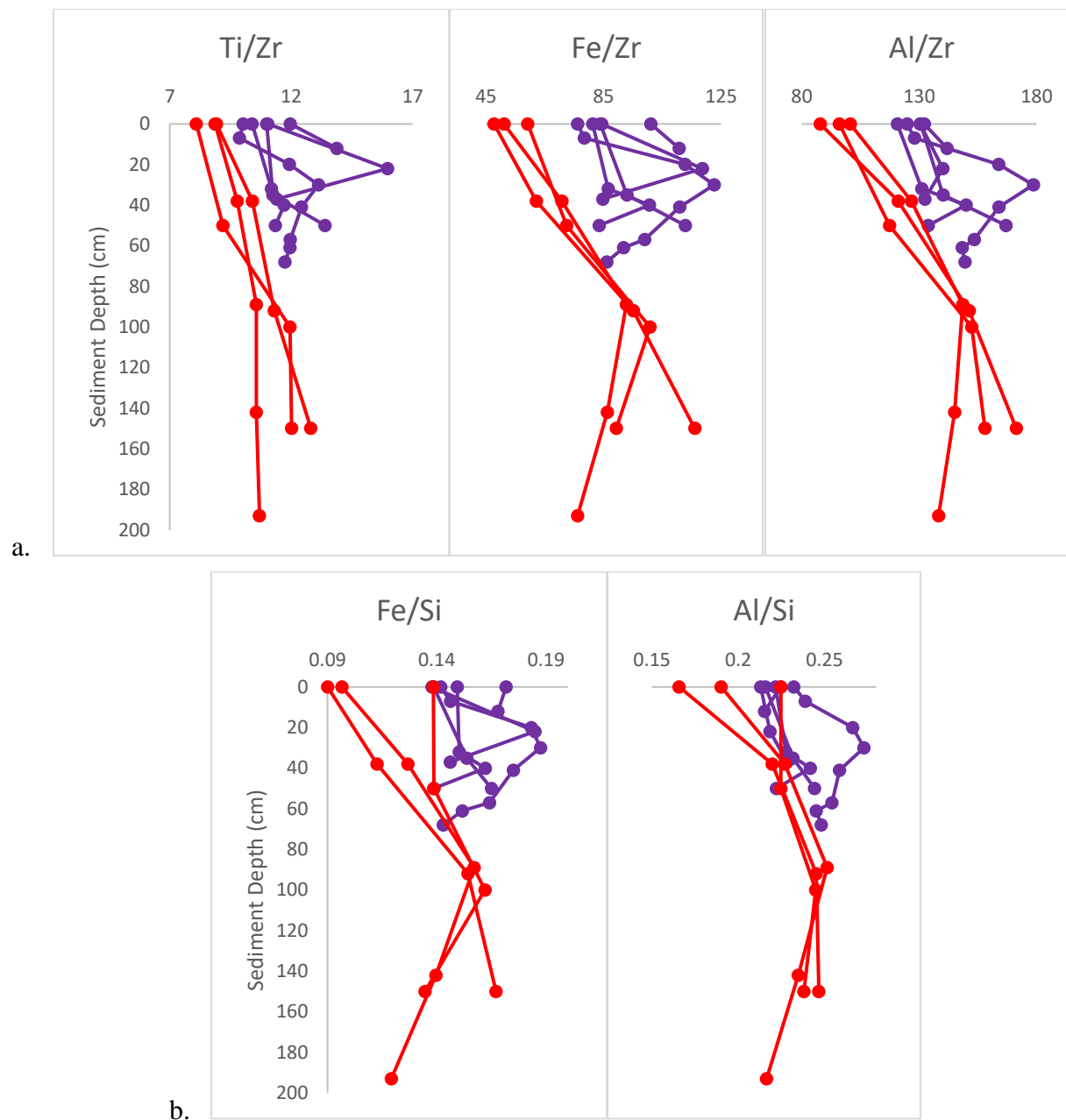


Figure 5.7-Ratios of conservative elements commonly found in wind-blown dust. Konza cores are red and Stockdale cores are purple. Elemental concentrations used were those determined by HHXRF. (a) Major element wt%/Zr wt% ratios (b) Major element wt%/Si wt%

Table 5.2-Element ratio data for Konza LTER core average, Stockdale kimberlite core average, source rock, and various loess samples. *Data from Konza cores 5 & 6 not included. **Data from core SDK not included. *Data determined by XRF from Shales rock chips collected 20km of both study sites. (1) Cullers et al., 2006. (2) Cullers, 1994. (3) Gallet et al., 1998.**

Source	Al/Si	Fe/Si	Ti/Zr	Fe/Zr	Al/Zr
Konza Average *	0.224	0.131	10.474	78.964	133.880
Stockdale Average **	0.238	0.159	11.868	95.650	143.048
Flint Hills Shale Average ***	0.326	0.195	24.252	250.871	419.741
SDK Surface (1)	0.078	0.402	NDA	NDA	NDA
Permian Shale Avg, Central KS (2)	0.233	0.098	NDA	NDA	NDA
Spitsbergen (Norway) Loess (periglacial dust) (3)	0.182	0.092	16.310	122.144	239.720
Argentina Loess (glacial dust w/volcanic glass from Patagonia) (3)	0.274	0.126	24.247	175.325	381.061
UK Loess (marine or paleoestuary dust) (3)	0.115	0.050	10.450	59.890	137.573
France Loess (marine or paleoestuary dust) (3)	0.123	0.063	9.602	45.959	89.440
UCC (4)	0.261	0.113	15.776	184.061	423.401

All three of these element ratios demonstrate that the soils have lower Al, Fe, and to a lesser extent, Ti relative to Zr in the upper part of the profile (**Error! Reference source not found.**, Table 2.1) This mostly likely due to the incorporation of loess. However, since the elements involved are conservative in nature, it is probable that there is an additional as yet unidentified factor operating here as well. Titanium and Zr are highly resistant to weathering in soils (Panahi, 2000) and because of this Ti/Zr ratios are stable enough in soils long term to be used to determine source rock for the soil. There is a slight decrease in the ratio at the surface of cores in both Konza and Stockdale. This suggests that addition of loess may be diluting these elements, which may possibly mean the source of the loess is closer rather than far. This is further evidenced by the lower ratios of Al/Zr and Fe/Zr in the shallow part of the cores.

Ratios of Al/Si and Fe/Si will also change with the addition of loess to a soil. The farther a dust is transported, the more it becomes enriched in Al and depleted in Si, most likely due to the increased clay proportion as larger and more dense silicate minerals (e.g. quartz and feldspar) drop out. Al/Si ratios of 0.22 to 0.36 are seen in Western U.S. dust when there is a mixture of both local and far sources (Mason and Jacobs, 1998), whereas far traveled dust, like that from the Saharan Dessert to Italy, has ratios from 0.35 to 0.47. However, there are many factors

influencing the shift in this ratio with depth such as parent bedrock composition and the extent of the weathering of the parent bedrock. As seen in **Error! Reference source not found.** (b), the Al/Si ratio for Konza ranges from 0.17 to 0.25 with an average of 0.22. Stockdale ranges from 0.21 to 0.30 with an average Al/Si ratio of 0.24. Table 2.1 shows Flint Hills shale, which is the primary parent rock for Konza, has a ratio of 0.33 whereas the Stockdale kimberlite outcrop surface has a ratio of 0.08. Given how the soil ratio changes from that of the bedrock in each area, it is a reasonable determination to state that the incorporation of loess has a marked impact on the ratios in both Konza and Stockdale.

Enrichment of Fe relative to Si also occurs in loess as it travels further from the source. As the parent rock in the two study areas weather, and clays form, this ratio will increase. Additionally, in Stockdale there will be mixing between country rock with the kimberlite alteration products, which will increase the Al/Si ratio, yet decrease the Fe/Si ratio. But element concentration measurements show that as Konza and Stockdale weather, the surface of the cores have a lower Al/Si and Fe/Si ratios than deeper in the core. The changes in these ratios with depth in both areas compared to parent rock can only be partially explained by weathering and clay formation. The influx of loess is altering these ratios and probably partially responsible for the lower ratios at the surface of the cores. Again though, a quantitative determination of the loess Al/Si and Fe/Si ratio or of the amount of soil-loess mixing is not possible given the data available.

There are no chemical data for the loess in this area, nor has a definitive source determination been made for the loess in this area. Furthermore, there is a clear distinction in the range of ratios for Konza as compared to Stockdale. All three Zr ratios are higher in Stockdale due to the extreme differences in parent rock geochemistry. Because of these data gaps, it is difficult to say with any confidence what the geochemical impact of the loess is on the soils in these areas, except to say that it is certainly a major factor in moderating the differences in the soils that surely would have been seen if parent rock composition and weathering extent were the sole factors in determining soil mineralogy.

5.4-Variations in microbial activity in Konza and Stockdale soils

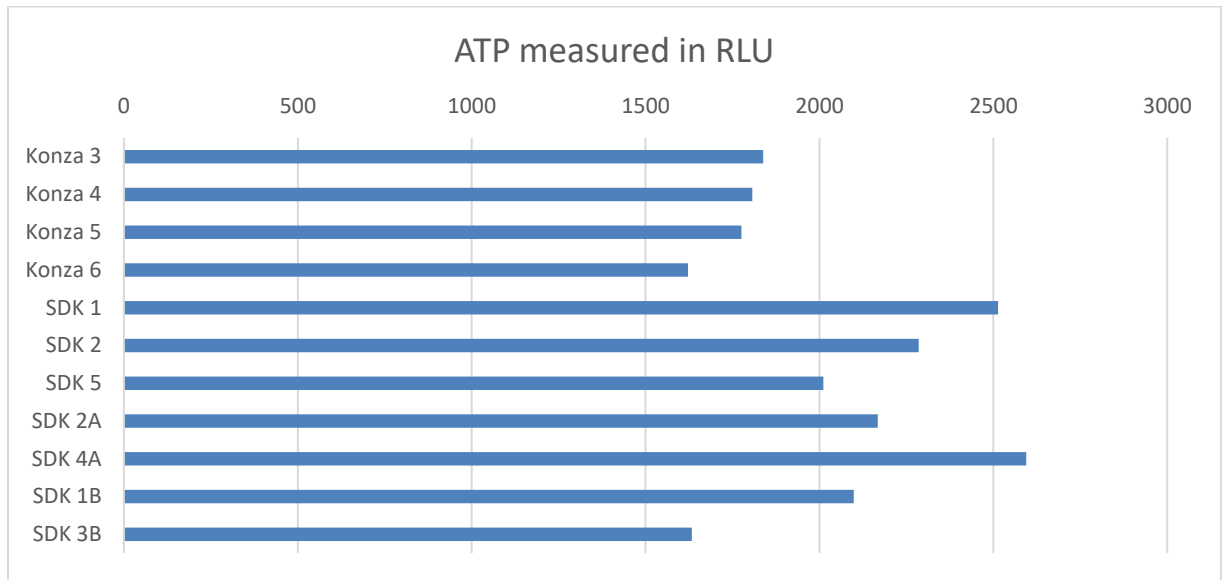


Figure 5.8-Relative amount of ATP in Konza and Stockdale cores. Results are measured in relative light units (RLU)

Adenosine Triphosphate (ATP) amounts can be used as a metric to assess the amount of microbial activity in the soil. Microorganisms are not only important for the health and productivity of soils, but also can play a role in mineral weathering in the soil. ATP levels in Konza soils are lower than those in most of the Stockdale kimberlite soils. One possible reason could be nutrient limitations. Microbial activity can be strongly constrained when there's a limited amount of P available (Cleveland et al., 2002). Iron availability is also integral in the production of ATP, as it is needed to reduce oxygen for ATP production (Nielands, 1995). As reported in the results section for XRF chemical analysis and ICP-OES chemical analysis, the concentrations of both P and Fe are higher in the area surrounding the Stockdale kimberlite. While the reasons for increased ATP at Stockdale as compared to Konza are no doubt more complicated than simple concentration levels of two elements, nutrient availability is likely to be a key factor.

Chapter 6 - Conclusion

The Flint Hills of Kansas are carved out of an interbedded limestone-shale system which is the home to Konza Prairie, a tall grass prairie whose geology is characteristic of this region. Also located in the Flint Hills are 13 kimberlite pipes. These diatremes of eruptive material, are ultramafic in nature and thus are vastly different from the surrounding country rock. Though the limestone mineralogy of this area is dominated by calcium carbonates, soils at Konza tend to be carbonate poor and approximately 1 m thick (Schaefer et al., 2007). Chemical data from HHXRF analysis and bulk extraction via aqua regia and subsequent ICP-OES analysis revealed calcium concentrations to be low in all cores except the bottom of core 5 and core 6. Both cores were located at the base of the N4D watershed and both cores terminated at the bedrock, which probably incorporated limestone chips into the soil. This resulted in the higher Ca concentrations of about 17%, at a depth of 70cm as opposed to the much lower 0.5% found at 30cm depth.

As the limestone weathers chemically, Ca leaches out of the soil. Since calcium carbonate is the primary mineral in limestone, when it disappears during chemical weathering, the remaining minerals being weathered are primarily from the mixture of shale layers and windblown loess. Mineralogy of the soils at Konza reveal that non-silicate minerals are a small component of the overall mineral assemblage found in soils here. Weathering resistant silicate minerals such as quartz, albite and microcline, dominate the mineralogy in the Konza cores. Also commonly seen in these cores are muscovite, calcite and sometimes dolomite. Particle size analysis shows Konza cores 5 and 6 at the base of the N4D watershed having a higher proportion of clay and fine silt compared to other cores. Clay mineral identification of Konza shows primarily clay mica (likely muscovite) and kaolinite to be dominant. Also in the clay size fractions, expandable 2:1 layer silicates and small amounts of dolomite were detected, but not calcite. The chemical index of alteration (CIA) which is a quantification of the extent to which sediment has been weathered, indicates that Konza soils have been weathered extensively as compared to the parent bedrock.

The Stockdale kimberlite diatreme because of the chemical composition of the magma, the minerals contained within the diatreme are Mg- and Fe-rich, low in silica, and contain high concentrations of trace metals which commonly substitute into these minerals. XRF and ICP-OES chemical data reveal that not only do the soils surrounding the kimberlite have higher Fe and Mg than the surrounding country rock but they also have higher trace element concentrations

as well. Iron in some Stockdale cores was about twice as high as Konza, Cu in Stockdale measured up to 3 times as much as Konza, and Ni concentrations were 10 times that measured at Konza. Because these elements are so much more prevalent in the kimberlite, the resulting minerals and weathering products are quite different from the surrounding country rock and are incorporated into the soil.

Also different from Konza, are the presence of so many high Fe and Mg bearing minerals such as biotite, chrysotile, enstatite, lizardite, olivine, phlogopite, kleberite, etc. which are contained in the soils surrounding the entire Stockdale kimberlite study site. Identifying many of these minerals, even the primary minerals, in these soils was not unexpected since the kimberlite lies directly underneath the stream and the stream intersects western edge of the kimberlite surface exposure carrying many of these minerals with it. In the uphill transect, biotite, chrysotile, enstatite, lizardite, magnesioferrite, magnetite, phengitic muscovite and phlogopite were detected. These minerals occur at all depths in the cores from this transect. At its highest point, core SDK 3B is approximately 3m higher in elevation than the kimberlite surface exposure. This indicates that as the kimberlite is weathering, is leaving a mineralogical signature or signal of this differential elemental content as compared to the interbedded limestone-shale country rock into which it has erupted.

Clay mineral identification reveals that in addition to many of the minerals found in the clay size fractions, though in differing amounts, smectite is also present in the area surrounding the Stockdale kimberlite. The analyzed samples from the kimberlite locations all contain smectite, likely high-Mg low charge smectites (Lee et al., 2003), in medium to high proportions of the total clay size fraction. Along the uphill transect SDK 1B has about ~20-50% of smectite and ~5-20% expandable 2:1 layer silicates, which is a similar proportion of expandable 2:1 layer silicates detected in the cores taken from Konza. In this core, there is co-mingling of smectite forming out of the ultrabasic mineral assemblage, primarily from serpentine (Estrade et al., 2015) and the incorporation of the expandable 2:1 layer silicate identified in the soils common in the limestone-shale country rock demonstrating a mixing of the weathering products and demonstrating the dilution of the Kimberlite signal. In core SDK 2B no smectite is present and there is more of the expandable 2:1 layer silicates. It could be said that this is the location at which the smectite signal for the kimberlite disappears.

The CIA was calculated for Stockdale cores SDK 1, 2, 5, 2A, 3A, 1B and 3B. The kimberlite surface has a calculated CIA of 28. At depth of 10 to 40 cm, which is directly above the Kimberlite, samples from upstream and next to the exposed edge all indicate that soils at this depth have been more weathered compared to the parent material. However, the CIA value of the surface sample for the same cores reveal much more extensive weathering. Except for SDK 3B, the soils around the kimberlite while they have been weathered, have not been weathered as heavily as those seen at Konza.

Because of their inclusions of parent material in the lower parts of their cores, each study site contained cores that are representations of the full weathering process. The lower part is an example of what weathering looks like when the bedrock is initially incorporated into the soil and begins to weather. The middle depths of each core are a transition zone and show how the soil chemistry and mineralogy changes with the addition of the elements from the parent rock. Core SDK 1B exemplifies this especially well. The surface samples from each core demonstrate how the parent rock influences the soil mineralogy after more extensive weathering when many cations have mobilized and been leached from the soil. This is also the case in each soil core where the influence of windblown dust, or loess is most notable. Ratios of conservative elements are lower in the shallow and surface portions of both study sites indicating that the loess may be being blown in from nearby areas. Konza soils have low CEC, retain little water, and make a poor choice for agriculture. In contrast, the kimberlite soils retain cations such as Mg^{2+} , have high CEC, and can hold water in the soil due to the presence of smectite-like clays. With further study, these soils may prove to be agriculturally advantageous either for growing crops directly or as a soil amendment for other areas.

From a purely economic standpoint, to say that understanding the processes involved in generating and maintaining soil is important is a massive understatement. However, it is also important to understand these processes from the standpoint of broadening scientific knowledge. The Critical Zone of planet Earth extends from the top of the canopy to the base of circulating groundwater systems (Brantley et al., 2008) and Critical Zone science aims to understand how integrated processes work in this area, interact in this area, and impact each other in this area. This study on the geochemistry of soil and weathering, along with all the work being done on Critical Zone processes, adds to this important body of knowledge. The more we as a scientific community fully understand these processes and can unravel all the complex interactions

necessary to develop soil and induce the characteristics we see in each type and in each area, the greater the likelihood we can apply that knowledge in a meaningful way in other places. Therefore, maintaining a holistic view of soil as a system and taking a global approach to researching the involved aspects—such as weathering, mineralogy, geochemistry, microbiology and element mobility—is key to understanding the integrated nature of the system.

Chapter 7 - References

- Blackburn, T. J., Stockli, D. F., Carlson, R. W., & Berendsen, P. (2008). (U–Th)/He dating of kimberlites—A case study from north-eastern Kansas. *Earth and Planetary Science Letters*, 275(1), 111-120.
- Borchardt, G. (1989). Smectites. *Minerals in soil environments*, (mineralsinsoile), 675-727.
- Brookins, D. G. (1970). The kimberlites of Riley County, Kansas. *Kansas Geological Survey Bulletin 200*, University of Kansas.
- Cleveland, C. C., Townsend, A. R., & Schmidt, S. K. (2002). Phosphorus limitation of microbial processes in moist tropical forests: evidence from short-term laboratory incubations and field studies. *Ecosystems*, 5(7), 0680-0691.
- Cullers, R. L. (1994). The controls on the major and trace element variation of shales, siltstones, and sandstones of Pennsylvanian-Permian age from uplifted continental blocks in Colorado to platform sediment in Kansas, USA. *Geochimica et Cosmochimica Acta*, 58(22), 4955-4972.
- Cullers, R. L., Berendsen, P., & Barczuk, A. (2006). *The Geology, Petrology, and Elemental Composition of Kimberlites from Riley and Marshall Counties, Kansas, USA* (Open File Report, pp. 1-41, Publication). Lawrence: Kansas Geological Survey.
- Cullers, R. L., Mullenax, J., Dimarco, M. J., & Nordeng, S. (1982). The trace element content and petrogenesis of kimberlites in Riley County, Kansas, USA. *American Mineralogist*, 67(3-4), 223-233.
- Dulekoz, E. (1969). Geochronology and clay mineralogy of the Eskridge Shale near Manhattan, Kansas. (Master's thesis, Kansas State University).
- Ebens, R. J., & Connor, J. J. (1980). *Geochemistry of loess and carbonate residuum* (No. 954-G).

- Eke, O. C. (2012). *Surface water and sediment geochemistry in understanding mobility of nitrates in mesic Kansas grassland* (Master's thesis, Kansas State University).
- Essington, M. E. (2004). *Soil and water chemistry: an integrative approach*. CRC press.
- Estrade, N., Cloquet, C., Echevarria, G., Sterckeman, T., Deng, T., Tang, Y., & Morel, J. L. (2015). Weathering and vegetation controls on nickel isotope fractionation in surface ultramafic environments (Albania). *Earth and Planetary Science Letters*, 423, 24-35.
- Gallet, S., Jahn, B. M., Lanoë, B. V. V., Dia, A., & Rossello, E. (1998). Loess geochemistry and its implications for particle origin and composition of the upper continental crust. *Earth and Planetary Science Letters*, 156(3-4), 157-172.
- Jackson, M. L., & Sherman, G. D. (1953). Chemical weathering of minerals in soils. *Advances in agronomy*, 5, 219-318.
- Jantz, D. R., Harner, R. F., Rowland, H. T., & Grier, D. A. (1975). United States Department of Agriculture Soil survey of Riley county and part of Geary county, Kansas.
- Jewett, J. M. (1941). *The geology of Riley and Geary counties, Kansas*. Kansas State Printing Plant, WC Austin, State Printer.
- Kansas Department of Agriculture Riley County. (2016). *Estimated Economic Impact of Agriculture, Food, and Food Processing Sectors, Riley County*, Retrieved January 8, 2017. <http://agriculture.ks.gov/docs/default-source/ag-marketing/county-ag-stats/2016-county-ag-stats/riley-ag-contribution-2016.pdf?sfvrsn=4>
- Kansas Department of Agriculture. (2016). *Estimated Economic Impact of Agriculture, Food, and Food Processing Sectors*. Retrieved January 8, 2017. <http://agriculture.ks.gov/about-kda/kansas-agriculture>
- Konert, M., & Vandenberghe, J. E. F. (1997). Comparison of laser grain size analysis with pipette and sieve analysis: a solution for the underestimation of the clay fraction. *Sedimentology*, 44(3), 523-535.

- Konza Prairie Long-Term Ecological Research (LTER). (2014). Retrieved August 08, 2016, from <http://lter.konza.ksu.edu/>
- Lange, I. M., Reynolds, R. C., & Lyons, J. B. (1966). K-Rb ratios in coexisting K-feldspars and biotites from some New England granites and metasediments. *Chemical Geology*, 1, 317-322.
- Lee, S. Y., & Kim, S. J. (2003). Dehydration behaviour hexadecyltrimethylammonium-exchanged smectite. *Clay Minerals*, 38(2), 225-232.
- Ma, L., Chabaux, F., Pelt, E., Blaes, E., Jin, L., & Brantley, S. (2010). Regolith production rates calculated with uranium-series isotopes at Susquehanna/Shale Hills Critical Zone Observatory. *Earth and Planetary Science Letters*, 297(1), 211-225.
- Macpherson, G. L., Roberts, J. A., Blair, J. M., Townsend, M. A., Fowle, D. A., & Beisner, K. R. (2008). Increasing shallow groundwater CO₂ and limestone weathering, Konza Prairie, USA. *Geochimica et Cosmochimica Acta*, 72(23), 5581-5599.
- Mason, J. A., & Jacobs, P. M. (1998). Chemical and particle-size evidence for addition of fine dust to soils of the midwestern United States. *Geology*, 26(12), 1135-1138.
- Meyer, H. O. A., & Brookins, D. G. (1976). Sapphirine, sillimanite, and garnet in granulite xenoliths from Stockdale kimberlite, Kansas. *American Mineralogist*, 61(11-12), 1194-1202.
- Moore, D. M., & Reynolds, R. C. (1989). *X-ray Diffraction and the Identification and Analysis of Clay Minerals* (Vol. 378, p. 155). Oxford: Oxford university press.
- Morkel, J., & Vermaak, M. K. G. (2006). The role of swelling clay in kimberlite weathering. *Mineral Processing and Extractive Metallurgy*, 115(3), 150-154.
- Muhs, D. R., Bettis, E. A., Aleinikoff, J. N., McGeehin, J. P., Beann, J., Skipp, G., ... & Benton, R. (2008). Origin and paleoclimatic significance of late Quaternary loess in Nebraska: evidence from stratigraphy, chronology, sedimentology, and geochemistry. *Geological Society of America Bulletin*, 120(11-12), 1378-1407.

- National Research Council. (2001). *Basic research opportunities in earth science*. national academies Press.
- Neilands, J. B. (1995). Siderophores: structure and function of microbial iron transport compounds. *Journal of Biological Chemistry*, 270(45), 26723-26726.
- Nesbitt, H., & Young, G. M. (1982). Early Proterozoic climates and plate motions inferred from major element chemistry of lutites. *Nature*, 299(5885), 715-717.
- Oviatt, C. G. (1998). Geomorphology of Konza prairie. *Grassland dynamics: long-term ecological research in tallgrass prairie*. Oxford University Press, New York, 35-47.
- Pecchioni, L. L. (1981). *Depositional environment of the Eskridge shale (lower Permian)* (Doctoral dissertation, Kansas State University).
- Poppe, L. J., Paskevich, V. F., Hathaway, J. C., & Blackwood, D. S. (2001). A laboratory manual for X-ray powder diffraction. *US Geological Survey Open-File Report*, 1(041), 1-88.
- Ransom, M., C. W. Rice, T. C. Todd, and W. A. Wehmuller. 1998. Pages 48–66 A. K. Knapp, J. M. Briggs, D. C. Hartnett, and S. L. Collins, editors. *Grassland dynamics: long-term ecological research in tallgrass prairie*. Oxford University Press, New York, New York, USA.
- Reheis, M. C., & Kihl, R. (1995). Dust deposition in southern Nevada and California, 1984–1989: Relations to climate, source area, and source lithology. *Journal of Geophysical Research: Atmospheres*, 100(D5), 8893-8918.
- Rosa, F., & Brookins, D. G. (1966). The mineralogy of the Stockdale kimberlite pipe, Riley County, Kansas. *Transactions of the Kansas Academy of Science (1903)*, 335-344.
- Rost, F., Beermann, E., & Amthauer, G. (1975). Chemical investigation of pyrope garnets in stockdale kimberlite intrusion, riley-county, Kansas. *American Mineralogist*, 60(7-8), 675-680.

- Rowe, H., Hughes, N., & Robinson, K. (2012). The quantification and application of handheld energy-dispersive x-ray fluorescence (ED-XRF) in mudrock chemostratigraphy and geochemistry. *Chemical Geology*, 324, 122-131.
- Runnels, R. T., & Schleicher, J. A. (1956). Chemical composition of eastern Kansas limestones. *Kansas Geological Survey Bulletin* 119.
- Schaefer, G. L., Cosh, M. H., & Jackson, T. J. (2007). The USDA natural resources conservation service soil climate analysis network (SCAN). *Journal of Atmospheric and Oceanic Technology*, 24(12), 2073-2077.
- Smith, R. M., Twiss, P. C., Krauss, R. K., & Brown, M. J. (1970). Dust deposition in relation to site, season, and climatic variables. *Soil Science Society of America Journal*, 34(1), 112-117.
- Soil Composition. (2007). Retrieved August 08, 2017, from https://www.ctahr.hawaii.edu/mauisoil/a_comp.aspx
- Swift, R. S., & Sparks, D. L. (1996). Methods of soil analysis: Part 3. Chemical methods. *Soil Science Society of America Book Series*, 5, 1018-1020.
- Tallgrass Prairie National Preserve (U.S. National Park Service). (2014). Retrieved August 08, 2017, from <https://www.nps.gov/tapr/index.htm>
- Taylor, S. R., & McLennan, S. M. (1985). The continental crust: its composition and evolution. Blackwell Scientific Publishing.
- Tsypin, M., & Macpherson, G. L. (2012). The effect of precipitation events on inorganic carbon in soil and shallow groundwater, Konza Prairie LTER Site, NE Kansas, USA. *Applied geochemistry*, 27(12), 2356-2369.
- US Climate Data. (n.d.). Temperature - Precipitation - Sunshine - Snowfall. Retrieved June 18, 2016, from <http://www.usclimatedata.com/climate/manhattan/kansas/united-states/usks0358>

- Wood, H. K., & Macpherson, G. L. (2005). Sources of Sr and implications for weathering of limestone under tallgrass prairie, northeastern Kansas. *Applied geochemistry*, 20(12), 2325-2342.
- Yang, S. Y., Li, C. X., Yang, D. Y., & Li, X. S. (2004). Chemical weathering of the loess deposits in the lower Changjiang Valley, China, and paleoclimatic implications. *Quaternary International*, 117(1), 27-34.

Appendix A - General Sample Location Descriptions

Konza Prairie (from Eke, 2012)

Sample ID	Date	# Tubes (1"x24")	Max depth of core (cm)	Latitude	Longitude	Elevation (m)
Konza 3	7-27-2010	4	153	N39°4.039'	W96°35.845'	398
Konza 4	7-27-2010	4	160	N39°4.046'	W96°35.886'	396.5
Konza 5	7-27-2010	2	70	N39°5.259'	W96°35.077'	385
Konza 6	7-27-2010	3	130	N39°5.324'	W96°35.075'	382
Konza 9	8-2-2010	4	203	N39°6.155'	W96°35.204'	345
Konza 10	8-2-2010	4	160	N39°5.773'	W96°34.257'	370.5

Stockdale Kimberlite

Sample ID	Date	Max depth of core (cm)	Latitude	Longitude	Elevation (m)	Description
SDK 1	10-3-2015	23	39.34197	-96.72416	384	western edge of surface exposure where creek bed crosses the fence line
SDK 2	10-3-2015	52	39.34203	-96.72431	384.9	creek bed upstream (north and west) from SDK 1 approximately 52ft (16m)
SDK 3	10-3-2015	34	39.34208	-96.72453	385	creek bed upstream (north and west) from SDK 2 approximately 65ft (20m)
SDK 4	10-11-2015	16	39.34240	-96.72455	385.5	creek bed upstream (north) from SDK 3 approximately 121ft (37m)
SDK 5	10-11-2015	26	39.34258	-96.72445	385.9	creek bed upstream (north and slightly east) from SDK 4 approximately 72ft (22m)
SDK 2A	10-3-2015	63	39.34185	-96.72423	383.9	creek bed downstream (south and west) from SDK 1 approximately 64ft (20m)
SDK 3A	10-11-2015	48	39.34174	-96.72442	383.8	creek bed downstream (south and west) from SDK 2A approximately 71ft (22m)
SDK 4A	10-11-2015	61	39.34152	-96.72468	383.5	creek bed downstream (south and west) from SDK 3A approximately 118ft (36m)
SDK 1B	10-17-2015	41	39.34198	-96.72400	385.6	due east along the fence line approximately 45ft (14m) and uphill from SDK 1; opposite side of exposure
SDK 2B	10-17-2015	79	39.34198	-96.72384	387.6	due east along the fence line approximately 46ft (14m) and uphill from SDK 1B
SDK 3B	10-17-2015	82	39.34198	-96.72364	388.7	due east along the fence line approximately 58ft (18m) and uphill from SDK 2B

Appendix B - X-Ray Fluorescence (XRF) Data

B.1 – Accuracy Table

Chemical data for standard material RTC-W-220, pressed powder pellet, Woodford Shale. Accepted values “For RTC-W-220, values for major elements are from lithium borate-fused disk analysis by WD-XRF at SGS; values for trace elements (ppm) from sodium peroxide fusion dissolution and analysis by ICP-MS and ICP-OES. Values for %S determined by LECO combustion/infrared analysis” (Rowe, 2012).

Elemental Concentrations	Accepted values	Rowe et al (2012) measured values	Measured values this study	σ Measured values this study
Mg (wt%)	0.67	0.8	0.46	0.12
Al	4.96	5.39	4.49	0.25
Si	32.6	33.7	28.03	1.12
P	0.07	0.05	0.07	0.01
S	3.34	2.18	2.42	0.09
K	2.07	2.31	2.32	0.04
Ca	0.13	0.23	0.11	0.02
Ti	0.23	0.27	0.27	0.01
Mn	0.015	0.012	0.024	0.0003
Fe	2.93	2.53	2.7	0.04
Ba (ppm)	2090	1884	1752	536
V	928	1114	927	13.6
Cr	110	98	107	3.2
Ni	130	153	145	3.1
Cu	83	147	89	5.7
Zn	823	844	888	38
Th	8.4	9	11	0.06
Rb	122	123	138	3
U	18.1	17	14	3
Sr	75.5	87	81	11
Y	35.4	34	33	0.2
Zr	80.3	95	114	2
Nb	9	9	10	0.01
Mo	79	83	72	4

B.2 – XRF Raw Data

In the following tables are the unprocessed data for the X-Ray Fluorescence analyses conducted on both the Konza Prairie and Stockdale Kimberlite samples for this study. Analyses were conducted using a Bruker Tracer III.

XRF Sample ID	Wt %	Mg	Al	Si	P	S	K	Ca	Ti	V	Cr	Mn	Fe	Co	Ni	Cu	Zn	Ga	As	Rb	Sr	Y	Zr	Nb	Mo	Ba	Pb	Th	U
TR-10-1-0-10-run1	GL2	0.04	4.46	19.49	0.01	0.15	1.84	1.92	0.38	0.01	0.01	0.08	2.79	0.00	0.00	0.00	0.01	0.00	0.00	0.01	0.01	0.00	0.04	0.00	0.00	0.00	0.00	0.00	0.00
TR-10-1-0-10-run2	GL2	BDL	4.52	19.40	0.01	0.14	1.82	1.91	0.39	0.01	0.01	0.08	2.80	0.00	0.00	0.00	0.01	0.00	0.00	0.01	0.01	0.00	0.04	0.00	0.00	0.04	0.00	0.00	0.00
TR-10-1-0-10-run3	GL2	BDL	4.24	19.06	0.01	0.15	1.80	2.01	0.37	0.01	0.01	0.07	2.78	0.00	0.00	0.00	0.01	0.00	0.00	0.01	0.01	0.00	0.05	0.00	0.01	0.09	0.00	0.00	0.00
TR-10-1-0-10-run4	GL2													0.00	0.00	0.00	0.01	0.00	0.00	0.01	0.01	0.00	0.05	0.00	0.00	0.00	0.00	0.00	0.00
TR-10-1-0-10-run5	GL2													0.00	0.00	0.00	0.01	0.00	0.00	0.01	0.01	0.00	0.05	0.00	0.01	0.01	0.00	0.00	0.00
TR-10-1-0-10-run6	GL2													0.00	0.00	0.00	0.01	0.00	0.00	0.01	0.01	0.00	0.05	0.00	0.01	0.08	0.00	0.00	0.00
	wt%	0.04	4.40	19.32	0.01	0.15	1.82	1.95	0.38	0.01	0.01	0.08	2.79	0.00	0.00	0.00	0.01	0.00	0.00	0.01	0.01	0.00	0.05	0.00	0.00	0.04	0.00	0.00	0.00
	Std. Dev.	N/A	0.15	0.22	0.00	0.00	0.02	0.05	0.01	0.00	0.00	0.00	0.01	0.00	0.00	0.00	0.00	0.00	0.00	0.00	0.00	0.00	0.00	0.00	0.00	0.04	0.00	0.00	0.00
	ppm	350.73	44027.63	193153.90	113.46	1464.89	18201.68	19451.72	3801.58	72.61	84.31	761.07	27917.07	6.71	45.04	36.49	88.86	14.09	14.13	102.04	92.20	41.08	460.15	13.24	49.22	350.25	14.76	7.89	0.86
	Oxide %	0.06	8.32	41.32	0.03	0.37	2.19	2.72	0.63	0.01	0.01	0.10	3.59	0.00	0.01	0.00	0.01	0.00	0.00	0.01	0.01	0.01	0.06	0.00	0.01	0.04	0.00	0.00	0.00
TR-10-2-50-60-run1	GL2	0.01	4.34	20.46	0.02	0.14	1.85	1.25	0.38	0.01	0.01	0.10	2.91	0.00	0.00	0.00	0.01	0.00	0.00	0.01	0.01	0.00	0.04	0.00	0.00	0.05	0.00	0.00	0.00
TR-10-2-50-60-run2	GL2	BDL	4.34	20.36	0.01	0.14	1.82	1.21	0.38	0.01	0.01	0.10	2.95	0.00	0.00	0.00	0.01	0.00	0.00	0.01	0.01	0.00	0.04	0.00	0.00	0.06	0.00	0.00	0.00
TR-10-2-50-60-run3	GL2	BDL	4.42	20.41	0.01	0.14	1.84	1.23	0.38	0.01	0.01	0.10	2.85	0.00	0.00	0.00	0.01	0.00	0.00	0.01	0.01	0.00	0.04	0.00	0.00	0.00	0.00	0.00	0.00
TR-10-2-50-60-run4	GL2													0.00	0.00	0.00	0.01	0.00	0.00	0.01	0.01	0.00	0.04	0.00	0.00	0.05	0.00	0.00	0.00
TR-10-2-50-60-run5	GL2													0.00	0.00	0.00	0.01	0.00	0.00	0.01	0.01	0.00	0.04	0.00	0.00	0.05	0.00	0.00	0.00
TR-10-2-50-60-run6	GL2													0.00	0.00	0.00	0.01	0.00	0.00	0.01	0.01	0.00	0.04	0.00	0.00	0.05	0.00	0.00	0.00
	wt%	0.01	4.36	20.41	0.01	0.14	1.84	1.23	0.38	0.01	0.01	0.10	2.91	0.00	0.00	0.00	0.01	0.00	0.00	0.01	0.01	0.00	0.04	0.00	0.00	0.04	0.00	0.00	0.00
	Std. Dev.	N/A	0.05	0.05	0.00	0.00	0.01	0.02	0.00	0.00	0.00	0.00	0.05	0.00	0.00	0.00	0.00	0.00	0.00	0.00	0.00	0.00	0.00	0.00	0.00	0.02	0.00	0.00	0.00
	ppm	94.32	43648.24	204079.03	141.89	1431.60	18359.07	12273.85	3795.52	87.81	85.56	972.06	29061.91	8.82	45.69	36.52	88.55	13.53	15.20	104.77	93.36	38.51	404.23	13.01	40.51	380.80	14.95	8.03	0.17
	Oxide %	0.02	8.25	43.66	0.03	0.36	2.21	1.72	0.63	0.02	0.01	0.13	3.74	0.00	0.01	0.00	0.01	0.00	0.00	0.01	0.01	0.00	0.05	0.00	0.01	0.04	0.00	0.00	0.00
TR-10-3-100-110-run1	GL2	0.08	4.47	18.53	0.01	0.14	1.84	3.64	0.38	0.01	0.01	0.07	3.03	0.00	0.00	0.00	0.01	0.00	0.00	0.01	0.01	0.00	0.03	0.00	0.00	0.04	0.00	0.00	0.00
TR-10-3-100-110-run2	GL2	0.03	4.48	18.54	0.01	0.14	1.83	3.64	0.38	0.01	0.01	0.07	3.02	0.00	0.00	0.00	0.01	0.00	0.00	0.01	0.01	0.00	0.03	0.00	0.00	0.02	0.00	0.00	0.00
TR-10-3-100-110-run3	GL2	0.06	4.48	18.70	0.01	0.14	1.85	3.65	0.38	0.00	0.01	0.07	3.02	0.00	0.00	0.00	0.01	0.00	0.00	0.01	0.01	0.00	0.03	0.00	0.00	0.02	0.00	0.00	0.00
TR-10-3-100-110-run4	GL2													0.00	0.01	0.00	0.01	0.00	0.00	0.01	0.01	0.00	0.03	0.00	0.00	0.04	0.00	0.00	0.00
TR-10-3-100-110-run5	GL2													0.00	0.01	0.00	0.01	0.00	0.00	0.01	0.01	0.00	0.03	0.00	0.00	0.00	0.00	0.00	0.00
TR-10-3-100-110-run6	GL2													0.00	0.00	0.00	0.01	0.00	0.00	0.01	0.01	0.00	0.03	0.00	0.00	0.00	0.00	0.00	0.00
	wt%	0.06	4.48	18.59	0.01	0.14	1.84	3.64	0.38	0.01	0.01	0.07	3.02	0.00	0.00	0.00	0.01	0.00	0.00	0.01	0.01	0.00	0.03	0.00	0.00	0.02	0.00	0.00	0.00
	Std. Dev.	0.03	0.01	0.09	0.00	0.00	0.01	0.01	0.00	0.00	0.00	0.00	0.01	0.00	0.00	0.00	0.00	0.00	0.00	0.00	0.00	0.00	0.00	0.00	0.00	0.02	0.00	0.00	0.00
	ppm	573.54	44750.71	185901.27	101.76	1386.87	18440.99	36439.04	3792.55	57.67	79.32	693.38	30206.89	10.25	48.12	41.35	93.93	14.42	14.25	109.81	133.19	37.12	309.31	12.04	27.90	198.81	14.81	8.44	0.12
	Oxide %	0.10	8.46	39.77	0.02	0.35	2.22	5.10	0.63	0.01	0.01	0.09	3.89	0.00	0.01	0.01	0.01	0.00	0.00	0.01	0.02	0.00	0.04	0.00	0.00	0.02	0.00	0.00	0.00
TR-10-4-150-160-run1	GL2	0.05	4.70	19.86	0.01	0.13	1.86	1.57	0.38	0.01	0.01	0.12	2.99	0.00	0.00	0.00	0.01	0.00	0.00	0.01	0.01	0.00	0.03	0.00	0.00	0.05	0.00	0.00	0.00
TR-10-4-150-160-run2	GL2	BDL	4.62	19.78	0.01	0.13	1.85	1.57	0.39	0.01	0.01	0.12	3.02	0.00	0.00	0.00	0.01	0.00	0.00	0.01	0.02	0.00	0.03	0.00	0.00	0.19	0.00	0.00	0.00
TR-10-4-150-160-run3	GL2	BDL	4.68	19.74	0.01	0.13	1.84	1.57	0.38	0.01	0.01	0.12	3.04	0.00	0.00	0.00	0.01	0.00	0.00	0.01	0.01	0.00	0.03	0.00	0.00	0.03	0.00	0.00	0.00
TR-10-4-150-160-run4	GL2													0.00	0.00	0.00	0.01	0.00	0.00	0.01	0.02	0.00	0.03	0.00	0.00	0.04	0.00	0.00	0.00
TR-10-4-150-160-run5	GL2													0.00	0.00	0.00	0.01	0.00	0.00	0.01	0.01	0.00	0.03	0.00	0.00	0.06	0.00	0.00	0.00
TR-10-4-150-160-run6	GL2													0.00	0.00	0.00	0.01	0.00	0.00	0.01	0.01	0.00	0.03	0.00	0.00	0.04	0.00	0.00	0.00
	wt%	0.05	4.67	19.79	0.01	0.13	1.85	1.57	0.38	0.01	0.01	0.12	3.02	0.00	0.00	0.00	0.01	0.00	0.00	0.01	0.01	0.00	0.03	0.00	0.00	0.07	0.00	0.00	0.00
	Std. Dev.	N/A	0.05	0.06	0.00	0.00	0.01	0.00	0.00	0.00	0.00	0.00	0.03	0.00	0.00	0.00	0.00	0.00	0.00	0.00	0.00	0.00	0.00	0.00	0.00	0.06	0.00	0.00	0.00
	ppm	516.04	46671.52	197925.44	113.38	1300.62	18526.38	15713.39	3832.36	84.04	79.58	1227.87	30161.75	11.07	47.54	40.54	102.16	15.06	12.27	119.78	148.22	38.91	313.19	13.08	27.21	663.28	14.51	9.07	0.00
	Oxide %	0.09	8.82	42.34	0.03	0.32	2.23	2.20	0.64	0.02	0.01	0.16	3.88	0.00	0.01	0.01	0.01	0.00	0.00	0.01	0.02	0.00	0.04	0.00	0.00	0.07	0.00	0.00	0.00
TR-3-1-1-10-run1	GL2	BDL	3.92	23.59	0.02	0.16	1.75	0.53	0.40	0.01	0.01	0.06	1.93	0.00	0.00	0.00	0.01	0.00	0.00	0.01	0.01	0.00	0.04	0.00	0.00	0.04	0.00	0.00	0.00
TR-3-1-1-10-run2	GL2	BDL	3.96	23.66	0.02	0.16	1.76	0.54	0.39	0.01	0.01	0.06	1.96	0.00	0.00	0.00	0.01	0.00	0.00	0.01	0.01	0.00	0.04	0.00	0.00	0.12	0.00	0.00	0.00
TR-3-1-1-10-run3	GL2	BDL	3.95	23.54	0.02	0.15	1.74	0.53	0.39	0.01	0.01	0.06	1.97	0.00	0.00	0.00	0.01	0.00	0.00	0.01	0.01	0.00	0.04	0.00	0.00	0.10	0.00	0.00	0.00
TR-3-1-1-10-run4	GL2													0.00	0.00	0.00	0.01	0.00	0.00	0.01	0.01	0.00	0.04	0.00	0.00	0.04	0.00	0.00	0.00
TR-3-1-1-10-run5	GL2													0.00	0.00	0.00	0.01	0.00	0.00	0.01	0.01	0.00	0.04	0.00	0.00	0.03	0.00	0.00	0.00
TR-3-1-1-10-run6	GL2													0.00	0.00	0.00	0.01	0.00	0.00	0.01	0.01	0.00	0.04	0.00	0.00	0.02	0.00	0.00	0.00
	wt%	BDL	3.94	23.60	0.02	0.16	1.75	0.54	0.39	0.01	0.01	0.06	1.95	0.00															

XRF Sample ID	Wt %	Mg	Al	Si	P	S	K	Ca	Ti	V	Cr	Mn	Fe	Co	Ni	Cu	Zn	Ga	As	Rb	Sr	Y	Zr	Nb	Mo	Ba	Pb	Th	U
TR-4-1T-0-10-run1	GL2	BDL	3.89	22.89	0.02	0.16	1.73	0.51	0.41	0.01	0.01	0.06	2.12	0.00	0.00	0.00	0.01	0.00	0.00	0.01	0.01	0.00	0.05	0.00	0.00	0.00	0.00	0.00	0.00
TR-4-1T-0-10-run2	GL2	BDL	1.89	12.24	BDL	0.11	0.68	0.14	0.19	0.02	0.03	0.07	-0.81	0.00	0.00	0.00	0.01	0.00	0.00	0.01	0.01	0.00	0.04	0.00	0.00	0.11	0.00	0.00	0.00
TR-4-1T-0-10-run3	GL2	BDL	1.64	11.22	BDL	0.10	0.59	0.10	0.17	0.03	0.03	0.07	-1.06	0.00	0.00	0.00	0.01	0.00	0.00	0.01	0.01	0.00	0.05	0.00	0.00	0.03	0.00	0.00	0.00
TR-4-1T-0-10-run4	GL2													0.00	0.00	0.00	0.01	0.00	0.00	0.01	0.01	0.00	0.05	0.00	0.00	0.06	0.00	0.00	0.00
TR-4-1T-0-10-run5	GL2													0.00	0.00	0.00	0.01	0.00	0.00	0.01	0.01	0.00	0.05	0.00	0.00	0.01	0.00	0.00	0.00
TR-4-1T-0-10-run6	GL2													0.00	0.00	0.00	0.01	0.00	0.00	0.01	0.01	0.00	0.04	0.00	0.00	0.03	0.00	0.00	0.00
	wt%	BDL	2.47	15.45	0.02	0.12	1.00	0.25	0.26	0.02	0.02	0.07	0.08	0.00	0.00	0.00	0.01	0.00	0.00	0.01	0.01	0.00	0.04	0.00	0.00	0.04	0.00	0.00	0.00
	Std. Dev.	N/A	1.24	6.46	N/A	0.03	0.64	0.22	0.13	0.01	0.01	0.01	1.77	0.00	0.00	0.00	0.00	0.00	0.00	0.00	0.00	0.00	0.00	0.00	0.00	0.04	0.00	0.00	0.00
	ppm	BDL	24742.54	154532.36	188.41	1232.86	10033.48	2491.12	2577.19	187.39	210.88	678.00	828.39	5.57	26.90	28.53	69.87	12.00	12.45	101.92	106.79	40.02	445.36	14.60	45.22	394.54	13.39	7.86	1.19
	Oxide %	BDL	4.68	33.06	0.04	0.31	1.21	0.35	0.43	0.03	0.03	0.09	0.11	0.00	0.00	0.00	0.01	0.00	0.00	0.01	0.01	0.01	0.06	0.00	0.01	0.04	0.00	0.00	0.00
TR-4-2-92-102-run1	GL2	BDL	5.08	20.94	0.01	0.13	1.82	0.51	0.40	0.01	0.01	0.07	3.05	0.00	0.00	0.00	0.01	0.00	0.00	0.01	0.01	0.00	0.03	0.00	0.00	0.10	0.00	0.00	0.00
TR-4-2-92-102-run2	GL2	BDL	5.15	21.00	0.01	0.13	1.81	0.51	0.38	0.01	0.01	0.07	3.06	0.00	0.00	0.00	0.01	0.00	0.00	0.01	0.01	0.00	0.03	0.00	0.00	0.00	0.00	0.00	0.00
TR-4-2-92-102-run3	GL2	BDL	5.10	21.08	0.01	0.13	1.82	0.51	0.39	0.01	0.01	0.07	3.03	0.00	0.00	0.00	0.01	0.00	0.00	0.01	0.01	0.00	0.03	0.00	0.00	0.07	0.00	0.00	0.00
TR-4-2-92-102-run4	GL2													0.00	0.00	0.00	0.01	0.00	0.00	0.01	0.01	0.00	0.03	0.00	0.00	0.15	0.00	0.00	0.00
TR-4-2-92-102-run5	GL2													0.00	0.00	0.00	0.01	0.00	0.00	0.01	0.01	0.00	0.03	0.00	0.00	0.00	0.00	0.00	0.00
TR-4-2-92-102-run6	GL2													0.00	0.00	0.00	0.01	0.00	0.00	0.01	0.01	0.00	0.03	0.00	0.00	0.00	0.00	0.00	0.00
	wt%	BDL	5.11	21.01	0.01	0.13	1.82	0.51	0.39	0.01	0.01	0.07	3.05	0.00	0.00	0.00	0.01	0.00	0.00	0.01	0.01	0.00	0.03	0.00	0.00	0.06	0.00	0.00	0.00
	Std. Dev.	N/A	0.04	0.07	0.00	0.00	0.00	0.00	0.01	0.00	0.00	0.00	0.02	0.00	0.00	0.00	0.00	0.00	0.00	0.00	0.00	0.00	0.00	0.00	0.00	0.06	0.00	0.00	0.00
	ppm	BDL	51106.88	210076.57	71.90	1296.76	18183.28	5105.29	3912.91	105.29	95.05	693.51	30487.78	10.26	41.86	37.39	87.23	15.54	11.99	118.91	100.42	38.61	336.16	13.13	29.43	597.97	14.49	9.01	0.00
	Oxide %	BDL	9.66	44.94	0.02	0.32	2.19	0.71	0.65	0.02	0.01	0.09	3.92	0.00	0.01	0.00	0.01	0.00	0.00	0.01	0.01	0.00	0.05	0.00	0.00	0.07	0.00	0.00	0.00
TR-4-3-150-160-run1	GL2	0.07	4.86	19.65	0.01	0.13	1.80	2.50	0.37	0.01	0.01	0.14	3.27	0.00	0.00	0.00	0.01	0.00	0.00	0.01	0.01	0.00	0.03	0.00	0.00	0.06	0.00	0.00	0.00
TR-4-3-150-160-run2	GL2	0.13	4.85	19.81	0.01	0.13	1.80	2.52	0.37	0.01	0.01	0.15	3.23	0.00	0.00	0.00	0.01	0.00	0.00	0.01	0.01	0.00	0.03	0.00	0.00	0.12	0.00	0.00	0.00
TR-4-3-150-160-run3	GL2	0.11	4.87	19.67	0.01	0.13	1.78	2.51	0.37	0.01	0.01	0.14	3.20	0.00	0.00	0.00	0.01	0.00	0.00	0.01	0.01	0.00	0.03	0.00	0.00	0.00	0.00	0.00	0.00
TR-4-3-150-160-run4	GL2													0.00	0.00	0.00	0.01	0.00	0.00	0.01	0.01	0.00	0.03	0.00	0.00	0.12	0.00	0.00	0.00
TR-4-3-150-160-run5	GL2													0.00	0.01	0.00	0.01	0.00	0.00	0.01	0.01	0.00	0.03	0.00	0.00	0.06	0.00	0.00	0.00
TR-4-3-150-160-run6	GL2													0.00	0.00	0.00	0.01	0.00	0.00	0.01	0.01	0.00	0.03	0.00	0.00	0.06	0.00	0.00	0.00
	wt%	0.10	4.86	19.71	0.01	0.13	1.79	2.51	0.37	0.01	0.01	0.14	3.23	0.00	0.00	0.00	0.01	0.00	0.00	0.01	0.01	0.00	0.03	0.00	0.00	0.07	0.00	0.00	0.00
	Std. Dev.	0.03	0.01	0.08	0.00	0.00	0.01	0.01	0.00	0.00	0.00	0.00	0.03	0.00	0.00	0.00	0.00	0.00	0.00	0.00	0.00	0.00	0.00	0.00	0.00	0.05	0.00	0.00	0.00
	ppm	1033.97	48612.16	197106.18	113.89	1279.58	17897.93	25093.52	3720.43	92.41	64.77	1434.88	32334.06	13.74	48.49	39.08	100.26	15.88	18.10	114.32	126.18	37.20	284.33	12.11	23.04	694.62	16.42	8.67	0.07
	Oxide %	0.17	9.19	42.17	0.03	0.32	2.16	3.51	0.62	0.02	0.01	0.19	4.16	0.00	0.01	0.00	0.01	0.00	0.00	0.01	0.01	0.00	0.04	0.00	0.00	0.08	0.00	0.00	0.00
TR-5-1-0-10-run1	GL2	BDL	4.40	21.02	0.01	0.15	2.00	0.73	0.39	0.01	0.01	0.06	2.77	0.00	0.00	0.00	0.01	0.00	0.00	0.01	0.01	0.00	0.03	0.00	0.00	0.00	0.00	0.00	0.00
TR-5-1-0-10-run2	GL2	BDL	4.48	21.10	0.01	0.15	2.02	0.73	0.39	0.01	0.01	0.06	2.82	0.00	0.00	0.00	0.01	0.00	0.00	0.01	0.01	0.00	0.03	0.00	0.00	0.01	0.00	0.00	0.00
TR-5-1-0-10-run3	GL2	BDL	4.47	20.99	0.01	0.14	2.01	0.73	0.40	0.01	0.01	0.06	2.79	0.00	0.00	0.00	0.01	0.00	0.00	0.01	0.01	0.00	0.04	0.00	0.00	0.05	0.00	0.00	0.00
TR-5-1-0-10-run4	GL2													0.00	0.00	0.00	0.01	0.00	0.00	0.01	0.01	0.00	0.04	0.00	0.00	0.09	0.00	0.00	0.00
TR-5-1-0-10-run5	GL2													0.00	0.00	0.00	0.01	0.00	0.00	0.01	0.01	0.00	0.04	0.00	0.00	0.03	0.00	0.00	0.00
TR-5-1-0-10-run6	GL2													0.00	0.00	0.00	0.01	0.00	0.00	0.01	0.01	0.00	0.04	0.00	0.00	0.06	0.00	0.00	0.00
	wt%	BDL	4.45	21.03	0.01	0.15	2.01	0.73	0.39	0.01	0.01	0.06	2.79	0.00	0.00	0.00	0.01	0.00	0.00	0.01	0.01	0.00	0.04	0.00	0.00	0.04	0.00	0.00	0.00
	Std. Dev.	N/A	0.04	0.06	0.00	0.00	0.01	0.00	0.01	0.00	0.00	0.00	0.02	0.00	0.00	0.00	0.00	0.00	0.00	0.00	0.00	0.00	0.00	0.00	0.00	0.03	0.00	0.00	0.00
	ppm	BDL	44476.95	210349.93	132.58	1489.18	20100.31	7292.01	3937.97	82.10	95.12	580.08	27936.00	8.79	40.97	35.16	83.09	13.85	10.48	110.69	84.57	37.98	358.97	13.40	33.20	406.55	13.45	8.52	1.30
	Oxide %	BDL	8.40	45.00	0.03	0.37	2.42	1.02	0.66	0.01	0.01	0.07	3.59	0.00	0.01	0.00	0.01	0.00	0.00	0.01	0.01	0.00	0.05	0.00	0.00	0.05	0.00	0.00	0.00
TR-5-2-60-70-run1	GL2	0.05	3.99	16.66	0.02	0.14	1.60	6.30	0.32	0.01	0.01	0.04	2.75	0.00	0.00	0.00	0.01	0.00	0.00	0.01	0.01	0.00	0.03	0.00	0.00	0.00	0.00	0.00	0.00
TR-5-2-60-70-run2	GL2	0.05	3.96	16.67	0.01	0.13	1.59	6.25	0.32	0.00	0.01	0.04	2.68	0.00	0.00	0.00	0.01	0.00	0.00	0.01	0.01	0.00	0.03	0.00	0.00	0.00	0.00	0.00	0.00
TR-5-2-60-70-run3	GL2	0.14	4.04	17.21	0.01	0.14	1.63	6.10	0.35	0.00	0.01	0.04	2.76	0.00	0.00	0.00	0.01	0.00	0.00	0.01	0.01	0.00	0.03	0.00	0.00	0.01	0.00	0.00	0.00
TR-5-2-60-70-run4	GL2													0.00	0.00	0.00	0.01	0.00	0.00	0.01	0.01	0.00	0.03	0.00	0.00	0.01	0.00	0.00	0.00
TR-5-2-60-70-run5	GL2													0.00	0.00	0.00	0.01	0.00	0.00	0.01	0.01	0.00	0.03	0.00	0.00	0.03	0.00	0.00	0.00
TR-5-2-60-70-run6	GL2													0.00	0.00	0.00	0.01	0.00	0.00	0.01	0.01	0.00	0.03	0.00	0.00	0.07	0.00	0.00	0.00
	wt%	0.08	4.00	16.84	0.01	0.14	1.60	6.22	0.33	0.00	0.01	0.04	2.73	0.00	0.00	0.00	0.01	0.00	0.00	0.01</									

XRF Sample ID	Wt %	Mg	Al	Si	P	S	K	Ca	Ti	V	Cr	Mn	Fe	Co	Ni	Cu	Zn	Ga	As	Rb	Sr	Y	Zr	Nb	Mo	Ba	Pb	Th	U
TR-9-1B-38-48-run1	GL2	BDL	4.89	22.11	0.01	0.12	1.98	0.51	0.41	0.01	0.01	0.05	2.84	0.00	0.00	0.00	0.01	0.00	0.00	0.01	0.01	0.00	0.04	0.00	0.00	0.00	0.00	0.00	0.00
TR-9-1B-38-48-run2	GL2	BDL	4.87	22.05	0.01	0.13	1.95	0.50	0.40	0.01	0.01	0.05	2.84	0.00	0.00	0.00	0.01	0.00	0.00	0.01	0.01	0.00	0.04	0.00	0.00	0.06	0.00	0.00	0.00
TR-9-1B-38-48-run3	GL2	BDL	4.91	22.11	0.01	0.13	1.98	0.51	0.39	0.01	0.01	0.06	2.80	0.00	0.00	0.00	0.01	0.00	0.00	0.01	0.01	0.00	0.04	0.00	0.00	0.00	0.00	0.00	0.00
TR-9-1B-38-48-run4	GL2													0.00	0.00	0.00	0.01	0.00	0.00	0.01	0.01	0.00	0.04	0.00	0.00	0.00	0.00	0.00	0.00
TR-9-1B-38-48-run5	GL2													0.00	0.00	0.00	0.01	0.00	0.00	0.01	0.01	0.00	0.04	0.00	0.00	0.05	0.00	0.00	0.00
TR-9-1B-38-48-run6	GL2													0.00	0.00	0.00	0.01	0.00	0.00	0.01	0.01	0.00	0.04	0.00	0.00	0.07	0.00	0.00	0.00
	wt%	BDL	4.89	22.09	0.01	0.13	1.97	0.51	0.40	0.01	0.01	0.05	2.83	0.00	0.00	0.00	0.01	0.00	0.00	0.01	0.01	0.00	0.04	0.00	0.00	0.03	0.00	0.00	0.00
	Std. Dev.	N/A	0.02	0.04	0.00	0.01	0.01	0.01	0.01	0.00	0.00	0.00	0.02	0.00	0.00	0.00	0.00	0.00	0.00	0.00	0.00	0.00	0.00	0.00	0.00	0.03	0.00	0.00	0.00
	ppm	BDL	48881.89	220878.96	93.08	1284.90	19686.38	5086.60	3995.20	82.50	97.20	545.37	28263.45	8.67	38.69	33.85	80.60	14.03	9.65	117.29	102.44	38.26	399.54	13.40	41.74	305.68	13.41	8.96	1.31
	Oxide %	BDL	9.24	47.25	0.02	0.32	2.37	0.71	0.67	0.01	0.01	0.07	3.64	0.00	0.00	0.00	0.01	0.00	0.00	0.01	0.01	0.00	0.05	0.00	0.01	0.03	0.00	0.00	0.00
TR-9-1T-0-10-run1	GL2	BDL	4.36	23.01	0.01	0.14	1.86	0.55	0.38	0.01	0.01	0.06	2.13	0.00	0.00	0.00	0.01	0.00	0.00	0.01	0.01	0.00	0.04	0.00	0.01	0.04	0.00	0.00	0.00
TR-9-1T-0-10-run2	GL2	BDL	4.32	23.33	0.02	0.14	1.86	0.56	0.39	0.01	0.01	0.06	2.13	0.00	0.00	0.00	0.01	0.00	0.00	0.01	0.01	0.00	0.05	0.00	0.00	0.02	0.00	0.00	0.00
TR-9-1T-0-10-run3	GL2	BDL	4.20	22.01	0.01	0.14	1.85	0.55	0.38	0.01	0.01	0.06	2.23	0.00	0.00	0.00	0.01	0.00	0.00	0.01	0.01	0.00	0.04	0.00	0.00	0.00	0.00	0.00	0.00
TR-9-1T-0-10-run4	GL2													0.00	0.00	0.00	0.01	0.00	0.00	0.01	0.01	0.00	0.04	0.00	0.00	0.00	0.00	0.00	0.00
TR-9-1T-0-10-run5	GL2													0.00	0.00	0.00	0.01	0.00	0.00	0.01	0.01	0.00	0.04	0.00	0.00	0.06	0.00	0.00	0.00
TR-9-1T-0-10-run6	GL2													0.00	0.00	0.00	0.01	0.00	0.00	0.01	0.01	0.00	0.04	0.00	0.00	0.00	0.00	0.00	0.00
	wt%	BDL	4.30	22.78	0.02	0.14	1.86	0.55	0.38	0.01	0.01	0.06	2.16	0.00	0.00	0.00	0.01	0.00	0.00	0.01	0.01	0.00	0.04	0.00	0.00	0.02	0.00	0.00	0.00
	Std. Dev.	N/A	0.08	0.69	0.00	0.00	0.01	0.00	0.00	0.00	0.00	0.00	0.05	0.00	0.00	0.00	0.00	0.00	0.00	0.00	0.00	0.00	0.00	0.00	0.00	0.02	0.00	0.00	0.00
	ppm	BDL	42956.87	227835.85	153.50	1420.37	18568.95	5533.95	3818.87	81.28	102.48	584.36	21637.26	5.21	32.18	31.36	71.92	12.18	10.72	105.98	116.54	39.36	432.67	13.96	47.86	207.53	12.92	8.04	1.27
	Oxide %	BDL	8.12	48.74	0.04	0.35	2.24	0.77	0.64	0.01	0.01	0.08	2.78	0.00	0.00	0.00	0.01	0.00	0.00	0.01	0.01	0.00	0.06	0.00	0.01	0.02	0.00	0.00	0.00
TR-9-2-89-99-run1	GL2	BDL	5.33	21.03	0.01	0.13	2.00	0.51	0.38	0.01	0.01	0.07	3.25	0.00	0.00	0.00	0.01	0.00	0.00	0.01	0.01	0.00	0.04	0.00	0.00	0.05	0.00	0.00	0.00
TR-9-2-89-99-run2	GL2	0.00	5.30	20.95	0.01	0.13	1.99	0.51	0.38	0.01	0.01	0.07	3.24	0.00	0.00	0.00	0.01	0.00	0.00	0.01	0.01	0.00	0.04	0.00	0.00	0.00	0.00	0.00	0.00
TR-9-2-89-99-run3	GL2	0.00	5.29	20.94	0.01	0.12	1.99	0.51	0.38	0.01	0.01	0.07	3.22	0.00	0.00	0.00	0.01	0.00	0.00	0.01	0.01	0.00	0.04	0.00	0.00	0.08	0.00	0.00	0.00
TR-9-2-89-99-run4	GL2													0.00	0.00	0.00	0.01	0.00	0.00	0.01	0.01	0.00	0.04	0.00	0.00	0.18	0.00	0.00	0.00
TR-9-2-89-99-run5	GL2													0.00	0.00	0.00	0.01	0.00	0.00	0.01	0.01	0.00	0.03	0.00	0.00	0.01	0.00	0.00	0.00
TR-9-2-89-99-run6	GL2													0.00	0.00	0.00	0.01	0.00	0.00	0.01	0.01	0.00	0.03	0.00	0.00	0.08	0.00	0.00	0.00
	wt%	0.00	5.31	20.97	0.01	0.13	2.00	0.51	0.38	0.01	0.01	0.07	3.24	0.00	0.00	0.00	0.01	0.00	0.00	0.01	0.01	0.00	0.04	0.00	0.00	0.06	0.00	0.00	0.00
	Std. Dev.	0.00	0.02	0.05	0.00	0.00	0.01	0.00	0.00	0.00	0.00	0.00	0.02	0.00	0.00	0.00	0.00	0.00	0.00	0.00	0.00	0.00	0.00	0.00	0.00	0.07	0.00	0.00	0.00
	ppm	17.57	53052.92	209721.61	68.28	1294.79	19971.39	5095.72	3823.54	106.68	91.11	706.10	32358.30	10.45	45.08	36.31	88.00	15.23	13.61	123.91	101.40	37.70	351.39	13.05	35.58	649.51	14.70	9.43	0.78
	Oxide %	0.00	10.02	44.87	0.02	0.32	2.41	0.71	0.64	0.02	0.01	0.09	4.16	0.00	0.01	0.00	0.01	0.00	0.00	0.01	0.01	0.00	0.05	0.00	0.01	0.07	0.00	0.00	0.00
TR-9-3-142-152-run1	GL2	0.01	5.28	21.81	0.01	0.13	1.88	0.52	0.37	0.01	0.01	0.05	2.98	0.00	0.00	0.00	0.01	0.00	0.00	0.01	0.01	0.00	0.03	0.00	0.00	0.00	0.00	0.00	0.00
TR-9-3-142-152-run2	GL2	0.03	5.28	21.75	0.01	0.13	1.87	0.52	0.37	0.01	0.01	0.05	2.96	0.00	0.00	0.00	0.01	0.00	0.00	0.01	0.01	0.00	0.03	0.00	0.00	0.10	0.00	0.00	0.00
TR-9-3-142-152-run3	GL2	BDL	5.13	21.58	0.01	0.13	1.85	0.51	0.37	0.01	0.01	0.05	2.92	0.00	0.00	0.00	0.01	0.00	0.00	0.01	0.01	0.00	0.03	0.00	0.00	0.08	0.00	0.00	0.00
TR-9-3-142-152-run4	GL2													0.00	0.00	0.00	0.01	0.00	0.00	0.01	0.01	0.00	0.03	0.00	0.00	0.00	0.00	0.00	0.00
TR-9-3-142-152-run5	GL2													0.00	0.00	0.00	0.01	0.00	0.00	0.01	0.01	0.00	0.03	0.00	0.00	0.00	0.00	0.00	0.00
TR-9-3-142-152-run6	GL2													0.00	0.00	0.00	0.01	0.00	0.00	0.01	0.01	0.00	0.04	0.00	0.00	0.00	0.00	0.00	0.00
	wt%	0.02	5.23	21.71	0.01	0.13	1.86	0.51	0.37	0.01	0.01	0.05	2.95	0.00	0.00	0.00	0.01	0.00	0.00	0.01	0.01	0.00	0.03	0.00	0.00	0.03	0.00	0.00	0.00
	Std. Dev.	0.01	0.08	0.12	0.00	0.00	0.01	0.00	0.00	0.00	0.00	0.00	0.03	0.00	0.00	0.00	0.00	0.00	0.00	0.00	0.00	0.00	0.00	0.00	0.00	0.05	0.00	0.00	0.00
	ppm	235.29	52273.18	217145.62	116.64	1318.58	18648.81	5147.32	3726.72	100.42	99.94	462.70	29518.21	9.13	36.61	33.34	80.51	14.49	12.26	114.03	127.23	37.69	344.90	13.02	33.34	299.70	13.86	8.64	0.64
	Oxide %	0.04	9.88	46.45	0.03	0.33	2.25	0.72	0.62	0.02	0.01	0.06	3.80	0.00	0.00	0.00	0.01	0.00	0.00	0.01	0.02	0.00	0.05	0.00	0.01	0.03	0.00	0.00	0.00
TR-9-4-193-203-run1	GL2	BDL	4.84	22.57	0.01	0.13	1.97	0.52	0.39	0.01	0.01	0.07	2.62	0.00	0.00	0.00	0.01	0.00	0.00	0.01	0.01	0.00	0.04	0.00	0.00	0.05	0.00	0.00	0.00
TR-9-4-193-203-run2	GL2	BDL	4.82	22.62	0.01	0.13	1.98	0.51	0.39	0.01	0.01	0.07	2.61	0.00	0.00	0.00	0.01	0.00	0.00	0.01	0.01	0.00	0.04	0.00	0.00	0.08	0.00	0.00	0.00
TR-9-4-193-203-run3	GL2	BDL	4.73	21.91	0.01	0.13	1.93	0.50	0.39	0.01	0.01	0.07	2.60	0.00	0.00	0.00	0.01	0.00	0.00	0.01	0.01	0.00	0.04	0.00	0.00	0.03	0.00	0.00	0.00
TR-9-4-193-203-run4	GL2													0.00	0.00	0.00	0.01	0.00	0.00	0.01	0.01	0.00	0.04	0.00	0.00	0.08	0.00	0.00	0.00
TR-9-4-193-203-run5	GL2													0.00	0.00	0.00	0.01	0.00	0.00	0.01	0.01	0.00	0.04	0.00	0.00	0.14	0.00	0.00	0.00
TR-9-4-193-203-run6	GL2													0.00	0.00	0.00	0.01	0.00	0.00	0.01	0.01	0.00	0.03	0.00	0.00	0.04	0.00	0.00	0.00
	wt%	BDL	4.80	22.37	0.01	0.13	1.96	0.51	0.39	0.01	0.01	0.07	2.61	0.00	0.00	0.00	0.01												

XRF Sample ID	Wt %	Mg	Al	Si	P	S	K	Ca	Ti	V	Cr	Mn	Fe	Co	Ni	Cu	Zn	Ga	As	Rb	Sr	Y	Zr	Nb	Mo	Ba	Pb	Th	U
TR-SDK-2A-40-50-run1	GL2	BDL	5.00	21.22	0.01	0.14	1.88	0.84	0.39	0.01	0.01	0.05	3.20	0.00	0.01	0.00	0.01	0.00	0.00	0.01	0.01	0.00	0.03	0.00	0.00	0.05	0.00	0.00	0.00
TR-SDK-2A-40-50-run2	GL2	0.05	5.11	21.25	0.01	0.14	1.88	0.85	0.39	0.01	0.01	0.05	3.17	0.00	0.01	0.00	0.01	0.00	0.00	0.01	0.01	0.00	0.03	0.00	0.00	0.00	0.00	0.00	0.00
TR-SDK-2A-40-50-run3	GL2	0.04	5.01	20.93	0.01	0.14	1.84	0.82	0.39	0.01	0.01	0.05	3.14	0.00	0.01	0.00	0.01	0.00	0.00	0.01	0.01	0.00	0.03	0.00	0.00	0.08	0.00	0.00	0.00
TR-SDK-2A-40-50-run4	GL2													0.00	0.01	0.00	0.01	0.00	0.00	0.01	0.01	0.00	0.03	0.00	0.00	0.14	0.00	0.00	0.00
TR-SDK-2A-40-50-run5	GL2													0.00	0.01	0.00	0.01	0.00	0.00	0.01	0.01	0.00	0.03	0.00	0.00	0.04	0.00	0.00	0.00
TR-SDK-2A-40-50-run6	GL2													0.00	0.01	0.00	0.01	0.00	0.00	0.01	0.01	0.00	0.03	0.00	0.00	0.03	0.00	0.00	0.00
	wt%	0.05	5.04	21.13	0.01	0.14	1.87	0.84	0.39	0.01	0.01	0.05	3.17	0.00	0.01	0.00	0.01	0.00	0.00	0.01	0.01	0.00	0.03	0.00	0.00	0.06	0.00	0.00	0.00
	Std. Dev.	0.01	0.06	0.17	0.00	0.00	0.02	0.01	0.00	0.00	0.00	0.00	0.03	0.00	0.00	0.00	0.00	0.00	0.00	0.00	0.00	0.00	0.00	0.00	0.00	0.05	0.00	0.00	0.00
	ppm	460.62	50403.46	211348.03	135.33	1416.49	18655.25	8377.94	3907.90	104.21	104.92	488.54	31689.48	12.27	63.68	39.23	83.87	14.73	15.00	114.92	99.47	38.48	328.11	14.04	28.57	556.94	15.03	8.69	0.35
	Oxide %	0.08	9.52	45.21	0.03	0.35	2.25	1.17	0.65	0.02	0.02	0.06	4.08	0.00	0.01	0.00	0.01	0.00	0.00	0.01	0.01	0.00	0.04	0.00	0.00	0.06	0.00	0.00	0.00
TR-SDK-2A-50-60-run1	GL2	0.23	4.94	22.19	0.02	0.14	1.69	0.84	0.39	0.01	0.01	0.14	2.96	0.00	0.01	0.00	0.01	0.00	0.00	0.01	0.01	0.00	0.03	0.00	0.00	0.13	0.00	0.00	0.00
TR-SDK-2A-50-60-run2	GL2	0.27	4.99	22.30	0.02	0.13	1.71	0.85	0.40	0.01	0.01	0.14	3.00	0.00	0.01	0.00	0.01	0.00	0.00	0.01	0.01	0.00	0.03	0.00	0.00	0.18	0.00	0.00	0.00
TR-SDK-2A-50-60-run3	GL2	0.44	5.33	23.62	0.02	0.13	1.70	0.88	0.41	0.01	0.01	0.12	3.04	0.00	0.01	0.00	0.01	0.00	0.00	0.01	0.01	0.00	0.03	0.00	0.00	0.16	0.00	0.00	0.00
TR-SDK-2A-50-60-run4	GL2													0.00	0.01	0.00	0.01	0.00	0.00	0.01	0.01	0.00	0.03	0.00	0.00	0.00	0.00	0.00	0.00
TR-SDK-2A-50-60-run5	GL2													0.00	0.01	0.01	0.01	0.00	0.00	0.01	0.01	0.00	0.03	0.00	0.00	0.09	0.00	0.00	0.00
TR-SDK-2A-50-60-run6	GL2													0.00	0.01	0.00	0.01	0.00	0.00	0.01	0.01	0.00	0.03	0.00	0.00	0.11	0.00	0.00	0.00
	wt%	0.31	5.09	22.70	0.02	0.13	1.70	0.85	0.40	0.01	0.01	0.13	3.00	0.00	0.01	0.00	0.01	0.00	0.00	0.01	0.01	0.00	0.03	0.00	0.00	0.11	0.00	0.00	0.00
	Std. Dev.	0.11	0.21	0.80	0.00	0.00	0.01	0.02	0.01	0.00	0.00	0.01	0.04	0.00	0.00	0.00	0.00	0.00	0.00	0.00	0.00	0.00	0.00	0.00	0.00	0.06	0.00	0.00	0.00
	ppm	3137.11	50880.18	227023.52	182.72	1346.44	17013.91	8549.30	4022.81	114.12	98.50	1331.18	30035.09	10.47	113.05	48.04	83.93	14.92	18.52	103.75	115.62	38.51	344.69	15.23	30.49	1116.43	16.29	7.86	0.12
	Oxide %	0.52	9.61	48.57	0.04	0.34	2.05	1.20	0.67	0.02	0.01	0.17	3.86	0.00	0.01	0.01	0.01	0.00	0.00	0.01	0.01	0.00	0.05	0.00	0.00	0.12	0.00	0.00	0.00
TR-SDK-2B-0-10-run1	GL2	0.10	4.57	20.98	0.01	0.15	1.56	0.57	0.40	0.01	0.01	0.06	2.91	0.00	0.00	0.00	0.01	0.00	0.00	0.01	0.01	0.00	0.04	0.00	0.00	0.12	0.00	0.00	0.00
TR-SDK-2B-0-10-run2	GL2	0.07	4.70	21.28	0.01	0.16	1.58	0.57	0.41	0.01	0.01	0.06	2.96	0.00	0.00	0.00	0.01	0.00	0.00	0.01	0.01	0.00	0.04	0.00	0.00	0.06	0.00	0.00	0.00
TR-SDK-2B-0-10-run3	GL2	0.06	4.68	21.24	0.01	0.15	1.58	0.57	0.40	0.01	0.01	0.06	2.95	0.00	0.00	0.00	0.01	0.00	0.00	0.01	0.01	0.00	0.04	0.00	0.00	0.21	0.00	0.00	0.00
TR-SDK-2B-0-10-run4	GL2													0.00	0.01	0.00	0.01	0.00	0.00	0.01	0.01	0.00	0.04	0.00	0.00	0.11	0.00	0.00	0.00
TR-SDK-2B-0-10-run5	GL2													0.00	0.00	0.00	0.01	0.00	0.00	0.01	0.01	0.00	0.04	0.00	0.00	0.01	0.00	0.00	0.00
TR-SDK-2B-0-10-run6	GL2													0.00	0.01	0.00	0.01	0.00	0.00	0.01	0.01	0.00	0.04	0.00	0.00	0.02	0.00	0.00	0.00
	wt%	0.08	4.65	21.16	0.01	0.15	1.58	0.57	0.40	0.01	0.01	0.06	2.94	0.00	0.00	0.00	0.01	0.00	0.00	0.01	0.01	0.00	0.04	0.00	0.00	0.09	0.00	0.00	0.00
	Std. Dev.	0.02	0.07	0.16	0.00	0.00	0.01	0.00	0.01	0.00	0.00	0.00	0.02	0.00	0.00	0.00	0.00	0.00	0.00	0.00	0.00	0.00	0.00	0.00	0.00	0.08	0.00	0.00	0.00
	ppm	795.18	46517.03	211645.34	132.25	1527.60	15751.40	5728.86	4031.67	92.77	110.15	578.70	29389.64	7.70	48.09	36.06	86.55	14.25	11.30	106.11	96.86	38.80	412.94	14.44	41.45	886.63	13.92	8.17	0.39
	Oxide %	0.13	8.79	45.28	0.03	0.38	1.90	0.80	0.67	0.02	0.02	0.07	3.78	0.00	0.01	0.00	0.01	0.00	0.00	0.01	0.01	0.00	0.06	0.00	0.01	0.10	0.00	0.00	0.00
TR-SDK-2B-16-28-run1	GL2	BDL	5.10	21.09	0.01	0.14	1.52	0.45	0.41	0.01	0.01	0.04	3.17	0.00	0.00	0.00	0.01	0.00	0.00	0.01	0.01	0.00	0.03	0.00	0.00	0.12	0.00	0.00	0.00
TR-SDK-2B-16-28-run2	GL2	BDL	5.15	21.20	0.01	0.14	1.53	0.45	0.41	0.01	0.01	0.04	3.16	0.00	0.01	0.00	0.01	0.00	0.00	0.01	0.01	0.00	0.03	0.00	0.00	0.00	0.00	0.00	0.00
TR-SDK-2B-16-28-run3	GL2	BDL	5.10	21.16	0.01	0.14	1.53	0.45	0.41	0.01	0.01	0.04	3.19	0.00	0.00	0.00	0.01	0.00	0.00	0.01	0.01	0.00	0.03	0.00	0.00	0.06	0.00	0.00	0.00
TR-SDK-2B-16-28-run4	GL2													0.00	0.00	0.00	0.01	0.00	0.00	0.01	0.01	0.00	0.03	0.00	0.00	0.09	0.00	0.00	0.00
TR-SDK-2B-16-28-run5	GL2													0.00	0.00	0.00	0.01	0.00	0.00	0.01	0.01	0.00	0.03	0.00	0.00	0.09	0.00	0.00	0.00
TR-SDK-2B-16-28-run6	GL2													0.00	0.01	0.00	0.01	0.00	0.00	0.01	0.01	0.00	0.03	0.00	0.00	0.05	0.00	0.00	0.00
	wt%	BDL	5.12	21.15	0.01	0.14	1.53	0.45	0.41	0.01	0.01	0.04	3.17	0.00	0.00	0.00	0.01	0.00	0.00	0.01	0.01	0.00	0.03	0.00	0.00	0.07	0.00	0.00	0.00
	Std. Dev.	N/A	0.03	0.06	0.00	0.00	0.00	0.00	0.00	0.00	0.00	0.00	0.02	0.00	0.00	0.00	0.00	0.00	0.00	0.00	0.00	0.00	0.00	0.00	0.00	0.04	0.00	0.00	0.00
	ppm	BDL	51156.72	211512.83	68.19	1424.50	15259.24	4524.63	4092.88	94.68	103.20	388.38	31719.95	10.59	49.02	36.97	88.66	15.56	12.05	116.48	89.54	38.58	332.40	13.87	28.39	683.84	14.31	8.74	0.00
	Oxide %	BDL	9.67	45.25	0.02	0.36	1.84	0.63	0.68	0.02	0.02	0.05	4.08	0.00	0.01	0.00	0.01	0.00	0.00	0.01	0.01	0.00	0.04	0.00	0.00	0.08	0.00	0.00	0.00
TR-SDK-2B-28-35-run1	GL2	BDL	4.97	20.78	0.01	0.15	1.55	0.49	0.40	0.01	0.01	0.05	3.13	0.00	0.01	0.00	0.01	0.00	0.00	0.01	0.01	0.00	0.03	0.00	0.00	0.04	0.00	0.00	0.00
TR-SDK-2B-28-35-run2	GL2	BDL	5.06	21.01	0.01	0.15	1.57	0.51	0.40	0.01	0.01	0.05	3.13	0.00	0.01	0.00	0.01	0.00	0.00	0.01	0.01	0.00	0.03	0.00	0.00	0.16	0.00	0.00	0.00
TR-SDK-2B-28-35-run3	GL2	BDL	5.02	20.87	0.01	0.15	1.57	0.50	0.40	0.01	0.01	0.05	3.11	0.00	0.01	0.00	0.01	0.00	0.00	0.01	0.01	0.00	0.03	0.00	0.00	0.00	0.00	0.00	0.00
TR-SDK-2B-28-35-run4	GL2													0.00	0.01	0.00	0.01	0.00	0.00	0.01	0.01	0.00	0.03	0.00	0.00	0.06	0.00	0.00	0.00
TR-SDK-2B-28-35-run5	GL2													0.00	0.01	0.00	0.01	0.00	0.00	0.01	0.01	0.00	0.03	0.00	0.00	0.05	0.00	0.00	0.00
TR-SDK-2B-28-35-run6	GL2													0.00	0.00	0.00	0.01	0.00	0.00	0.01	0.01	0.00	0.03	0.00	0.00	0.16	0.00	0.00	0.00
	wt%	BDL	5.02	20.89	0.01	0.15	1.56	0.50	0.40	0.01	0.01	0.05	3.12	0.00	0.01														

XRF Sample ID	Wt %	Mg	Al	Si	P	S	K	Ca	Ti	V	Cr	Mn	Fe	Co	Ni	Cu	Zn	Ga	As	Rb	Sr	Y	Zr	Nb	Mo	Ba	Pb	Th	U
TR-SDK-3-30-34-run1	GL2	0.59	3.01	10.18	BDL	0.15	1.28	15.52	0.26	0.00	0.00	0.04	2.56	0.00	0.00	0.00	0.01	0.00	0.00	0.01	0.01	0.00	0.02	0.00	0.00	0.03	0.00	0.00	0.00
TR-SDK-3-30-34-run2	GL2	0.54	3.16	10.36	BDL	0.15	1.31	15.29	0.26	0.00	0.01	0.04	2.60	0.00	0.00	0.00	0.01	0.00	0.00	0.01	0.01	0.00	0.02	0.00	0.00	0.12	0.00	0.00	0.00
TR-SDK-3-30-34-run3	GL2	0.55	2.98	10.21	BDL	0.14	1.30	15.26	0.25	0.00	0.00	0.04	2.62	0.00	0.01	0.00	0.01	0.00	0.00	0.01	0.01	0.00	0.02	0.00	0.00	0.02	0.00	0.00	0.00
TR-SDK-3-30-34-run4	GL2													0.00	0.00	0.00	0.01	0.00	0.00	0.01	0.01	0.00	0.02	0.00	0.00	0.00	0.00	0.00	0.00
TR-SDK-3-30-34-run5	GL2													0.00	0.00	0.00	0.01	0.00	0.00	0.01	0.01	0.00	0.02	0.00	0.00	0.02	0.00	0.00	0.00
TR-SDK-3-30-34-run6	GL2													0.00	0.00	0.00	0.01	0.00	0.00	0.01	0.01	0.00	0.02	0.00	0.00	0.02	0.00	0.00	0.00
	wt%	0.56	3.05	10.25	N/A	0.15	1.29	15.36	0.26	0.00	0.00	0.04	2.59	0.00	0.00	0.00	0.01	0.00	0.00	0.01	0.01	0.00	0.02	0.00	0.00	0.05	0.00	0.00	0.00
	Std. Dev.	0.03	0.10	0.10	N/A	0.00	0.01	0.14	0.01	0.00	0.00	0.00	0.03	0.00	0.00	0.00	0.00	0.00	0.00	0.00	0.00	0.00	0.00	0.00	0.00	0.05	0.00	0.00	0.00
	ppm	5640.23	30529.60	102491.32	N/A	1457.72	12939.61	153570.24	2590.17	32.96	47.13	419.09	25919.19	11.34	47.92	40.91	78.39	12.97	11.83	92.45	74.18	32.09	170.32	8.95	7.31	492.23	13.64	7.14	0.00
	Oxide %	0.94	5.77	21.93	N/A	0.36	1.56	21.49	0.43	0.01	0.01	0.05	3.33	0.00	0.01	0.01	0.01	0.00	0.00	0.01	0.01	0.00	0.02	0.00	0.00	0.05	0.00	0.00	0.00
TR-SDK-3A-0-9-run1	GL2	0.14	4.41	19.52	0.02	0.17	1.59	1.31	0.39	0.01	0.01	0.12	3.06	0.00	0.01	0.00	0.01	0.00	0.00	0.01	0.01	0.00	0.04	0.00	0.00	0.09	0.00	0.00	0.00
TR-SDK-3A-0-9-run2	GL2	0.16	4.44	19.46	0.02	0.18	1.59	1.30	0.38	0.01	0.01	0.12	3.12	0.00	0.01	0.00	0.01	0.00	0.00	0.01	0.01	0.00	0.04	0.00	0.00	0.09	0.00	0.00	0.00
TR-SDK-3A-0-9-run3	GL2	0.13	4.43	19.45	0.02	0.18	1.59	1.32	0.38	0.01	0.01	0.12	3.07	0.00	0.01	0.00	0.01	0.00	0.00	0.01	0.01	0.00	0.04	0.00	0.00	0.00	0.00	0.00	0.00
TR-SDK-3A-0-9-run4	GL2													0.00	0.01	0.00	0.01	0.00	0.00	0.01	0.01	0.00	0.04	0.00	0.00	0.17	0.00	0.00	0.00
TR-SDK-3A-0-9-run5	GL2													0.00	0.01	0.00	0.01	0.00	0.00	0.01	0.01	0.00	0.04	0.00	0.00	0.11	0.00	0.00	0.00
TR-SDK-3A-0-9-run6	GL2													0.00	0.01	0.00	0.01	0.00	0.00	0.01	0.01	0.00	0.03	0.00	0.00	0.14	0.00	0.00	0.00
	wt%	0.14	4.43	19.48	0.02	0.18	1.59	1.31	0.38	0.01	0.01	0.12	3.08	0.00	0.01	0.00	0.01	0.00	0.00	0.01	0.01	0.00	0.03	0.00	0.00	0.10	0.00	0.00	0.00
	Std. Dev.	0.01	0.02	0.04	0.00	0.01	0.00	0.01	0.00	0.00	0.00	0.00	0.03	0.00	0.00	0.00	0.00	0.00	0.00	0.00	0.00	0.00	0.00	0.00	0.00	0.06	0.00	0.00	0.00
	ppm	1412.87	44258.03	194753.18	200.57	1779.68	15872.62	13085.41	3826.36	102.06	89.81	1241.19	30844.94	10.94	117.59	45.48	93.20	13.48	11.07	99.95	126.14	37.61	347.21	16.14	29.89	992.60	13.80	7.55	0.00
	Oxide %	0.23	8.36	41.66	0.05	0.44	1.91	1.83	0.64	0.02	0.01	0.16	3.97	0.00	0.01	0.01	0.01	0.00	0.00	0.01	0.01	0.00	0.05	0.00	0.00	0.11	0.00	0.00	0.00
TR-SDK-3A-16-22-run1	GL2	0.51	4.44	18.90	0.01	0.17	1.48	1.48	0.42	0.01	0.01	0.17	2.97	0.00	0.02	0.01	0.01	0.00	0.00	0.01	0.01	0.00	0.03	0.00	0.00	0.10	0.00	0.00	0.00
TR-SDK-3A-16-22-run2	GL2	0.41	4.41	18.99	0.02	0.17	1.48	1.48	0.41	0.01	0.01	0.17	2.93	0.00	0.02	0.01	0.01	0.00	0.00	0.01	0.01	0.00	0.03	0.00	0.00	0.16	0.00	0.00	0.00
TR-SDK-3A-16-22-run3	GL2	0.57	4.50	19.41	0.02	0.16	1.48	1.45	0.42	0.01	0.01	0.16	2.98	0.00	0.02	0.01	0.01	0.00	0.00	0.01	0.01	0.00	0.03	0.00	0.00	0.00	0.00	0.00	0.00
TR-SDK-3A-16-22-run4	GL2													0.00	0.02	0.01	0.01	0.00	0.00	0.01	0.01	0.00	0.03	0.00	0.00	0.07	0.00	0.00	0.00
TR-SDK-3A-16-22-run5	GL2													0.00	0.02	0.01	0.01	0.00	0.00	0.01	0.02	0.00	0.03	0.00	0.00	0.20	0.00	0.00	0.00
TR-SDK-3A-16-22-run6	GL2													0.00	0.02	0.01	0.01	0.00	0.00	0.01	0.01	0.00	0.03	0.00	0.00	0.08	0.00	0.00	0.00
	wt%	0.50	4.45	19.10	0.02	0.17	1.48	1.47	0.42	0.01	0.01	0.17	2.96	0.00	0.02	0.01	0.01	0.00	0.00	0.01	0.01	0.00	0.03	0.00	0.00	0.10	0.00	0.00	0.00
	Std. Dev.	0.08	0.05	0.27	0.00	0.01	0.00	0.01	0.01	0.00	0.00	0.00	0.03	0.00	0.00	0.00	0.00	0.00	0.00	0.00	0.00	0.00	0.00	0.00	0.00	0.07	0.00	0.00	0.00
	ppm	4958.70	44505.95	191011.33	163.54	1667.32	14803.84	14687.45	4204.60	91.27	92.95	1651.86	29619.75	13.41	190.75	57.74	92.03	14.42	13.86	96.36	143.15	37.79	329.68	19.48	27.78	1008.59	14.84	7.45	1.14
	Oxide %	0.82	8.41	40.86	0.04	0.42	1.78	2.06	0.70	0.02	0.01	0.21	3.81	0.00	0.02	0.01	0.01	0.00	0.00	0.01	0.02	0.00	0.04	0.00	0.00	0.11	0.00	0.00	0.00
TR-SDK-3A-27-32-run1	GL2	0.56	4.30	19.49	0.01	0.15	1.47	1.08	0.43	0.01	0.01	0.13	2.96	0.00	0.02	0.01	0.01	0.00	0.00	0.01	0.01	0.00	0.03	0.00	0.00	0.18	0.00	0.00	0.00
TR-SDK-3A-27-32-run2	GL2	0.71	4.55	20.37	0.02	0.15	1.51	1.15	0.44	0.01	0.01	0.14	2.98	0.00	0.02	0.01	0.01	0.00	0.00	0.01	0.01	0.00	0.03	0.00	0.00	0.24	0.00	0.00	0.00
TR-SDK-3A-27-32-run3	GL2	0.68	4.23	19.74	0.01	0.16	1.46	1.18	0.44	0.01	0.01	0.15	2.98	0.00	0.02	0.01	0.01	0.00	0.00	0.01	0.01	0.00	0.03	0.00	0.00	0.15	0.00	0.00	0.00
TR-SDK-3A-27-32-run4	GL2													0.00	0.02	0.01	0.01	0.00	0.00	0.01	0.01	0.00	0.03	0.00	0.00	0.04	0.00	0.00	0.00
TR-SDK-3A-27-32-run5	GL2													0.00	0.02	0.01	0.01	0.00	0.00	0.01	0.01	0.00	0.03	0.00	0.00	0.10	0.00	0.00	0.00
TR-SDK-3A-27-32-run6	GL2													0.00	0.02	0.01	0.01	0.00	0.00	0.01	0.02	0.00	0.03	0.00	0.00	0.14	0.00	0.00	0.00
	wt%	0.65	4.36	19.87	0.01	0.15	1.48	1.14	0.44	0.01	0.01	0.14	2.97	0.00	0.02	0.01	0.01	0.00	0.00	0.01	0.01	0.00	0.03	0.00	0.00	0.14	0.00	0.00	0.00
	Std. Dev.	0.08	0.16	0.45	0.00	0.00	0.02	0.05	0.01	0.00	0.00	0.01	0.01	0.00	0.00	0.00	0.00	0.00	0.00	0.00	0.00	0.00	0.00	0.00	0.00	0.07	0.00	0.00	0.00
	ppm	6524.21	43598.64	198653.20	134.86	1522.98	14799.12	11383.17	4362.74	96.12	113.04	1405.62	29731.10	15.60	219.52	63.69	86.93	14.40	14.78	93.38	143.96	36.84	338.51	20.29	28.84	1419.84	14.97	7.21	0.00
	Oxide %	1.08	8.24	42.50	0.03	0.38	1.78	1.59	0.73	0.02	0.02	0.18	3.82	0.00	0.03	0.01	0.01	0.00	0.00	0.01	0.02	0.00	0.05	0.00	0.00	0.16	0.00	0.00	0.00
TR-SDK-3A-43-49-run1	GL2	0.53	4.48	20.22	0.02	0.14	1.49	1.02	0.49	0.01	0.01	0.10	2.82	0.00	0.02	0.01	0.01	0.00	0.00	0.01	0.01	0.00	0.03	0.00	0.00	0.11	0.00	0.00	0.00
TR-SDK-3A-43-49-run2	GL2	0.67	4.44	20.19	0.01	0.14	1.48	1.01	0.46	0.01	0.01	0.10	2.92	0.00	0.02	0.01	0.01	0.00	0.00	0.01	0.01	0.00	0.03	0.00	0.00	0.17	0.00	0.00	0.00
TR-SDK-3A-43-49-run3	GL2	0.58	4.41	20.08	0.01	0.14	1.47	1.00	0.45	0.01	0.01	0.09	2.99	0.00	0.02	0.01	0.01	0.00	0.00	0.01	0.01	0.00	0.03	0.00	0.00	0.02	0.00	0.00	0.00
TR-SDK-3A-43-49-run4	GL2													0.00	0.02	0.01	0.01	0.00	0.00	0.01	0.01	0.00	0.03	0.00	0.00	0.18	0.00	0.00	0.00
TR-SDK-3A-43-49-run5	GL2													0.00	0.02	0.01	0.01	0.00	0.00	0.01	0.01	0.00	0.03	0.00	0.00	0.08	0.00	0.00	0.00
TR-SDK-3A-43-49-run6	GL2													0.00	0.02	0.01	0.01	0.00	0.00	0.01	0.01	0.00	0.03	0.00	0.00	0.05	0.00	0.00	0.00
	wt%	0.59	4.44	20.16	0.01	0.14	1.48	1.01	0.47	0.01	0.01	0.10	2.91	0.00</															

XRF Sample ID	Wt %	Mg	Al	Si	P	S	K	Ca	Ti	V	Cr	Mn	Fe	Co	Ni	Cu	Zn	Ga	As	Rb	Sr	Y	Zr	Nb	Mo	Ba	Pb	Th	U
TR-SDK-3B-57-61-run1	GL2	BDL	5.24	20.51	0.00	0.13	1.57	0.38	0.42	0.01	0.01	0.05	3.30	0.00	0.00	0.00	0.01	0.00	0.00	0.01	0.01	0.00	0.03	0.00	0.00	0.00	0.00	0.00	0.00
TR-SDK-3B-57-61-run2	GL2	BDL	5.18	20.44	0.00	0.13	1.56	0.38	0.42	0.01	0.01	0.05	3.33	0.00	0.00	0.00	0.01	0.00	0.00	0.01	0.01	0.00	0.03	0.00	0.00	0.11	0.00	0.00	0.00
TR-SDK-3B-57-61-run3	GL2	BDL	5.25	20.63	0.00	0.13	1.58	0.39	0.42	0.01	0.01	0.05	3.31	0.00	0.00	0.00	0.01	0.00	0.00	0.01	0.01	0.00	0.04	0.00	0.00	0.07	0.00	0.00	0.00
TR-SDK-3B-57-61-run4	GL2													0.00	0.00	0.00	0.01	0.00	0.00	0.01	0.01	0.00	0.04	0.00	0.00	0.00	0.00	0.00	0.00
TR-SDK-3B-57-61-run5	GL2													0.00	0.00	0.00	0.01	0.00	0.00	0.01	0.01	0.00	0.03	0.00	0.00	0.10	0.00	0.00	0.00
TR-SDK-3B-57-61-run6	GL2													0.00	0.00	0.00	0.01	0.00	0.00	0.01	0.01	0.00	0.03	0.00	0.00	0.10	0.00	0.00	0.00
	wt%	BDL	5.22	20.53	0.00	0.13	1.57	0.38	0.42	0.01	0.01	0.05	3.32	0.00	0.00	0.00	0.01	0.00	0.00	0.01	0.01	0.00	0.03	0.00	0.00	0.06	0.00	0.00	0.00
	Std. Dev.	N/A	0.04	0.09	0.00	0.00	0.01	0.00	0.00	0.00	0.00	0.00	0.02	0.00	0.00	0.00	0.00	0.00	0.00	0.00	0.00	0.00	0.00	0.00	0.00	0.05	0.00	0.00	0.00
	ppm	BDL	52225.90	205291.72	32.30	1330.41	15717.38	3824.29	4180.12	92.90	92.28	490.43	33167.10	11.51	45.63	37.17	86.59	15.85	13.30	119.30	85.26	39.98	344.01	14.20	31.24	635.07	15.13	9.00	-0.01
	Oxide %	BDL	9.87	43.92	0.01	0.33	1.89	0.54	0.70	0.02	0.01	0.06	4.27	0.00	0.01	0.00	0.01	0.00	0.00	0.01	0.01	0.01	0.05	0.00	0.00	0.07	0.00	0.00	0.00
TR-SDK-3B-61-68-run1	GL2	BDL	5.22	21.12	0.01	0.12	1.59	0.37	0.42	0.01	0.01	0.04	3.07	0.00	0.00	0.00	0.01	0.00	0.00	0.01	0.01	0.00	0.04	0.00	0.00	0.05	0.00	0.00	0.00
TR-SDK-3B-61-68-run2	GL2	BDL	5.28	21.46	0.01	0.13	1.62	0.38	0.43	0.01	0.01	0.05	3.10	0.00	0.00	0.00	0.01	0.00	0.00	0.01	0.01	0.00	0.04	0.00	0.00	0.15	0.00	0.00	0.00
TR-SDK-3B-61-68-run3	GL2	BDL	5.21	21.29	0.01	0.13	1.60	0.38	0.43	0.01	0.01	0.04	3.03	0.00	0.00	0.00	0.01	0.00	0.00	0.01	0.01	0.00	0.04	0.00	0.00	0.02	0.00	0.00	0.00
TR-SDK-3B-61-68-run4	GL2													0.00	0.00	0.00	0.01	0.00	0.00	0.01	0.01	0.00	0.04	0.00	0.00	0.17	0.00	0.00	0.00
TR-SDK-3B-61-68-run5	GL2													0.00	0.00	0.00	0.01	0.00	0.00	0.01	0.01	0.00	0.04	0.00	0.00	0.13	0.00	0.00	0.00
TR-SDK-3B-61-68-run6	GL2													0.00	0.00	0.00	0.01	0.00	0.00	0.01	0.01	0.00	0.04	0.00	0.00	0.05	0.00	0.00	0.00
	wt%	BDL	5.24	21.29	0.01	0.13	1.60	0.38	0.43	0.01	0.01	0.04	3.07	0.00	0.00	0.00	0.01	0.00	0.00	0.01	0.01	0.00	0.04	0.00	0.00	0.09	0.00	0.00	0.00
	Std. Dev.	N/A	0.04	0.17	0.00	0.00	0.02	0.01	0.00	0.00	0.00	0.00	0.03	0.00	0.00	0.00	0.00	0.00	0.00	0.00	0.00	0.00	0.00	0.00	0.00	0.06	0.00	0.00	0.00
	ppm	BDL	52393.19	212913.72	54.64	1278.92	16026.30	3757.40	4286.80	86.45	101.61	444.14	30660.95	10.40	46.68	35.82	86.26	15.42	8.60	120.39	85.32	39.53	355.60	14.10	31.65	939.72	13.80	9.11	0.19
	Oxide %	BDL	9.90	45.55	0.01	0.32	1.93	0.53	0.72	0.02	0.01	0.06	3.94	0.00	0.01	0.00	0.01	0.00	0.00	0.01	0.01	0.01	0.05	0.00	0.00	0.10	0.00	0.00	0.00
TR-SDK-3B-68-76-run1	GL2	BDL	5.50	21.79	0.01	0.13	1.66	0.38	0.44	0.01	0.01	0.04	2.97	0.00	0.00	0.00	0.01	0.00	0.00	0.01	0.01	0.00	0.03	0.00	0.00	0.12	0.00	0.00	0.00
TR-SDK-3B-68-76-run2	GL2	BDL	5.56	21.78	0.00	0.13	1.66	0.38	0.43	0.01	0.01	0.04	2.93	0.00	0.00	0.00	0.01	0.00	0.00	0.01	0.01	0.00	0.03	0.00	0.00	0.05	0.00	0.00	0.00
TR-SDK-3B-68-76-run3	GL2	BDL	5.50	21.73	0.00	0.12	1.67	0.39	0.45	0.01	0.01	0.04	2.93	0.00	0.00	0.00	0.01	0.00	0.00	0.01	0.01	0.00	0.04	0.00	0.00	0.05	0.00	0.00	0.00
TR-SDK-3B-68-76-run4	GL2													0.00	0.00	0.00	0.01	0.00	0.00	0.01	0.01	0.00	0.04	0.00	0.00	0.07	0.00	0.00	0.00
TR-SDK-3B-68-76-run5	GL2													0.00	0.00	0.00	0.01	0.00	0.00	0.01	0.01	0.00	0.03	0.00	0.00	0.03	0.00	0.00	0.00
TR-SDK-3B-68-76-run6	GL2													0.00	0.00	0.00	0.01	0.00	0.00	0.01	0.01	0.00	0.04	0.00	0.00	0.02	0.00	0.00	0.00
	wt%	BDL	5.52	21.77	0.00	0.13	1.66	0.38	0.44	0.01	0.01	0.04	2.95	0.00	0.00	0.00	0.01	0.00	0.00	0.01	0.01	0.00	0.04	0.00	0.00	0.06	0.00	0.00	0.00
	Std. Dev.	N/A	0.04	0.03	0.00	0.00	0.01	0.00	0.01	0.00	0.00	0.00	0.02	0.00	0.00	0.00	0.00	0.00	0.00	0.00	0.00	0.00	0.00	0.00	0.00	0.04	0.00	0.00	0.00
	ppm	BDL	55209.61	217666.27	45.07	1278.61	16604.83	3821.42	4391.16	85.22	101.18	429.50	29459.32	9.12	43.91	37.25	85.82	15.37	12.54	119.96	82.88	40.19	356.92	14.21	31.75	581.84	14.53	9.07	0.00
	Oxide %	BDL	10.43	46.57	0.01	0.32	2.00	0.53	0.73	0.02	0.01	0.06	3.79	0.00	0.01	0.00	0.01	0.00	0.00	0.01	0.01	0.01	0.05	0.00	0.00	0.06	0.00	0.00	0.00
TR-SDK-3B-7-16-run1	GL2	BDL	4.92	20.95	0.01	0.16	1.57	0.48	0.40	0.01	0.01	0.05	3.02	0.00	0.00	0.00	0.01	0.00	0.00	0.01	0.01	0.00	0.04	0.00	0.00	0.00	0.00	0.00	0.00
TR-SDK-3B-7-16-run2	GL2	BDL	4.89	20.84	0.01	0.15	1.57	0.48	0.40	0.01	0.01	0.05	3.03	0.00	0.00	0.00	0.01	0.00	0.00	0.01	0.01	0.00	0.04	0.00	0.00	0.02	0.00	0.00	0.00
TR-SDK-3B-7-16-run3	GL2	BDL	4.78	20.83	0.01	0.15	1.55	0.48	0.39	0.01	0.01	0.05	3.06	0.00	0.00	0.00	0.01	0.00	0.00	0.01	0.01	0.00	0.04	0.00	0.00	0.00	0.00	0.00	0.00
TR-SDK-3B-7-16-run4	GL2													0.00	0.00	0.00	0.01	0.00	0.00	0.01	0.01	0.00	0.04	0.00	0.00	0.00	0.00	0.00	0.00
TR-SDK-3B-7-16-run5	GL2													0.00	0.00	0.00	0.01	0.00	0.00	0.01	0.01	0.00	0.04	0.00	0.00	0.00	0.00	0.00	0.00
TR-SDK-3B-7-16-run6	GL2													0.00	0.00	0.00	0.01	0.00	0.00	0.01	0.01	0.00	0.04	0.00	0.00	0.02	0.00	0.00	0.00
	wt%	BDL	4.87	20.87	0.01	0.15	1.56	0.48	0.40	0.01	0.01	0.05	3.04	0.00	0.00	0.00	0.01	0.00	0.00	0.01	0.01	0.00	0.04	0.00	0.00	0.01	0.00	0.00	0.00
	Std. Dev.	N/A	0.07	0.06	0.00	0.00	0.01	0.00	0.01	0.00	0.00	0.00	0.02	0.00	0.00	0.00	0.00	0.00	0.00	0.00	0.00	0.00	0.00	0.00	0.00	0.01	0.00	0.00	0.00
	ppm	BDL	48652.81	208711.69	89.70	1532.59	15633.29	4771.34	3954.20	97.27	101.77	510.85	30368.48	8.72	46.25	36.28	84.38	15.04	13.65	109.34	94.73	39.49	394.14	13.82	39.99	59.11	14.71	8.23	0.86
	Oxide %	BDL	9.19	44.65	0.02	0.38	1.88	0.67	0.66	0.02	0.01	0.07	3.91	0.00	0.01	0.00	0.01	0.00	0.00	0.01	0.01	0.01	0.05	0.00	0.01	0.01	0.00	0.00	0.00
TR-SDK-4-0-16-run1	GL2	0.04	4.73	20.31	0.02	0.15	1.79	1.32	0.38	0.01	0.01	0.10	2.94	0.00	0.00	0.00	0.01	0.00	0.00	0.01	0.01	0.00	0.04	0.00	0.00	0.07	0.00	0.00	0.00
TR-SDK-4-0-16-run2	GL2	0.03	4.86	20.71	0.02	0.15	1.82	1.36	0.39	0.01	0.01	0.10	2.92	0.00	0.00	0.00	0.01	0.00	0.00	0.01	0.01	0.00	0.04	0.00	0.00	0.06	0.00	0.00	0.00
TR-SDK-4-0-16-run3	GL2	0.04	4.74	20.91	0.02	0.16	1.81	1.30	0.39	0.01	0.01	0.11	2.87	0.00	0.00	0.00	0.01	0.00	0.00	0.01	0.01	0.00	0.03	0.00	0.00	0.08	0.00	0.00	0.00
TR-SDK-4-0-16-run4	GL2													0.00	0.00	0.00	0.01	0.00	0.00	0.01	0.01	0.00	0.03	0.00	0.00	0.11	0.00	0.00	0.00
TR-SDK-4-0-16-run5	GL2													0.00	0.00	0.00	0.01	0.00	0.00	0.01	0.01	0.00	0.04	0.00	0.00	0.04	0.00	0.00	0.00
TR-SDK-4-0-16-run6	GL2													0.00	0.00	0.00	0.01	0.00	0.00	0.01	0.01	0.00	0.04	0.00	0.00	0.05	0.00	0.00	0.00
	wt%	0.03	4.78	20.64	0.02	0.16	1.81	1.33	0.39	0.01	0.01	0.10	2.91	0.00	0.00	0.00	0.01	0.00	0.00	0.01	0.01	0.00							

XRF Sample ID	Wt %	Mg	Al	Si	P	S	K	Ca	Ti	V	Cr	Mn	Fe	Co	Ni	Cu	Zn	Ga	As	Rb	Sr	Y	Zr	Nb	Mo	Ba	Pb	Th	U
TR-SDK-4A-37-42-run1	GL2	0.21	4.59	20.57	0.01	0.13	1.60	1.15	0.41	0.01	0.01	0.06	2.81	0.00	0.01	0.00	0.01	0.00	0.00	0.01	0.01	0.00	0.04	0.00	0.00	0.10	0.00	0.00	0.00
TR-SDK-4A-37-42-run2	GL2	0.21	4.64	20.55	0.01	0.12	1.59	1.13	0.41	0.01	0.01	0.06	2.86	0.00	0.01	0.00	0.01	0.00	0.00	0.01	0.01	0.00	0.04	0.00	0.00	0.08	0.00	0.00	0.00
TR-SDK-4A-37-42-run3	GL2	0.15	4.55	20.44	0.01	0.13	1.60	1.14	0.40	0.01	0.01	0.06	2.83	0.00	0.01	0.00	0.01	0.00	0.00	0.01	0.01	0.00	0.03	0.00	0.00	0.21	0.00	0.00	0.00
TR-SDK-4A-37-42-run4	GL2													0.00	0.01	0.00	0.01	0.00	0.00	0.01	0.01	0.00	0.03	0.00	0.00	0.09	0.00	0.00	0.00
TR-SDK-4A-37-42-run5	GL2													0.00	0.01	0.01	0.01	0.00	0.00	0.01	0.01	0.00	0.03	0.00	0.00	0.05	0.00	0.00	0.00
TR-SDK-4A-37-42-run6	GL2													0.00	0.01	0.01	0.01	0.00	0.00	0.01	0.01	0.00	0.03	0.00	0.00	0.20	0.00	0.00	0.00
	wt%	0.19	4.59	20.52	0.01	0.13	1.60	1.14	0.41	0.01	0.01	0.06	2.83	0.00	0.01	0.00	0.01	0.00	0.00	0.01	0.01	0.00	0.04	0.00	0.00	0.12	0.00	0.00	0.00
	Std. Dev.	0.03	0.05	0.07	0.00	0.00	0.01	0.01	0.00	0.00	0.00	0.00	0.03	0.00	0.00	0.00	0.00	0.00	0.00	0.00	0.00	0.00	0.00	0.00	0.00	0.07	0.00	0.00	0.00
	ppm	1886.01	45932.48	205194.27	118.05	1272.12	16006.78	11418.18	4058.62	86.53	110.13	613.69	28336.33	10.58	134.03	48.62	84.17	14.37	10.87	102.13	125.13	38.36	352.91	16.16	34.22	1224.59	14.13	7.85	0.84
	Oxide %	0.31	8.68	43.90	0.03	0.32	1.93	1.60	0.68	0.02	0.02	0.08	3.65	0.00	0.02	0.01	0.01	0.00	0.00	0.01	0.01	0.00	0.05	0.00	0.01	0.14	0.00	0.00	0.00
TR-SDK-5-0-12-run1	GL2	BDL	4.54	19.99	0.01	0.16	1.81	1.07	0.38	0.01	0.01	0.10	3.06	0.00	0.01	0.00	0.01	0.00	0.00	0.01	0.01	0.00	0.03	0.00	0.00	0.15	0.00	0.00	0.00
TR-SDK-5-0-12-run2	GL2	BDL	4.64	19.58	0.01	0.16	1.78	1.05	0.36	0.01	0.01	0.09	3.06	0.00	0.00	0.00	0.01	0.00	0.00	0.01	0.01	0.00	0.03	0.00	0.00	0.02	0.00	0.00	0.00
TR-SDK-5-0-12-run3	GL2	BDL	4.68	20.69	0.02	0.15	1.83	1.07	0.39	0.01	0.01	0.11	2.95	0.00	0.00	0.00	0.01	0.00	0.00	0.01	0.01	0.00	0.02	0.00	0.00	0.03	0.00	0.00	0.00
TR-SDK-5-0-12-run4	GL2													0.00	0.00	0.00	0.01	0.00	0.00	0.01	0.01	0.00	0.02	0.00	0.00	0.00	0.00	0.00	0.00
TR-SDK-5-0-12-run5	GL2													0.00	0.00	0.00	0.01	0.00	0.00	0.01	0.01	0.00	0.03	0.00	0.00	0.04	0.00	0.00	0.00
TR-SDK-5-0-12-run6	GL2													0.00	0.01	0.00	0.01	0.00	0.00	0.01	0.01	0.00	0.03	0.00	0.00	0.00	0.00	0.00	0.00
	wt%	BDL	4.62	20.09	0.01	0.15	1.80	1.06	0.38	0.01	0.01	0.10	3.02	0.00	0.00	0.00	0.01	0.00	0.00	0.01	0.01	0.00	0.03	0.00	0.00	0.04	0.00	0.00	0.00
	Std. Dev.	N/A	0.08	0.56	0.00	0.00	0.02	0.01	0.02	0.00	0.00	0.01	0.06	0.00	0.00	0.00	0.00	0.00	0.00	0.00	0.00	0.00	0.00	0.00	0.00	0.06	0.00	0.00	0.00
	ppm	BDL	46198.53	200854.92	137.58	1529.51	18040.26	10637.42	3776.83	99.63	85.27	975.37	30246.19	9.31	42.26	32.47	78.53	13.19	15.21	104.23	91.79	35.83	305.55	13.54	23.17	401.45	14.81	7.82	0.00
	Oxide %	BDL	8.73	42.97	0.03	0.38	2.17	1.49	0.63	0.02	0.01	0.13	3.89	0.00	0.01	0.00	0.01	0.00	0.00	0.01	0.01	0.00	0.04	0.00	0.00	0.04	0.00	0.00	0.00
TR-SDK-5-16-20-run1	GL2	0.05	4.87	19.93	0.01	0.14	1.83	1.96	0.39	0.01	0.01	0.08	3.11	0.00	0.01	0.00	0.01	0.00	0.00	0.01	0.01	0.00	0.03	0.00	0.00	0.02	0.00	0.00	0.00
TR-SDK-5-16-20-run2	GL2	0.04	4.89	19.86	0.02	0.15	1.85	1.99	0.38	0.01	0.01	0.08	3.11	0.00	0.01	0.00	0.01	0.00	0.00	0.01	0.01	0.00	0.03	0.00	0.00	0.04	0.00	0.00	0.00
TR-SDK-5-16-20-run3	GL2	0.04	4.99	20.08	0.02	0.15	1.88	2.00	0.38	0.01	0.01	0.08	3.14	0.00	0.01	0.00	0.01	0.00	0.00	0.01	0.01	0.00	0.03	0.00	0.00	0.00	0.00	0.00	0.00
TR-SDK-5-16-20-run4	GL2													0.00	0.01	0.00	0.01	0.00	0.00	0.01	0.01	0.00	0.03	0.00	0.00	0.01	0.00	0.00	0.00
TR-SDK-5-16-20-run5	GL2													0.00	0.01	0.00	0.01	0.00	0.00	0.01	0.01	0.00	0.03	0.00	0.00	0.11	0.00	0.00	0.00
TR-SDK-5-16-20-run6	GL2													0.00	0.00	0.00	0.01	0.00	0.00	0.01	0.01	0.00	0.03	0.00	0.00	0.11	0.00	0.00	0.00
	wt%	0.04	4.92	19.96	0.02	0.15	1.85	1.98	0.38	0.01	0.01	0.08	3.12	0.00	0.01	0.00	0.01	0.00	0.00	0.01	0.01	0.00	0.03	0.00	0.00	0.05	0.00	0.00	0.00
	Std. Dev.	0.01	0.07	0.11	0.00	0.00	0.02	0.02	0.00	0.00	0.00	0.00	0.02	0.00	0.00	0.00	0.00	0.00	0.00	0.00	0.00	0.00	0.00	0.00	0.00	0.05	0.00	0.00	0.00
	ppm	429.85	49163.14	199584.19	153.96	1467.73	18545.86	19839.59	3836.47	92.76	82.19	789.93	31193.17	12.57	52.13	38.01	88.03	16.11	18.51	114.95	98.43	37.74	326.20	12.82	29.36	473.29	16.61	8.78	0.49
	Oxide %	0.07	9.29	42.70	0.04	0.37	2.23	2.78	0.64	0.02	0.01	0.10	4.01	0.00	0.01	0.00	0.01	0.00	0.00	0.01	0.01	0.00	0.04	0.00	0.00	0.05	0.00	0.00	0.00
TR-SDK-5-20-26-run1	GL2	0.15	4.65	18.54	0.01	0.15	1.87	2.48	0.37	0.01	0.01	0.09	3.27	0.00	0.01	0.00	0.01	0.00	0.00	0.01	0.01	0.00	0.03	0.00	0.00	0.05	0.00	0.00	0.00
TR-SDK-5-20-26-run2	GL2	0.16	4.67	18.30	0.01	0.14	1.84	2.44	0.37	0.01	0.01	0.08	3.20	0.00	0.01	0.00	0.01	0.00	0.00	0.01	0.01	0.00	0.03	0.00	0.00	0.12	0.00	0.00	0.00
TR-SDK-5-20-26-run3	GL2	0.09	4.73	18.28	0.01	0.15	1.86	2.44	0.37	0.01	0.01	0.09	3.25	0.00	0.01	0.00	0.01	0.00	0.00	0.01	0.01	0.00	0.03	0.00	0.00	0.14	0.00	0.00	0.00
TR-SDK-5-20-26-run4	GL2													0.00	0.01	0.00	0.01	0.00	0.00	0.01	0.01	0.00	0.03	0.00	0.00	0.05	0.00	0.00	0.00
TR-SDK-5-20-26-run5	GL2													0.00	0.01	0.00	0.01	0.00	0.00	0.01	0.01	0.00	0.03	0.00	0.00	0.16	0.00	0.00	0.00
TR-SDK-5-20-26-run6	GL2													0.00	0.01	0.00	0.01	0.00	0.00	0.01	0.01	0.00	0.03	0.00	0.00	0.05	0.00	0.00	0.00
	wt%	0.13	4.68	18.37	0.01	0.15	1.85	2.45	0.37	0.01	0.01	0.09	3.24	0.00	0.01	0.00	0.01	0.00	0.00	0.01	0.01	0.00	0.03	0.00	0.00	0.09	0.00	0.00	0.00
	Std. Dev.	0.04	0.04	0.14	0.00	0.01	0.02	0.02	0.00	0.00	0.00	0.00	0.04	0.00	0.00	0.00	0.00	0.00	0.00	0.00	0.00	0.00	0.00	0.00	0.00	0.05	0.00	0.00	0.00
	ppm	1330.07	46821.08	183724.36	90.80	1490.82	18547.50	24532.24	3734.53	93.74	77.78	861.20	32399.61	13.10	53.69	39.78	86.30	16.02	24.06	116.28	90.56	38.85	320.34	12.57	26.59	947.19	18.02	8.80	0.83
	Oxide %	0.22	8.85	39.30	0.02	0.37	2.23	3.43	0.62	0.02	0.01	0.11	4.17	0.00	0.01	0.00	0.01	0.00	0.00	0.01	0.01	0.00	0.04	0.00	0.00	0.11	0.00	0.00	0.00
TR-SDK-5-25-27-run1	GL2	BDL	4.67	18.98	0.01	0.15	1.82	2.00	0.38	0.01	0.01	0.09	3.16	0.00	0.00	0.00	0.01	0.00	0.00	0.01	0.01	0.00	0.03	0.00	0.00	0.11	0.00	0.00	0.00
TR-SDK-5-25-27-run2	GL2	0.04	4.69	19.07	0.01	0.15	1.82	1.97	0.38	0.01	0.01	0.09	3.09	0.00	0.00	0.00	0.01	0.00	0.00	0.01	0.01	0.00	0.03	0.00	0.00	0.14	0.00	0.00	0.00
TR-SDK-5-25-27-run3	GL2	BDL	4.50	19.06	0.02	0.14	1.79	2.01	0.38	0.01	0.01	0.09	3.09	0.00	0.00	0.00	0.01	0.00	0.00	0.01	0.01	0.00	0.03	0.00	0.00	0.01	0.00	0.00	0.00
TR-SDK-5-25-27-run4	GL2													0.00	0.01	0.00	0.01	0.00	0.00	0.01	0.01	0.00	0.03	0.00	0.00	0.08	0.00	0.00	0.00
TR-SDK-5-25-27-run5	GL2													0.00	0.01	0.00	0.01	0.00	0.00	0.01	0.01	0.00	0.03	0.00	0.00	0.01	0.00	0.00	0.00
TR-SDK-5-25-27-run6	GL2													0.00	0.00	0.00	0.01	0.00	0.00	0.01	0.01	0.00	0.03	0.00	0.00	0.04	0.00	0.00	0.00
	wt%	0.04	4.62	19.04	0.01	0.14	1.81	1.99	0.38	0.01	0.01	0.09	3.11	0.00	0.01	0.00	0.01												

B.3 – XRF Processed Data per Core Location (wt %)

Konza 3

Depth (cm)	Mg	Al	Si	P	S	K	Ca
0	0.00	4.03	24.14	0.03	0.15	1.73	0.55
35	0.02	5.32	21.45	0.02	0.12	1.81	0.50
86	0.00	5.14	21.83	0.02	0.12	1.81	0.53
143	0.00	4.86	22.23	0.02	0.12	1.82	0.59

Depth (cm)	Ti	V	Cr	Mn	Fe	Co	Ni
0	0.38	0.01	0.01	0.06	2.07	0.00	0.00
35	0.37	0.01	0.01	0.06	3.21	0.00	0.00
86	0.37	0.01	0.01	0.06	2.92	0.00	0.00
143	0.37	0.01	0.01	0.06	2.86	0.00	0.00

Depth (cm)	Cu	Zn	Ga	As	Rb	Sr	Y
0	0.00	0.01	0.00	0.00	0.01	0.01	0.00
35	0.00	0.01	0.00	0.00	0.01	0.01	0.00
86	0.00	0.01	0.00	0.00	0.01	0.01	0.00
143	0.00	0.01	0.00	0.00	0.01	0.02	0.00

Depth (cm)	Zr	Nb	Mo	Ba	Pb	Th	U
0	0.04	0.00	0.00	0.06	0.00	0.00	0.00
35	0.03	0.00	0.00	0.06	0.00	0.00	0.00
86	0.03	0.00	0.00	0.05	0.00	0.00	0.00
143	0.03	0.00	0.00	0.12	0.00	0.00	0.00

Konza 4

Depth (cm)	Mg	Al	Si	P	S	K	Ca
0	0.00	3.91	23.60	0.03	0.15	1.73	0.49
38	0.00	4.87	22.13	0.02	0.14	1.84	0.40
92	0.00	5.08	20.73	0.01	0.11	1.81	0.52
150	0.15	4.87	19.74	0.02	0.12	1.76	2.52

Depth (cm)	Ti	V	Cr	Mn	Fe	Co	Ni
0	0.40	0.01	0.01	0.06	2.12	0.00	0.00
38	0.42	0.01	0.01	0.06	2.49	0.00	0.00
92	0.38	0.01	0.01	0.06	3.20	0.00	0.00
150	0.36	0.01	0.01	0.12	3.30	0.00	0.00

Depth (cm)	Cu	Zn	Ga	As	Rb	Sr	Y
0	0.00	0.01	0.00	0.00	0.01	0.01	0.00
38	0.00	0.01	0.00	0.00	0.01	0.01	0.00
92	0.00	0.01	0.00	0.00	0.01	0.01	0.00
150	0.00	0.01	0.00	0.00	0.01	0.01	0.00

Depth (cm)	Zr	Nb	Mo	Ba	Pb	Th	U
0	0.04	0.00	0.00	0.04	0.00	0.00	0.00
38	0.04	0.00	0.00	0.07	0.00	0.00	0.00
92	0.03	0.00	0.00	0.06	0.00	0.00	0.00
150	0.03	0.00	0.00	0.07	0.00	0.00	0.00

Konza 5

Depth (cm)	Mg	Al	Si	P	S	K	Ca
0	0.00	4.44	20.82	0.02	0.14	2.03	0.74
60	0.06	4.04	17.10	0.02	0.13	1.64	6.12

Depth (cm)	Ti	V	Cr	Mn	Fe	Co	Ni
0	0.39	0.01	0.01	0.06	2.86	0.00	0.00
60	0.33	0.00	0.01	0.04	2.82	0.00	0.00

Depth (cm)	Cu	Zn	Ga	As	Rb	Sr	Y
0	0.00	0.01	0.00	0.00	0.01	0.01	0.00
60	0.00	0.01	0.00	0.00	0.01	0.01	0.00

Depth (cm)	Zr	Nb	Mo	Ba	Pb	Th	U
0	0.04	0.00	0.00	0.04	0.00	0.00	0.00
60	0.03	0.00	0.00	0.02	0.00	0.00	0.00

Konza 6

Depth (cm)	Mg	Al	Si	P	S	K	Ca
0	0.00	4.61	20.61	0.01	0.15	1.66	0.52
30	0.02	5.76	17.62	0.00	0.14	1.52	0.61
70	0.42	3.10	9.50	0.00	0.13	1.31	17.21
120	0.43	3.35	10.81	0.00	0.13	1.53	15.90

Depth (cm)	Ti	V	Cr	Mn	Fe	Co	Ni
0	0.38	0.01	0.01	0.05	2.94	0.00	0.00
30	0.35	0.01	0.01	0.06	4.70	0.00	0.01
70	0.22	0.00	0.00	0.03	2.77	0.00	0.01
120	0.24	0.00	0.00	0.04	2.71	0.00	0.01

Depth (cm)	Cu	Zn	Ga	As	Rb	Sr	Y
0	0.00	0.01	0.00	0.00	0.01	0.01	0.00
30	0.00	0.02	0.00	0.00	0.01	0.00	0.00
70	0.01	0.02	0.00	0.00	0.01	0.01	0.00
120	0.01	0.02	0.00	0.00	0.01	0.01	0.00

Depth (cm)	Zr	Nb	Mo	Ba	Pb	Th	U
0	0.04	0.00	0.00	0.04	0.00	0.00	0.00
30	0.03	0.00	0.00	0.04	0.00	0.00	0.00
70	0.01	0.00	0.00	0.02	0.00	0.00	0.00
120	0.01	0.00	0.00	0.02	0.00	0.00	0.00

Konza 9

Depth (cm)	Mg	Al	Si	P	S	K	Ca
0	0.00	4.36	22.89	0.02	0.13	1.86	0.56
38	0.00	5.06	22.30	0.02	0.12	2.00	0.55
89	0.01	5.22	20.75	0.01	0.12	1.96	0.51
142	0.00	5.00	21.30	0.01	0.12	1.86	0.52
193	0.00	4.81	22.23	0.02	0.12	1.95	0.53

Depth (cm)	Ti	V	Cr	Mn	Fe	Co	Ni
0	0.38	0.01	0.01	0.05	2.21	0.00	0.00
38	0.39	0.01	0.01	0.05	2.83	0.00	0.00
89	0.37	0.01	0.01	0.06	3.26	0.00	0.00
142	0.36	0.01	0.01	0.05	2.97	0.00	0.00
193	0.37	0.01	0.01	0.07	2.65	0.00	0.00

Depth (cm)	Cu	Zn	Ga	As	Rb	Sr	Y
0	0.00	0.01	0.00	0.00	0.01	0.01	0.00
38	0.00	0.01	0.00	0.00	0.01	0.01	0.00
89	0.00	0.01	0.00	0.00	0.01	0.01	0.00
142	0.00	0.01	0.00	0.00	0.01	0.01	0.00
193	0.00	0.01	0.00	0.00	0.01	0.01	0.00

Depth (cm)	Zr	Nb	Mo	Ba	Pb	Th	U
0	0.04	0.00	0.00	0.02	0.00	0.00	0.00
38	0.04	0.00	0.00	0.03	0.00	0.00	0.00
89	0.04	0.00	0.00	0.06	0.00	0.00	0.00
142	0.03	0.00	0.00	0.03	0.00	0.00	0.00
193	0.03	0.00	0.00	0.07	0.00	0.00	0.00

Konza 10

Depth (cm)	Mg	Al	Si	P	S	K	Ca
0	0.02	4.42	19.66	0.03	0.13	1.79	1.96
50	0.02	4.74	21.11	0.02	0.14	1.86	1.29
100	0.14	4.71	19.24	0.02	0.13	1.86	3.53
150	0.05	4.95	20.77	0.02	0.12	1.90	1.49

Depth (cm)	Ti	V	Cr	Mn	Fe	Co	Ni
0	0.37	0.01	0.01	0.07	2.72	0.00	0.00
50	0.37	0.01	0.01	0.10	2.93	0.00	0.00
100	0.37	0.01	0.01	0.07	3.12	0.00	0.00
150	0.38	0.01	0.01	0.13	2.80	0.00	0.00

Depth (cm)	Cu	Zn	Ga	As	Rb	Sr	Y
0	0.00	0.01	0.00	0.00	0.01	0.01	0.00
50	0.00	0.01	0.00	0.00	0.01	0.01	0.00
100	0.00	0.01	0.00	0.00	0.01	0.01	0.00
150	0.00	0.01	0.00	0.00	0.01	0.01	0.00

Depth (cm)	Zr	Nb	Mo	Ba	Pb	Th	U
0	0.05	0.00	0.00	0.04	0.00	0.00	0.00
50	0.04	0.00	0.00	0.04	0.00	0.00	0.00
100	0.03	0.00	0.00	0.02	0.00	0.00	0.00
150	0.03	0.00	0.00	0.07	0.00	0.00	0.00

SDK 1							
Depth (cm)	Mg	Al	Si	P	S	K	Ca
0	0.17	4.14	18.41	0.02	0.15	1.57	1.24
12	0.82	4.06	18.86	0.04	0.14	1.45	1.26
Depth (cm)	Ti	V	Cr	Mn	Fe	Co	Ni
0	0.37	0.01	0.01	0.08	3.16	0.00	0.02
12	0.40	0.01	0.01	0.09	3.17	0.00	0.03
Depth (cm)	Cu	Zn	Ga	As	Rb	Sr	Y
0	0.01	0.01	0.00	0.00	0.01	0.01	0.00
12	0.01	0.01	0.00	0.00	0.01	0.02	0.00
Depth (cm)	Zr	Nb	Mo	Ba	Pb	Th	U
0	0.03	0.00	0.00	0.07	0.00	0.00	0.00
12	0.03	0.00	0.00	0.10	0.00	0.00	0.00

SDK 2							
Depth (cm)	Mg	Al	Si	P	S	K	Ca
0	0.00	4.38	20.30	0.04	0.14	1.79	0.93
35	0.00	4.73	20.38	0.02	0.14	1.75	0.85
50	0.17	4.86	19.91	0.02	0.12	1.72	1.20
Depth (cm)	Ti	V	Cr	Mn	Fe	Co	Ni
0	0.37	0.01	0.01	0.06	2.81	0.00	0.00
35	0.38	0.01	0.01	0.06	3.14	0.00	0.01
50	0.39	0.01	0.01	0.04	3.29	0.00	0.01
Depth (cm)	Cu	Zn	Ga	As	Rb	Sr	Y
0	0.00	0.01	0.00	0.00	0.01	0.01	0.00
35	0.00	0.01	0.00	0.00	0.01	0.01	0.00
50	0.00	0.01	0.00	0.00	0.01	0.01	0.00
Depth (cm)	Zr	Nb	Mo	Ba	Pb	Th	U
0	0.03	0.00	0.00	0.05	0.00	0.00	0.00
35	0.03	0.00	0.00	0.03	0.00	0.00	0.00
50	0.03	0.00	0.00	0.09	0.00	0.00	0.00

SDK 3							
Depth (cm)	Mg	Al	Si	P	S	K	Ca
0	0.00	4.58	20.01	0.02	0.14	1.84	1.07
30	0.53	3.33	11.03	0.01	0.13	1.35	15.37
Depth (cm)	Ti	V	Cr	Mn	Fe	Co	Ni
0	0.38	0.01	0.01	0.12	3.08	0.00	0.00
30	0.26	0.00	0.01	0.04	2.68	0.00	0.00
Depth (cm)	Cu	Zn	Ga	As	Rb	Sr	Y
0	0.00	0.01	0.00	0.00	0.01	0.01	0.00
30	0.00	0.01	0.00	0.00	0.01	0.01	0.00
Depth (cm)	Zr	Nb	Mo	Ba	Pb	Th	U
0	0.04	0.00	0.00	0.06	0.00	0.00	0.00
30	0.02	0.00	0.00	0.05	0.00	0.00	0.00

SDK 4							
Depth (cm)	Mg	Al	Si	P	S	K	Ca
0	0.00	4.73	20.09	0.02	0.14	1.79	1.32
28	0.00	4.49	20.59	0.03	0.13	1.76	1.35
56	0.35	4.48	19.12	0.03	0.11	1.58	1.49
Depth (cm)	Ti	V	Cr	Mn	Fe	Co	Ni
0	0.38	0.01	0.01	0.11	2.82	0.00	0.00
28	0.43	0.01	0.01	0.10	2.75	0.00	0.00
56	0.40	0.01	0.01	0.16	3.15	0.00	0.02
Depth (cm)	Cu	Zn	Ga	As	Rb	Sr	Y
0	0.00	0.01	0.00	0.00	0.01	0.01	0.00
28	0.00	0.01	0.00	0.00	0.01	0.01	0.00
56	0.01	0.01	0.00	0.00	0.01	0.01	0.00
Depth (cm)	Zr	Nb	Mo	Ba	Pb	Th	U
0	0.03	0.00	0.00	0.07	0.00	0.00	0.00
28	0.04	0.00	0.00	0.07	0.00	0.00	0.00
56	0.03	0.00	0.00	0.09	0.00	0.00	0.00

SDK 5							
Depth (cm)	Mg	Al	Si	P	S	K	Ca
0	0.02	4.88	20.48	0.02	0.14	1.84	1.10
16	0.04	4.84	19.36	0.02	0.14	1.83	2.08
20	0.17	4.92	19.22	0.02	0.14	1.89	2.57
25	0.01	4.55	18.65	0.02	0.14	1.82	1.96
Depth (cm)	Ti	V	Cr	Mn	Fe	Co	Ni
0	0.38	0.01	0.01	0.11	3.13	0.00	0.00
16	0.37	0.01	0.01	0.08	3.12	0.00	0.01
20	0.37	0.01	0.01	0.10	3.28	0.00	0.01
25	0.36	0.01	0.01	0.10	3.06	0.00	0.01
Depth (cm)	Cu	Zn	Ga	As	Rb	Sr	Y
0	0.00	0.01	0.00	0.00	0.01	0.01	0.00
16	0.00	0.01	0.00	0.00	0.01	0.01	0.00
20	0.00	0.01	0.00	0.00	0.01	0.01	0.00
25	0.00	0.01	0.00	0.00	0.01	0.01	0.00
Depth (cm)	Zr	Nb	Mo	Ba	Pb	Th	U
0	0.03	0.00	0.00	0.04	0.00	0.00	0.00
16	0.03	0.00	0.00	0.05	0.00	0.00	0.00
20	0.03	0.00	0.00	0.09	0.00	0.00	0.00
25	0.03	0.00	0.00	0.07	0.00	0.00	0.00

SDK 2A							
Depth (cm)	Mg	Al	Si	P	S	K	Ca
0	0.01	4.40	19.86	0.03	0.16	1.67	1.18
32	0.09	4.53	19.91	0.02	0.13	1.62	1.31
40	0.00	4.92	20.35	0.01	0.13	1.81	0.83
50	0.15	4.61	20.76	0.02	0.12	1.65	0.85
Depth (cm)	Ti	V	Cr	Mn	Fe	Co	Ni
0	0.38	0.01	0.01	0.08	2.97	0.00	0.01
32	0.39	0.01	0.01	0.10	2.99	0.00	0.01
40	0.38	0.01	0.01	0.05	3.30	0.00	0.01
50	0.39	0.01	0.01	0.12	2.88	0.00	0.01
Depth (cm)	Cu	Zn	Ga	As	Rb	Sr	Y
0	0.00	0.01	0.00	0.00	0.01	0.01	0.00
32	0.00	0.01	0.00	0.00	0.01	0.01	0.00
40	0.00	0.01	0.00	0.00	0.01	0.01	0.00
50	0.00	0.01	0.00	0.00	0.01	0.01	0.00
Depth (cm)	Zr	Nb	Mo	Ba	Pb	Th	U
0	0.04	0.00	0.00	0.05	0.00	0.00	0.00
32	0.03	0.00	0.00	0.09	0.00	0.00	0.00
40	0.03	0.00	0.00	0.06	0.00	0.00	0.00
50	0.03	0.00	0.00	0.11	0.00	0.00	0.00

SDK 3A							
Depth (cm)	Mg	Al	Si	P	S	K	Ca
0	0.11	4.28	19.34	0.02	0.16	1.56	1.21
16	0.48	4.43	19.22	0.03	0.14	1.47	1.53
27	0.43	4.16	19.31	0.03	0.13	1.47	1.15
43	0.00	0.85	8.32	0.00	0.00	1.19	0.81
Depth (cm)	Ti	V	Cr	Mn	Fe	Co	Ni
0	0.38	0.01	0.01	0.12	3.11	0.00	0.01
16	0.42	0.01	0.01	0.15	3.13	0.00	0.02
27	0.44	0.01	0.01	0.13	3.00	0.00	0.02
43	0.42	0.00	0.01	0.09	3.14	0.00	0.02
Depth (cm)	Cu	Zn	Ga	As	Rb	Sr	Y
0	0.00	0.01	0.00	0.00	0.01	0.01	0.00
16	0.01	0.01	0.00	0.00	0.01	0.01	0.00
27	0.01	0.01	0.00	0.00	0.01	0.01	0.00
43	0.01	0.01	0.00	0.00	0.01	0.01	0.00
Depth (cm)	Zr	Nb	Mo	Ba	Pb	Th	U
0	0.03	0.00	0.00	0.10	0.00	0.00	0.00
16	0.03	0.00	0.00	0.10	0.00	0.00	0.00
27	0.03	0.00	0.00	0.14	0.00	0.00	0.00
43	0.03	0.00	0.00	0.10	0.00	0.00	0.00

SDK 4A							
Depth (cm)	Mg	Al	Si	P	S	K	Ca
0	0.01	4.11	19.31	0.03	0.18	1.57	2.06
22	1.07	4.01	18.34	0.02	0.12	1.31	1.37
37	0.21	4.67	20.47	0.03	0.11	1.62	1.23
Depth (cm)	Ti	V	Cr	Mn	Fe	Co	Ni
0	0.35	0.01	0.01	0.07	2.66	0.00	0.00
22	0.46	0.01	0.01	0.18	3.39	0.00	0.04
37	0.40	0.01	0.01	0.06	2.99	0.00	0.01
Depth (cm)	Cu	Zn	Ga	As	Rb	Sr	Y
0	0.00	0.01	0.00	0.00	0.01	0.02	0.00
22	0.01	0.01	0.00	0.00	0.01	0.01	0.00
37	0.00	0.01	0.00	0.00	0.01	0.01	0.00
Depth (cm)	Zr	Nb	Mo	Ba	Pb	Th	U
0	0.03	0.00	0.00	0.05	0.00	0.00	0.00
22	0.03	0.00	0.00	0.11	0.00	0.00	0.00
37	0.04	0.00	0.00	0.12	0.00	0.00	0.00

SDK 1B							
Depth (cm)	Mg	Al	Si	P	S	K	Ca
0	0.21	4.32	20.20	0.02	0.15	1.50	0.68
7	0.78	4.24	19.53	0.02	0.14	1.37	0.65
14	3.26	2.94	15.60	0.02	0.12	0.77	0.65
20	3.89	2.39	13.80	0.02	0.11	0.50	0.61
28	4.41	2.58	14.83	0.02	0.11	0.58	0.59
36	7.51	1.73	12.71	0.02	0.12	0.29	1.08
Depth (cm)	Ti	V	Cr	Mn	Fe	Co	Ni
0	0.43	0.01	0.01	0.06	3.01	0.00	0.02
7	0.46	0.01	0.02	0.08	3.68	0.00	0.03
14	0.57	0.01	0.03	0.18	4.71	0.01	0.06
20	0.58	0.01	0.03	0.26	5.26	0.01	0.07
28	0.54	0.02	0.03	0.17	4.99	0.01	0.07
36	0.49	0.01	0.04	0.14	5.22	0.01	0.08
Depth (cm)	Cu	Zn	Ga	As	Rb	Sr	Y
0	0.00	0.01	0.00	0.00	0.01	0.01	0.00
7	0.01	0.01	0.00	0.00	0.01	0.01	0.00
14	0.02	0.01	0.00	0.00	0.01	0.01	0.00
20	0.02	0.01	0.00	0.00	0.01	0.01	0.00
28	0.02	0.01	0.00	0.00	0.01	0.01	0.00
36	0.02	0.01	0.00	0.00	0.00	0.02	0.00
Depth (cm)	Zr	Nb	Mo	Ba	Pb	Th	U
0	0.03	0.00	0.00	0.08	0.00	0.00	0.00
7	0.03	0.00	0.00	0.16	0.00	0.00	0.00
14	0.02	0.00	0.00	0.20	0.00	0.00	0.00
20	0.02	0.00	0.00	0.19	0.00	0.00	0.00
28	0.02	0.00	0.00	0.23	0.00	0.00	0.00
36	0.01	0.00	0.00	0.21	0.00	0.00	0.00

SDK 2B							
Depth (cm)	Mg	Al	Si	P	S	K	Ca
0	0.01	4.69	21.29	0.03	0.13	1.61	0.58
16	0.03	5.28	21.62	0.02	0.13	1.58	0.50
28	0.00	5.40	20.87	0.01	0.12	1.53	0.44
42	0.00	5.27	21.00	0.02	0.12	1.55	0.42
54	0.00	5.12	21.43	0.02	0.12	1.60	0.40
71	0.00	4.74	21.11	0.02	0.14	1.86	1.29

Depth (cm)	Ti	V	Cr	Mn	Fe	Co	Ni
0	0.40	0.01	0.01	0.05	2.80	0.00	0.00
16	0.40	0.01	0.01	0.04	3.32	0.00	0.00
28	0.40	0.01	0.01	0.04	3.48	0.00	0.01
42	0.42	0.01	0.01	0.05	3.36	0.00	0.01
54	0.44	0.01	0.01	0.05	3.34	0.00	0.01
71	0.37	0.01	0.01	0.10	2.93	0.00	0.01

Depth (cm)	Cu	Zn	Ga	As	Rb	Sr	Y
0	0.00	0.01	0.00	0.00	0.01	0.01	0.00
16	0.00	0.01	0.00	0.00	0.01	0.01	0.00
28	0.00	0.01	0.00	0.00	0.01	0.01	0.00
42	0.00	0.01	0.00	0.00	0.01	0.01	0.00
54	0.00	0.01	0.00	0.00	0.01	0.01	0.00
71	0.00	0.01	0.00	0.00	0.01	0.01	0.00

Depth (cm)	Zr	Nb	Mo	Ba	Pb	Th	U
0	0.04	0.00	0.00	0.09	0.00	0.00	0.00
16	0.03	0.00	0.00	0.07	0.00	0.00	0.00
28	0.03	0.00	0.00	0.08	0.00	0.00	0.00
42	0.03	0.00	0.00	0.08	0.00	0.00	0.00
54	0.03	0.00	0.00	0.07	0.00	0.00	0.00
71	0.04	0.00	0.00	0.06	0.00	0.00	0.00

SKD 3B							
Depth (cm)	Mg	Al	Si	P	S	K	Ca
0	0.00	4.82	20.73	0.01	0.14	1.60	0.57
7	0.01	5.05	21.13	0.02	0.14	1.58	0.52
20	0.01	5.35	20.08	0.01	0.13	1.51	0.43
30	0.01	5.46	20.01	0.01	0.12	1.52	0.44
41	0.03	5.38	20.79	0.01	0.12	1.59	0.43
57	0.01	5.28	20.75	0.02	0.11	1.60	0.42
61	0.00	5.28	21.51	0.02	0.11	1.63	0.42
68	0.00	5.34	21.49	0.01	0.12	1.64	0.39
Depth (cm)	Ti	V	Cr	Mn	Fe	Co	Ni
0	0.39	0.01	0.01	0.06	2.94	0.00	0.01
7	0.39	0.01	0.01	0.05	3.09	0.00	0.00
20	0.39	0.01	0.01	0.06	3.68	0.00	0.01
30	0.40	0.01	0.01	0.11	3.75	0.00	0.01
41	0.41	0.01	0.01	0.06	3.64	0.00	0.01
57	0.41	0.01	0.01	0.05	3.41	0.00	0.00
61	0.43	0.01	0.01	0.05	3.26	0.00	0.00
68	0.42	0.01	0.01	0.04	3.07	0.00	0.00
Depth (cm)	Cu	Zn	Ga	As	Rb	Sr	Y
0	0.00	0.01	0.00	0.00	0.01	0.01	0.00
7	0.00	0.01	0.00	0.00	0.01	0.01	0.00
20	0.00	0.01	0.00	0.00	0.01	0.01	0.00
30	0.00	0.01	0.00	0.00	0.01	0.01	0.00
41	0.00	0.01	0.00	0.00	0.01	0.01	0.00
57	0.00	0.01	0.00	0.00	0.01	0.01	0.00
61	0.00	0.01	0.00	0.00	0.01	0.01	0.00
68	0.00	0.01	0.00	0.00	0.01	0.01	0.00
Depth (cm)	Zr	Nb	Mo	Ba	Pb	Th	U
0	0.04	0.00	0.00	0.05	0.00	0.00	0.00
7	0.04	0.00	0.00	0.01	0.00	0.00	0.00
20	0.03	0.00	0.00	0.04	0.00	0.00	0.00
30	0.03	0.00	0.00	0.09	0.00	0.00	0.00
41	0.03	0.00	0.00	0.07	0.00	0.00	0.00
57	0.03	0.00	0.00	0.06	0.00	0.00	0.00
61	0.04	0.00	0.00	0.09	0.00	0.00	0.00
68	0.04	0.00	0.00	0.06	0.00	0.00	0.00

Appendix C - Particle Size (PSA) Data

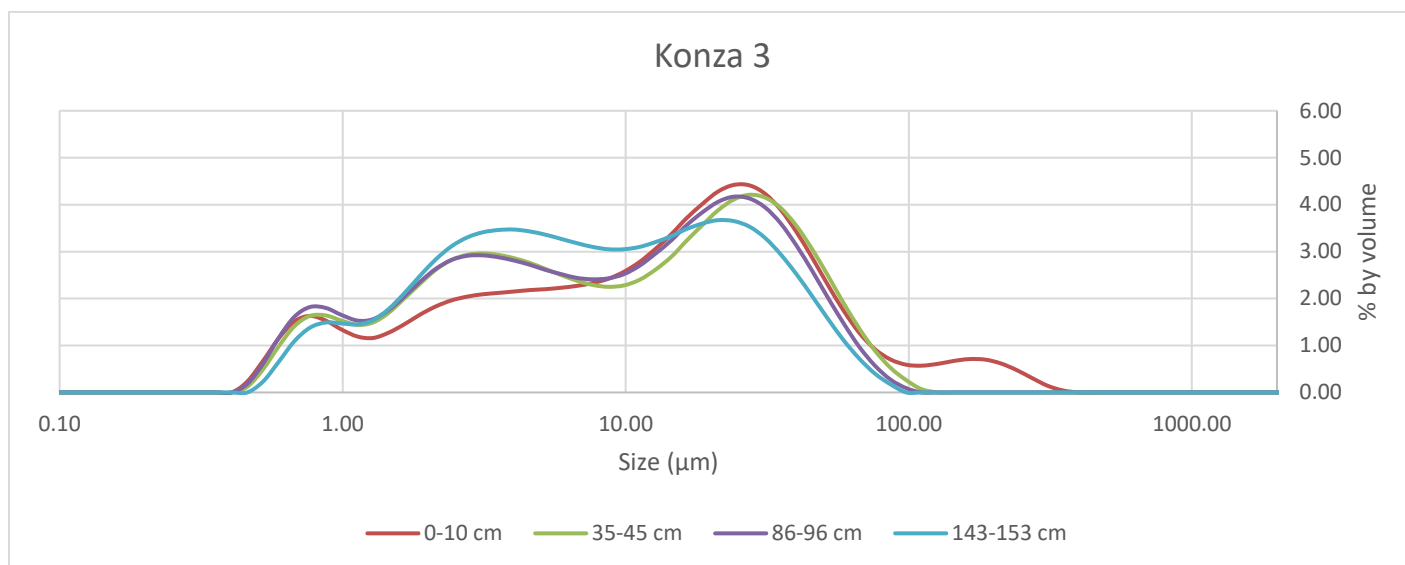
C.1 – Raw Data

In the following tables are the unprocessed data for the particle size analyses conducted on both the Konza Prairie and Stockdale Kimberlite samples for this study. Analyses were conducted using a Mastersizer 3000.

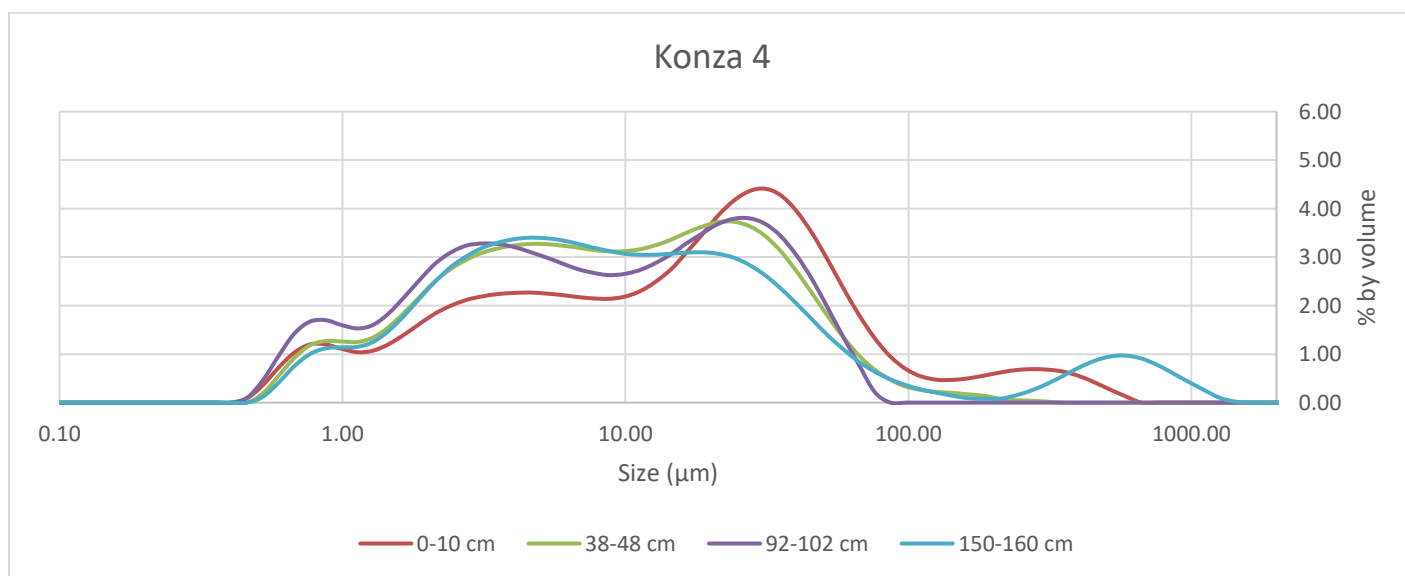
Size (µm)	Konza core 3 0 cm	Konza core 3 35 cm	Konza core 3 86 cm	Konza core 3 143cm	Konza core 4 0 cm	Konza core 4 38 cm	Konza core 4 92 cm	Konza core 4 150cm	Konza core 5 0 cm	Konza core 5 60 cm	Konza core 6 0 cm	Konza core 6 30 cm	Konza core 6 70 cm	Konza core 6 120cm	Konza core 9 0 cm	Konza core 9 38 cm	Konza core 9 89 cm	Konza core 9 142cm	Konza core 9 193cm	Konza core10 0 cm	Konza core10 50 cm	Konza core10 100cm	Konza core10 150cm
0.01	0.00	0.00	0.00	0.00	0.00	0.00	0.00	0.00	0.00	0.00	0.00	0.00	0.00	0.00	0.00	0.00	0.00	0.00	0.00	0.00	0.00	0.00	
0.0114	0.00	0.00	0.00	0.00	0.00	0.00	0.00	0.00	0.00	0.00	0.00	0.00	0.00	0.00	0.00	0.00	0.00	0.00	0.00	0.00	0.00	0.00	
0.0129	0.00	0.00	0.00	0.00	0.00	0.00	0.00	0.00	0.00	0.00	0.00	0.00	0.00	0.00	0.00	0.00	0.00	0.00	0.00	0.00	0.00	0.00	
0.0147	0.00	0.00	0.00	0.00	0.00	0.00	0.00	0.00	0.00	0.00	0.00	0.00	0.00	0.00	0.00	0.00	0.00	0.00	0.00	0.00	0.00	0.00	
0.0167	0.00	0.00	0.00	0.00	0.00	0.00	0.00	0.00	0.00	0.00	0.00	0.00	0.00	0.00	0.00	0.00	0.00	0.00	0.00	0.00	0.00	0.00	
0.0189	0.00	0.00	0.00	0.00	0.00	0.00	0.00	0.00	0.00	0.00	0.00	0.00	0.00	0.00	0.00	0.00	0.00	0.00	0.00	0.00	0.00	0.00	
0.0215	0.00	0.00	0.00	0.00	0.00	0.00	0.00	0.00	0.00	0.00	0.00	0.00	0.00	0.00	0.00	0.00	0.00	0.00	0.00	0.00	0.00	0.00	
0.0244	0.00	0.00	0.00	0.00	0.00	0.00	0.00	0.00	0.00	0.00	0.00	0.00	0.00	0.00	0.00	0.00	0.00	0.00	0.00	0.00	0.00	0.00	
0.0278	0.00	0.00	0.00	0.00	0.00	0.00	0.00	0.00	0.00	0.00	0.00	0.00	0.00	0.00	0.00	0.00	0.00	0.00	0.00	0.00	0.00	0.00	
0.0315	0.00	0.00	0.00	0.00	0.00	0.00	0.00	0.00	0.00	0.00	0.00	0.00	0.00	0.00	0.00	0.00	0.00	0.00	0.00	0.00	0.00	0.00	
0.0358	0.00	0.00	0.00	0.00	0.00	0.00	0.00	0.00	0.00	0.00	0.00	0.00	0.00	0.00	0.00	0.00	0.00	0.00	0.00	0.00	0.00	0.00	
0.0407	0.00	0.00	0.00	0.00	0.00	0.00	0.00	0.00	0.00	0.00	0.00	0.00	0.00	0.00	0.00	0.00	0.00	0.00	0.00	0.00	0.00	0.00	
0.0463	0.00	0.00	0.00	0.00	0.00	0.00	0.00	0.00	0.00	0.00	0.00	0.00	0.00	0.00	0.00	0.00	0.00	0.00	0.00	0.00	0.00	0.00	
0.0526	0.00	0.00	0.00	0.00	0.00	0.00	0.00	0.00	0.00	0.00	0.00	0.00	0.00	0.00	0.00	0.00	0.00	0.00	0.00	0.00	0.00	0.00	
0.0597	0.00	0.00	0.00	0.00	0.00	0.00	0.00	0.00	0.00	0.00	0.00	0.00	0.00	0.00	0.00	0.00	0.00	0.00	0.00	0.00	0.00	0.00	
0.0679	0.00	0.00	0.00	0.00	0.00	0.00	0.00	0.00	0.00	0.00	0.00	0.00	0.00	0.00	0.00	0.00	0.00	0.00	0.00	0.00	0.00	0.00	
0.0771	0.00	0.00	0.00	0.00	0.00	0.00	0.00	0.00	0.00	0.00	0.00	0.00	0.00	0.00	0.00	0.00	0.00	0.00	0.00	0.00	0.00	0.00	
0.0876	0.00	0.00	0.00	0.00	0.00	0.00	0.00	0.00	0.00	0.00	0.00	0.00	0.00	0.00	0.00	0.00	0.00	0.00	0.00	0.00	0.00	0.00	
0.0995	0.00	0.00	0.00	0.00	0.00	0.00	0.00	0.00	0.00	0.00	0.00	0.00	0.00	0.00	0.00	0.00	0.00	0.00	0.00	0.00	0.00	0.00	
0.113	0.00	0.00	0.00	0.00	0.00	0.00	0.00	0.00	0.00	0.00	0.00	0.00	0.00	0.00	0.00	0.00	0.00	0.00	0.00	0.00	0.00	0.00	
0.128	0.00	0.00	0.00	0.00	0.00	0.00	0.00	0.00	0.00	0.00	0.00	0.00	0.00	0.00	0.00	0.00	0.00	0.00	0.00	0.00	0.00	0.00	
0.146	0.00	0.00	0.00	0.00	0.00	0.00	0.00	0.00	0.00	0.00	0.00	0.00	0.00	0.00	0.00	0.00	0.00	0.00	0.00	0.00	0.00	0.00	
0.166	0.00	0.00	0.00	0.00	0.00	0.00	0.00	0.00	0.00	0.00	0.00	0.00	0.00	0.00	0.00	0.00	0.00	0.00	0.00	0.00	0.00	0.00	
0.188	0.00	0.00	0.00	0.00	0.00	0.00	0.00	0.00	0.00	0.00	0.00	0.00	0.00	0.00	0.00	0.00	0.00	0.00	0.00	0.00	0.00	0.00	
0.214	0.00	0.00	0.00	0.00	0.00	0.00	0.00	0.00	0.00	0.00	0.00	0.00	0.00	0.00	0.00	0.00	0.00	0.00	0.00	0.00	0.00	0.00	
0.243	0.00	0.00	0.00	0.00	0.00	0.00	0.00	0.00	0.00	0.00	0.00	0.00	0.00	0.00	0.00	0.00	0.00	0.00	0.00	0.00	0.00	0.00	
0.276	0.00	0.00	0.00	0.00	0.00	0.00	0.00	0.00	0.00	0.00	0.00	0.00	0.00	0.00	0.00	0.00	0.00	0.00	0.00	0.00	0.00	0.00	
0.314	0.00	0.00	0.00	0.00	0.00	0.00	0.00	0.00	0.00	0.00	0.00	0.00	0.00	0.00	0.00	0.00	0.00	0.00	0.00	0.00	0.00	0.00	
0.357	0.00	0.00	0.00	0.00	0.00	0.00	0.00	0.00	0.00	0.00	0.00	0.00	0.00	0.00	0.00	0.00	0.00	0.00	0.00	0.00	0.00	0.00	
0.405	0.00	0.00	0.00	0.00	0.00	0.00	0.00	0.00	0.00	0.00	0.08	0.00	0.00	0.00	0.00	0.00	0.00	0.00	0.00	0.00	0.00	0.00	
0.46	0.23	0.12	0.18	0.00	0.09	0.00	0.10	0.00	0.27	0.00	0.45	0.14	0.10	0.38	0.28	0.40	0.34	0.17	0.09	0.00	0.00	0.00	
0.523	0.67	0.49	0.61	0.23	0.36	0.19	0.46	0.12	0.80	0.10	1.01	0.56	0.45	1.08	0.74	0.99	0.98	0.58	0.40	0.11	0.00	0.16	
0.594	1.15	0.98	1.16	0.65	0.72	0.55	0.96	0.41	1.39	0.32	1.57	1.13	0.96	1.81	1.23	1.59	1.69	1.08	0.85	0.35	0.18	0.47	
0.675	1.51	1.41	1.61	1.09	1.03	0.92	1.42	0.75	1.83	0.59	1.92	1.63	1.40	2.30	1.59	2.00	2.20	1.48	1.26	0.62	0.38	0.81	
0.767	1.63	1.63	1.82	1.38	1.20	1.18	1.67	1.00	1.99	0.80	1.99	1.91	1.63	2.39	1.69	2.11	2.37	1.66	1.50	0.83	0.56	1.06	
0.872	1.53	1.64	1.80	1.49	1.20	1.27	1.70	1.12	1.90	0.90	1.82	1.95	1.62	2.16	1.59	1.94	2.23	1.62	1.54	0.92	0.67	1.18	
0.991	1.34	1.53	1.65	1.47	1.11	1.26	1.60	1.14	1.70	0.92	1.56	1.87	1.51	1.81	1.39	1.67	1.96	1.47	1.47	0.94	0.71	1.19	
1.13	1.19	1.44	1.53	1.45	1.04	1.25	1.53	1.15	1.56	0.93	1.39	1.86	1.44	1.59	1.23	1.46	1.76	1.35	1.41	0.95	0.73	1.20	
1.28	1.16	1.49	1.56	1.54	1.07	1.34	1.60	1.25	1.58	0.99	1.38	2.02	1.54	1.65	1.20	1.42	1.76	1.36	1.46	1.01	0.79	1.29	
1.45	1.27	1.69	1.75	1.77	1.20	1.55	1.83	1.47	1.77	1.13	1.53	2.37	1.84	1.97	1.30	1.54	1.95	1.52	1.65	1.16	0.91	1.48	
1.65	1.45	2.00	2.04	2.11	1.40	1.85	2.17	1.79	2.06	1.34	1.77	2.84	2.28	2.46	1.46	1.76	2.26	1.78	1.92	1.39	1.09	1.77	
1.88	1.66	2.32	2.36	2.49	1.63	2.19	2.54	2.16	2.37	1.58	2.01	3.32	2.76	2.98	1.64	1.99	2.59	2.06	2.21	1.64	1.29	2.09	
2.13	1.83	2.61	2.63	2.83	1.84	2.51	2.87	2.50	2.64	1.81	2.20	3.73	3.21	3.44	1.78	2.17	2.87	2.29	2.46	1.89	1.49	2.39	
2.42	1.96	2.82	2.82	3.11	2.00	2.76	3.10	2.80	2.82	2.02	2.31	4.00	3.56	3.79	1.86	2.27	3.04	2.45	2.63	2.11	1.68	2.65	
2.75	2.04	2.93	2.91	3.30	2.12	2.95	3.24	3.02	2.92	2.19	2.34	4.12	3.81	4.03	1.89	2.30	3.11	2.53	2.72	2.30	1.85	2.86	
3.12	2.09	2.96	2.92	3.41	2.19	3.09	3.28	3.19	2.95	2.34	2.31	4.11	3.95	4.16	1.88	2.28	3.10	2.54	2.74	2.46	2.01	3.03	
3.55	2.12	2.93	2.88	3.46	2.24	3.18	3.27	3.30	2.94	2.48	2.25	4.02	4.03	4.24	1.86	2.24	3.04	2.50	2.72	2.62	2.16	3.16	
4.03	2.15	2.86	2.81	3.47	2.26	3.24	3.21	3.37	2.90	2.60	2.18	3.86	4.04	4.28	1.84	2.19	2.95	2.44	2.66	2.76	2.32	3.27	
4.58	2.18	2.76	2.72	3.43	2.27	3.27	3.11	3.40	2.84	2.71	2.09	3.67	4.00	4.30	1.82	2.13	2.85	2.35	2.58	2.89	2.47	3.35	
5.21	2.20	2.63	2.61	3.36	2.25	3.27	3.00	3.39	2.77	2.80	2.00	3.45	3.92	4.30	1.79	2.08	2.74	2.25	2.49	3.00	2.60	3.40	
5.92	2.23	2.50	2.52	3.27	2.22	3.24	2.88	3.35	2.68	2.87	1.91	3.21	3.80	4.28	1.77	2.02	2.64	2.16	2.40	3.09	2.73	3.42	
6.72	2.27	2.38	2.44	3.18	2.18	3.20	2.76	3.28	2.60	2.92	1.82	2.98	3.66	4.23	1.75	1.98	2.55	2.07	2.32	3.16	2.84	3.41	
7.64	2.33	2.29	2.41	3.10	2.15	3.15	2.68	3.20	2.54	2.97	1.76	2.76	3.49	4.15	1.75	1.96	2.49	2.02	2.27	3.21	2.94	3.38	
8.68	2.42	2.25	2.43	3.05	2.14	3.12	2.63	3.13	2.50	3.02	1.72	2.57	3.32	4.03	1.78	1.97	2.47	2.02	2.27	3.24	3.04	3.34	
9.86	2.57	2.28	2.52	3.05	2.18	3.12	2.65	3.07	2.50	3.09	1.74	2.41	3.15	3.87	1.86	2.03	2.51	2.09	2.32	3.26	3.15	3.31	
11.2	2.78	2.40	2.70	3.10	2.29	3.16	2.73	3.05	2.56	3.17	1.83	2.29	2.98	3.67	2.02	2.17	2.60	2.24	2.45	3.28	3.27	3.28	
12.7	3.05	2.61	2.95	3.20	2.48	3.24	2.87	3.05															

Size (µm)	SDK 1		SDK 2		SDK 3		SDK 4		SDK 5		SDK 6		SDK 7		SDK 8		SDK 9		SDK 10		SDK 11		SDK 12		SDK 13		SDK 14		SDK 15		SDK 16		SDK 17		SDK 18		SDK 19		SDK 20		SDK 21		SDK 22		SDK 23		SDK 24		SDK 25		SDK 26		SDK 27		SDK 28		SDK 29		SDK 30		SDK 31		SDK 32		SDK 33		SDK 34		SDK 35		SDK 36		SDK 37		SDK 38		SDK 39		SDK 40		SDK 41		SDK 42		SDK 43		SDK 44		SDK 45		SDK 46		SDK 47		SDK 48		SDK 49		SDK 50		SDK 51		SDK 52		SDK 53		SDK 54		SDK 55		SDK 56		SDK 57		SDK 58		SDK 59		SDK 60		SDK 61		SDK 62		SDK 63		SDK 64		SDK 65		SDK 66		SDK 67		SDK 68		SDK 69		SDK 70		SDK 71		SDK 72		SDK 73		SDK 74		SDK 75		SDK 76		SDK 77		SDK 78		SDK 79		SDK 80		SDK 81		SDK 82		SDK 83		SDK 84		SDK 85		SDK 86		SDK 87		SDK 88		SDK 89		SDK 90		SDK 91		SDK 92		SDK 93		SDK 94		SDK 95		SDK 96		SDK 97		SDK 98		SDK 99		SDK 100																																																																																																																																																																																																																																																																																																																																																																																																																																																																																																										
	0-11 cm	12-15 cm	0-13 cm	16-19 cm	20-23 cm	24-27 cm	28-31 cm	32-35 cm	36-39 cm	40-43 cm	44-47 cm	48-51 cm	52-55 cm	56-59 cm	60-63 cm	64-67 cm	68-71 cm	72-75 cm	76-79 cm	80-83 cm	84-87 cm	88-91 cm	92-95 cm	96-99 cm	100-103 cm	104-107 cm	108-111 cm	112-115 cm	116-119 cm	120-123 cm	124-127 cm	128-131 cm	132-135 cm	136-139 cm	140-143 cm	144-147 cm	148-151 cm	152-155 cm	156-159 cm	160-163 cm	164-167 cm	168-171 cm	172-175 cm	176-179 cm	180-183 cm	184-187 cm	188-191 cm	192-195 cm	196-199 cm	200-203 cm	204-207 cm	208-211 cm	212-215 cm	216-219 cm	220-223 cm	224-227 cm	228-231 cm	232-235 cm	236-239 cm	240-243 cm	244-247 cm	248-251 cm	252-255 cm	256-259 cm	260-263 cm	264-267 cm	272-275 cm	276-279 cm	280-283 cm	284-287 cm	288-291 cm	292-295 cm	296-299 cm	300-303 cm	304-307 cm	308-311 cm	312-315 cm	316-319 cm	320-323 cm	324-327 cm	328-331 cm	332-335 cm	336-339 cm	340-343 cm	344-347 cm	348-351 cm	352-355 cm	356-359 cm	360-363 cm	364-367 cm	368-371 cm	372-375 cm	376-379 cm	380-383 cm	384-387 cm	388-391 cm	392-395 cm	396-399 cm	400-403 cm	404-407 cm	408-411 cm	412-415 cm	416-419 cm	420-423 cm	424-427 cm	428-431 cm	432-435 cm	436-439 cm	440-443 cm	444-447 cm	448-451 cm	452-455 cm	456-459 cm	460-463 cm	464-467 cm	468-471 cm	472-475 cm	476-479 cm	480-483 cm	484-487 cm	488-491 cm	492-495 cm	496-499 cm	500-503 cm	504-507 cm	508-511 cm	512-515 cm	516-519 cm	520-523 cm	524-527 cm	528-531 cm	532-535 cm	536-539 cm	540-543 cm	544-547 cm	548-551 cm	552-555 cm	556-559 cm	560-563 cm	564-567 cm	568-571 cm	572-575 cm	576-579 cm	580-583 cm	584-587 cm	588-591 cm	592-595 cm	596-599 cm	600-603 cm	604-607 cm	608-611 cm	612-615 cm	616-619 cm	620-623 cm	624-627 cm	628-631 cm	632-635 cm	636-639 cm	640-643 cm	644-647 cm	648-651 cm	652-655 cm	656-659 cm	660-663 cm	664-667 cm	668-671 cm	672-675 cm	676-679 cm	680-683 cm	684-687 cm	688-691 cm	692-695 cm	696-699 cm	700-703 cm	704-707 cm	708-711 cm	712-715 cm	716-719 cm	720-723 cm	724-727 cm	728-731 cm	732-735 cm	736-739 cm	740-743 cm	744-747 cm	748-751 cm	752-755 cm	756-759 cm	760-763 cm	764-767 cm	768-771 cm	772-775 cm	776-779 cm	780-783 cm	784-787 cm	788-791 cm	792-795 cm	796-799 cm	800-803 cm	804-807 cm	808-811 cm	812-815 cm	816-819 cm	820-823 cm	824-827 cm	828-831 cm	832-835 cm	836-839 cm	840-843 cm	844-847 cm	848-851 cm	852-855 cm	856-859 cm	860-863 cm	864-867 cm	868-871 cm	872-875 cm	876-879 cm	880-883 cm	884-887 cm	888-891 cm	892-895 cm	896-899 cm	900-903 cm	904-907 cm	908-911 cm	912-915 cm	916-919 cm	920-923 cm	924-927 cm	928-931 cm	932-935 cm	936-939 cm	940-943 cm	944-947 cm	948-951 cm	952-955 cm	956-959 cm	960-963 cm	964-967 cm	968-971 cm	972-975 cm	976-979 cm	980-983 cm	984-987 cm	988-991 cm	992-995 cm	996-999 cm	1000-1003 cm	1004-1007 cm	1008-1011 cm	1012-1015 cm	1016-1019 cm	1020-1023 cm	1024-1027 cm	1028-1031 cm	1032-1035 cm	1036-1039 cm	1040-1043 cm	1044-1047 cm	1048-1051 cm	1052-1055 cm	1056-1059 cm	1060-1063 cm	1064-1067 cm	1068-1071 cm	1072-1075 cm	1076-1079 cm	1080-1083 cm	1084-1087 cm	1088-1091 cm	1092-1095 cm	1096-1099 cm	1100-1103 cm	1104-1107 cm	1108-1111 cm	1112-1115 cm	1116-1119 cm	1120-1123 cm	1124-1127 cm	1128-1131 cm	1132-1135 cm	1136-1139 cm	1140-1143 cm	1144-1147 cm	1148-1151 cm	1152-1155 cm	1156-1159 cm	1160-1163 cm	1164-1167 cm	1168-1171 cm	1172-1175 cm	1176-1179 cm	1180-1183 cm	1184-1187 cm	1188-1191 cm	1192-1195 cm	1196-1199 cm	1200-1203 cm	1204-1207 cm	1208-1211 cm	1212-1215 cm	1216-1219 cm	1220-1223 cm	1224-1227 cm	1228-1231 cm	1232-1235 cm	1236-1239 cm	1240-1243 cm	1244-1247 cm	1248-1251 cm	1252-1255 cm	1256-1259 cm	1260-1263 cm	1264-1267 cm	1268-1271 cm	1272-1275 cm	1276-1279 cm	1280-1283 cm	1284-1287 cm	1288-1291 cm	1292-1295 cm	1296-1299 cm	1300-1303 cm	1304-1307 cm	1308-1311 cm	1312-1315 cm	1316-1319 cm	1320-1323 cm	1324-1327 cm	1328-1331 cm	1332-1335 cm	1336-1339 cm	1340-1343 cm	1344-1347 cm	1348-1351 cm	1352-1355 cm	1356-1359 cm	1360-1363 cm	1364-1367 cm	1368-1371 cm	1372-1375 cm	1376-1379 cm	1380-1383 cm	1384-1387 cm	1388-1391 cm	1392-1395 cm	1396-1399 cm	1400-1403 cm	1404-1407 cm	1408-1411 cm	1412-1415 cm	1416-1419 cm	1420-1423 cm	1424-1427 cm	1428-1431 cm	1432-1435 cm	1436-1439 cm	1440-1443 cm	1444-1447 cm	1448-1451 cm	1452-1455 cm	1456-1459 cm	1460-1463 cm	1464-1467 cm	1468-1471 cm	1472-1475 cm	1476-1479 cm	1480-1483 cm	1484-1487 cm	1488-1491 cm	1492-1495 cm	1496-1499 cm	1500-1503 cm	1504-1507 cm	1508-1511 cm	1512-1515 cm	1516-1519 cm	1520-1523 cm	1524-1527 cm	1528-1531 cm	1532-1535 cm	1536-1539 cm	1540-1543 cm	1544-1547 cm	1548-1551 cm	1552-1555 cm	1556-1559 cm	1560-1563 cm	1564-1567 cm	1568-1571 cm	1572-1575 cm	1576-1579 cm	1580-1583 cm	1584-1587 cm	1588-1591 cm	1592-1595 cm	1596-1599 cm	1600-1603 cm	1604-1607 cm	1608-1611 cm	1612-1615 cm	1616-1619 cm	1620-1623 cm	1624-1627 cm	1628-1631 cm	1632-1635 cm	1636-1639 cm	1640-1643 cm	1644-1647 cm	1648-1651 cm	1652-1655 cm	1656-1659 cm	1660-1663 cm	1664-1667 cm	1668-1671 cm	1672-1675 cm	1676-1679 cm	1680-1683 cm	1684-1687 cm	1688-1691 cm	1692-1695 cm	1696-1699 cm	1700-1703 cm	1704-1707 cm	1708-1711 cm	1712-1715 cm	1716-1719 cm	1720-1723 cm	1724-1727 cm	1728-1731 cm	1732-1735 cm	1736-1739 cm	1740-1743 cm	1744-1747 cm	1748-1751 cm	1752-1755 cm	1756-1759 cm	1760-1763 cm	1764-1767 cm	1768-1771 cm	1772-1775 cm	1776-1779 cm	1780-1783 cm	1784-1787 cm	1788-1791 cm	1792-1795 cm	1796-1799 cm	1800-1803 cm	1804-1807 cm	1808-1811 cm	1812-1815 cm	1816-1819 cm	1820-1823 cm	1824-1827 cm	1828-1831 cm	1832-1835 cm	1836-1839 cm	1840-1843 cm	1844-1847 cm	1848-1851 cm	1852-1855 cm	1856-1859 cm	1860-1863 cm	1864-1867 cm	1868-1871 cm	1872-1875 cm	1876-1879 cm	1880-1883 cm	1884-1887 cm	1888-1891 cm	1892-1895 cm	1896-1899 cm	1900-1903 cm	1904-1907 cm	1908-1911 cm	1912-1915 cm	1916-1919 cm	1920-1923 cm	1924-1927 cm	1928-1931 cm	1932-1935 cm	1936-1939 cm	1940-1943 cm	1944-1947 cm	1948-1951 cm	1952-1955 cm	1956-1959 cm	1960-1963 cm	1964-1967 cm	1968-1971 cm	1972-1975 cm	1976-1979 cm	1980-1983 cm	1984-1987 cm	1988-1991 cm	1992-1995 cm	1996-1999 cm	2000-2003 cm	2004-2007 cm	2008-2011 cm	2012-2015 cm	2016-2019 cm	2020-2023 cm	2024-2027 cm	2028-2031 cm	2032-2035 cm	2036-2039 cm	2040-2043 cm	2044-2047 cm	2048-2051 cm	2052-2055 cm	2056-2059 cm	2060-2063 cm	2064-2067 cm	2068-2071 cm	2072-2075 cm	2076-2079 cm	2080-2083 cm	2084-2087 cm	2088-2091 cm	2092-2095 cm	2096-2099 cm	2100-2103 cm	2104-2107 cm	2108-2111 cm	2112-2115 cm	2116-2119 cm	2120-2123 cm	2124-2127 cm	2128-2131 cm	2132-2135 cm	2136-2139 cm	2140-2143 cm	2144-2147 cm	2148-2151 cm	2152-2155 cm	2156-2159 cm	2160-2163 cm	2164-2167 cm	2168-2171 cm	2172-2175 cm	2176-2179 cm	2180-2183 cm	2184-2187 cm	2188-2191 cm	2192-2195 cm	2196-2199 cm	2200-2203 cm	2204-2207 cm	2208-2211 cm	2212-2215 cm	2216-2219 cm	2220-2223 cm	2224-2227 cm	2228-2231 cm	2232-2235 cm	2236-2239 cm	2240-2243 cm	2244-2247 cm	2248-2251 cm	2252-2255 cm	2256-2259 cm	2260-2263 cm	2264-2267 cm	2268-2271 cm	2272-2275 cm	2276-2279 cm	2280-2283 cm	2284-2287 cm	2288-2291 cm	2292-2295 cm	2296-2299 cm	2300-2303 cm	2304-2307 cm	2308-2311 cm	2312-2315 cm	2316-2319 cm	2320-2323 cm	2324-2327 cm	2328-2331 cm	2332-2335 cm	2336-2339 cm	2340-2343 cm	2344-2347 cm	2348-2351 cm	2352-2355 cm	2356-2359 cm	2360-2363 cm	2364-2367 cm	2368-2371 cm	2372-2375 cm	2376-2379 cm	2380-2383 cm	2384-2387 cm	2388-2391 cm	2392-2395 cm	2396-2399 cm	2400-2403 cm	2404-2407 cm	2408-2411 cm	2412-2415 cm	2416-2419 cm	2420-2423 cm	2424-2427 cm	2428-2431 cm	2432-2435 cm	2436-2439 cm	2440-2443 cm	2444-2447 cm	2448-2451 cm	2452-2455 cm	2456-2459 cm	2460-2463 cm	2464-2467 cm	2468-2471 cm	2472-2475 cm	2476-2479 cm	2480-2483 cm	2484-2487 cm	2488-2491 cm	2492-2495 cm	2496-2499 cm	2500-2503 cm	2504-2507 cm	2508-2511 cm	2512-2515 cm	2516-2519 cm	2520-2523 cm	2524-2527 cm	2528-2531 cm	2532-2535 cm	2536-2539 cm	2540-2543 cm	2544-2547 cm	2548-2551 cm	2552-2555 cm	2556-2559 cm	2560-2563 cm	2564-2567 cm	2568-2571 cm	2572-2575 cm	2576-2579 cm	2580-2583 cm	2584-2587 cm	2588-2591 cm	2592-2595 cm	2596-2599 cm	2600-2603 cm	2604-2607 cm	2608-2611 cm	2612-2615 cm	2616-2619 cm	2620-2623 cm	2624-2627 cm	2628-2631 cm	2632-2635 cm	2636-2639 cm	2640-2643 cm	2644-2647 cm	2648-2651 cm	2652-2655 cm	2656-2659 cm	2660-2663 cm	2664-2667 cm	2668-2671 cm	2672-2675 cm	2676-2679 cm	2680-2683 cm	2684-2687 cm	2688-2691 cm	2692-2695 cm	2696-2699 cm	2700-2703 cm	2704-2707 cm	2708-2711 cm	2712-2715 cm	2716-2719 cm	2720-2723 cm	2724-2727 cm	2728-2731 cm	2732-2735 cm	2736-2739 cm	2740-2743 cm	2744-2747 cm	2748-2751 cm	2752-2755 cm	2756-2759 cm	2760-2763 cm

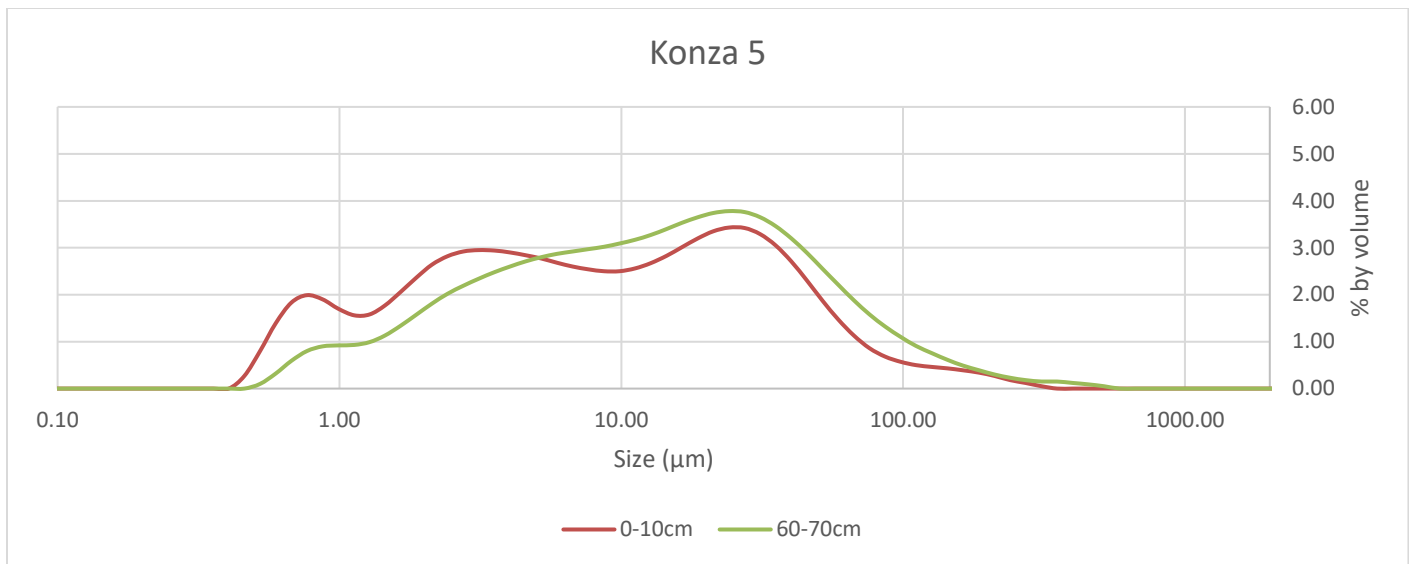
C.2 – Particle Size Data, Graphed Data and Summarized



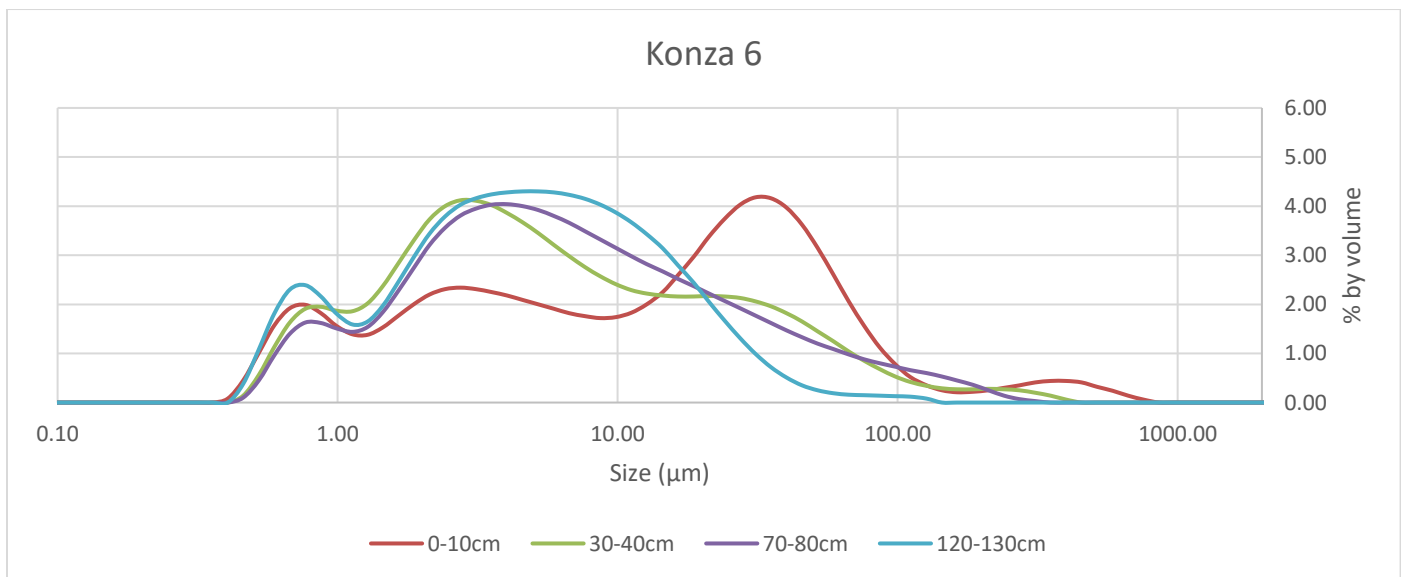
Particle	Size (μm)	0-10 cm	35-45 cm	86-96 cm	143-153 cm	Avg
Clay	0-8 μm	38.19	46.41	47.74	51.59	45.98
Silt	8-50 μm	49.44	46.11	46.86	44.46	46.72
Sand	> 50 μm	12.36	7.49	5.39	3.97	7.30



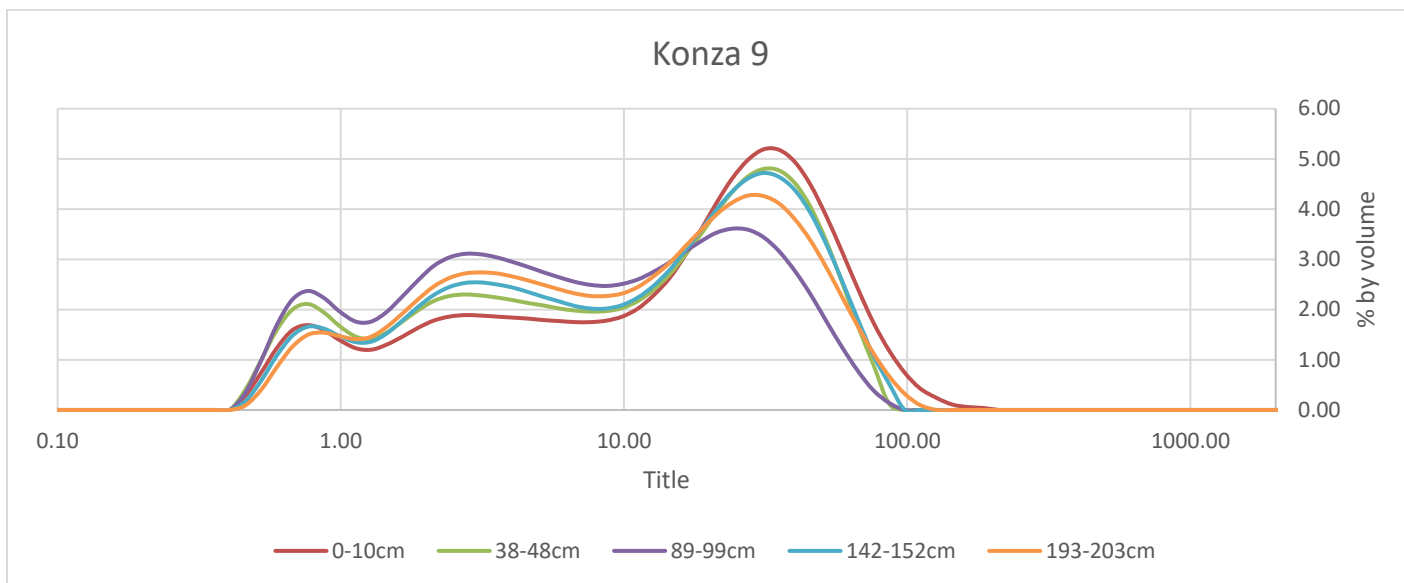
Particle	Size (μm)	0-10 cm	38-48 cm	92-102 cm	150-160 cm	Avg
Clay	0-8 μm	35.77	47.41	50.98	47.16	45.33
Silt	8-50 μm	46.92	45.77	44.71	39.22	44.16
Sand	> 50 μm	17.30	6.77	4.31	13.62	10.50



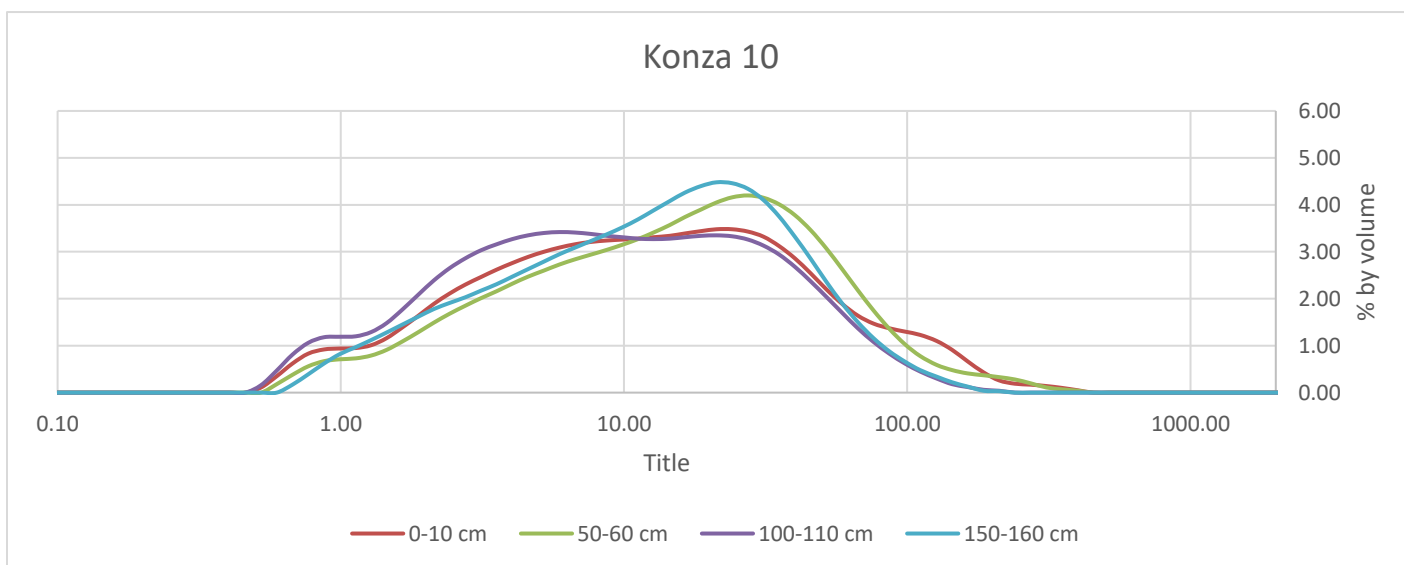
Particle	Size (μm)	0-10cm	60-70cm	Avg
Clay	0-8 μm	49.82	37.31	43.57
Silt	8-50 μm	40.82	47.61	44.22
Sand	> 50 μm	9.32	15.06	12.19



Particle	Size (μm)	0-10cm	30-40cm	70-80cm	120-130cm	Avg
Clay	0-8 μm	41.65	61.51	59.00	67.78	57.49
Silt	8-50 μm	42.18	29.94	32.23	30.98	33.83
Sand	> 50 μm	16.19	8.59	8.77	1.22	8.69

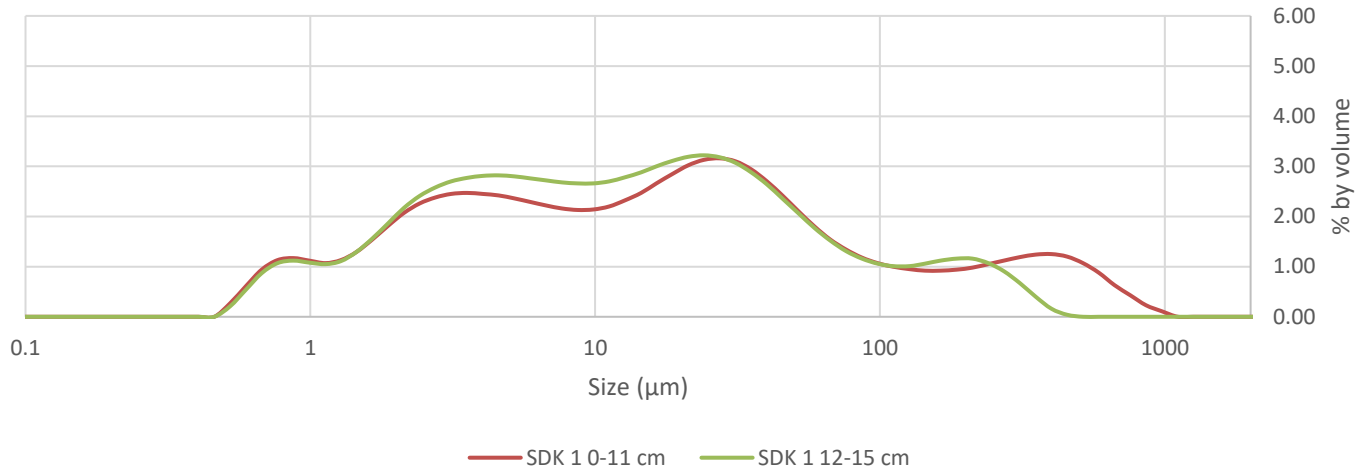


Particle	Size (μm)	0-10cm	38-48cm	89-99cm	142-152cm	193-203cm	Avg
Clay	0-8 μm	35.33	42.49	53.47	41.73	43.75	45.36
Silt	8-50 μm	50.73	48.90	42.18	48.97	47.29	46.84
Sand	> 50 μm	13.97	8.60	4.33	9.29	8.98	7.80



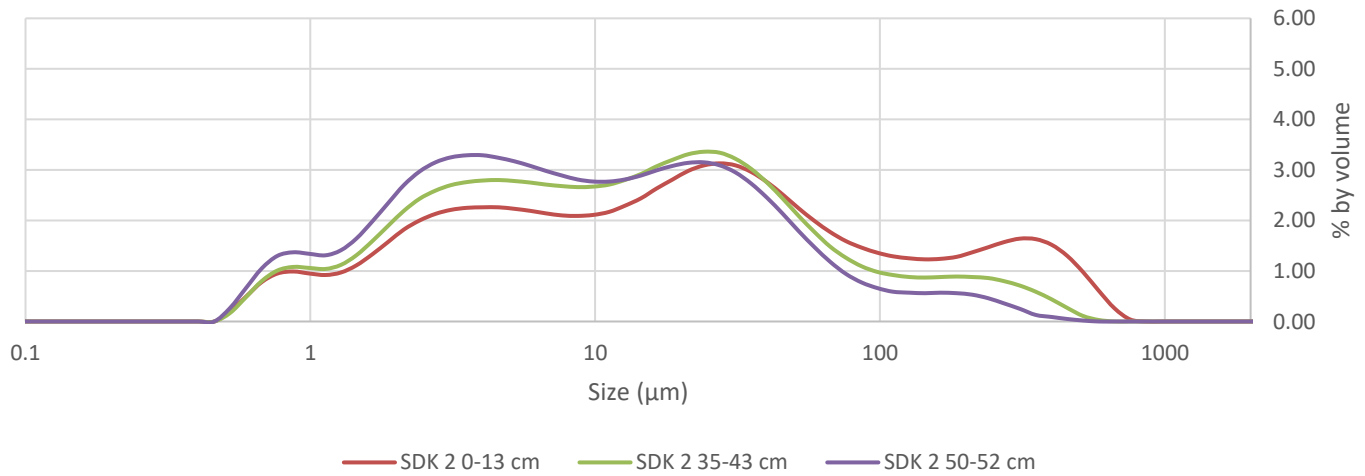
Particle	Size (μm)	0-10 cm	50-60 cm	100-110 cm	150-160 cm	Avg
Clay	0-8 μm	39.41	32.40	47.02	35.80	38.66
Silt	8-50 μm	45.49	51.89	44.19	54.50	49.02
Sand	> 50 μm	15.12	15.68	8.79	9.70	12.32

SDK 1

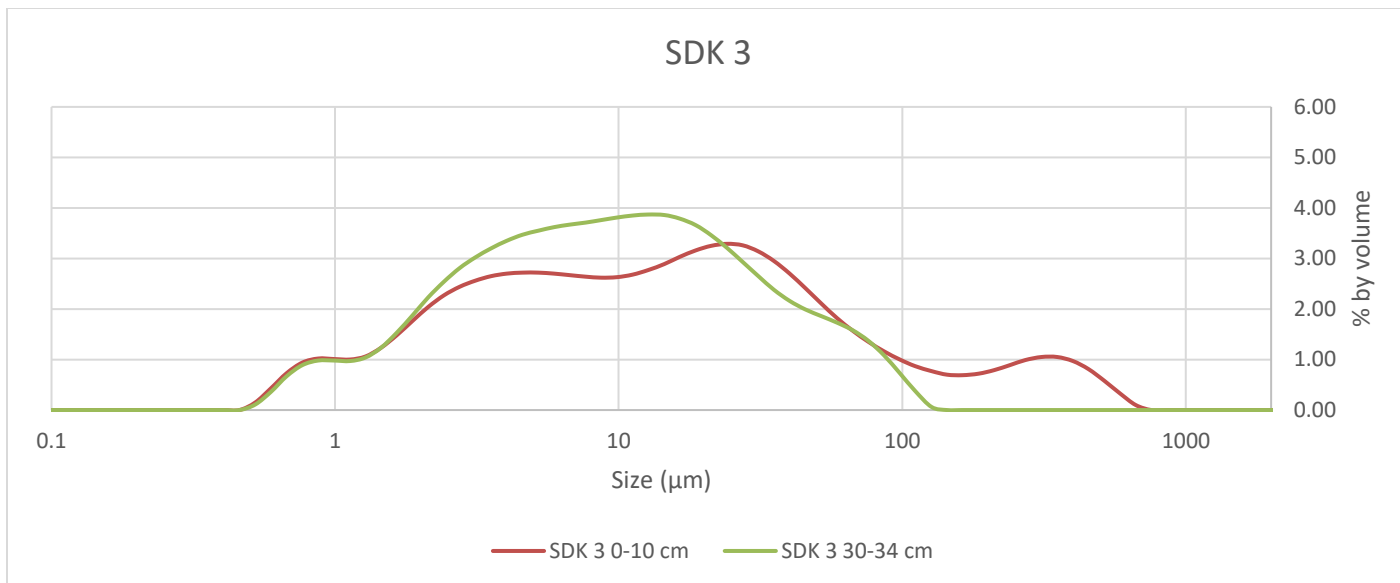


Particle	Size (μm)	SDK 1 0-11 cm	SDK 1 12-15 cm	AVG
Clay	0-8 μm	37.62	40.99	39.31
Silt	8-50 μm	37.23	40.32	38.78
Sand	> 50 μm	25.14	18.65	21.90

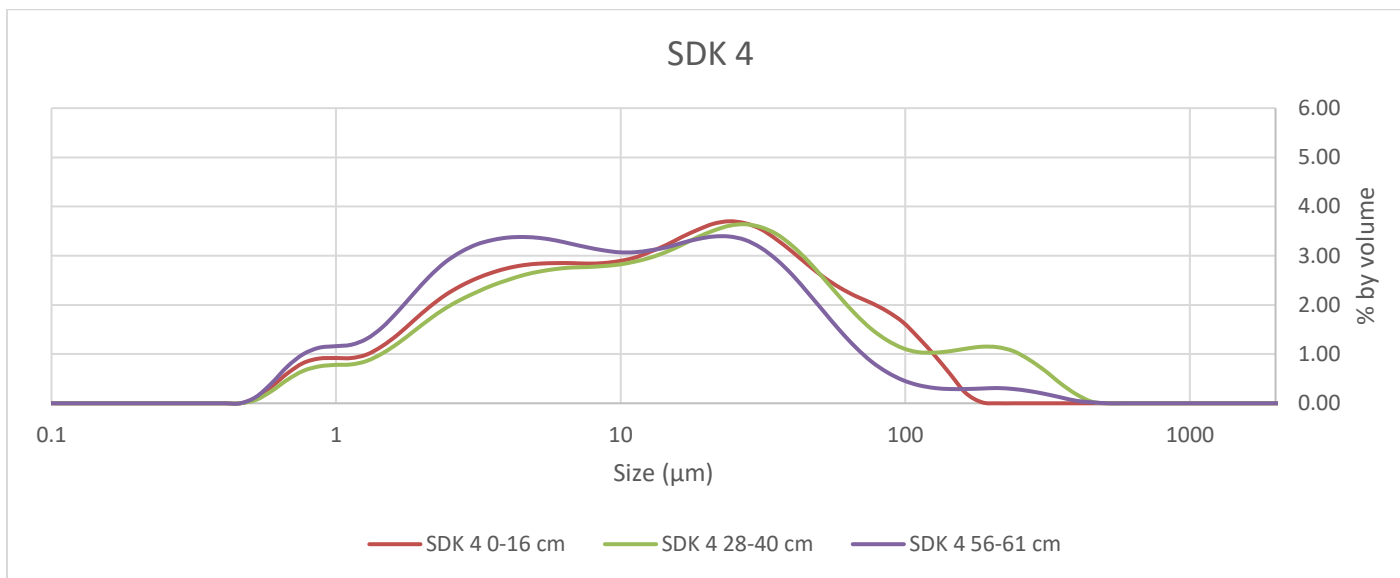
SDK 2



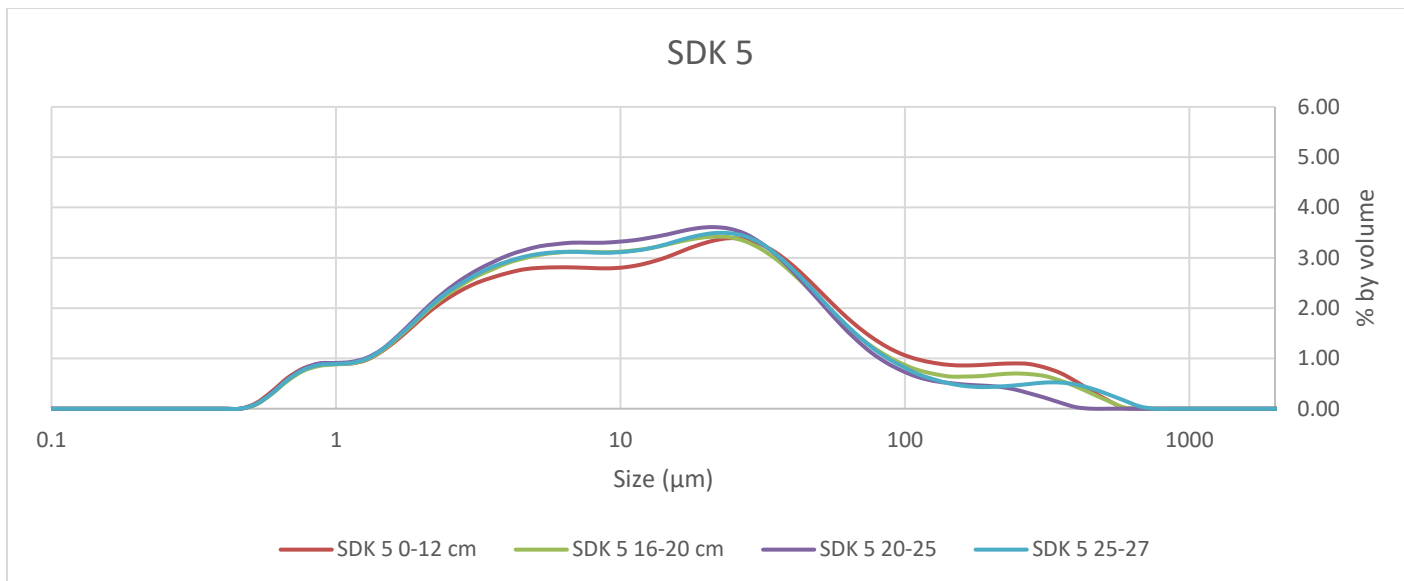
Particle	Size (μm)	SDK 2 0-13 cm	SDK 2 35-43 cm	SDK 2 50-52 cm	AVG
Clay	0-8 μm	33.86	40.74	48.69	41.10
Silt	8-50 μm	37.06	41.46	39.76	39.43
Sand	> 50 μm	29.09	17.80	11.55	19.48



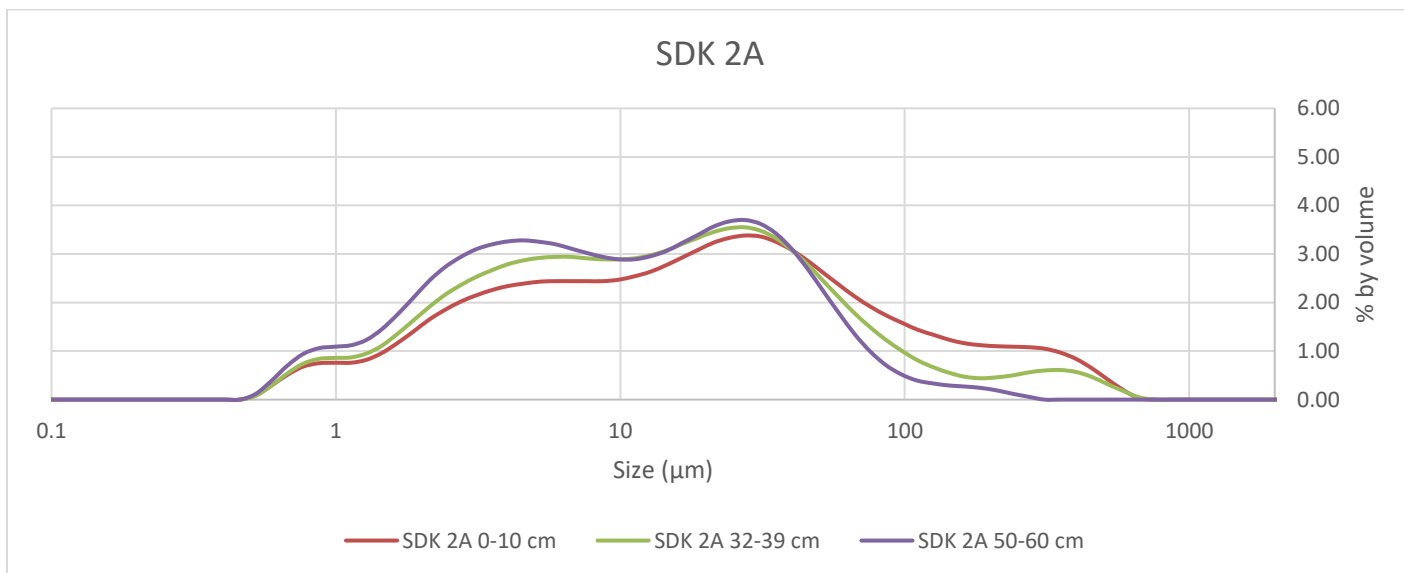
Particle	Size (μm)	SDK 3 0-10 cm	SDK 3 30-34 cm	AVG
Clay	0-8 μm	38.93	45.81	42.37
Silt	8-50 μm	40.78	45.38	43.08
Sand	> 50 μm	20.32	8.79	14.56



Particle	Size (μm)	SDK 4 0-16 cm	SDK 4 28-40 cm	SDK 4 56-61 cm	AVG
Clay	0-8 μm	38.55	34.81	47.64	40.33
Silt	8-50 μm	45.68	45.00	43.16	44.61
Sand	> 50 μm	15.78	20.16	9.22	15.05

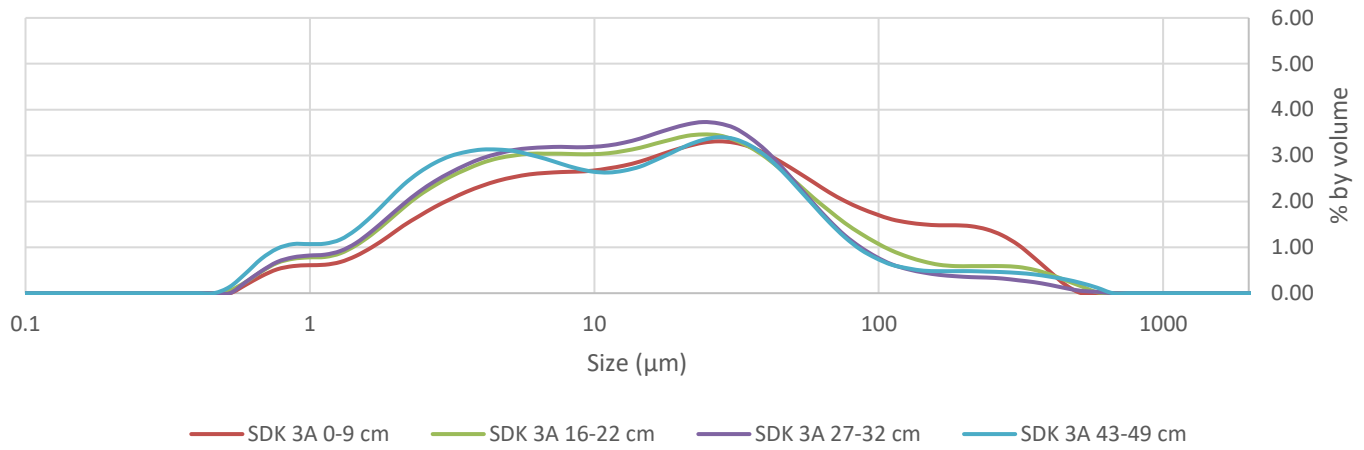


Particle	Size (μm)	SDK 5 0-12 cm	SDK 5 16-20 cm	SDK 5 20-25	SDK 5 25-27	AVG
Clay	0-8 μm	37.94	39.91	41.82	40.36	40.01
Silt	8-50 μm	42.63	43.96	46.13	44.64	44.34
Sand	> 50 μm	19.40	16.13	12.06	14.98	15.64



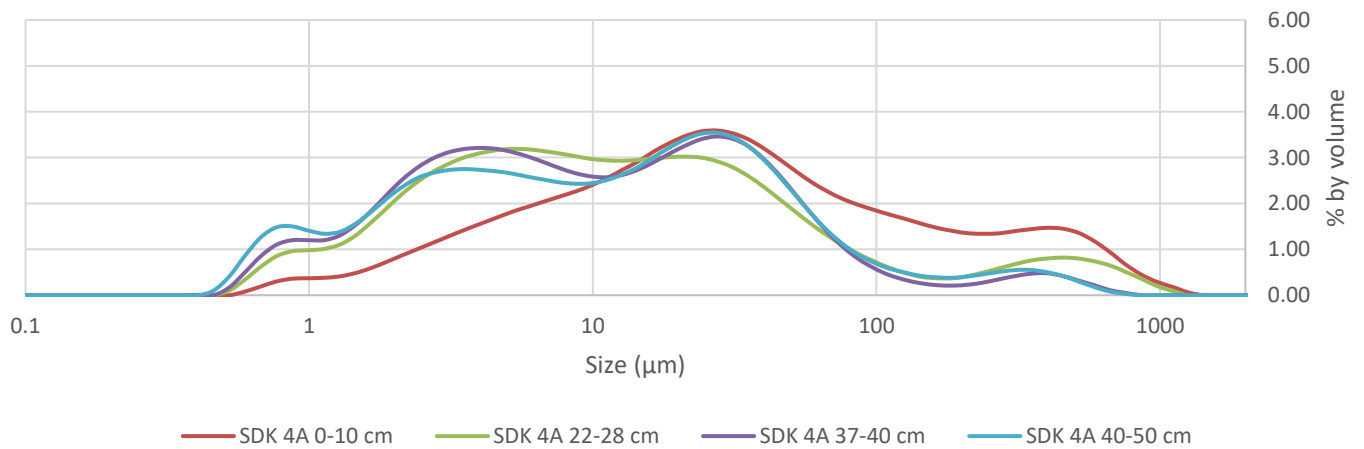
Particle	Size (μm)	SDK 2A 0-10 cm	SDK 2A 32-39 cm	SDK 2A 50-60 cm	AVG
Clay	0-8 μm	32.61	38.28	45.51	38.80
Silt	8-50 μm	41.34	44.45	45.10	43.63
Sand	> 50 μm	26.02	17.26	9.42	17.57

SDK 3A



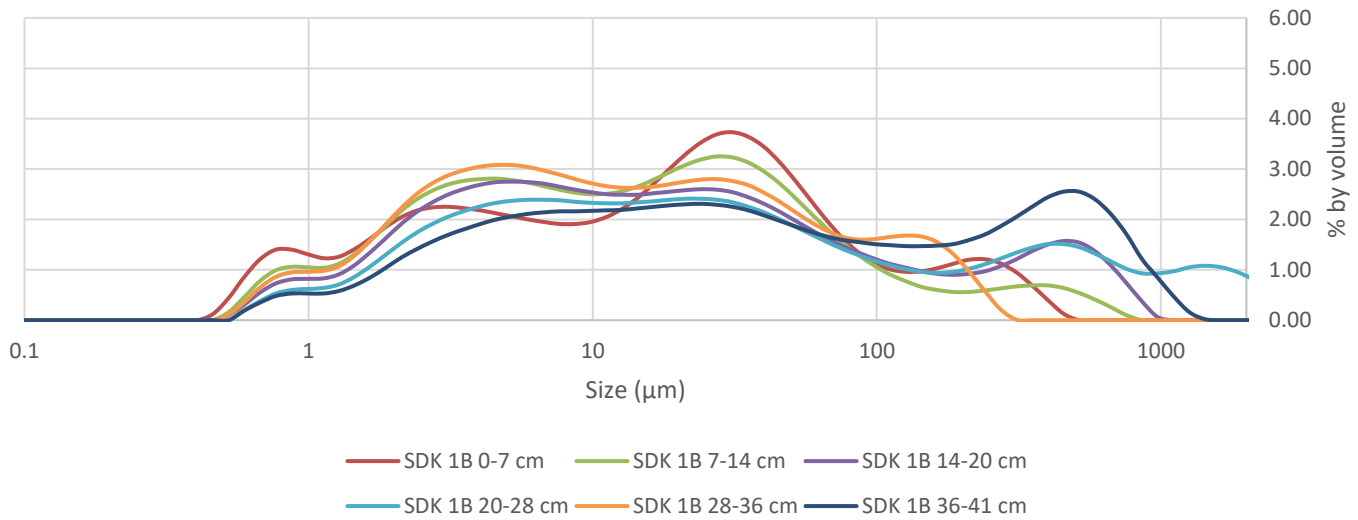
Particle	Size (μm)	SDK 3A 0-9 cm	SDK 3A 16-22 cm	SDK 3A 27-32 cm	SDK 3A 43-49 cm	AVG
Clay	0-8 μm	31.07	37.99	39.50	43.80	38.09
Silt	8-50 μm	41.92	44.48	47.27	41.59	43.82
Sand	> 50 μm	27.03	17.53	13.23	14.57	18.09

SDK 4A



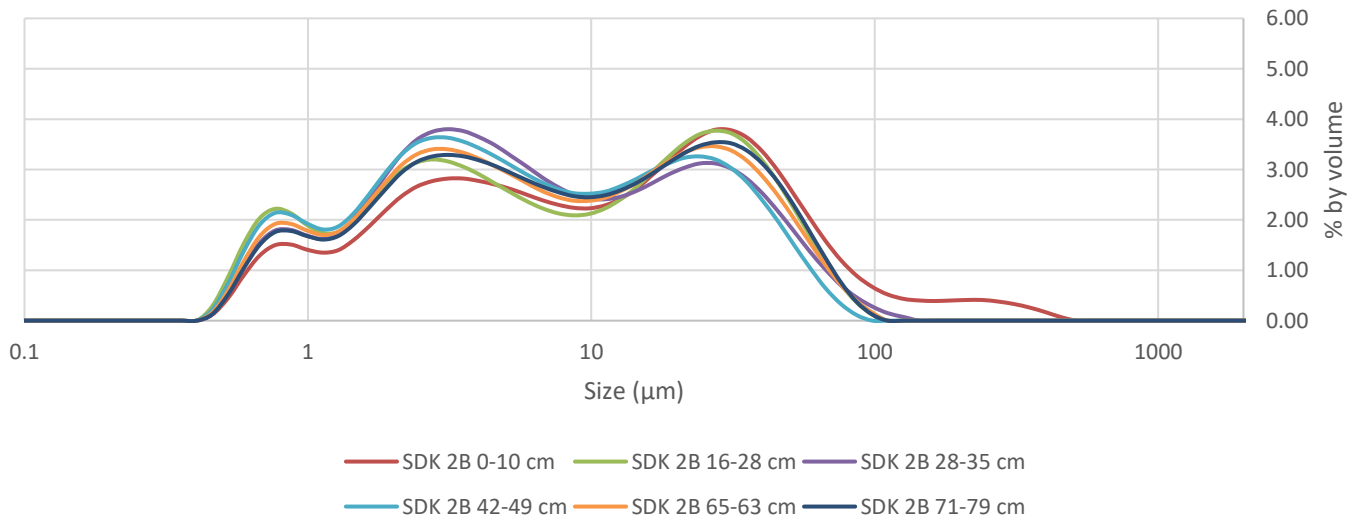
Particle	Size (μm)	SDK 4A 0-10 cm	SDK 4A 22-28 cm	SDK 4A 37-40 cm	SDK 4A 40-50 cm	AVG
Clay	0-8 μm	20.83	42.86	45.88	43.92	38.37
Silt	8-50 μm	43.02	39.59	41.53	41.73	41.47
Sand	> 50 μm	36.16	17.55	12.62	14.34	20.17

SDK 1B

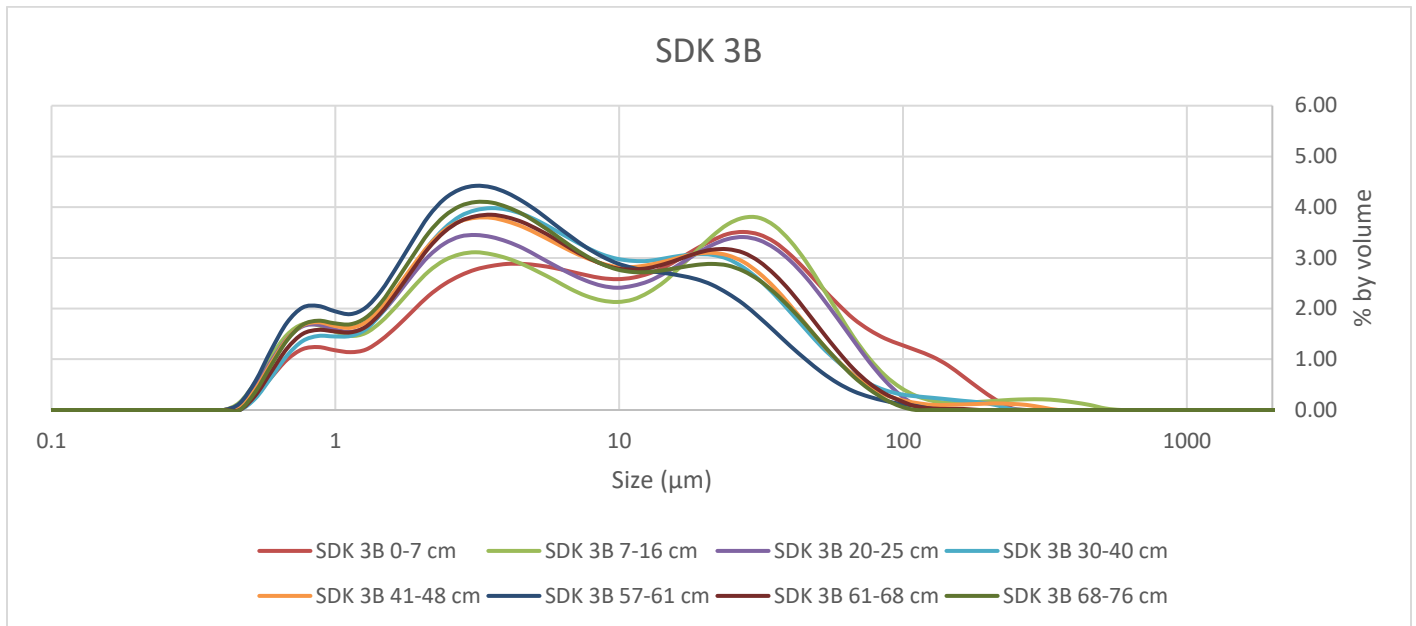


Particle	Size (μm)	SDK 1B 0-7 cm	SDK 1B 7-14 cm	SDK 1B 14-20 cm	SDK 1B 20-28 cm	SDK 1B 28-36 cm	SDK 1B 36-41 cm	AVG
Clay	0-8 μm	39.19	42.98	39.55	32.83	44.98	28.07	37.93
Silt	8-50 μm	41.58	39.92	34.27	31.85	36.79	30.53	35.82
Sand	> 50 μm	19.23	17.10	26.17	35.30	18.20	41.39	26.23

SDK 2B



Particle	Size (μm)	SDK 2B 0-10 cm	SDK 2B 16-28 cm	SDK 2B 28-35 cm	SDK 2B 42-49 cm	SDK 2B 65-63 cm	SDK 2B 71-79 cm	AVG
Clay	0-8 μm	46.64	53.94	58.86	59.85	55.65	54.01	54.83
Silt	8-50 μm	42.78	41.99	37.09	38.02	40.41	41.71	40.33
Sand	> 50 μm	10.56	4.08	4.06	2.15	3.93	4.27	4.84



Particle	Size (μm)	SDK 3B 0-7 cm	SDK 3B 7-16 cm	SDK 3B 20-25 cm	SDK 3B 30-40 cm	SDK 3B 41-48 cm	SDK 3B 57-61 cm	SDK 3B 61-68 cm	SDK 3B 68-76 cm	AVG
Clay	0-8 μm	45.24	50.22	54.53	59.59	59.67	68.82	58.69	62.68	57.43
Silt	8-50 μm	42.18	42.09	40.40	36.40	36.75	29.59	38.18	34.97	37.57
Sand	> 50 μm	12.61	7.68	5.08	4.04	3.59	1.56	3.14	2.32	5.00

Appendix D - Bulk Powder X-Ray Diffraction (XRD) Data

For all analyses from both Konza Prairie and for Stockdale Kimberlite, “Vermiculite” as identified by Highscore Plus may or may not truly be vermiculite. Unnamed 2:1 layer silicate is more accurate. A blank cell indicates mineral was not identified in this sample.

D.1-Konza Diffraction Analyses

Konza Core 3

Mineral	Konza 3 0-10cm	Konza 3 25-35cm	Konza 3 86-96cm	Konza 3 143-153cm
Albite	x	x	x	
Albite, Calcian				x
Quartz	x	x	x	x
Vermiculite**			x	x
Zeolite	x			
Other Minerals	Alunite			Mica

Konza Core 4

Mineral	Konza 4 0-10cm	Konza 4 38-48cm	Konza 4 92-102cm	Konza 4 150-160cm
Albite	x	x	x	x
Calcite				x
Microcline			x	
Muscovite	x			x
Quartz	x	x	x	x
Zeolite			x	x
Other Minerals	Anorthoclase		Dolomite	Orthoclase

Konza Core 5

Mineral	Konza 5 0-10cm	Konza 5 60-70cm
Albite		x
Albite, Calcian	x	
Calcite		x
Microcline	x	
Muscovite	x	
Quartz	x	x

Konza Core 6

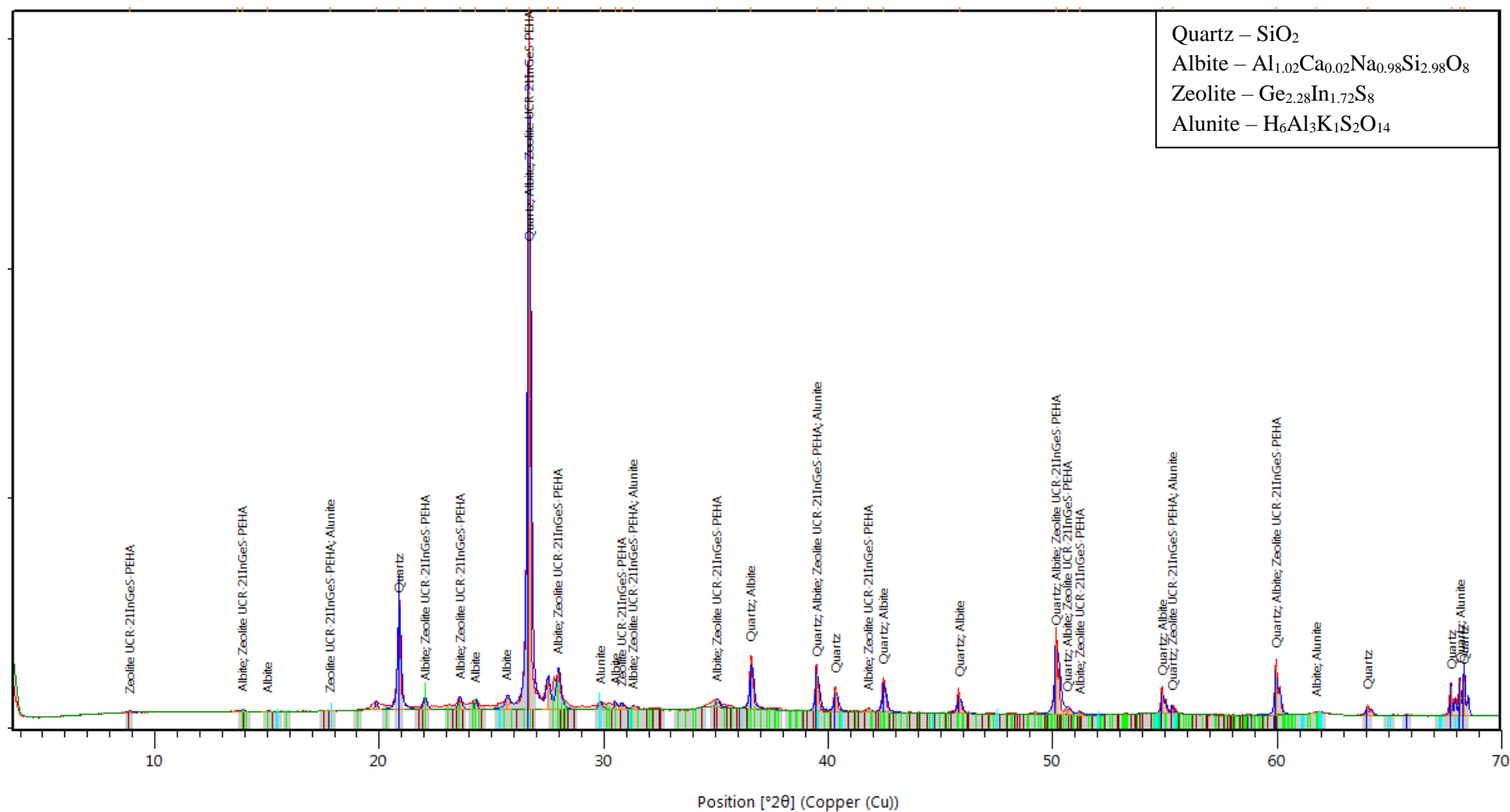
Mineral	Konza 6 0-10cm	Konza 6 30-40cm	Konza 6 70-80cm	Konza 6 120-130cm
Albite	x	x		
Calcite			x	x
Muscovite	x	x		
Quartz	x	x	x	x
Other Minerals	Nontronite		Illite	Illite Cristobalite

Konza Core 9

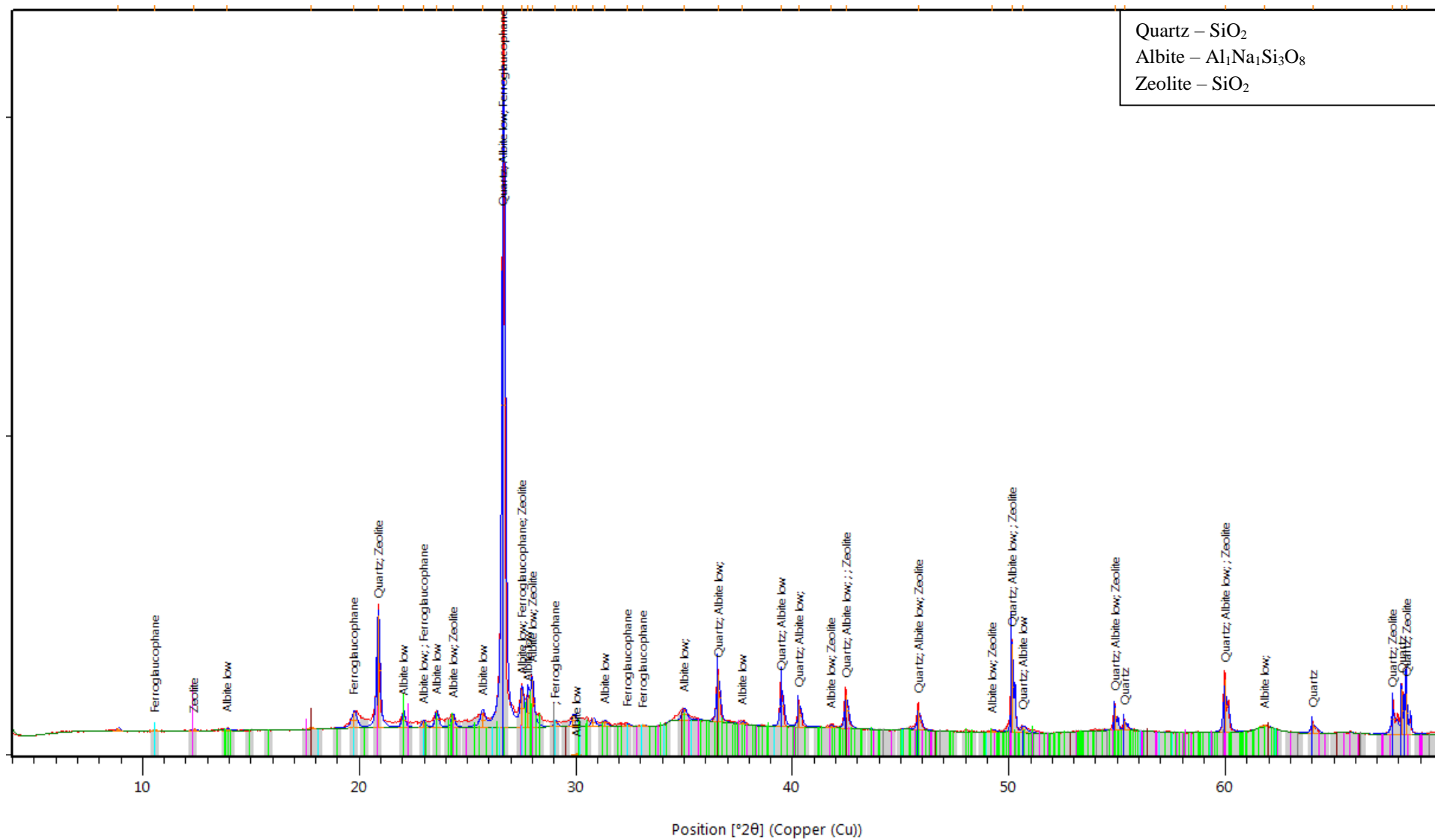
Mineral	Konza 9 0-10cm	Konza 9 38-48cm	Konza 9 89-99cm	Konza 9 142-152cm	Konza 9 193-203cm
Albite			x		
Albite, Calcian	x	x		x	x
Dolomite	x	x			
Microcline				x	
Muscovite	x	x	x	x	
Quartz	x	x	x	x	x
Vermiculite**					x
Zeolite	x				x
Other Minerals	Anorthoclase		Anorthoclase	Nepheline	Anorthoclase

Konza Core 10

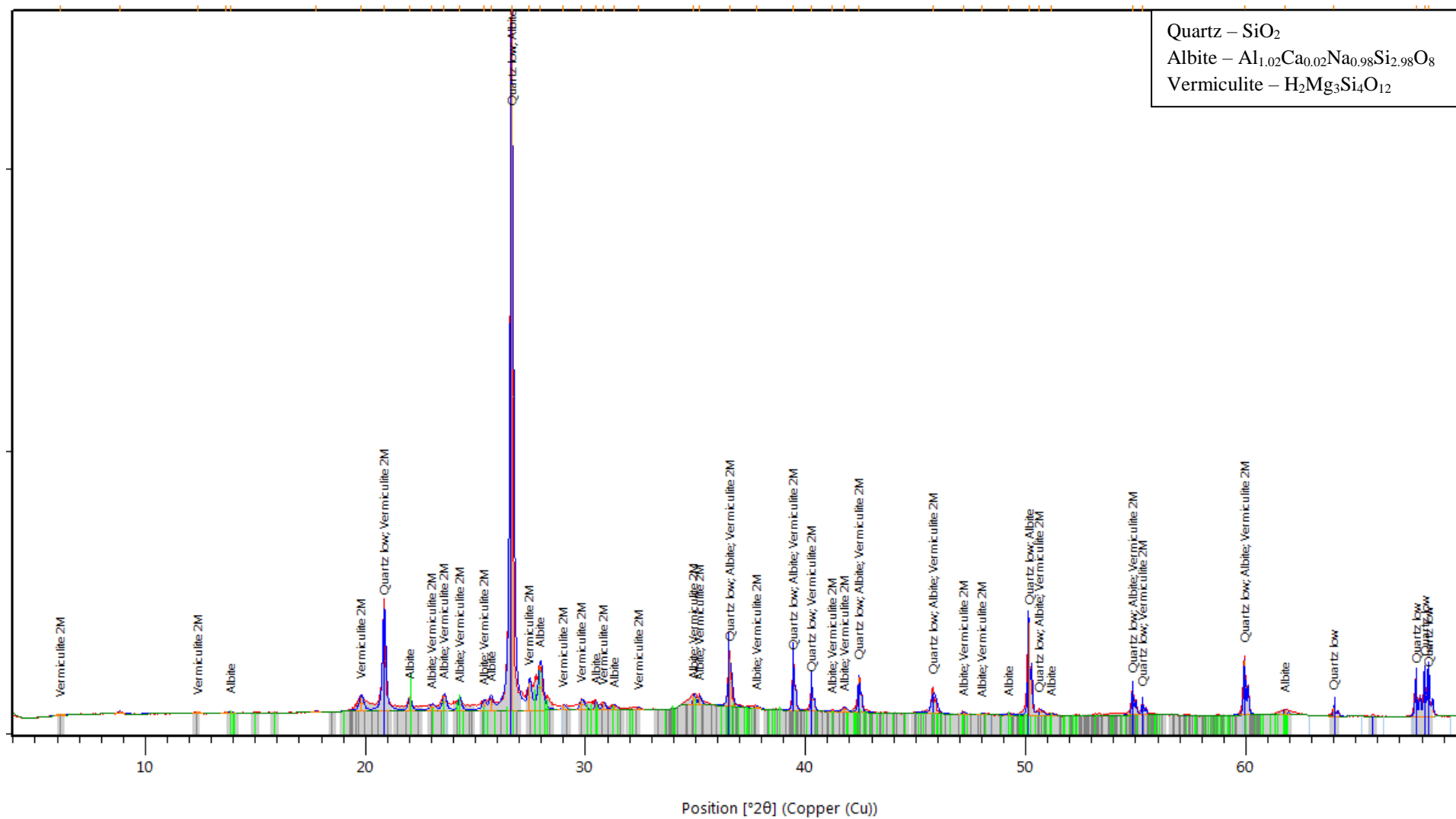
Mineral	Konza 10 0-10cm	Konza 10 50-60cm	Konza 10 100-110cm	Konza 10 150-160cm
Albite	x	x	x	x
Calcite	x	x	x	x
Microcline	x	x		
Muscovite		x		x
Quartz	x	x	x	x
Vermiculite**			x	x
Zeolite				x
Other Minerals	Mg Silicate			



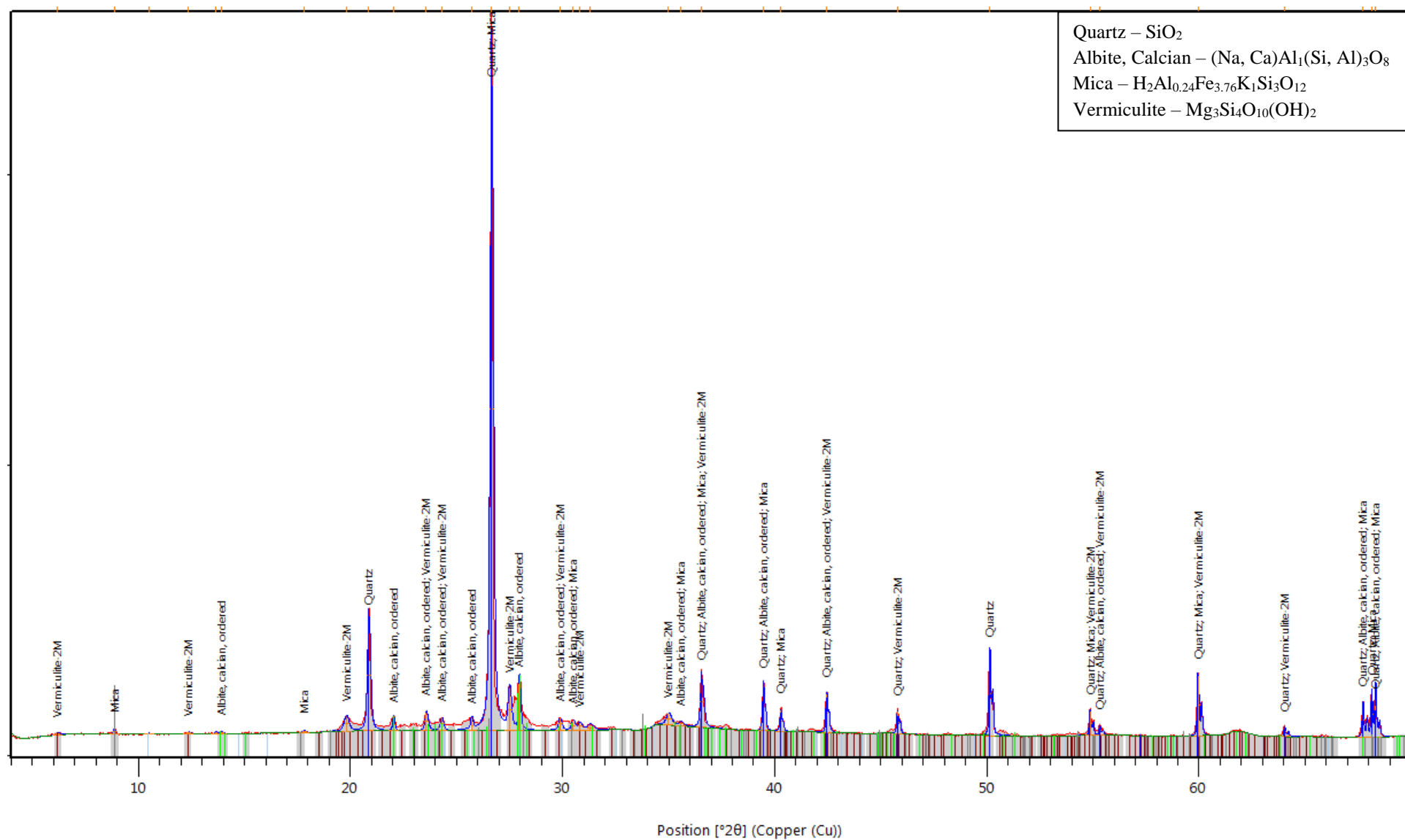
Konza Core 3, 0-10 cm



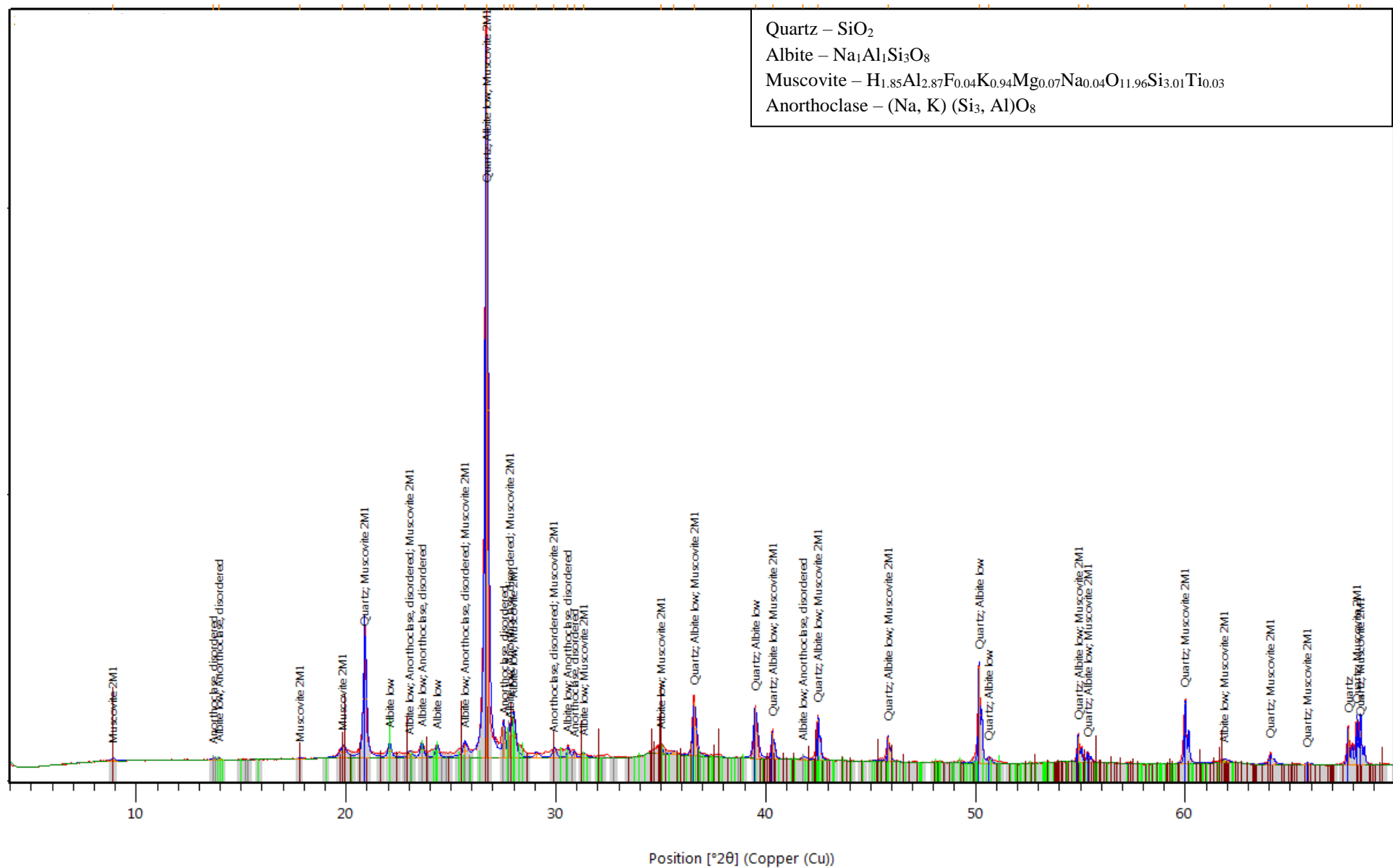
Konza Core 3, 25-45 cm



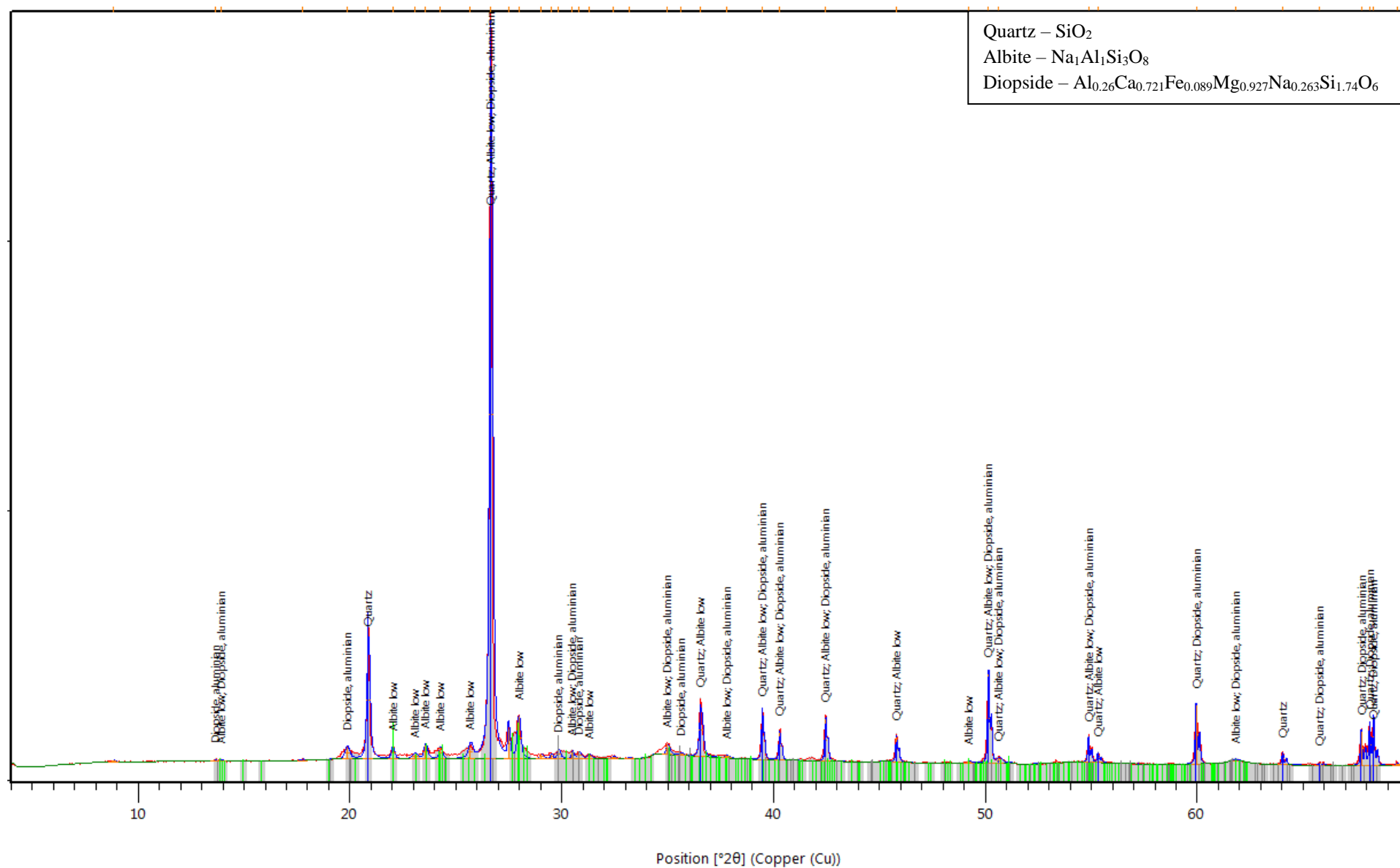
Konza Core 3, 86-96 cm



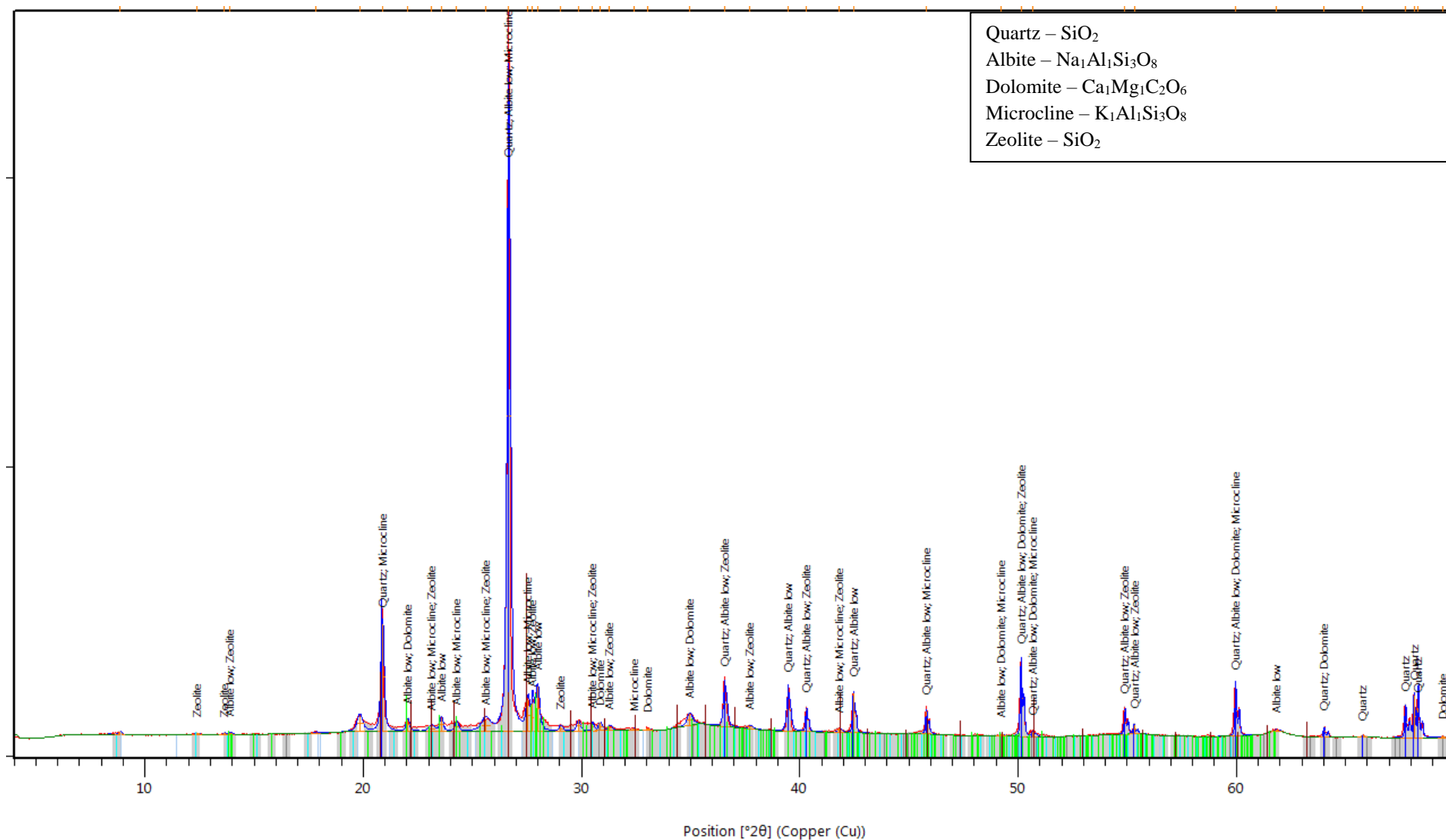
Konza Core 3, 143-153 cm



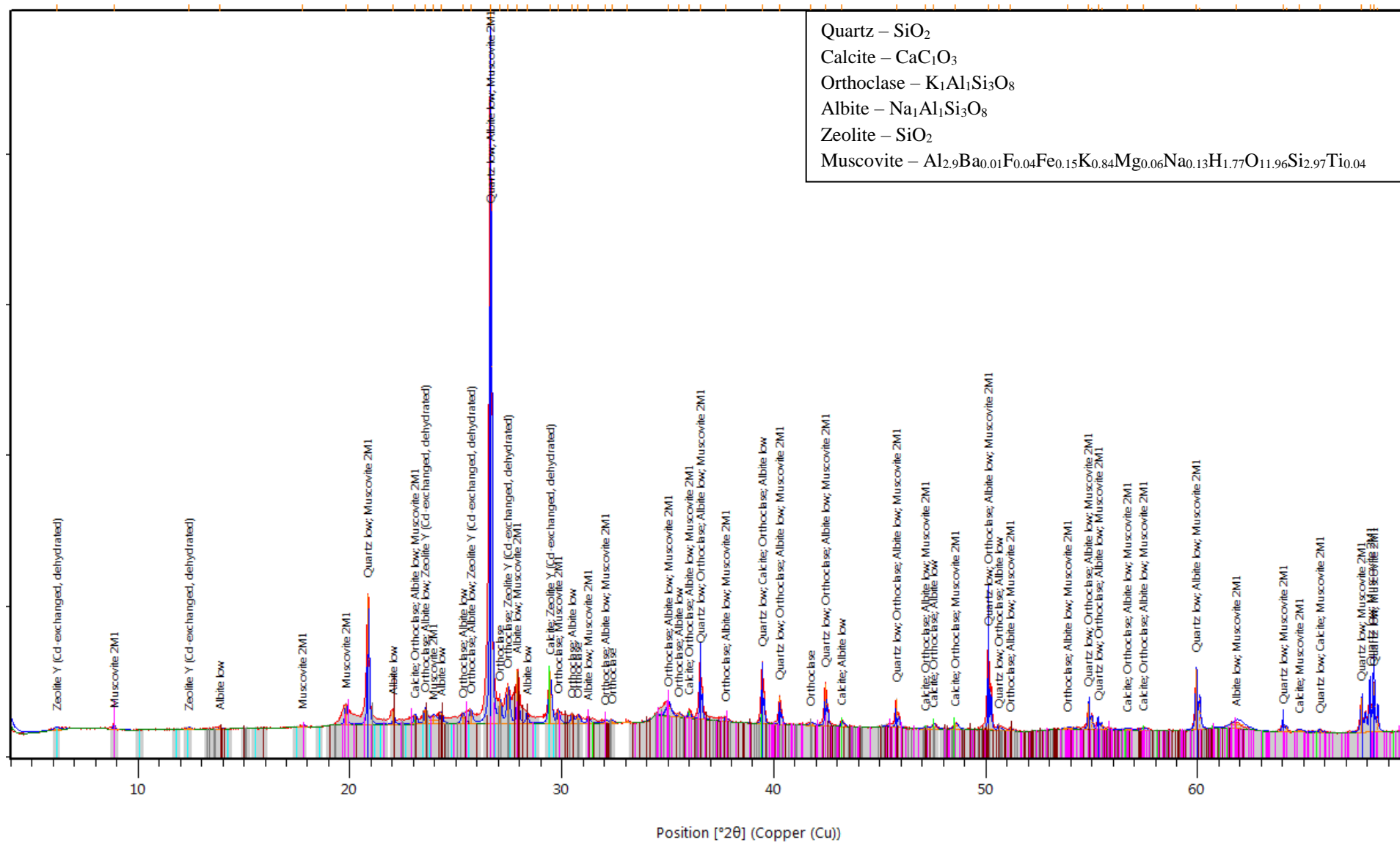
Konza Core 4, 0-10 cm



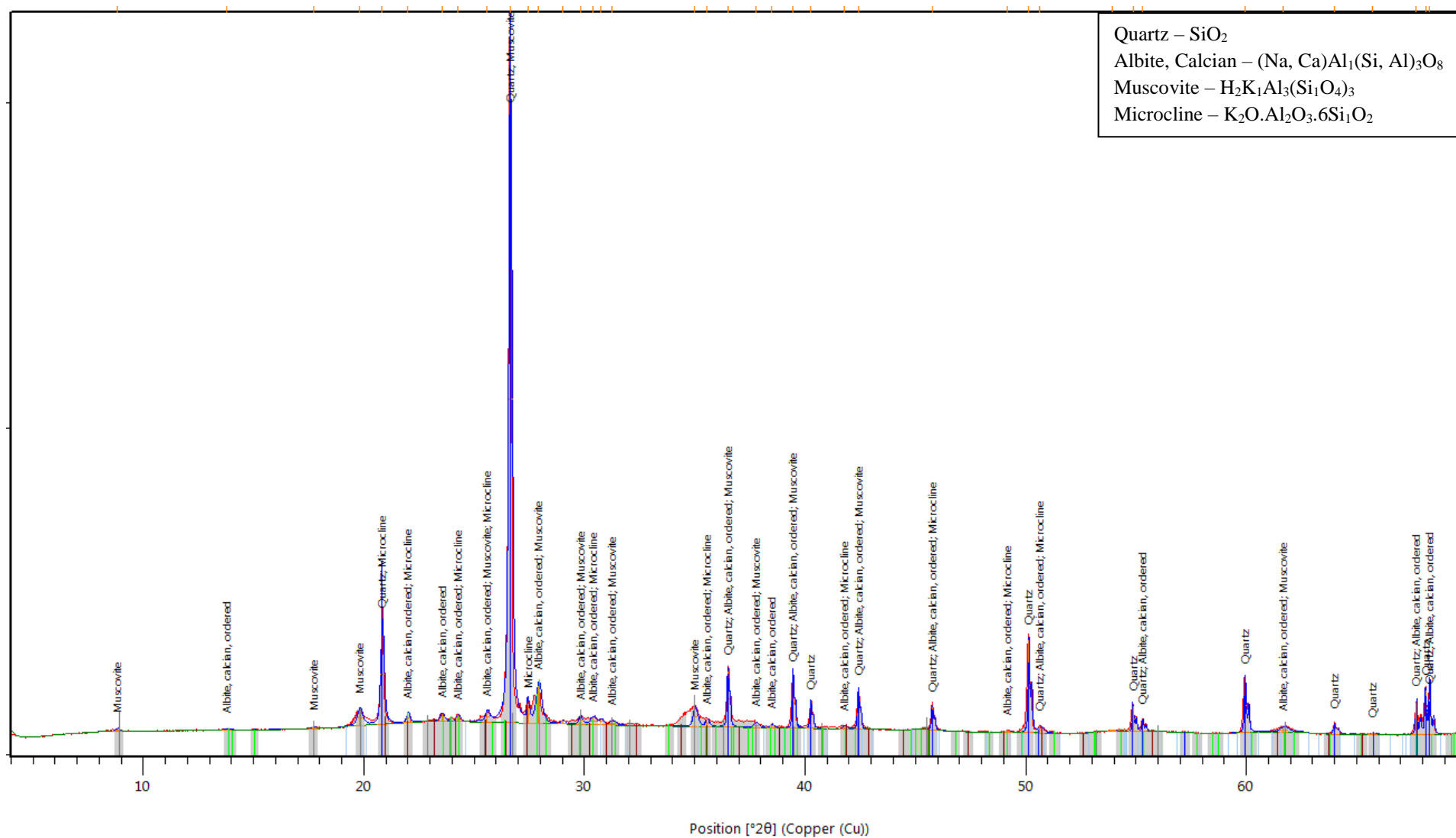
Konza Core 4, 38-48 cm



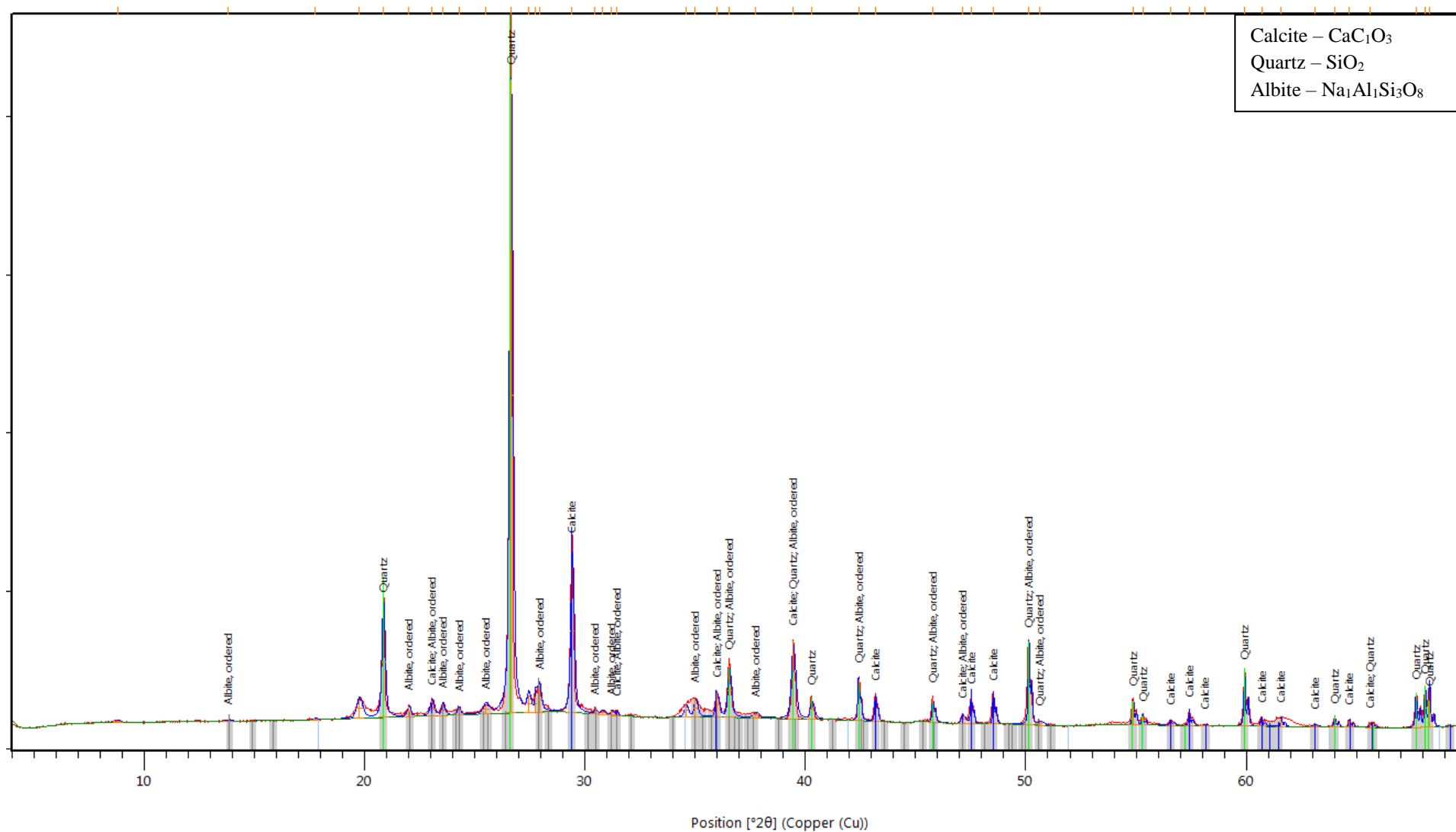
Konza Core 4, 92-102 cm



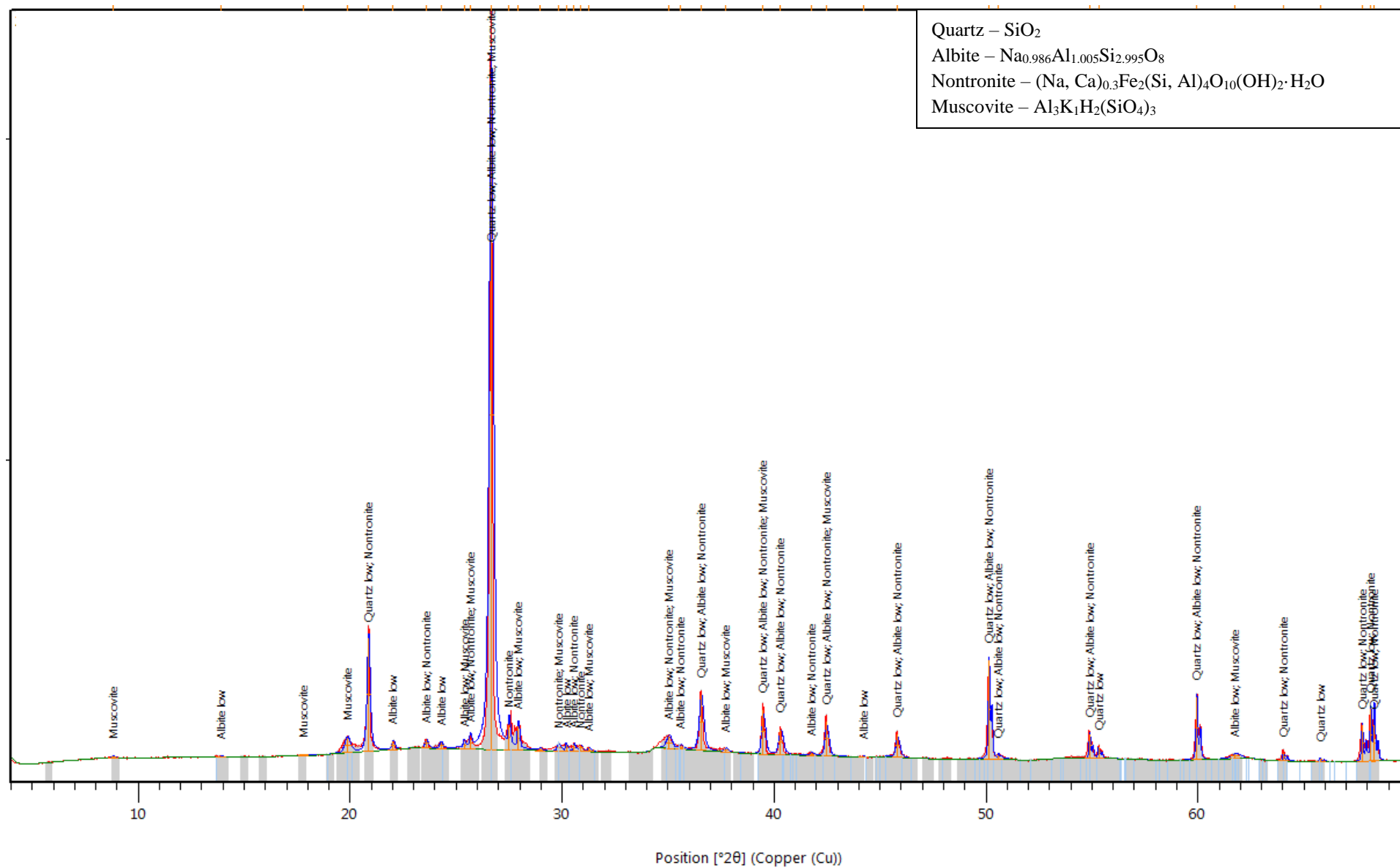
Konza Core 4, 150-160 cm



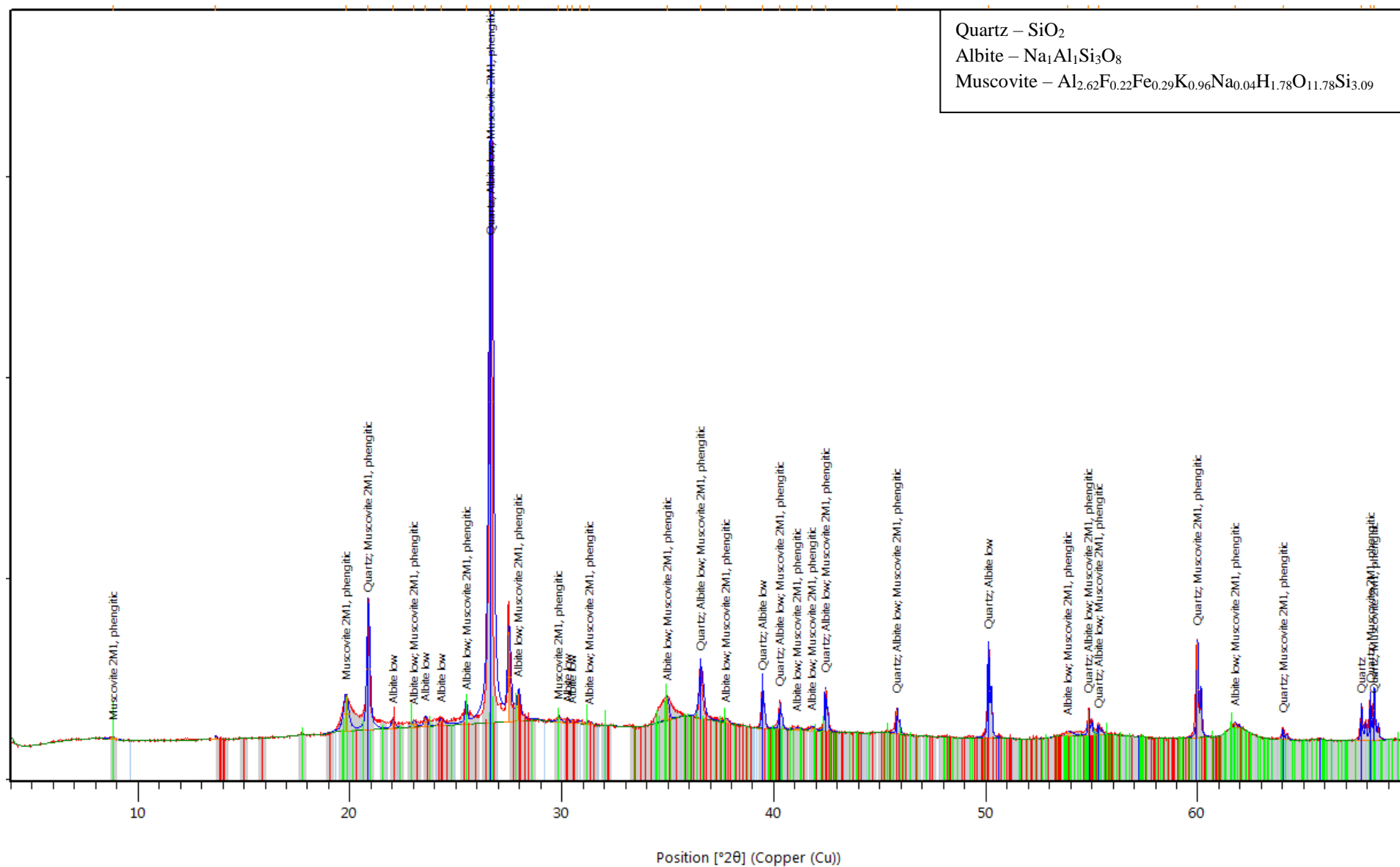
Konza Core 5, 0-10 cm



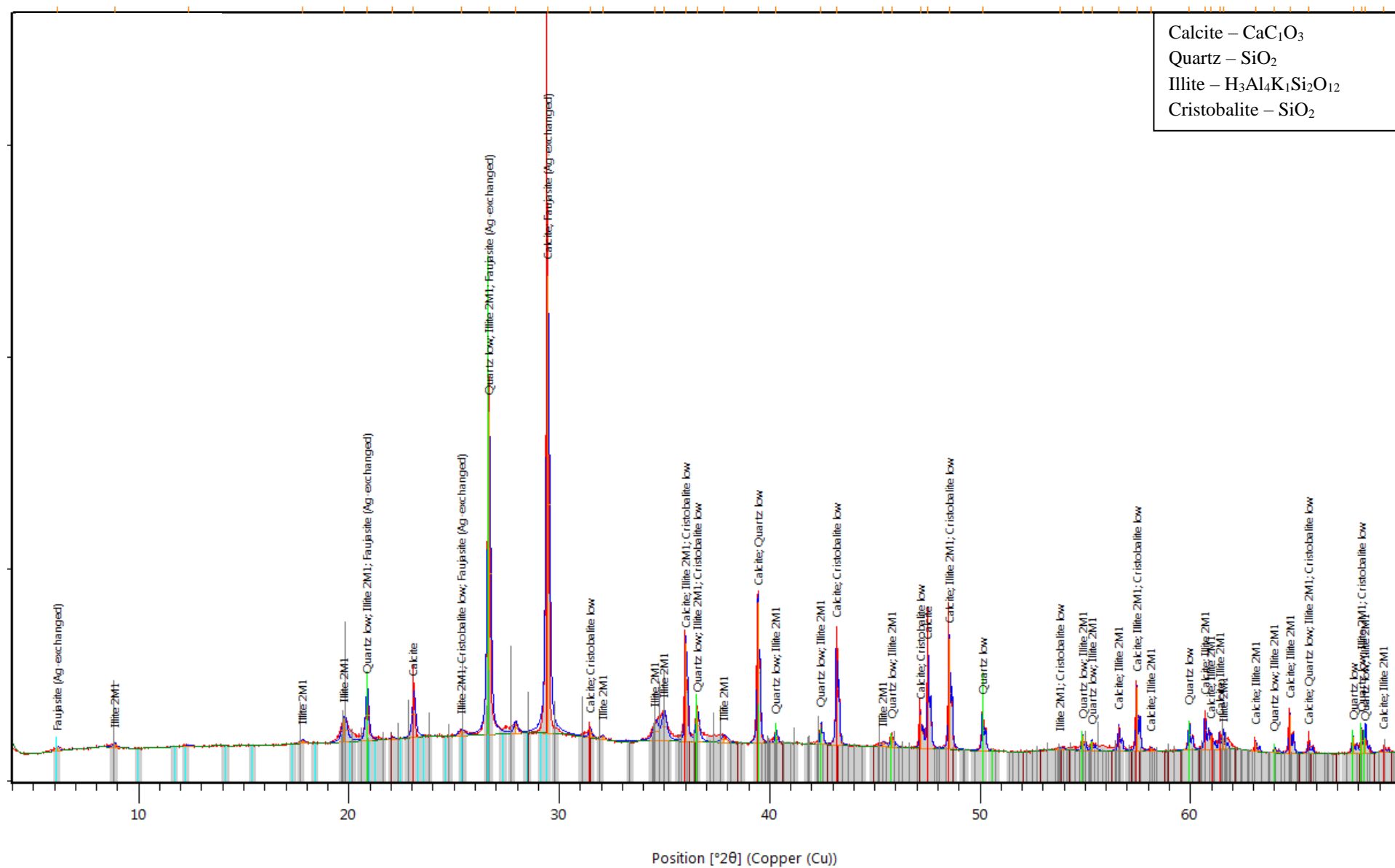
Konza Core 5, 60-70 cm



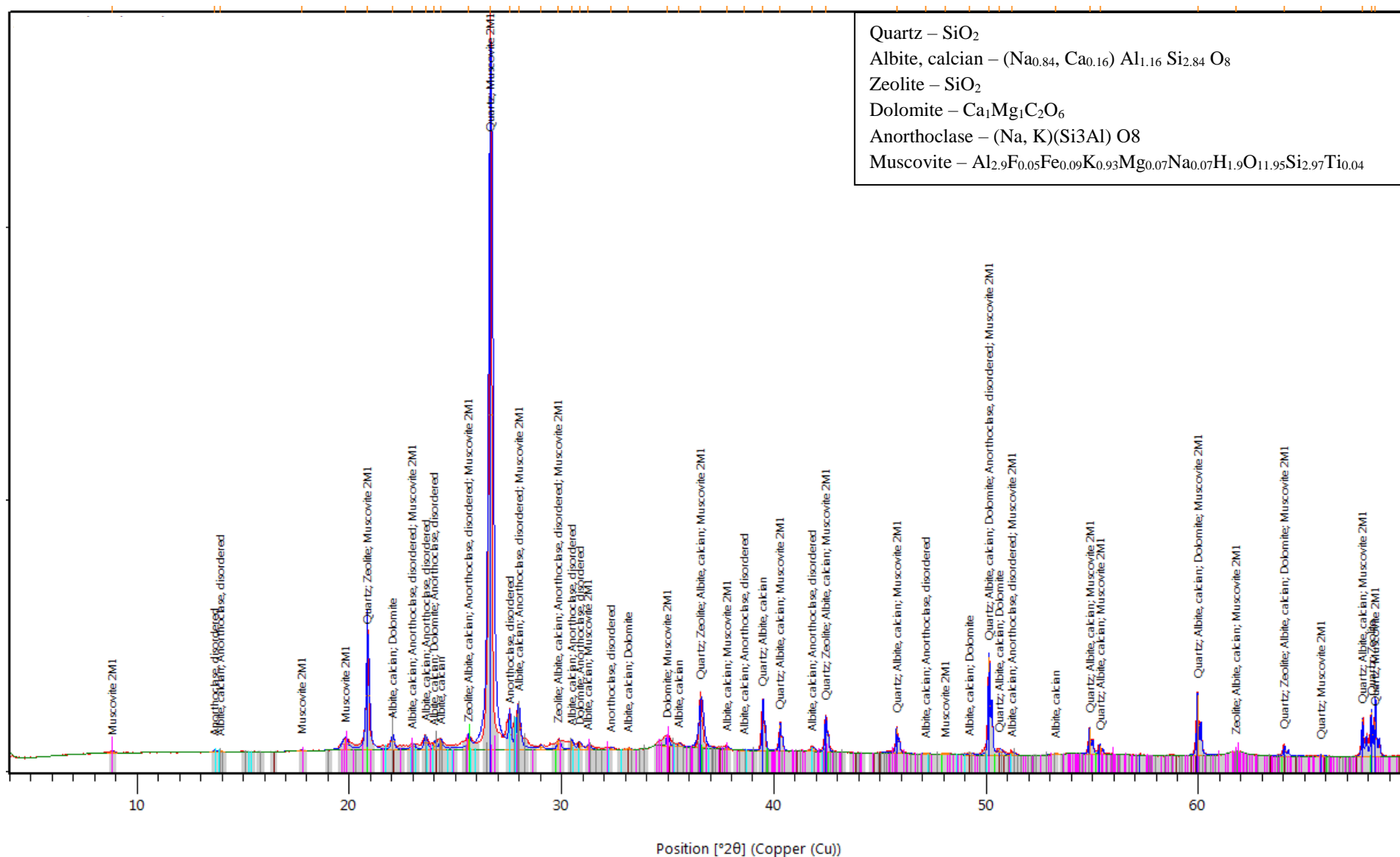
Konza Core 6, 0-10 cm



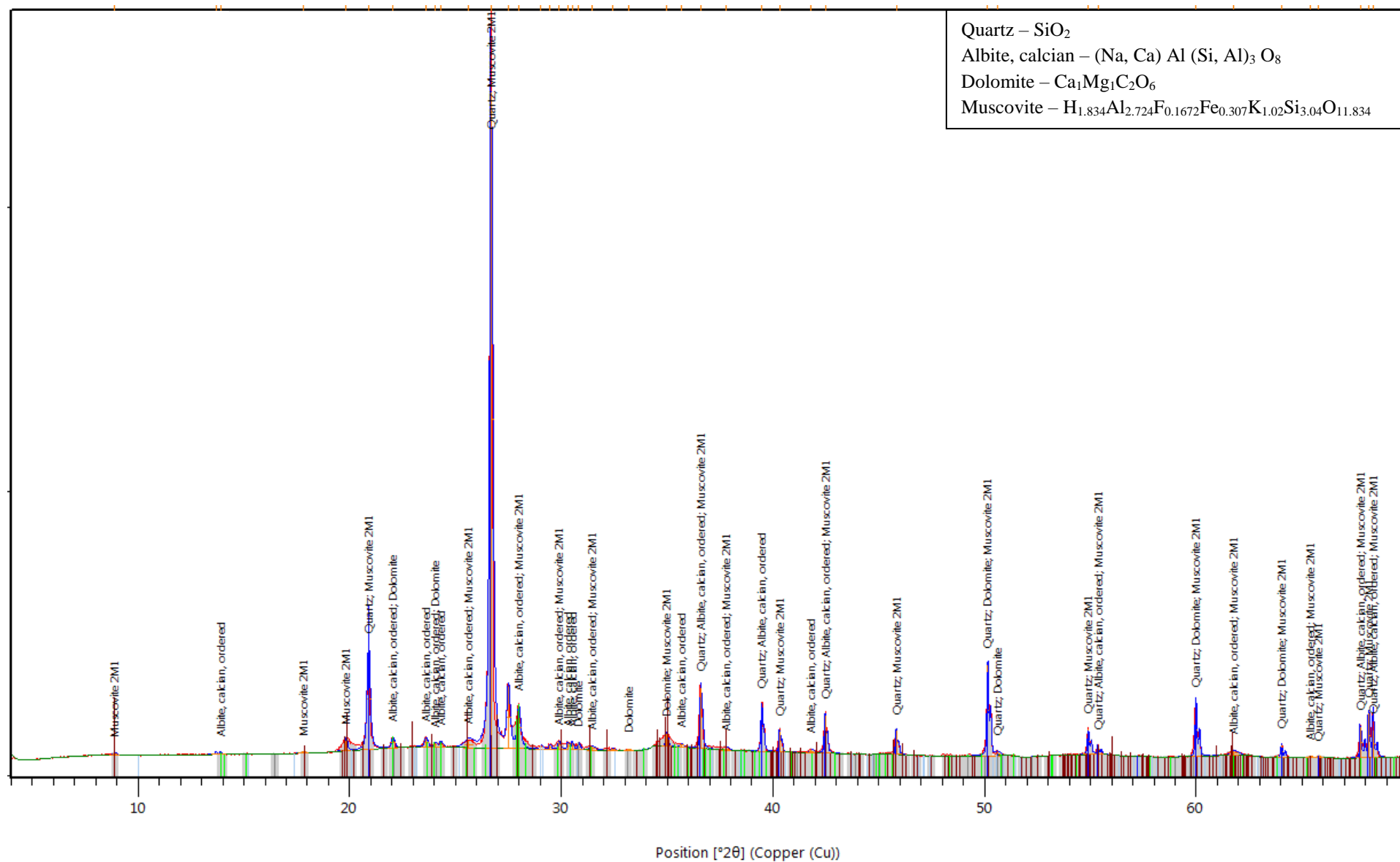
Konza Core 6, 30-40 cm



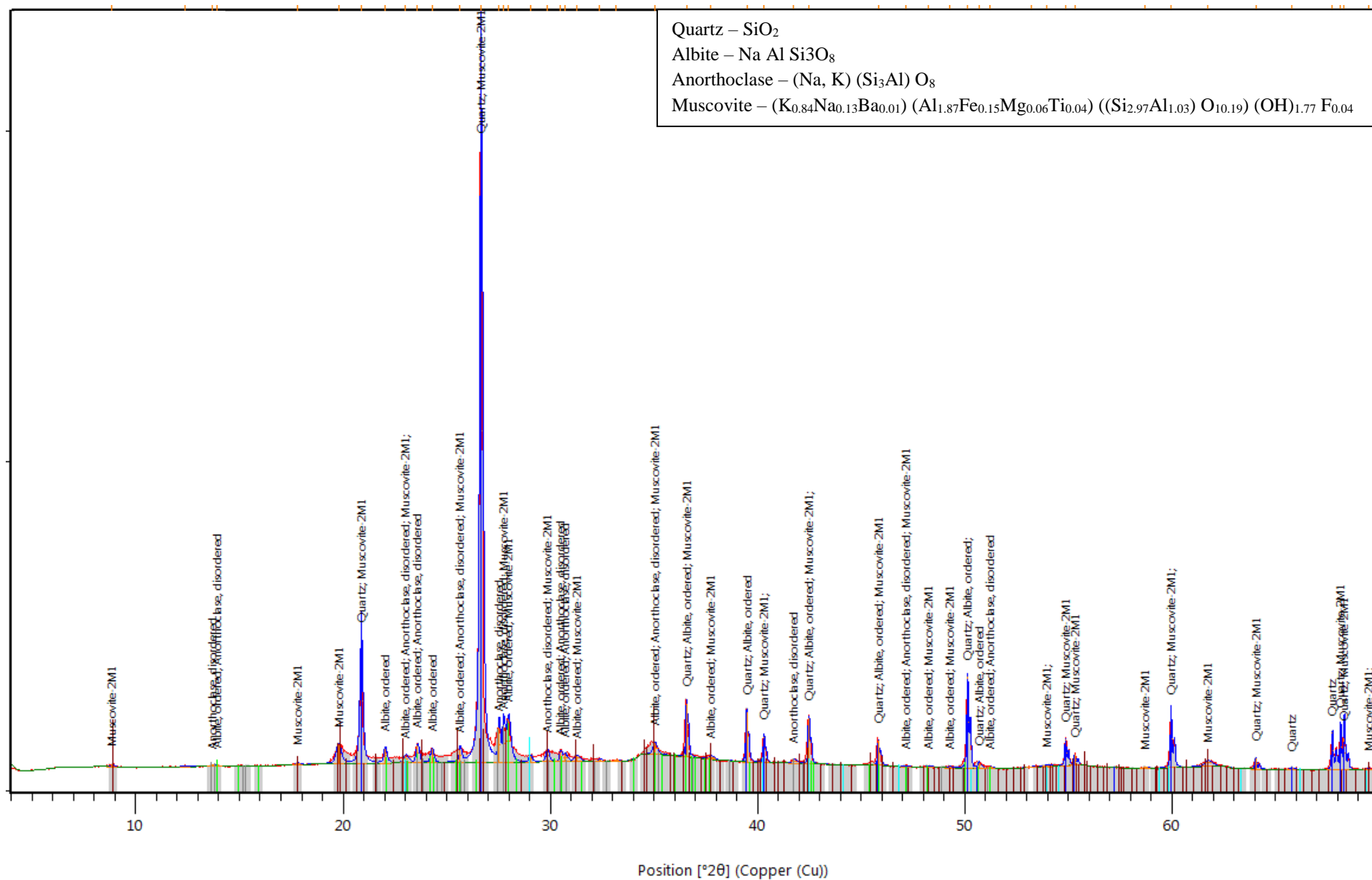
Konza Core 6, 120-130 cm



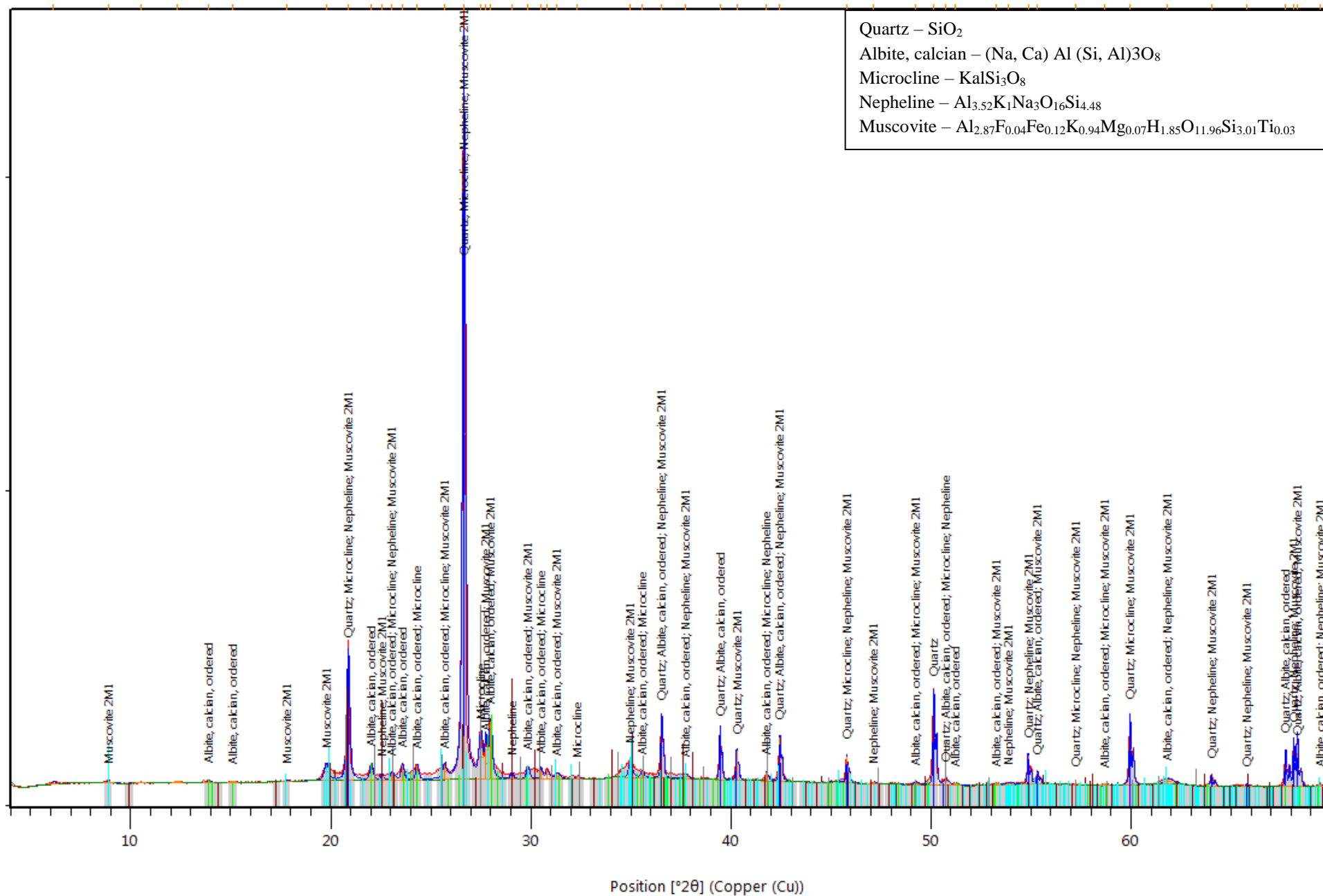
Konza Core 9, 0-10 cm



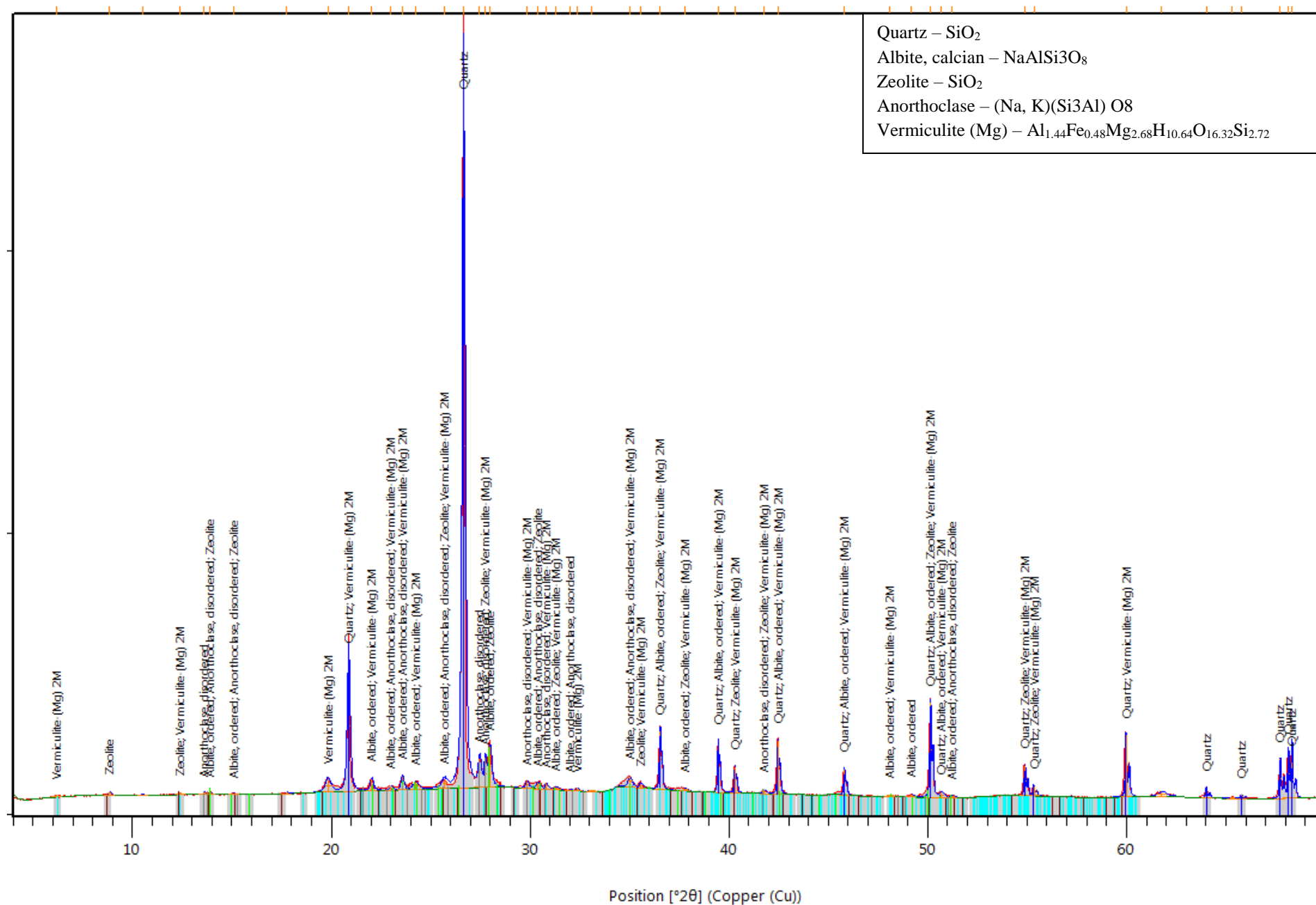
Konza Core 9, 38-48 cm



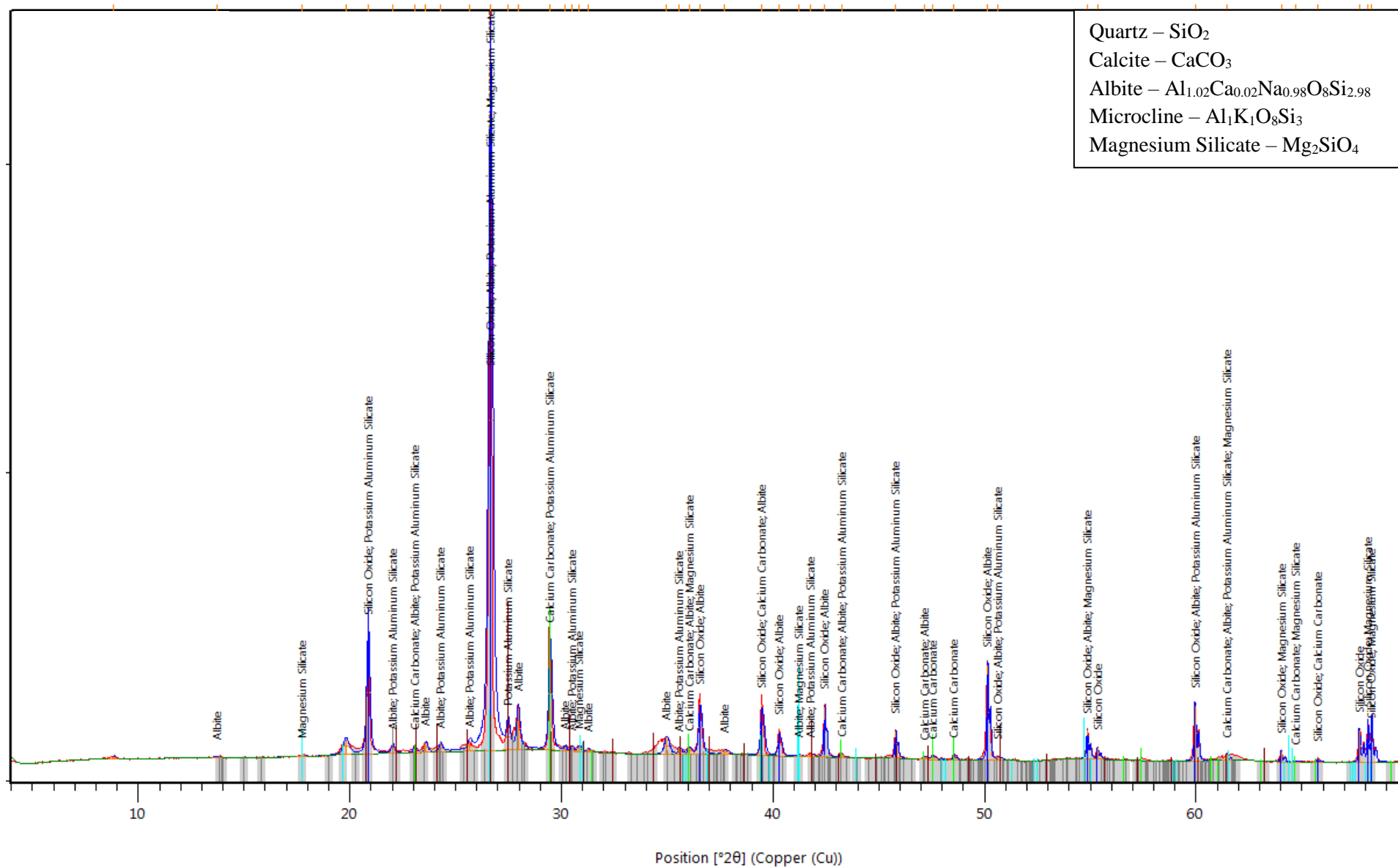
Konza Core 9, 89-99 cm



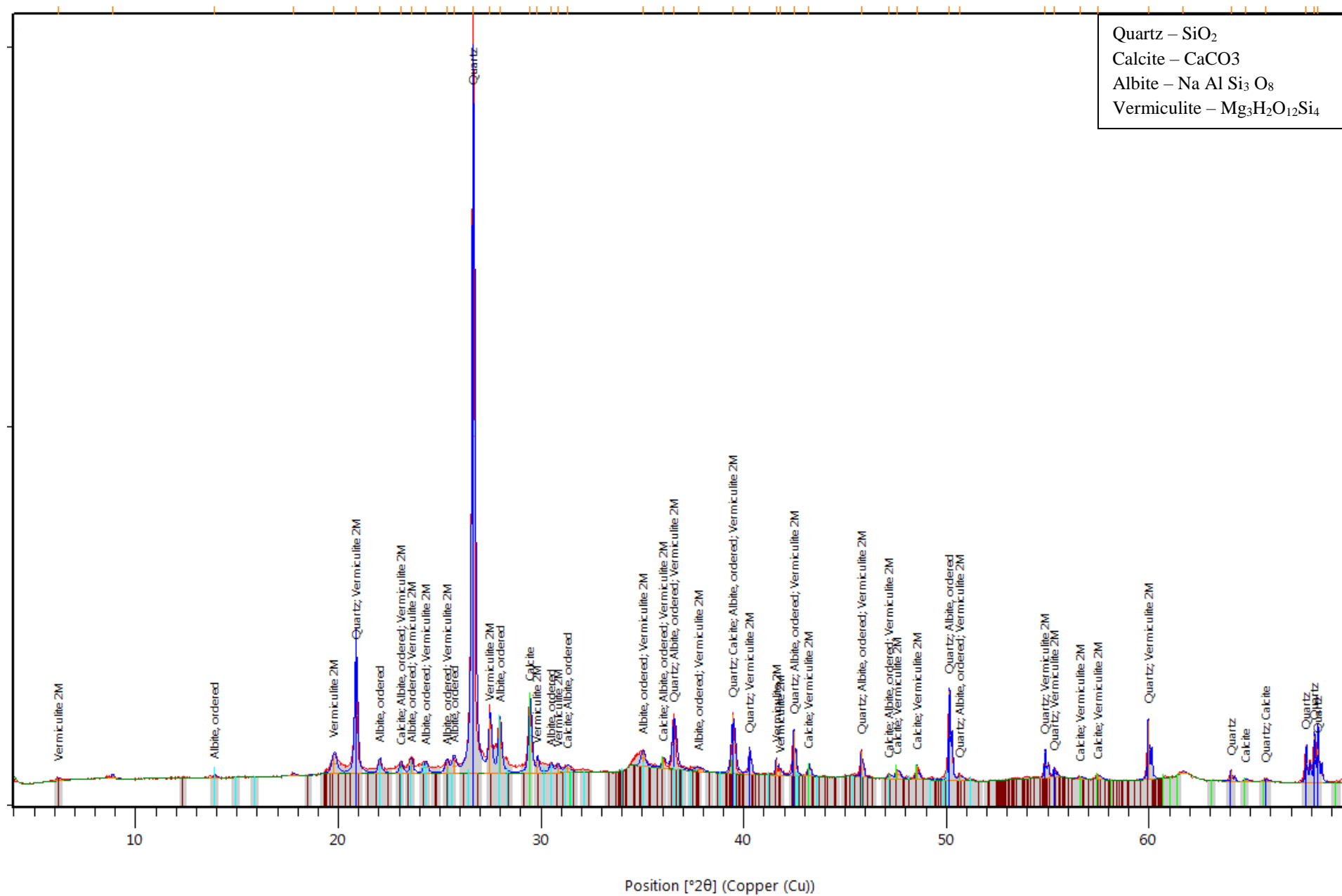
Konza Core 9, 142-152 cm



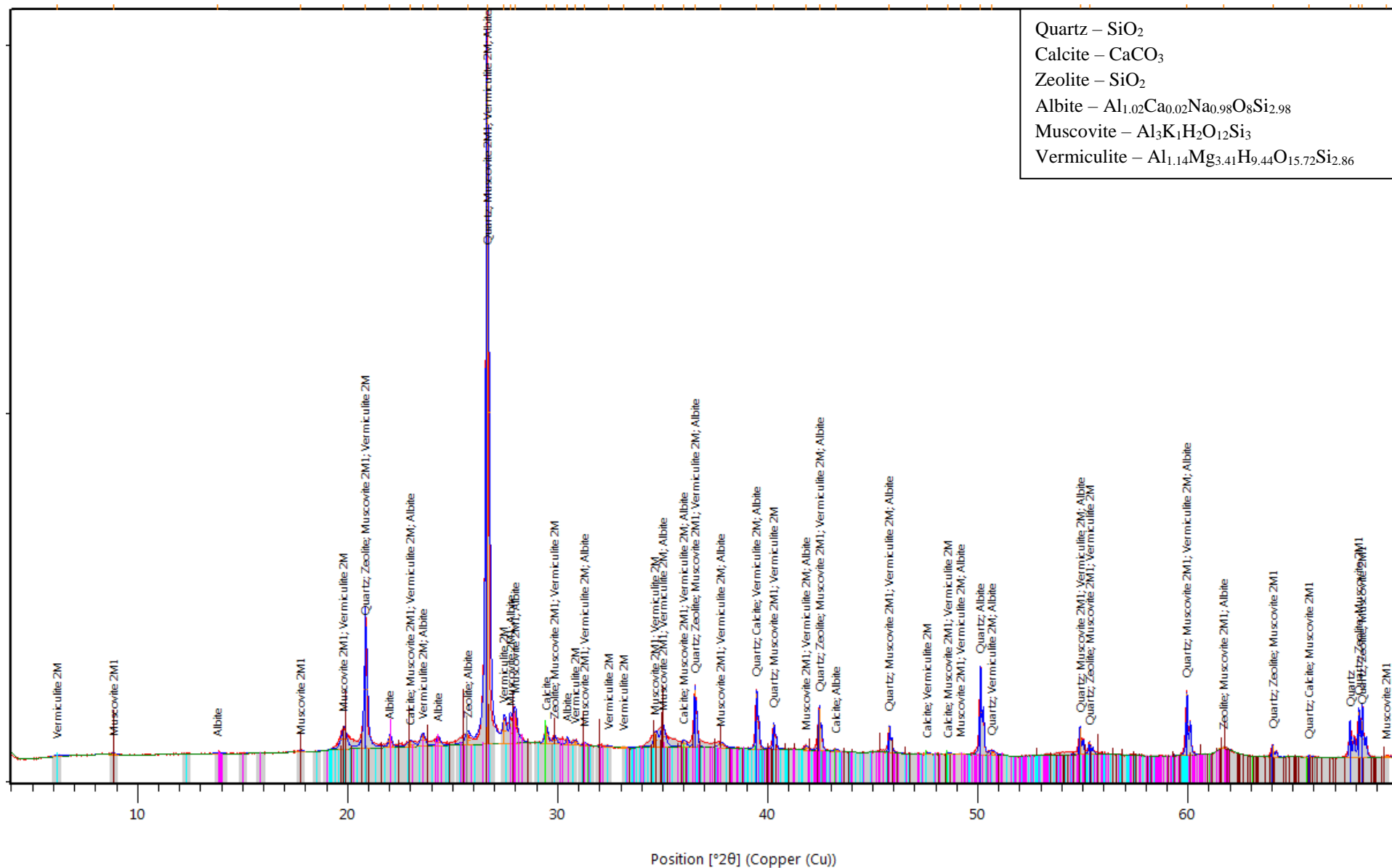
Konza Core 9, 193-203 cm



Konza Core 10, 0-10cm



Konza Core 10, 100-110 cm



Konza Core 10, 150-160 cm

D.2-Stockdale Diffraction Analyses

Stockdale Core SDK1

Core Transect →	Upstream	
	SDK 1 0-11cm	SDK 1 12-15cm
Albite	x (calcian)	x
Dolomite		x
Enstatite	x	
Lizardite	x	x
Magnetite	x	x
Microcline		x
Muscovite	x	x
Quartz	x	x

Stockdale Core SDK2

Core Transect →	Upstream		
	SDK 2 0-13cm	SDK 2 35-45cm	SDK 2 50-52cm
Albite	x	x	x
Anorthite	x		
Calcite			x
Enstatite		x	
Kleberite	x		
Muscovite	x	x	x
Quartz	x	x	x
Vermiculite**			x

Stockdale Core SDK3

Core Transect →	Upstream	
	SDK 3 0-10cm	SDK 3 30-34cm
Albite	x	
Calcite	x	x
Dolomite		x
Microcline	x	
Muscovite	x	
Phlogopite		x
Quartz	x	x
Vermiculite**		x

Stockdale Core SDK4

Core Transect →	Upstream		
	SDK 4 0-16cm	SDK 4 28-40cm	SDK 4 56-61cm
Albite	x	x	x
Biotite	x		
Calcite	x	x	x
Kleberite		x	
Mica, unnamed			x
Microcline	x	x	x
Muscovite		x	
Olivine	x		
Quartz	x	x	x
Other Minerals			Siderophyllite

Stockdale Core SDK5

Core Transect →	Upstream			
	SDK 5 0-12cm	SDK 5 16-20cm	SDK 5 20-25cm	SDK 5 25-27cm
Albite	x	x	x	x
Anorthoclase				x
Biotite				x
Calcite		x	x	x
Dolomite			x	x
Kleberite	x			
Microcline			x	
Muscovite	x	x	x	
Quartz	x	x	x	x
Vermiculite**	x	x		

Stockdale Core SDK2A

Core Transect →	Downstream			
	SDK 2A 0-10cm	SDK 2A 32-39cm	SDK 2A 40-50cm	SDK 2A 50-60cm
Albite	x	x	x	x
Anorthoclase			x	x
Calcite		x		
Chrysotile		x		
Microcline				x
Muscovite			x	x
Olivine	x			
Quartz	x	x	x	x
Vermiculite**	x			
Zeolite	x			

Stockdale Core SDK3A

Core Transect →	Downstream			
	SDK 3A 0-9cm	SDK 3A 16-22cm	SDK 3A 27-32cm	SDK 3A 43-49cm
Albite	x	x	x	x
Calcite			x	x
Dolomite			x	
Kleberite		x	x	x
Lizardite			x	
Mica, unnamed	x			
Microcline	x			
Muscovite		x		x
Quartz	x	x	x	x
Vermiculite**				x
Zeolite	x			
Other Minerals		Clinochlore		

Stockdale Core SDK4A

Core Transect →	Downstream		
	SDK 4A 0-10cm	SDK 4A 22-28cm	SDK 4A 37-42cm
Albite	x	x	x
Calcite	x		
Magnetite		x	x
Mica, unnamed			x
Muscovite		x	
Quartz	x	x	x
Vermiculite**	x		
Other Minerals			Perovskite

Stockdale Core SDK1B

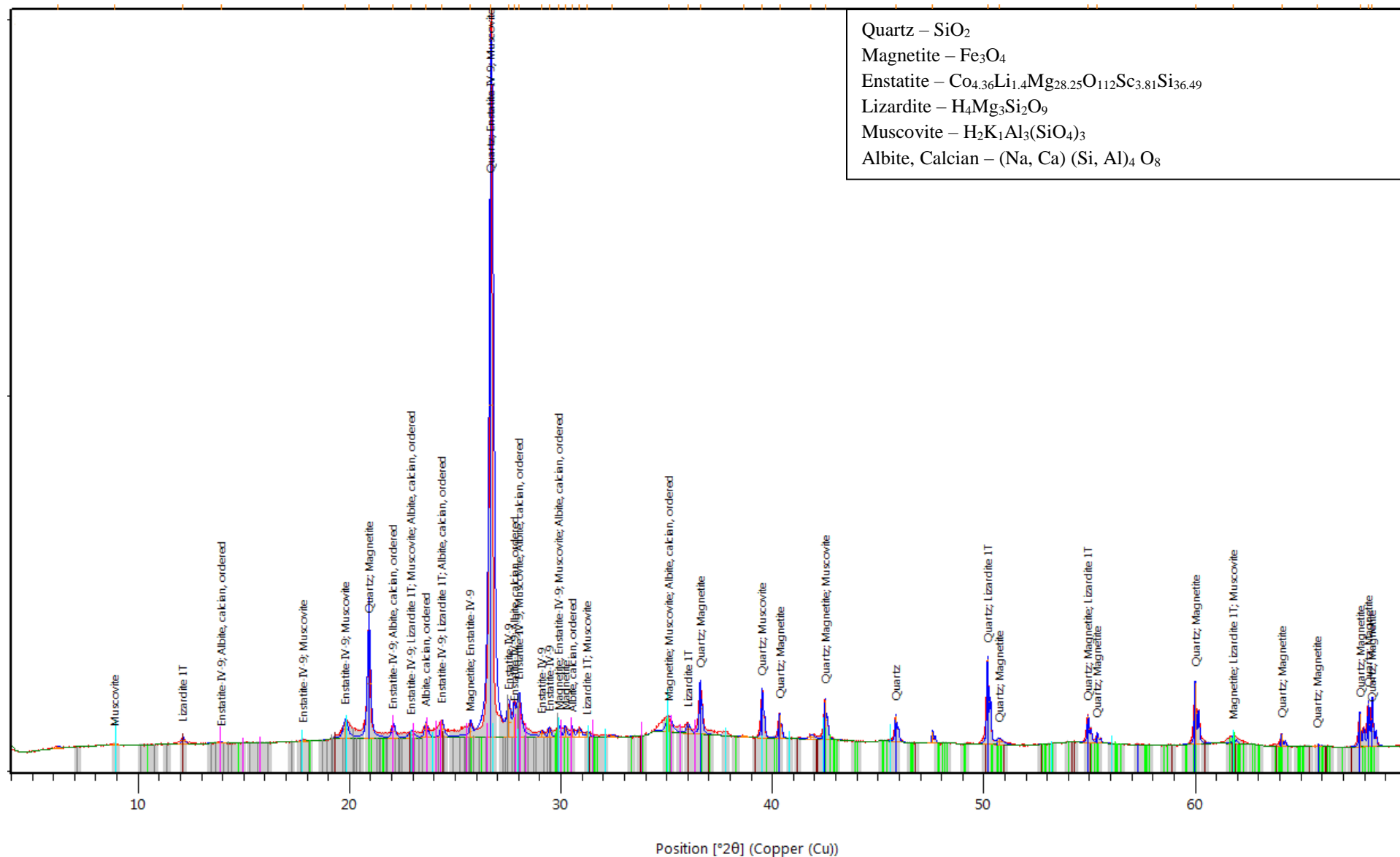
Core Transect →	Uphill					
	SDK 1B 0-7cm	SDK 1B 7-14cm	SDK 1B 14-21cm	SDK 1B 21-28cm	SDK 1B 28-36cm	SDK 1B 36-41cm
Albite	x	x	x		x	
Anorthite				x		
Chrysotile						x
Lizardite		x	x	x	x	x
Magnesioferrite					x	
Microcline		x	x			
Muscovite	x	x				
Phlogopite					x	
Quartz	x	x	x	x	x	x
Vermiculite**	x	x	x	x	x	x
Other Minerals						Feldspar, unnamed

Stockdale Core SDK2B

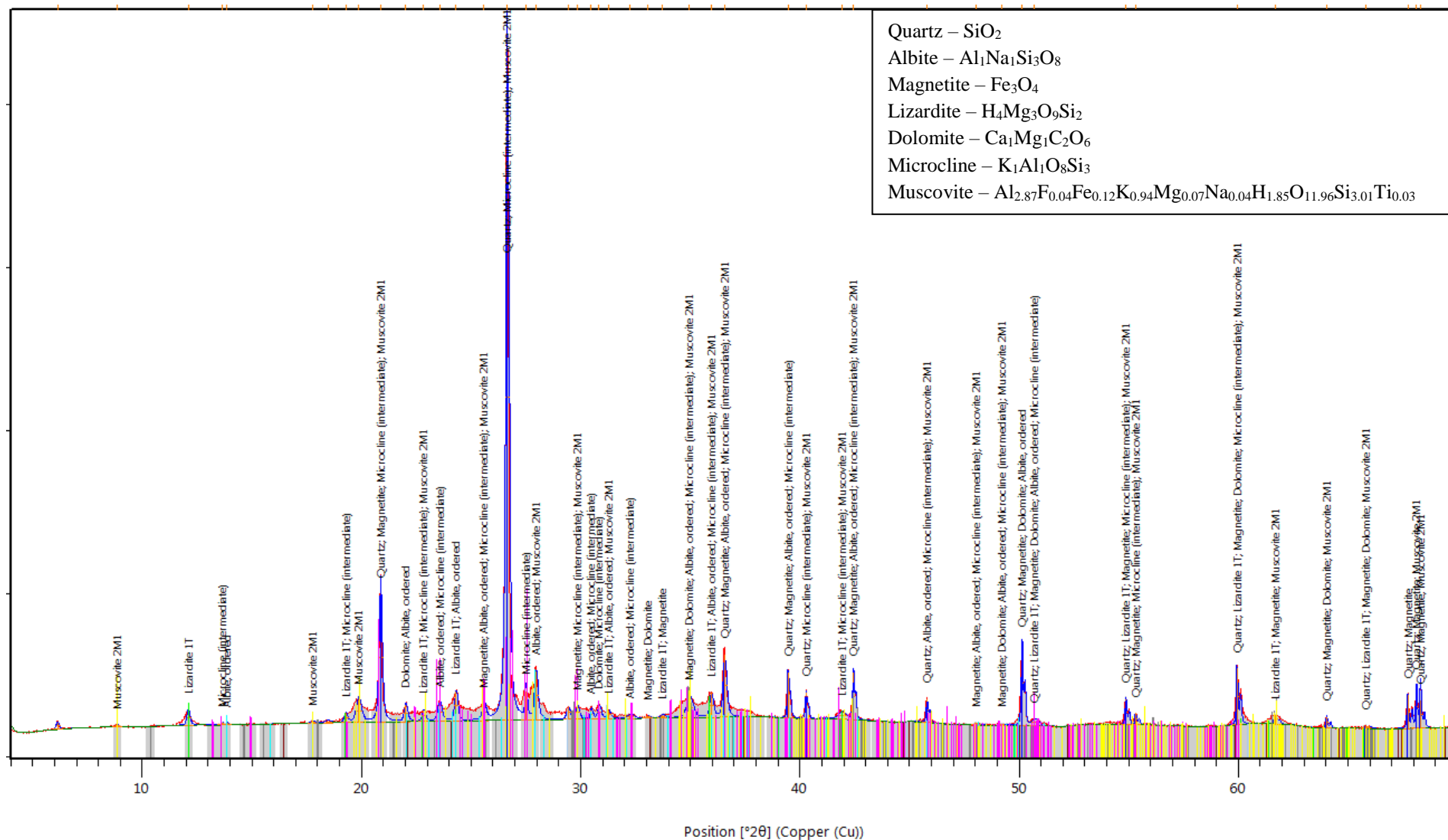
Core Transect →	Uphill					
	SDK 2B 0-13cm	SDK 2B 16-28cm	SDK 2B 28-35cm	SDK 2B 42-49cm	SDK 2B 54-63cm	SDK 2B 71-79cm
Albite	x	x	x	x	x	x
Biotite						x
Chrysotile					x	
Lizardite		x				
Magnesioferrite		x				
Magnetite			x			x
Microcline	x				x	
Muscovite	x			x	x	
Muscovite, phengitic			x			
Phlogopite		x				
Quartz	x	x	x	x	x	x
Vermiculite**	x	x	x	x		x

Stockdale Core SDK3B

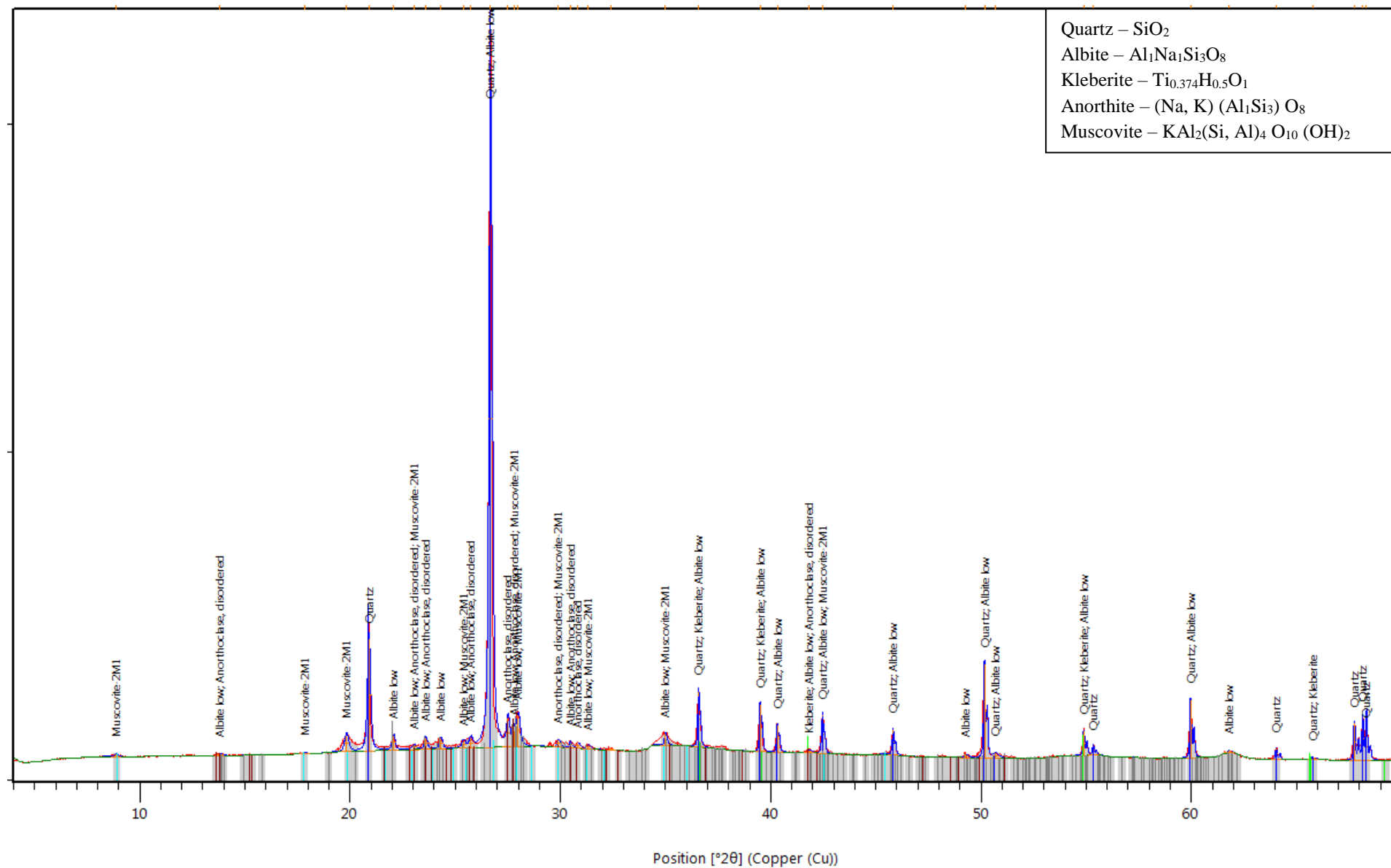
Core Transect→	Uphill							
	SDK 3B 0-7cm	SDK 3B 7-16cm	SDK 3B 20-25cm	SDK 3B 30-40cm	SDK 3B 41-48cm	SDK 3B 57-61cm	SDK 3B 61-68cm	SDK 3B 68-76cm
Albite	x	x	x	x	x	x	x	x
Dolomite	x							x
Enstatite								x
Kleberite			x					x
Magnetite		x						
Microcline		x						
Muscovite		x	x	x		x	x	x
Muscovite, phengitic					x			
Quartz	x	x	x	x	x	x	x	x
Vermiculite**			x	x	x		x	
Other Minerals				Feldspar, Na		Clino- pyroxine	Diopside	



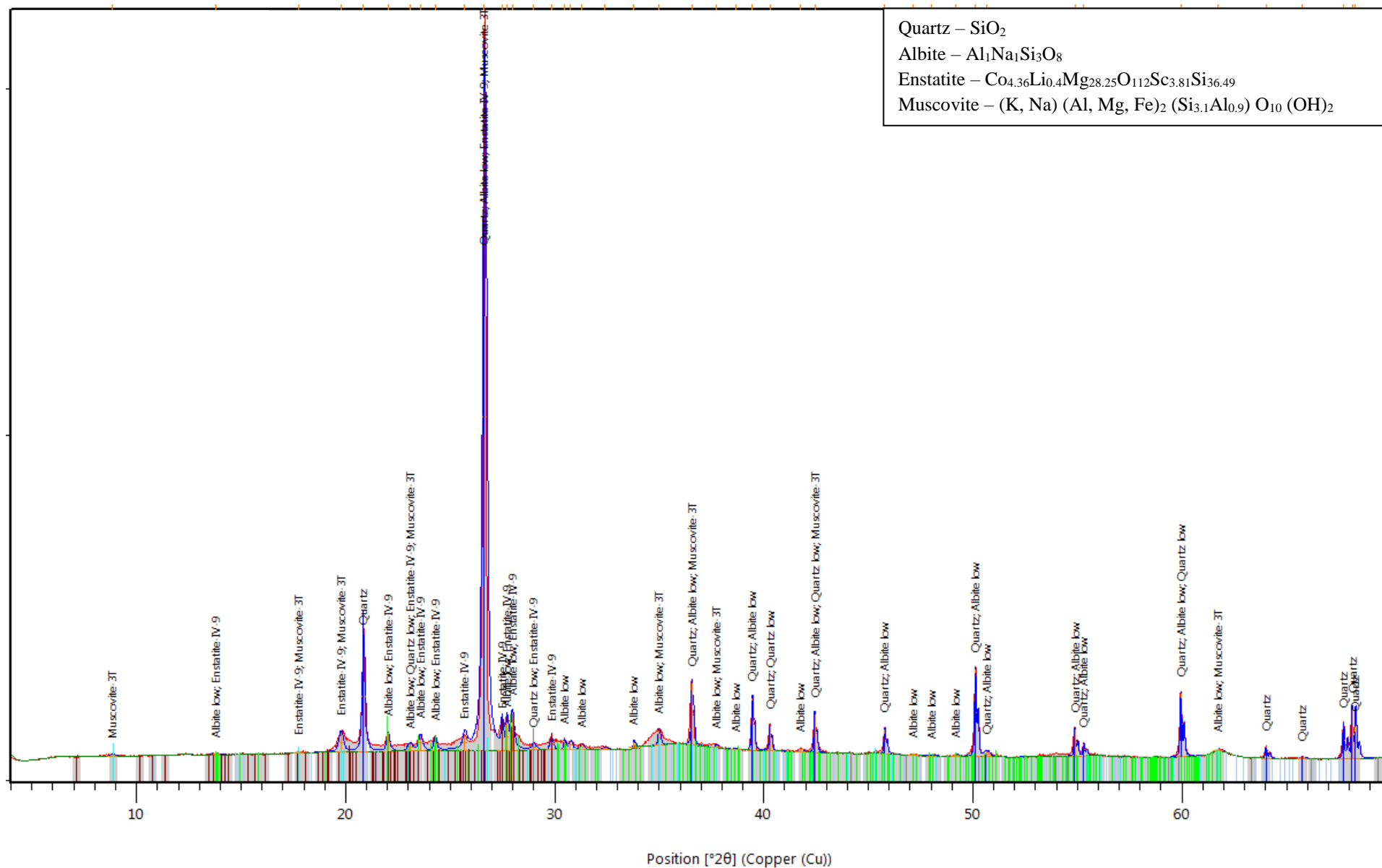
Stockdale Core SDK 1, 0-11 cm



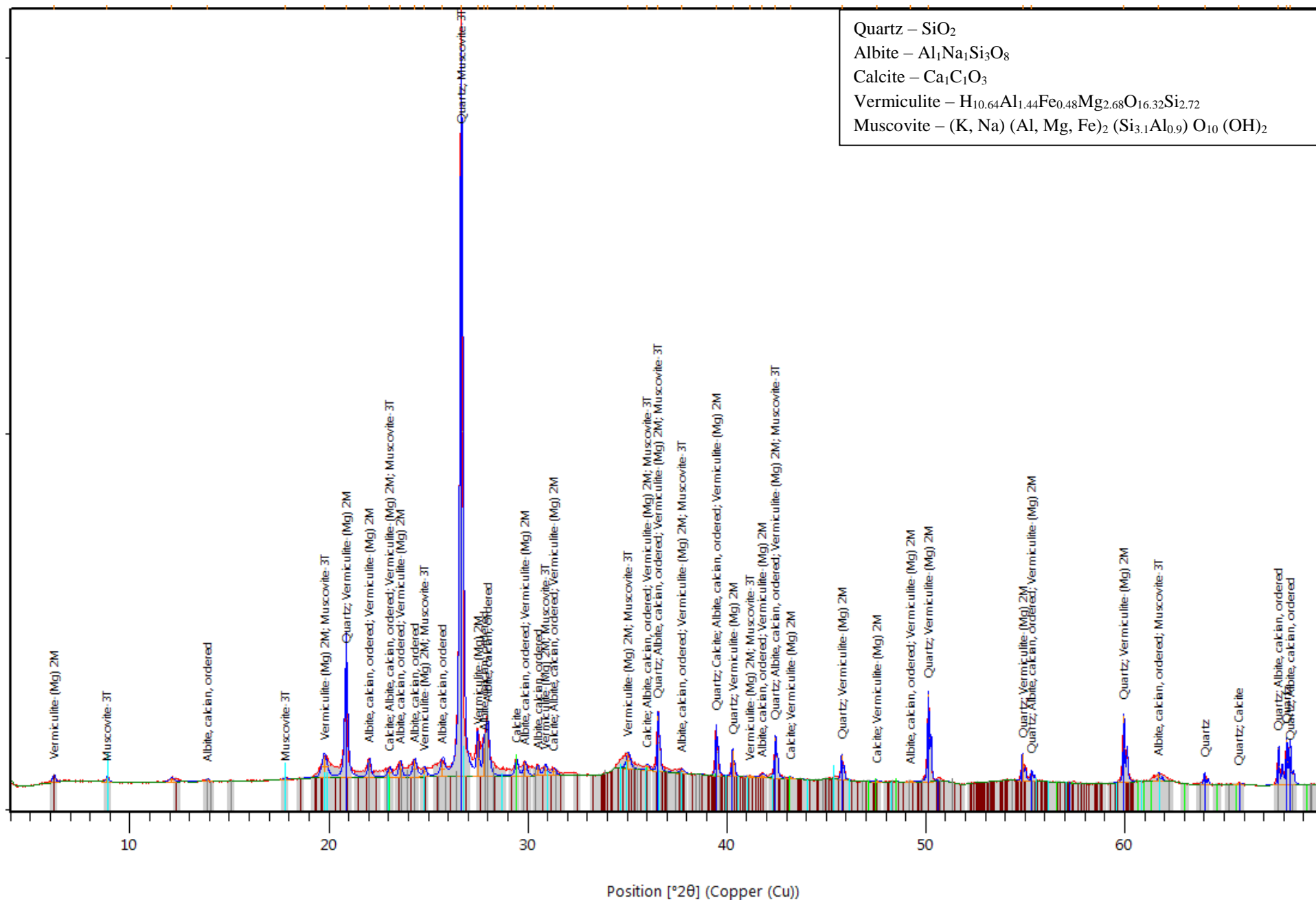
Stockdale Core SDK 1, 12-15 cm



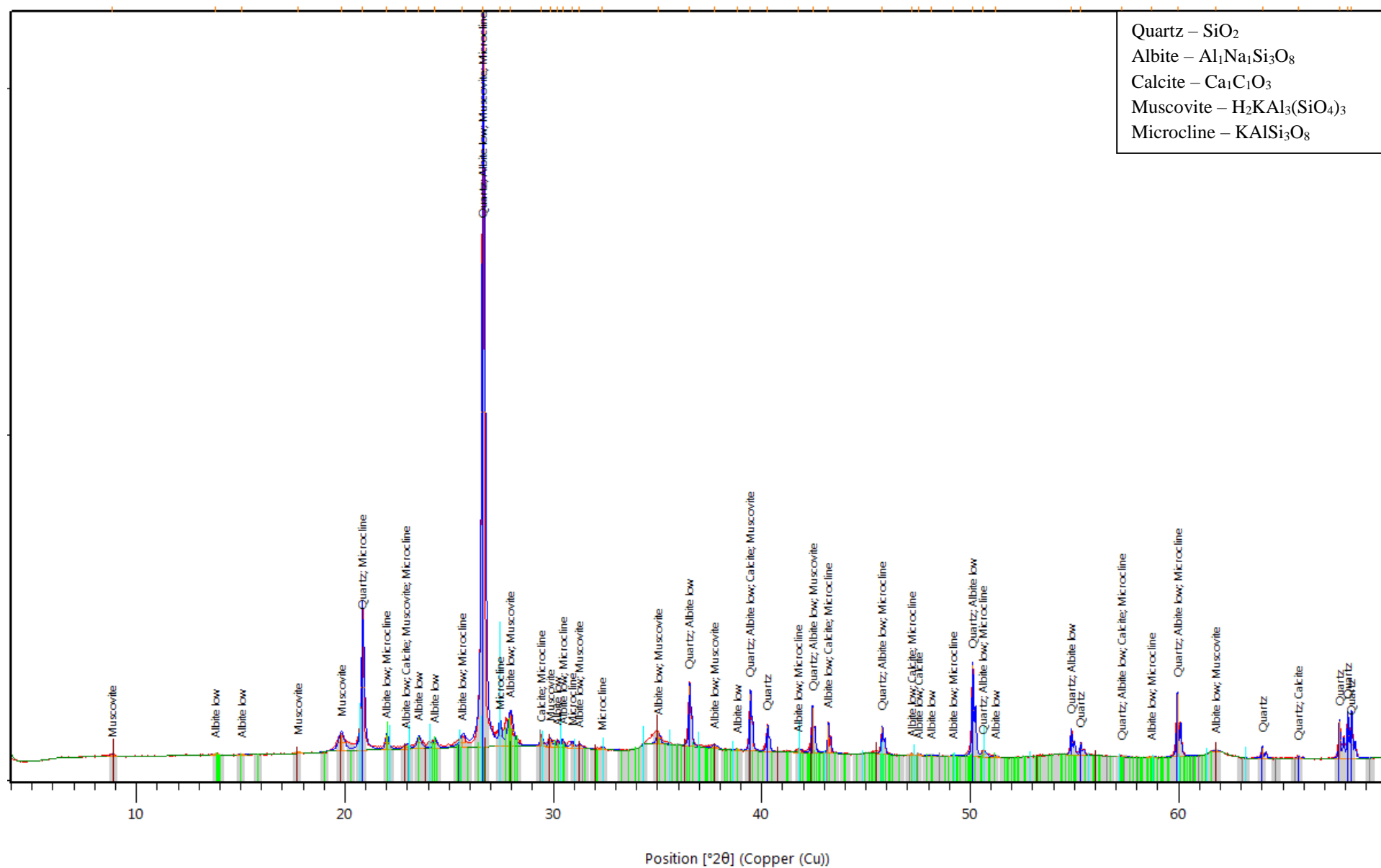
Stockdale Core SDK 2, 0-13 cm



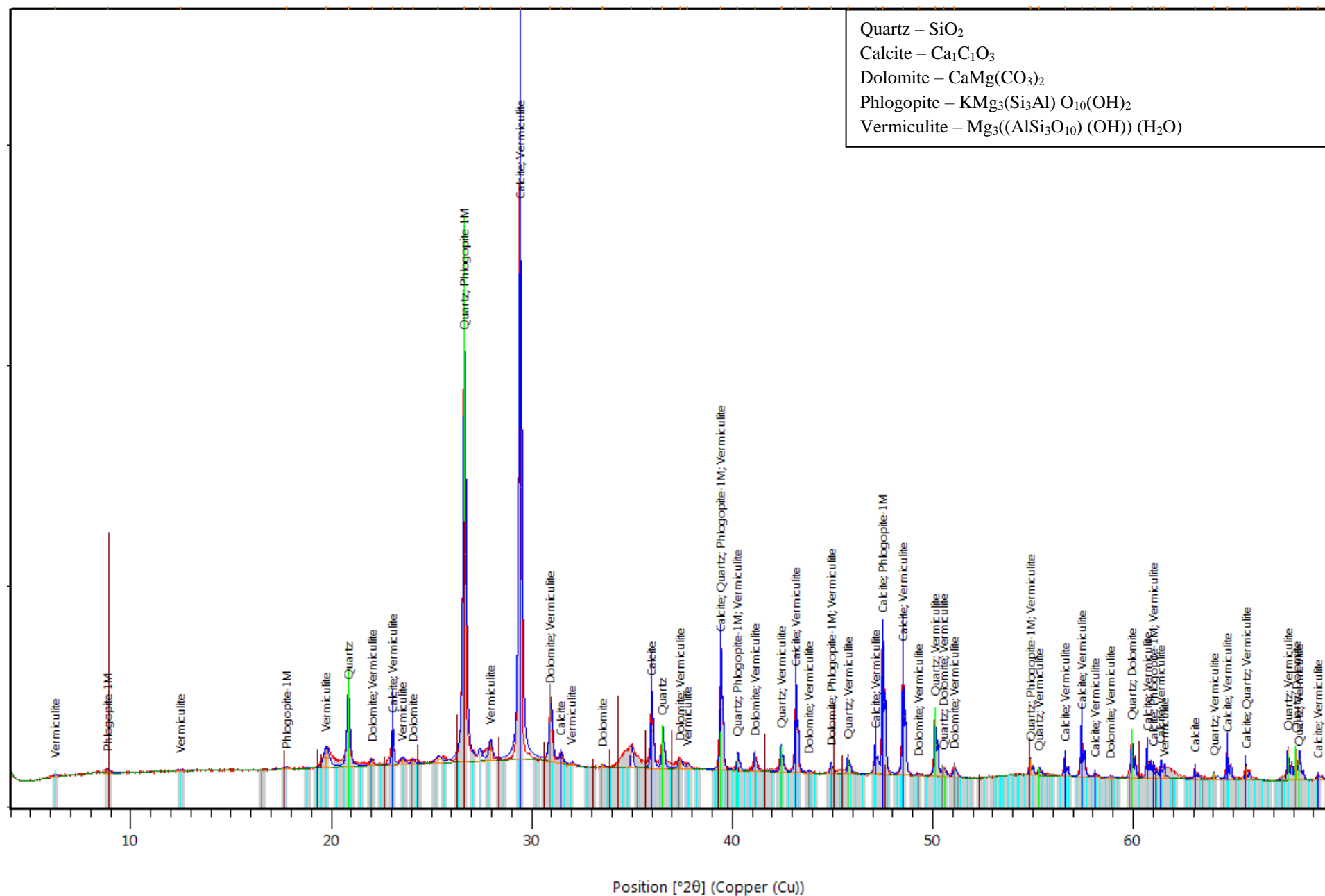
Stockdale Core SDK 2, 35-43 cm



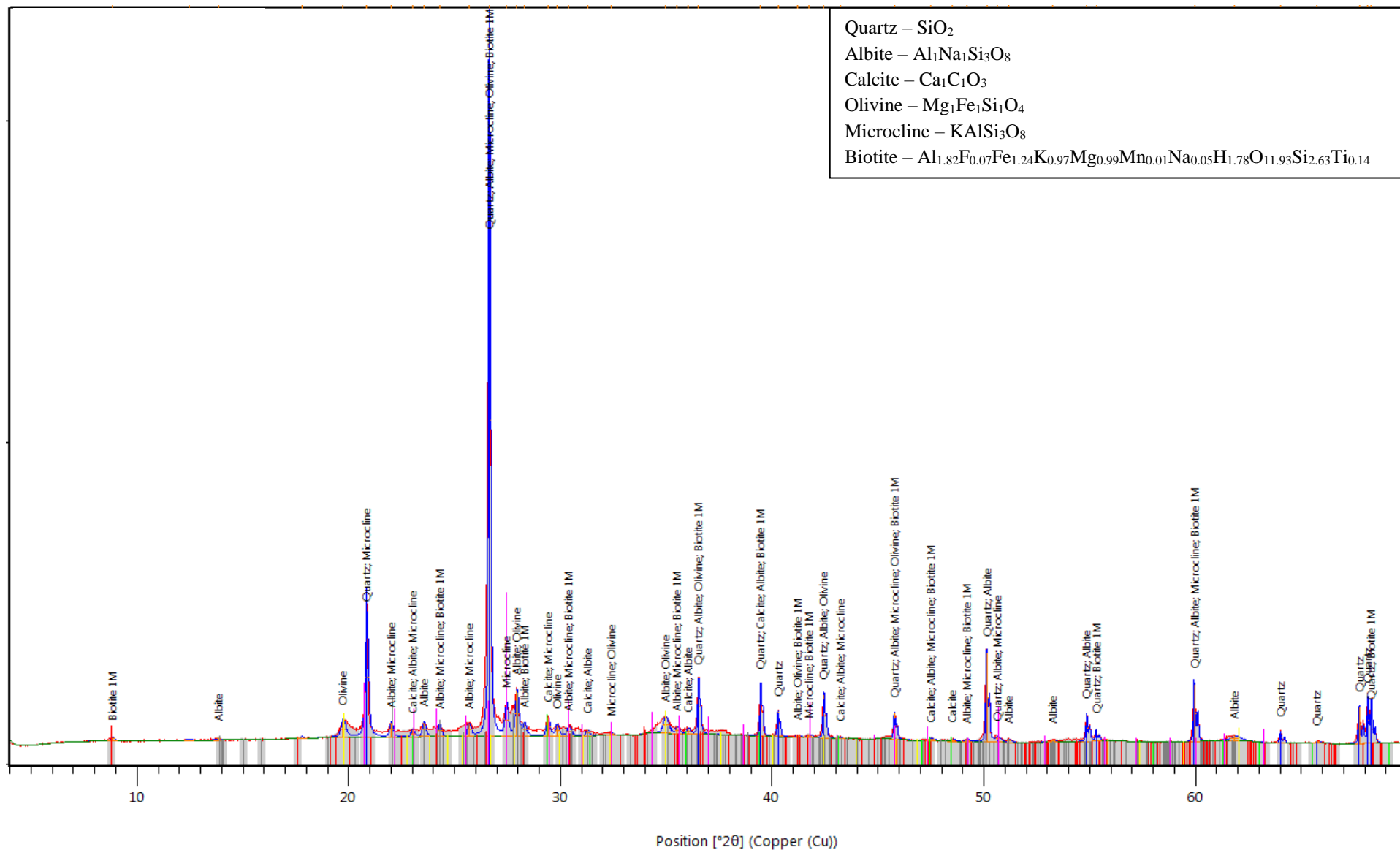
Stockdale Core SDK 2, 50-52 cm



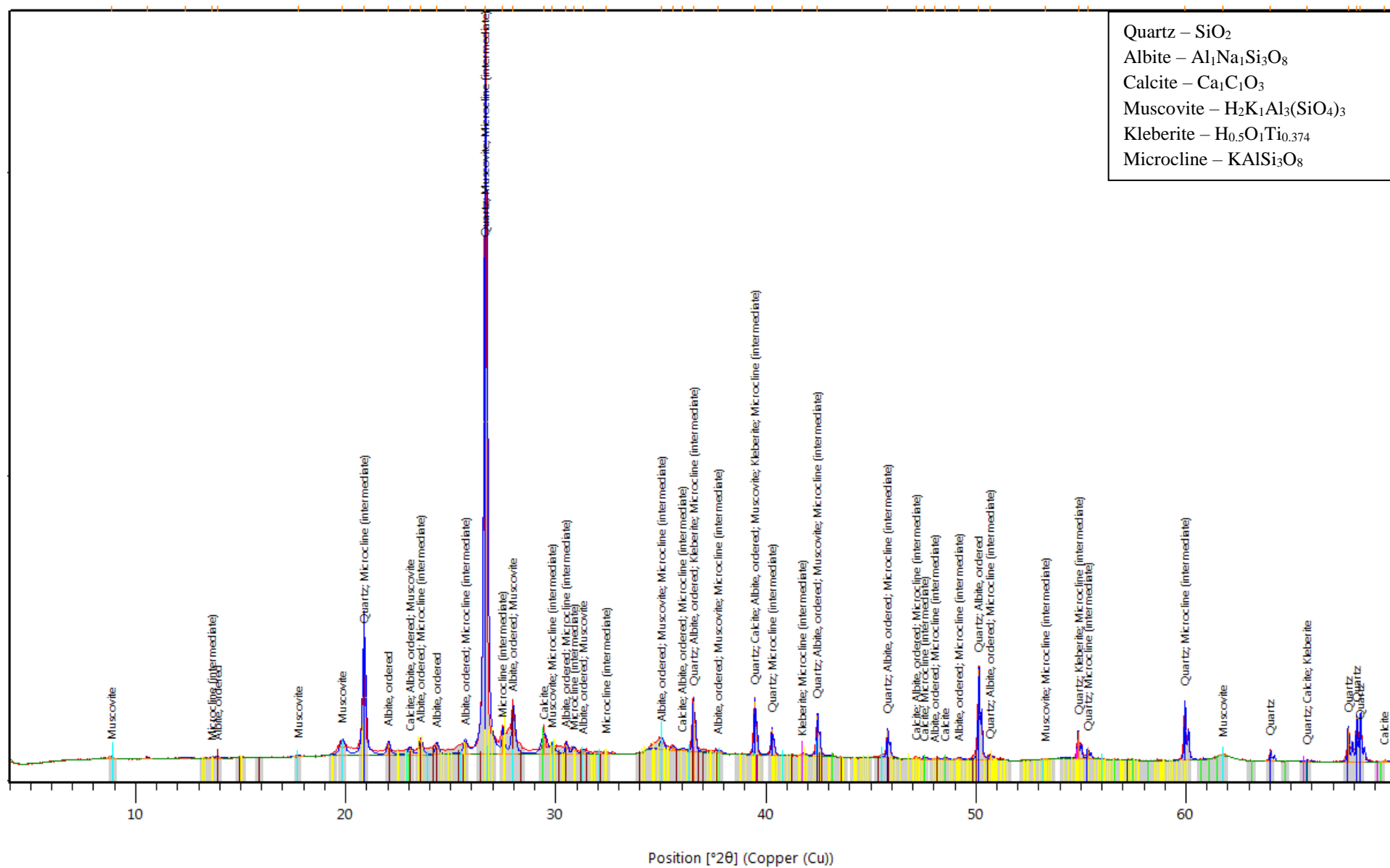
Stockdale Core SDK 3, 0-10 cm



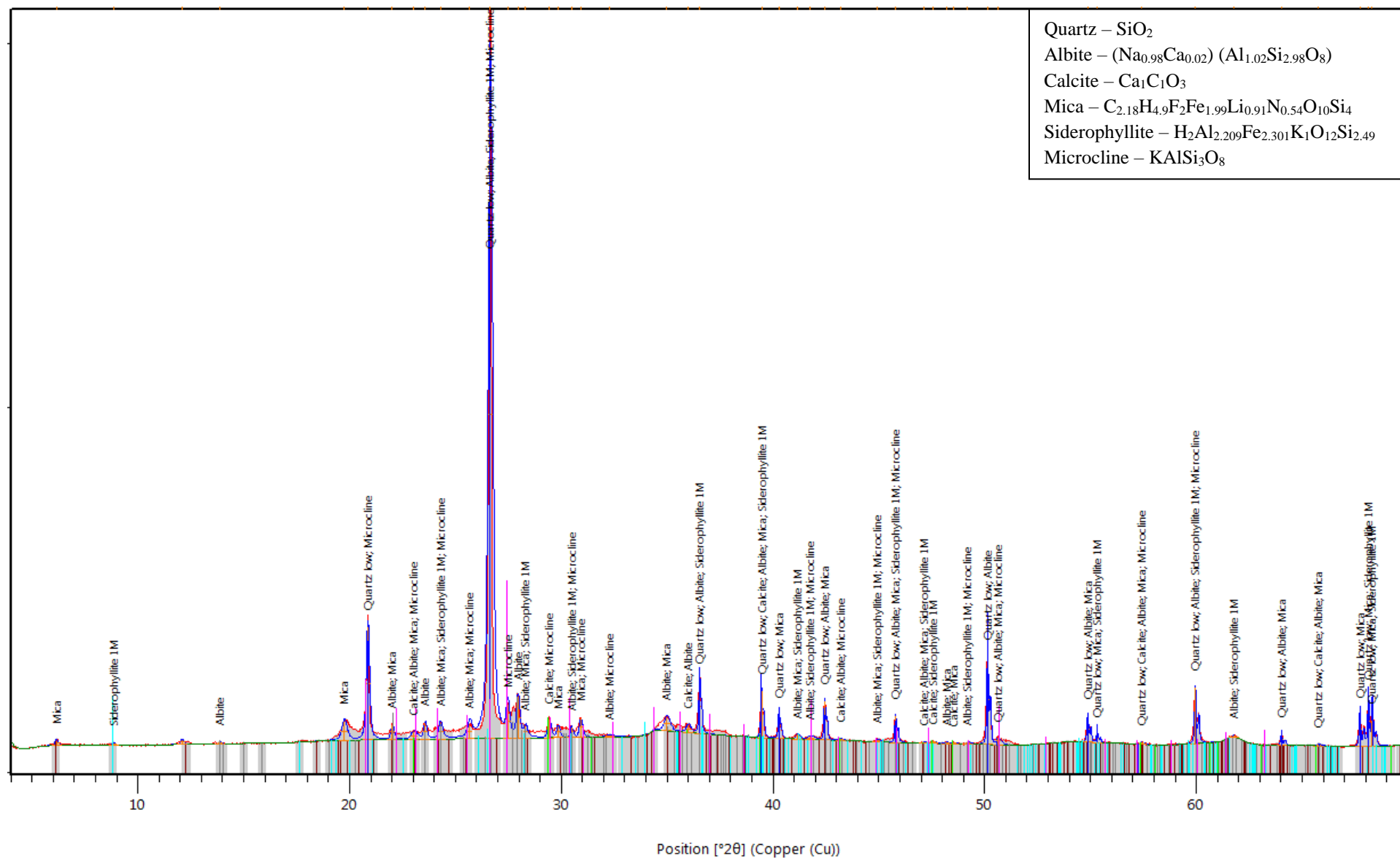
Stockdale Core SDK 3, 30-34 cm



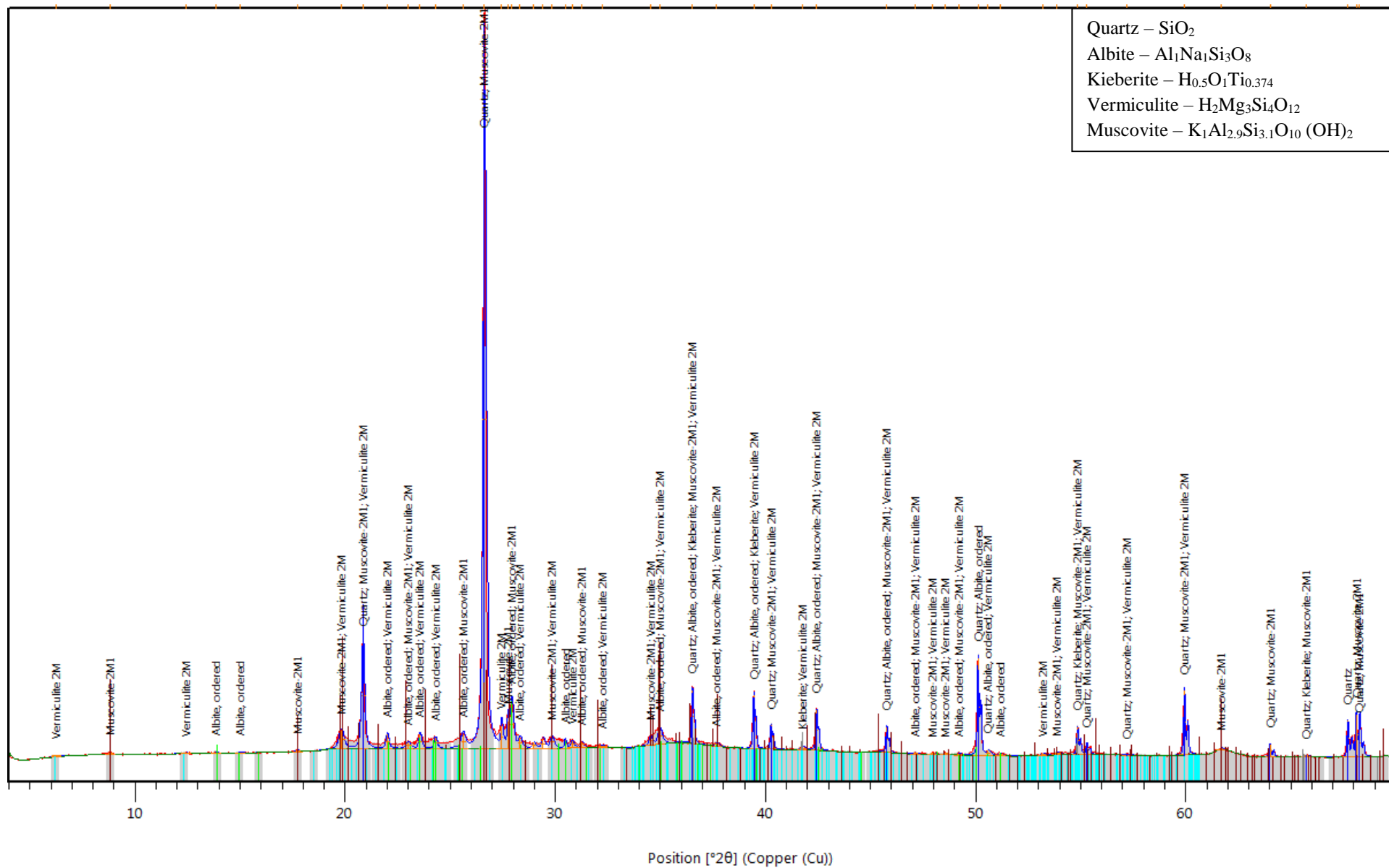
Stockdale Core SDK 4, 0-16 cm



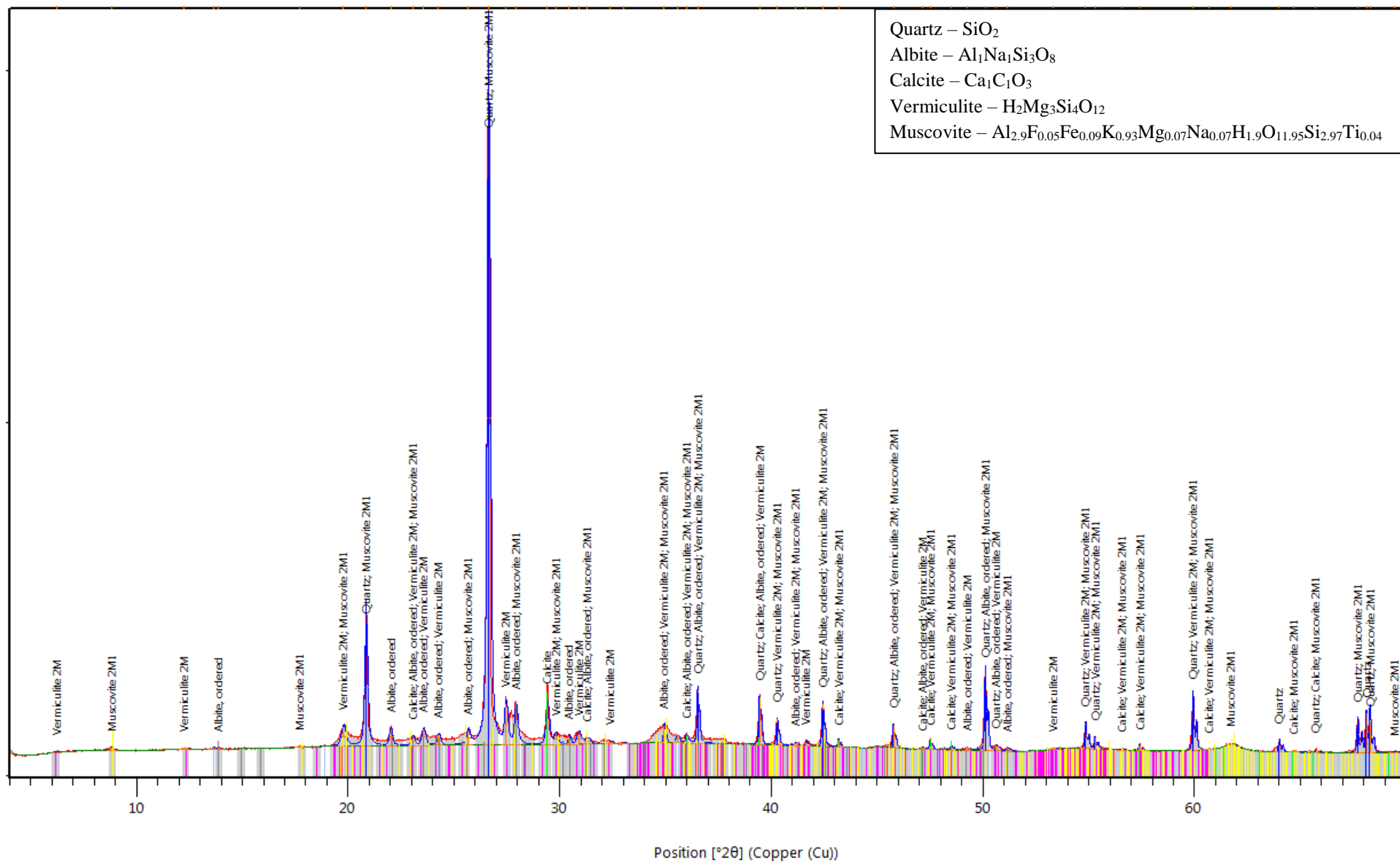
Stockdale Core SDK 4, 28-40 cm



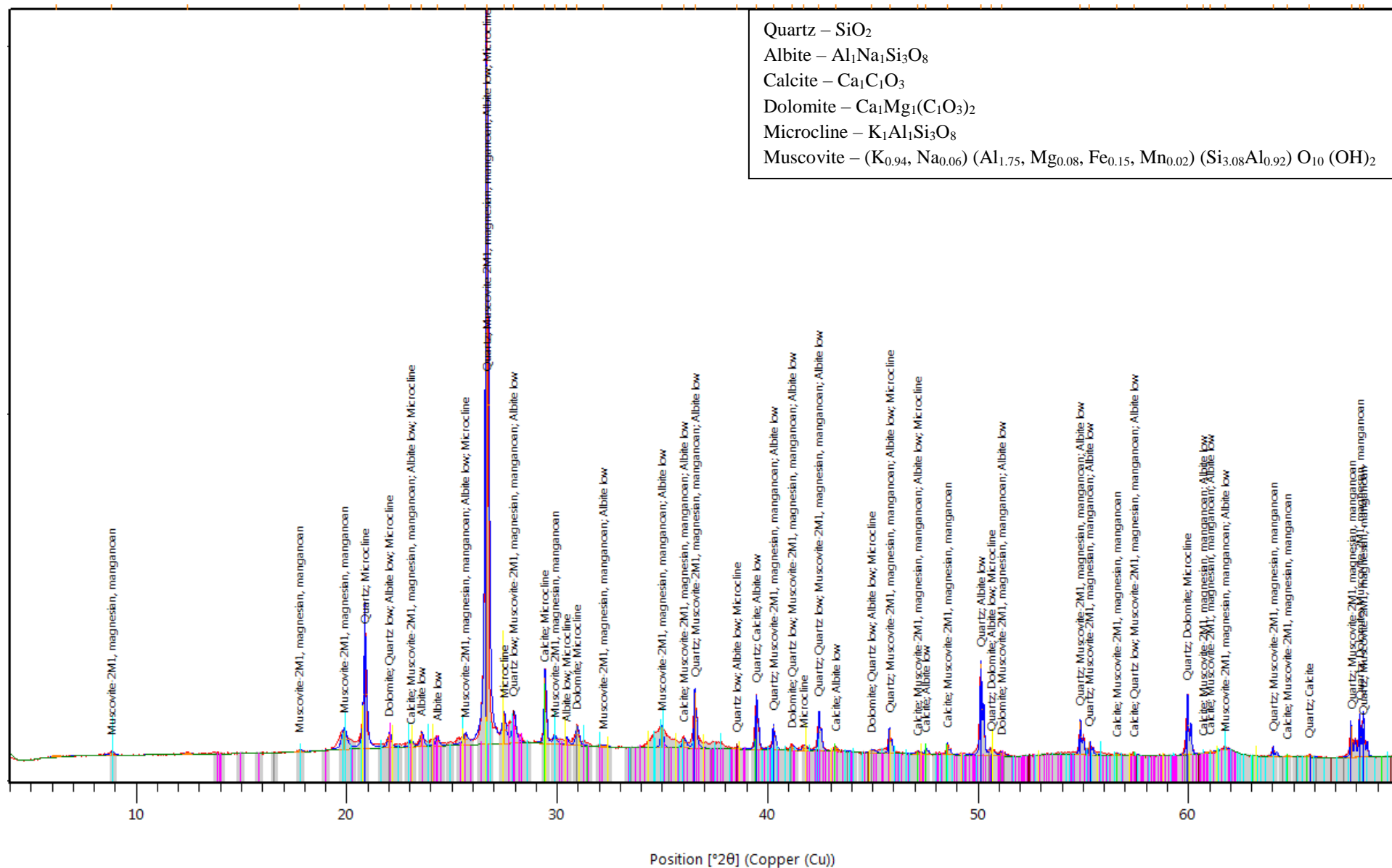
Stockdale Core SDK 4, 56-61 cm



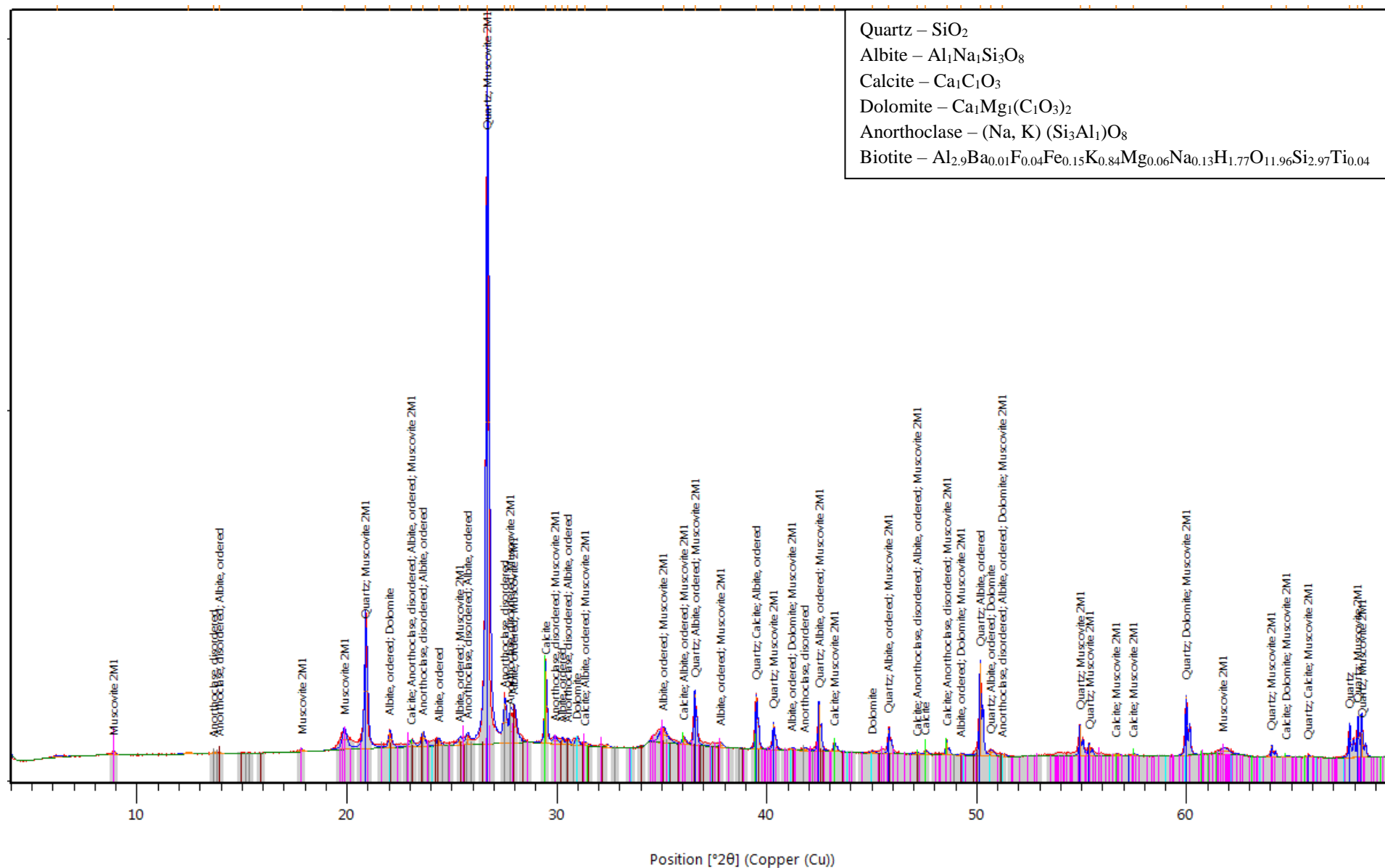
Stockdale Core SDK 5, 0-12 cm



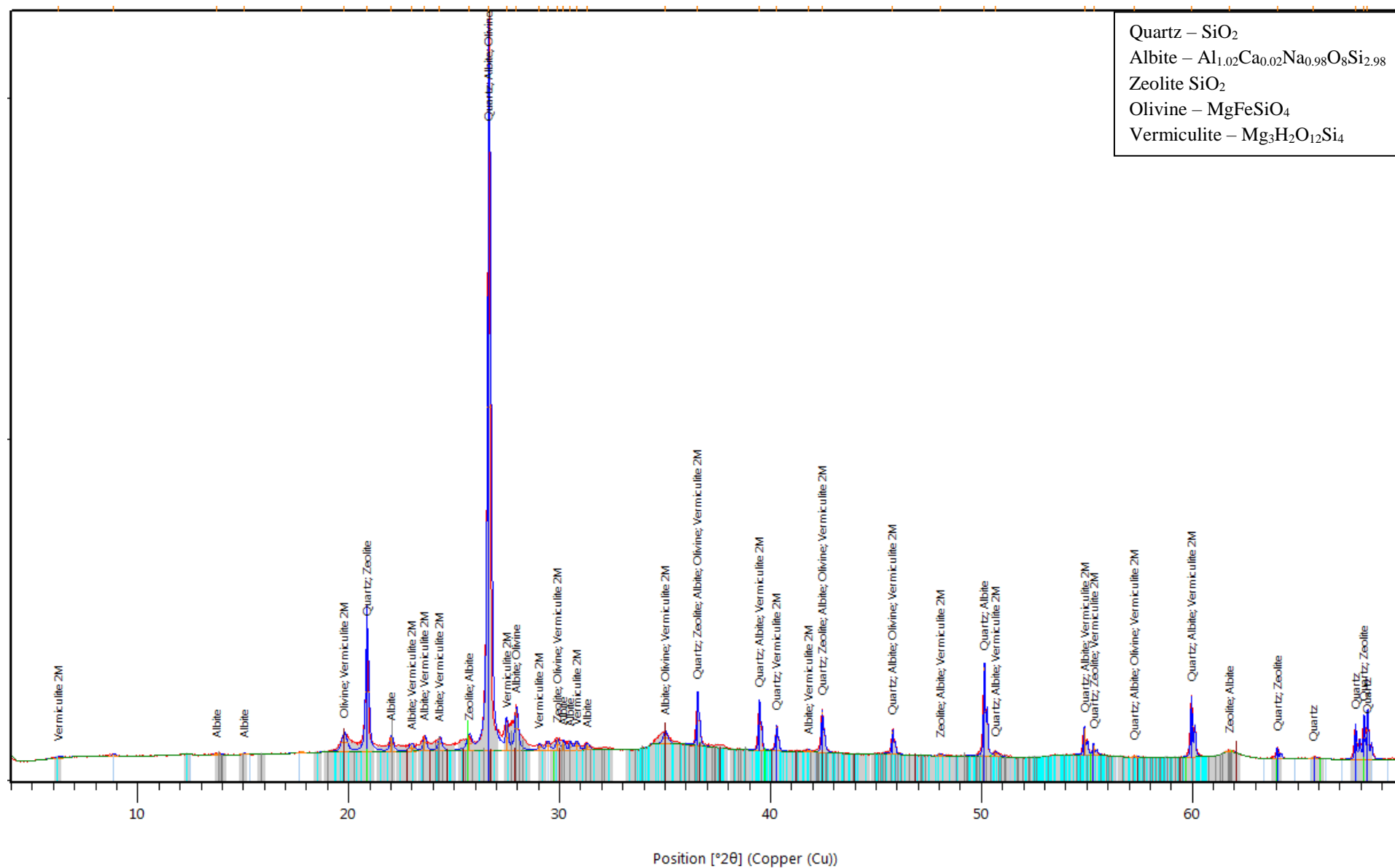
Stockdale Core SDK 5, 16-20 cm



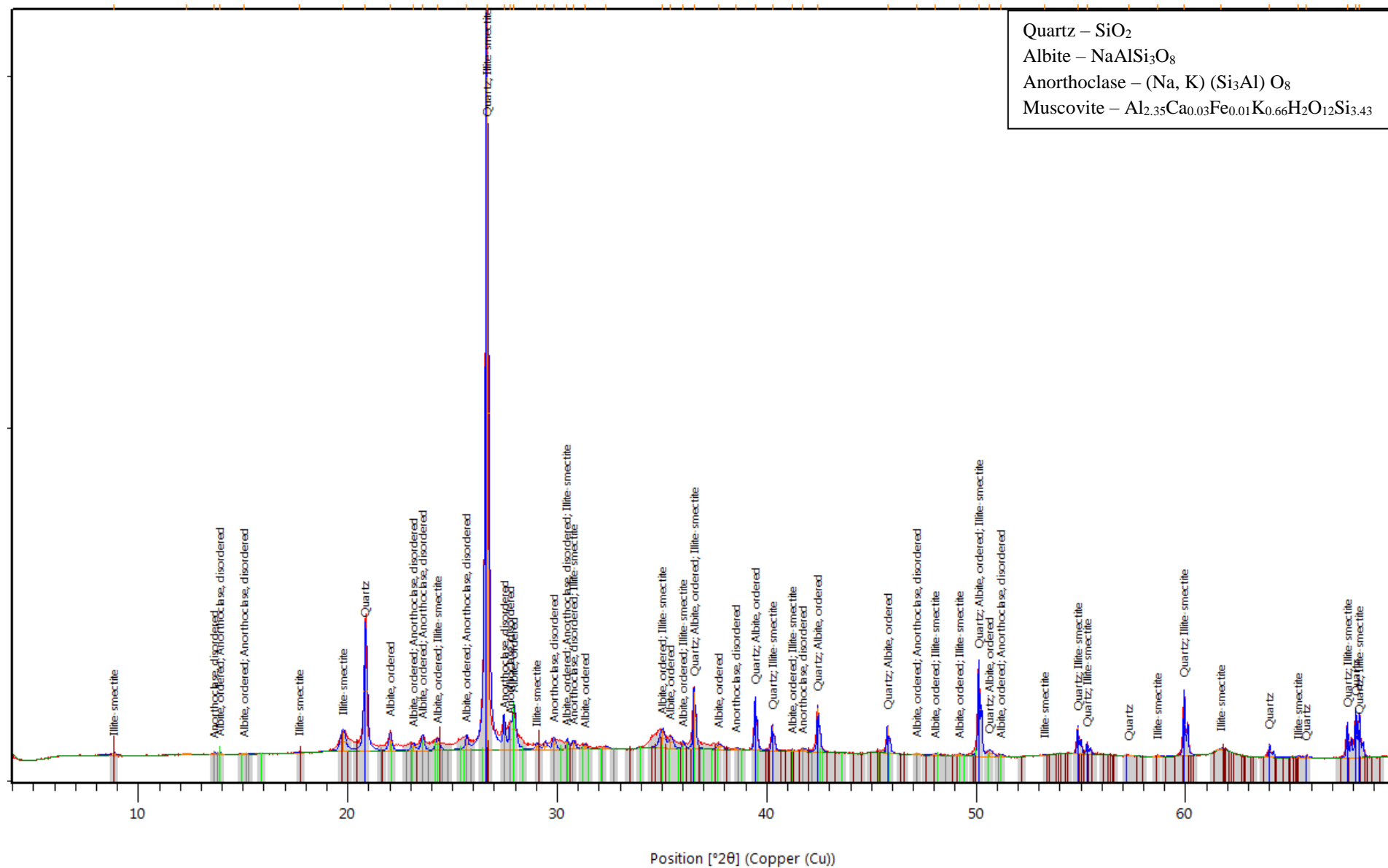
Stockdale Core SDK 5, 20-25 cm



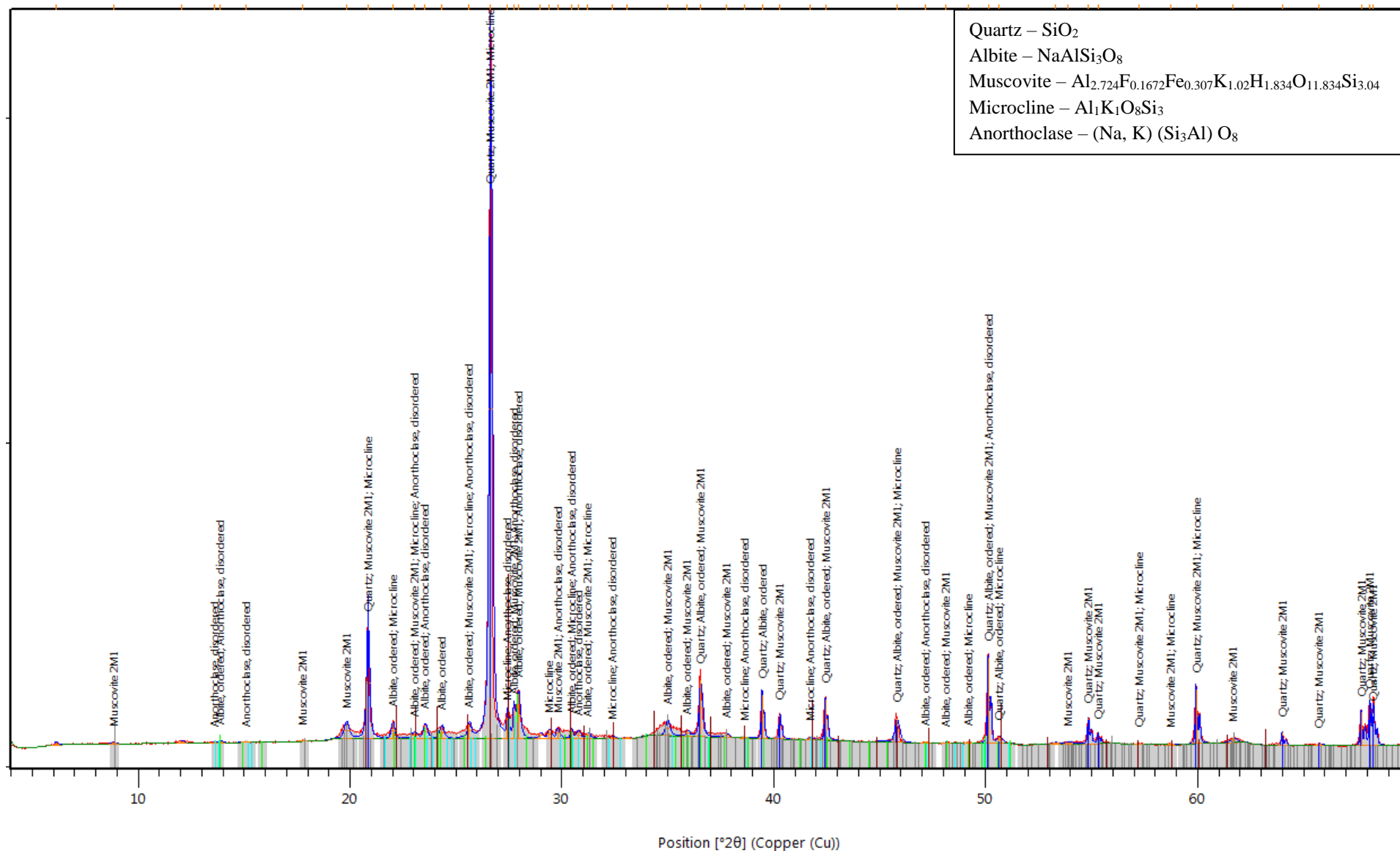
Stockdale Core SDK 5, 25-27 cm



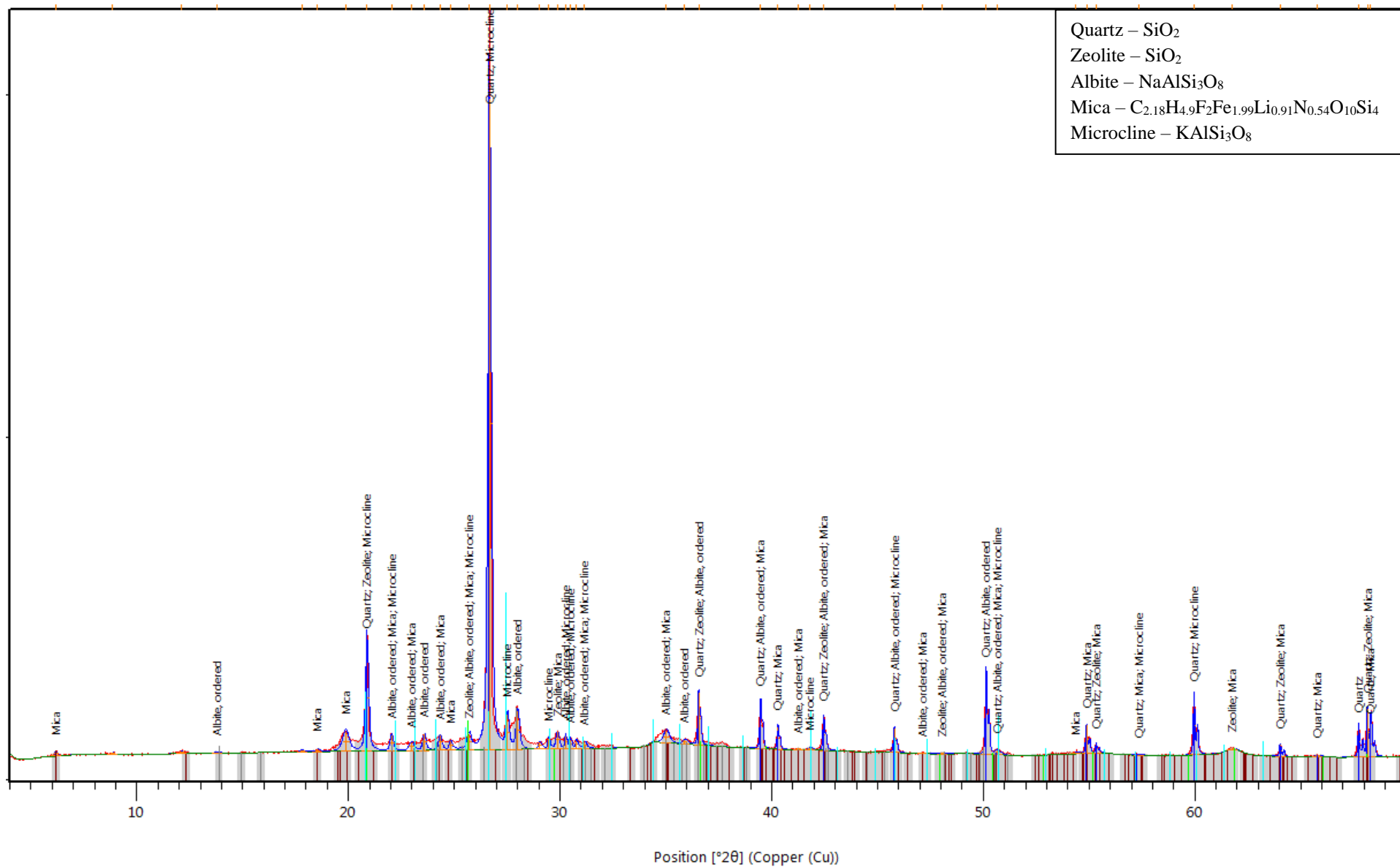
Stockdale Core SDK 2A, 0-10 cm



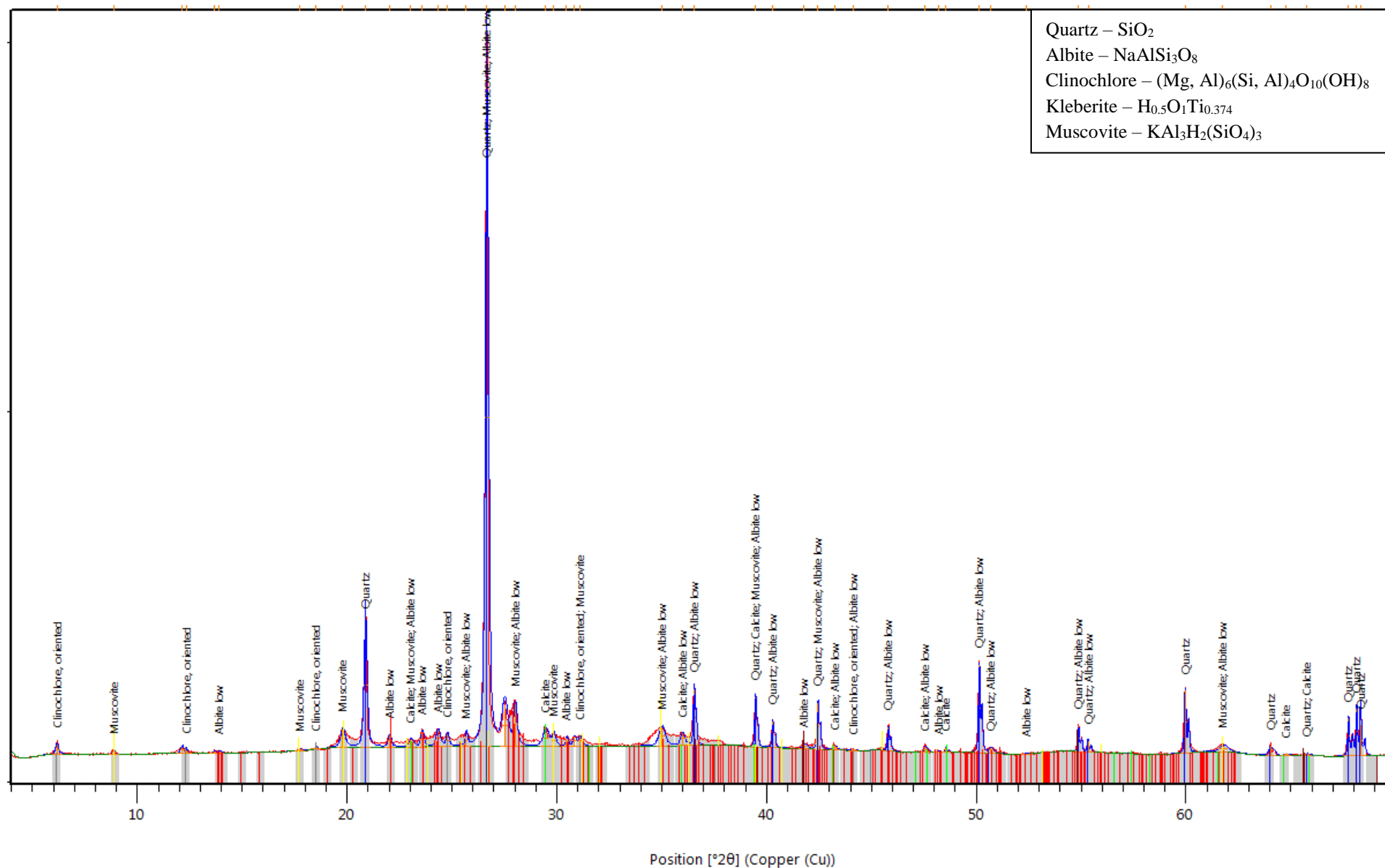
Stockdale Core SDK 2A, 40-50 cm



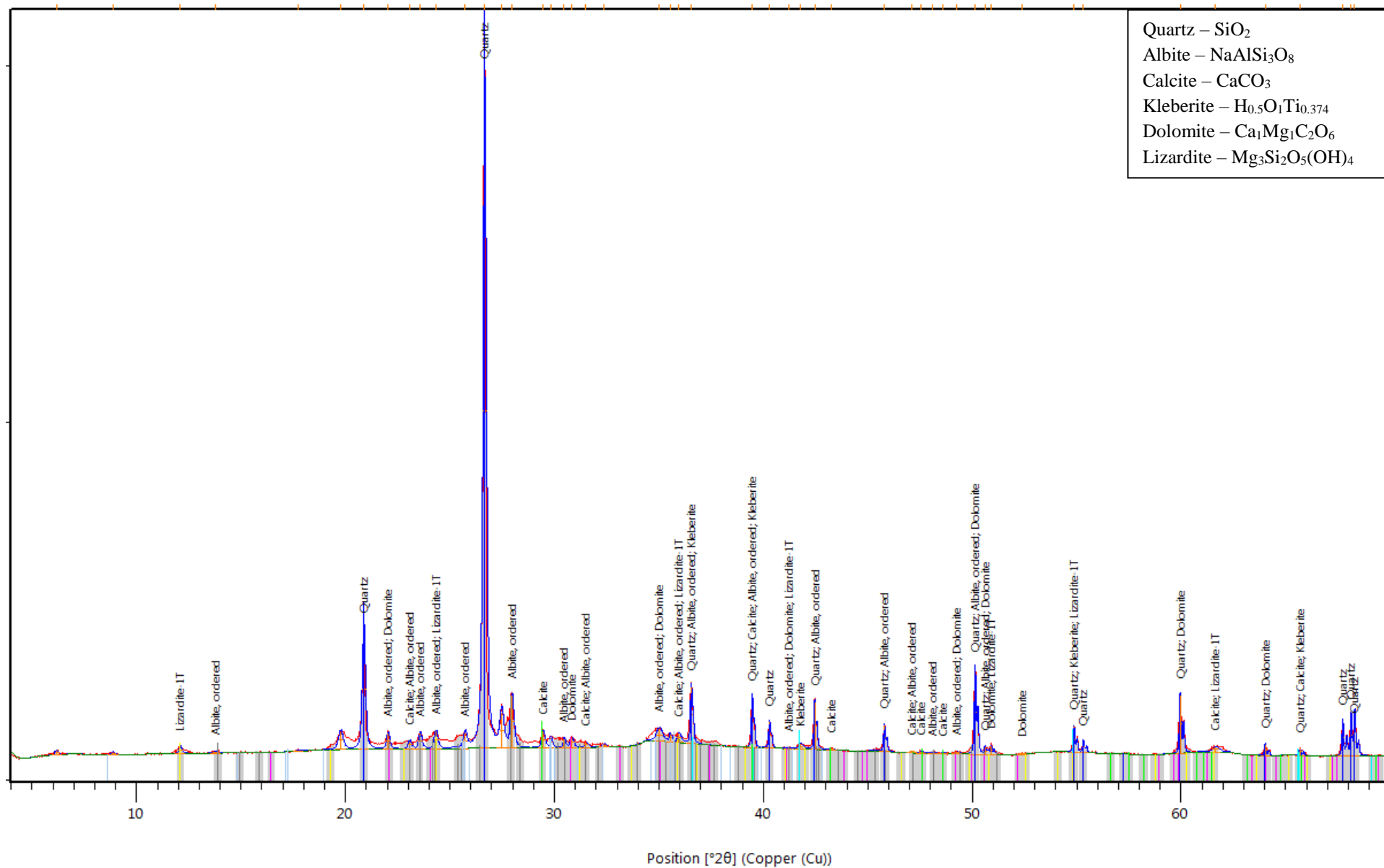
Stockdale Core SDK 2A, 50-60 cm



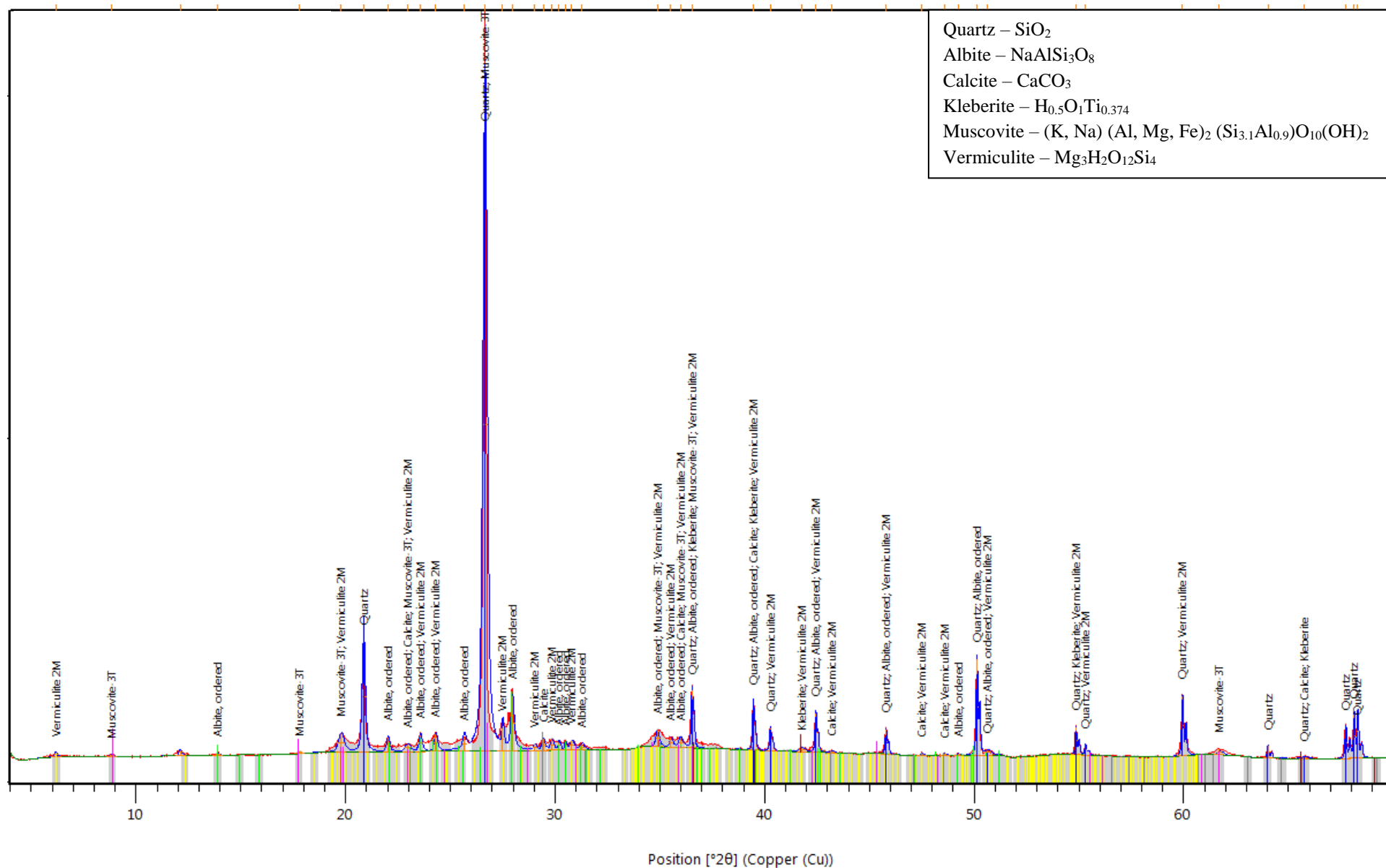
Stockdale Core SDK 3A, 0-9 cm



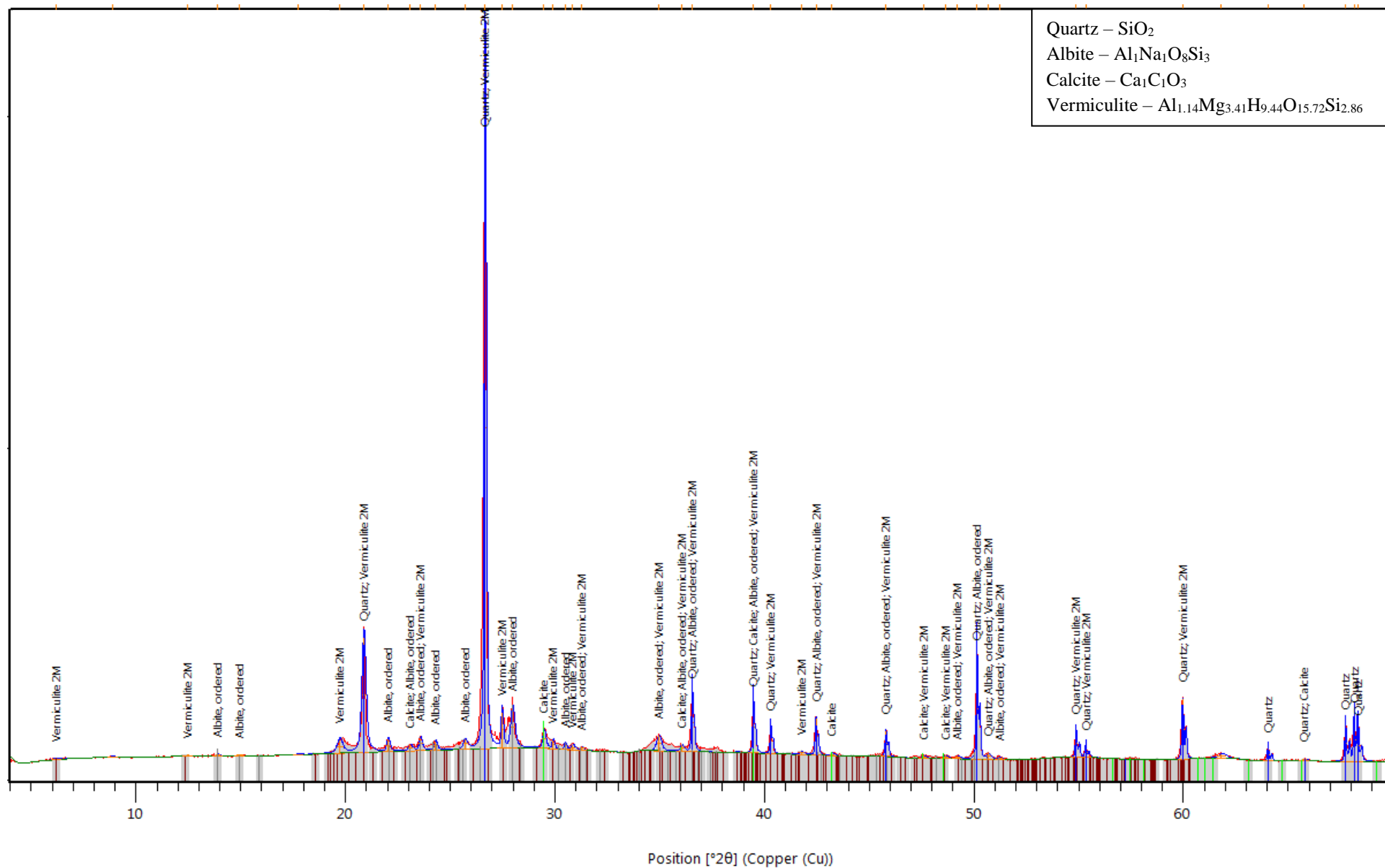
Stockdale Core SDK 3A, 16-22 cm



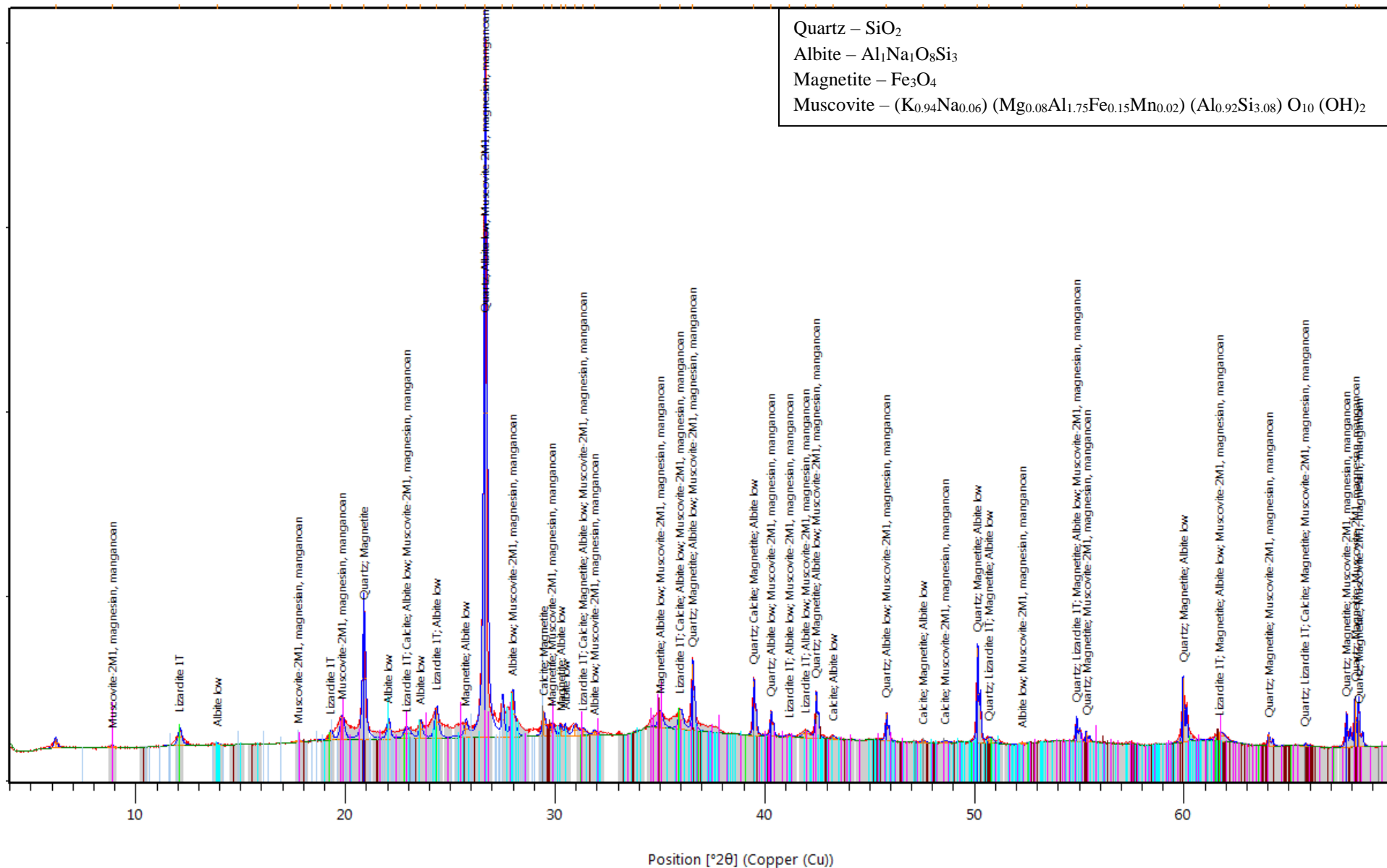
Stockdale Core SDK 3A, 27-32 cm



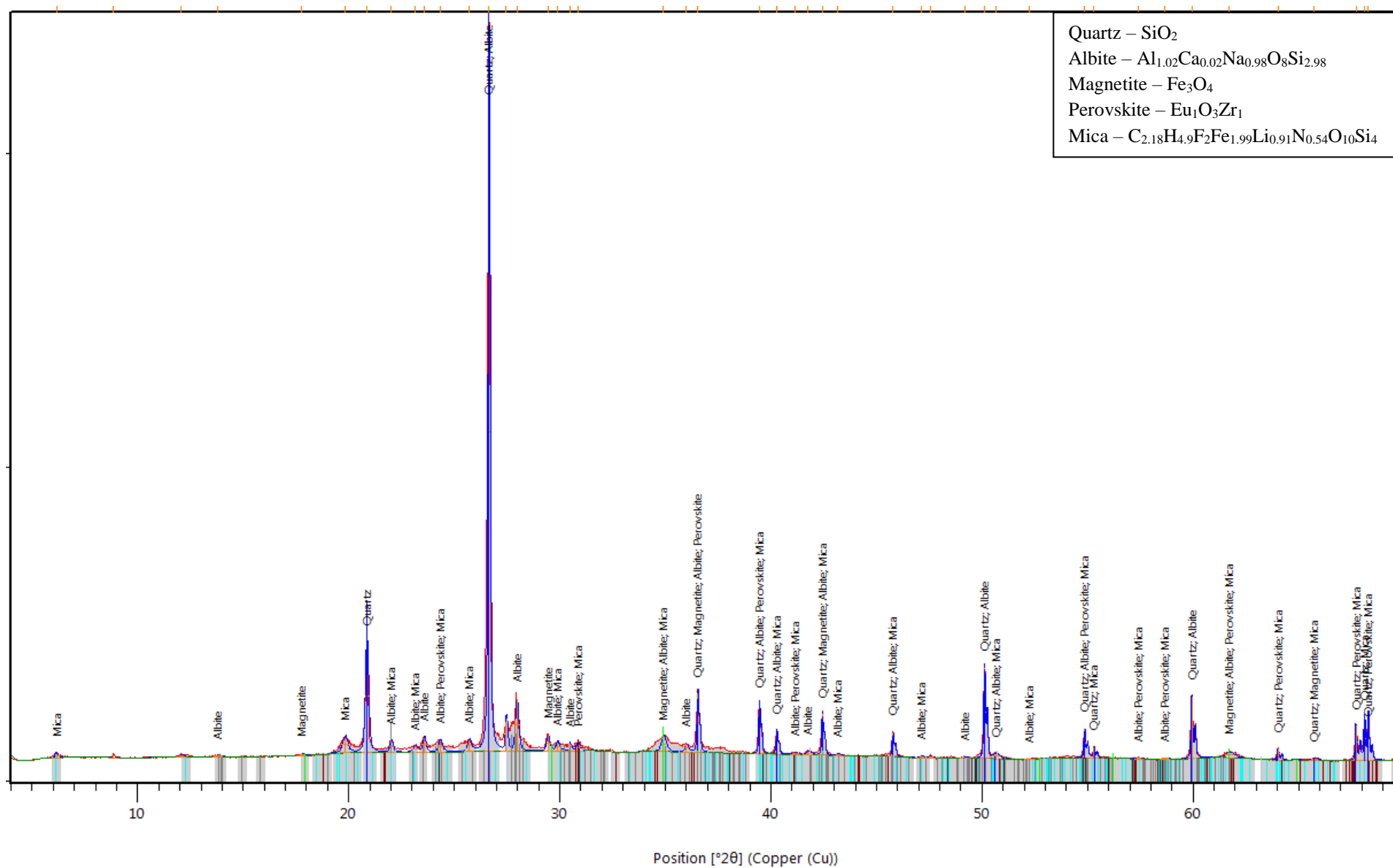
Stockdale Core SDK 3A, 43-49 cm



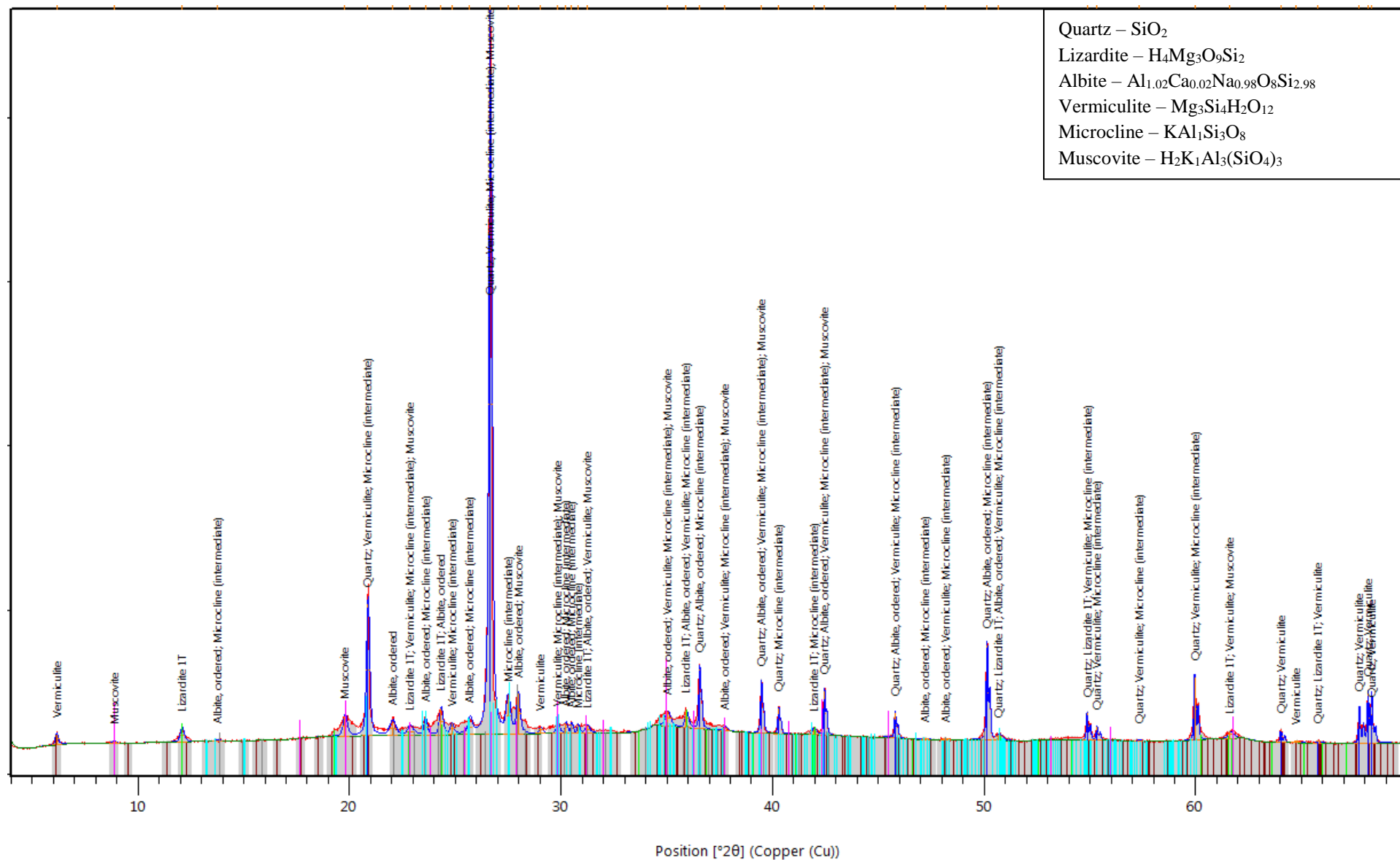
Stockdale Core SDK 4A, 0-10 cm



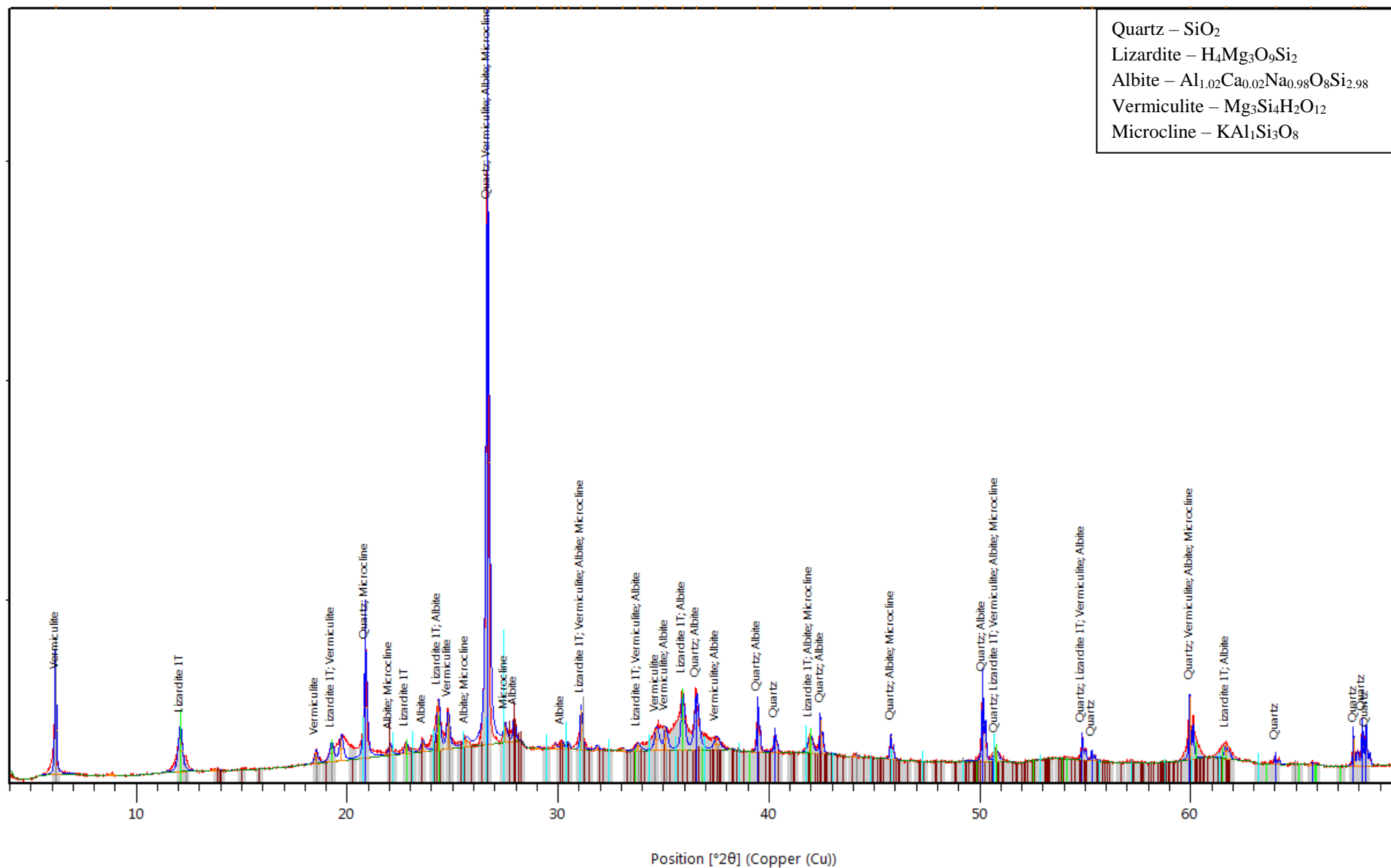
Stockdale Core SDK 4A, 22-28 cm



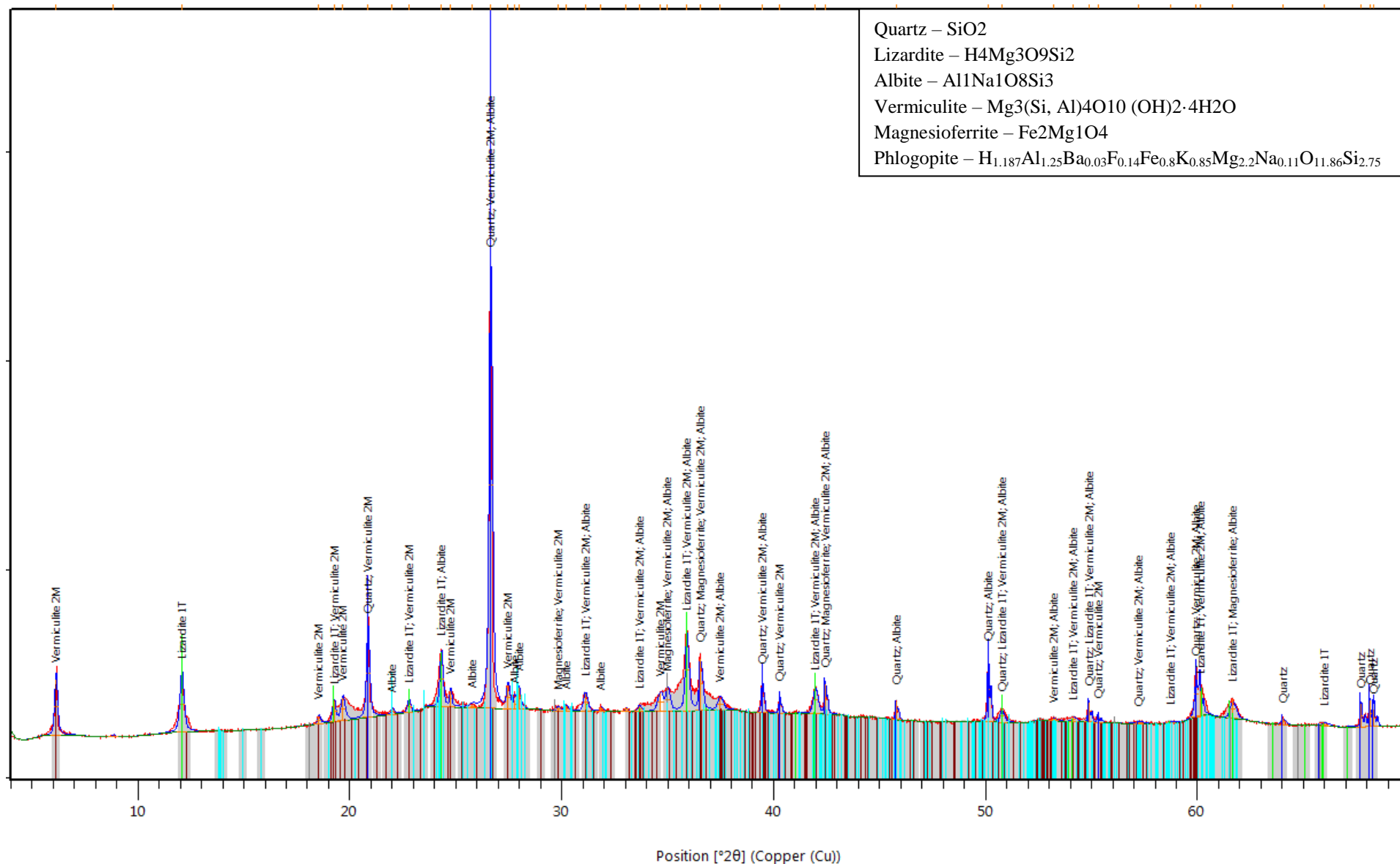
Stockdale Core SDK 4A, 37-42 cm



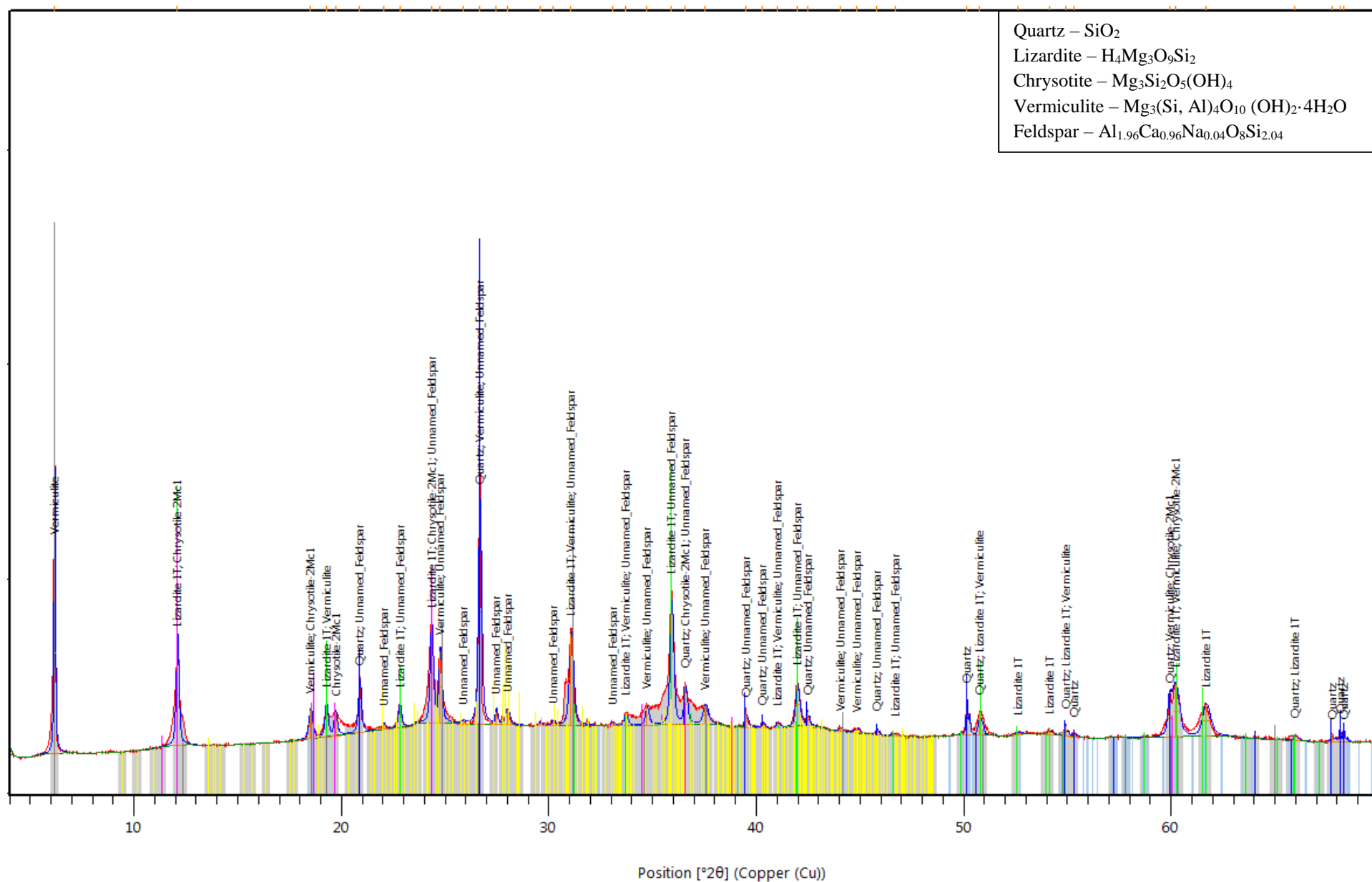
Stockdale Core SDK 1B, 7-14 cm



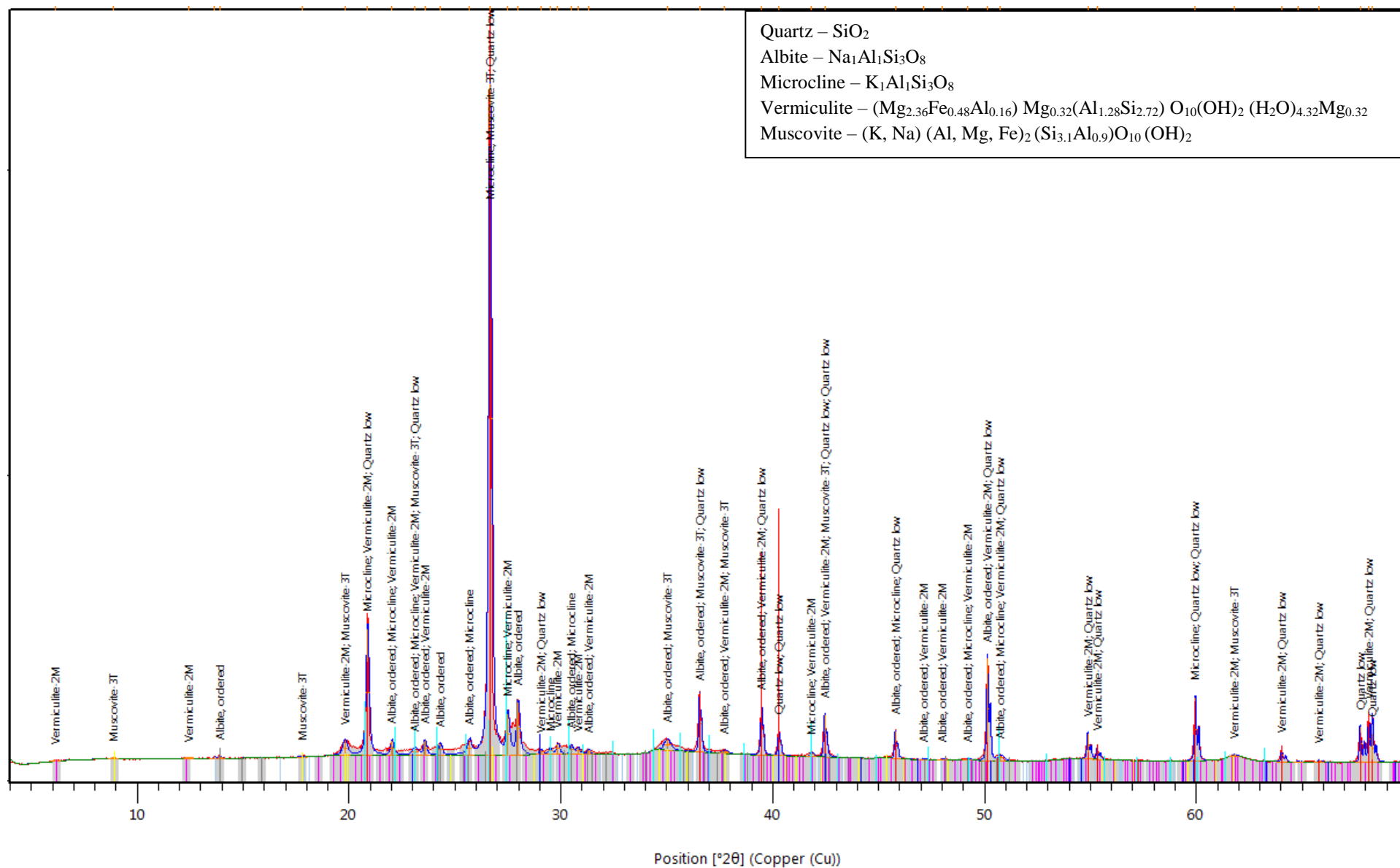
Stockdale Core SDK 1B, 14-20 cm



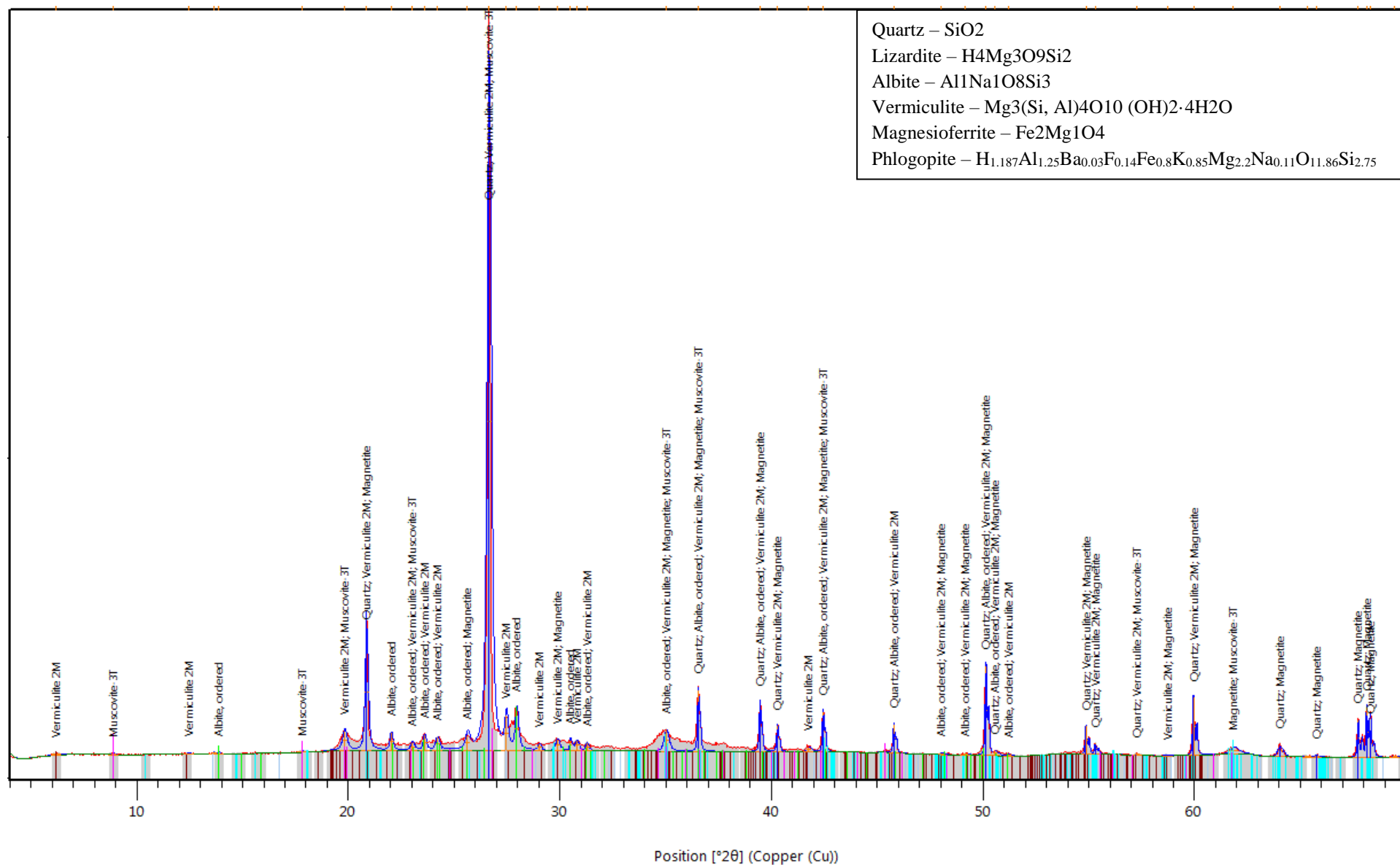
Stockdale Core SDK 1B, 28-36 cm



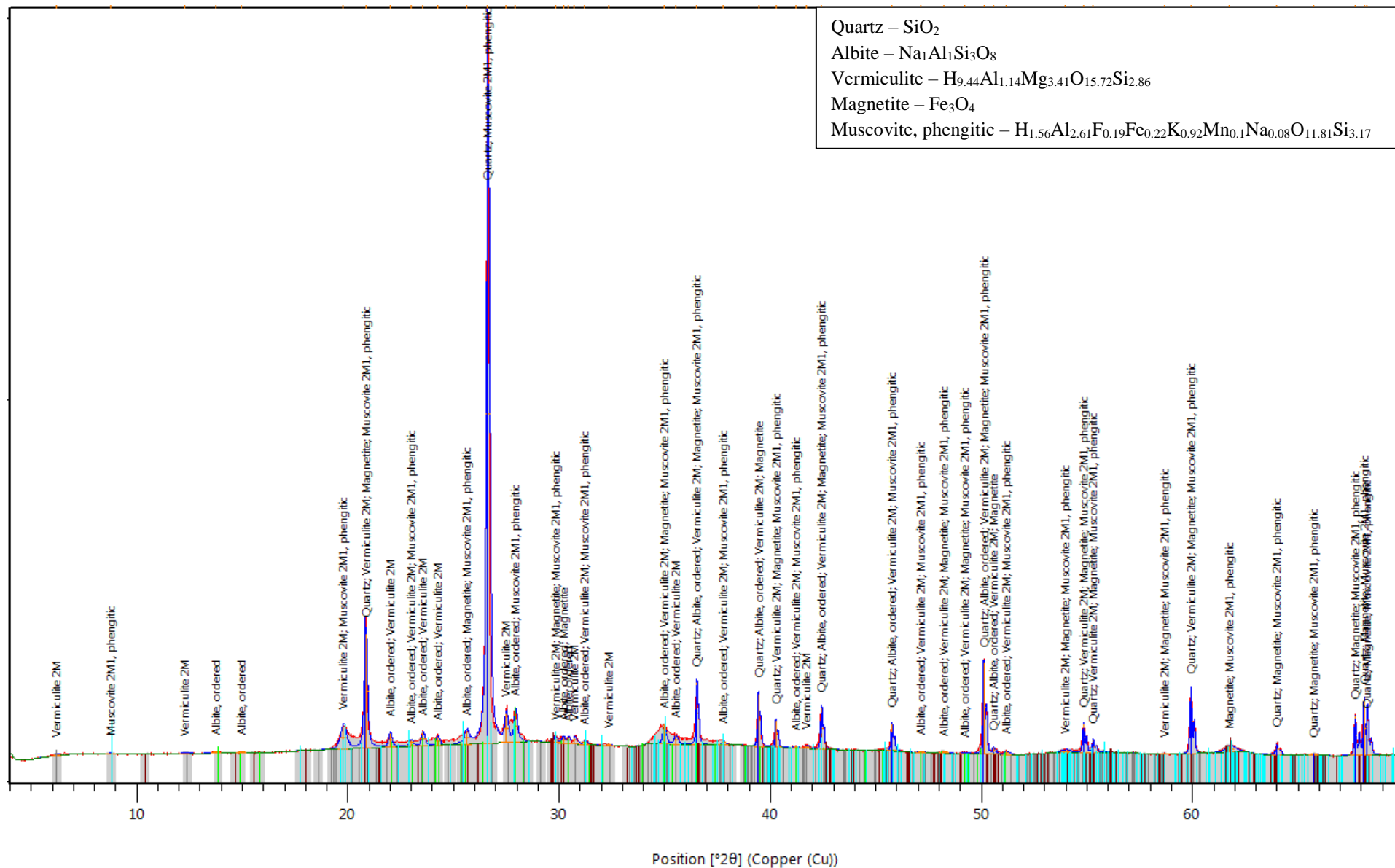
Stockdale Core SKD 1B, 36-41 cm



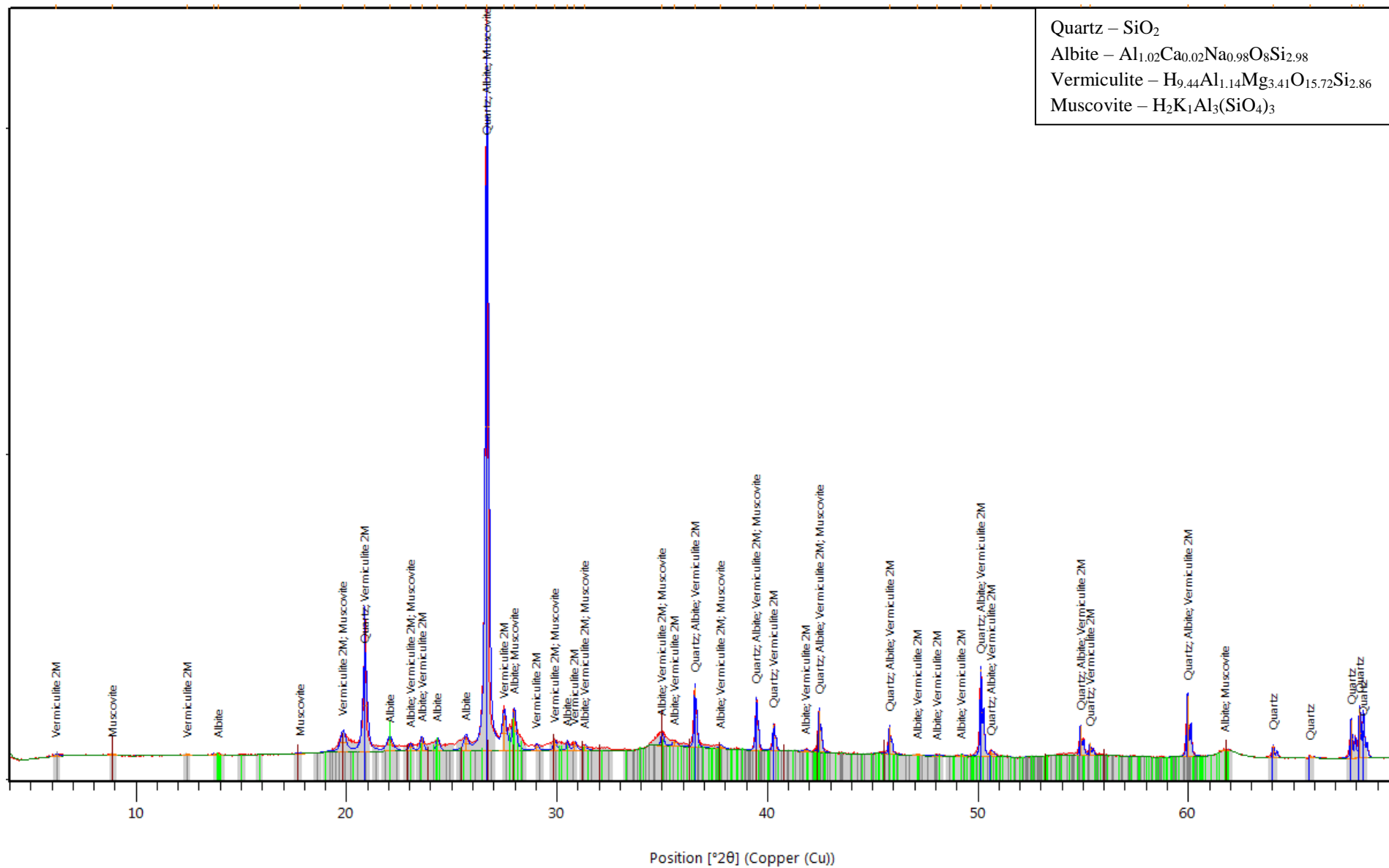
Stockdale Core SDK 2B, 0-10 cm



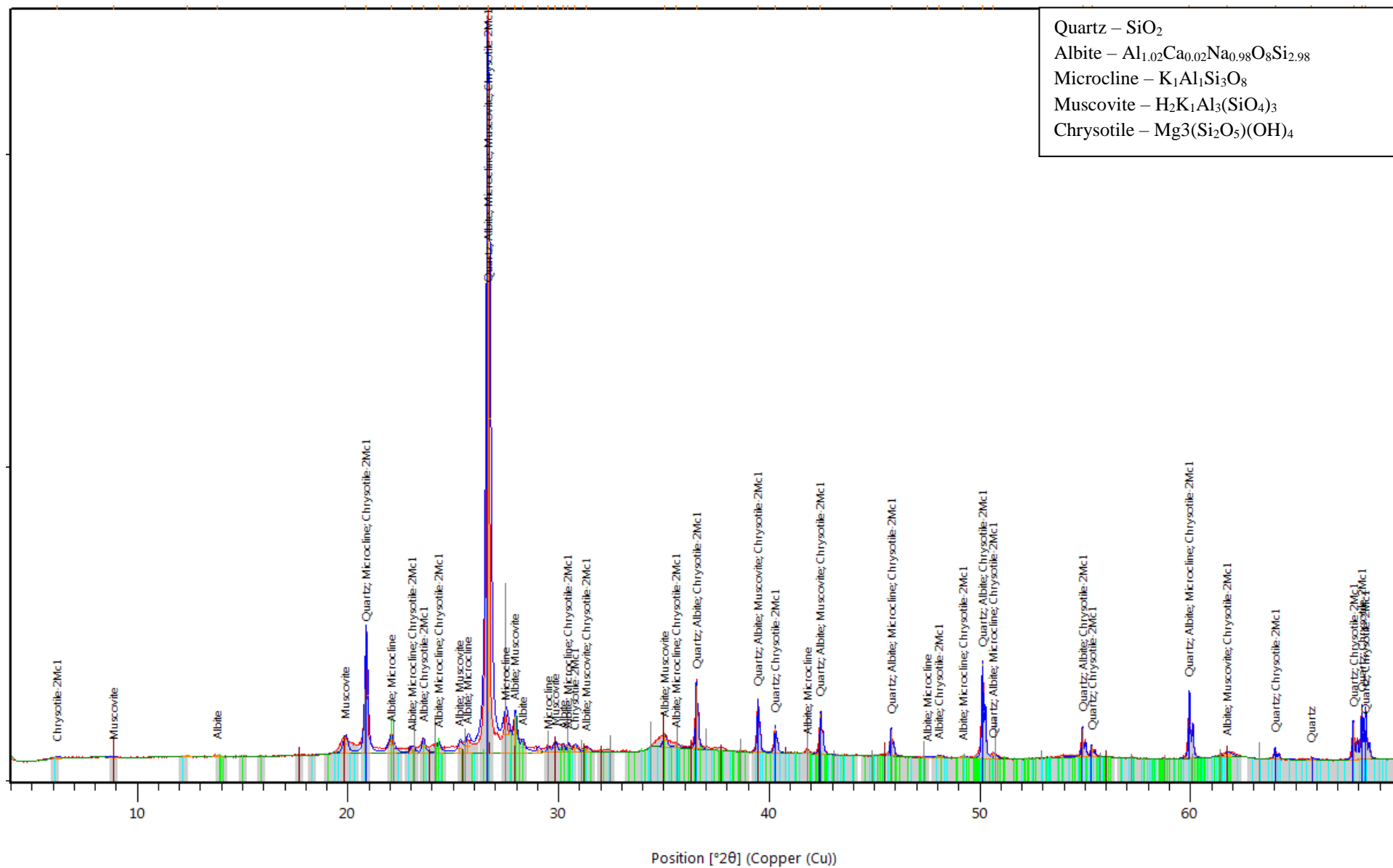
Stockdale Core SDK 2B, 16-28 cm



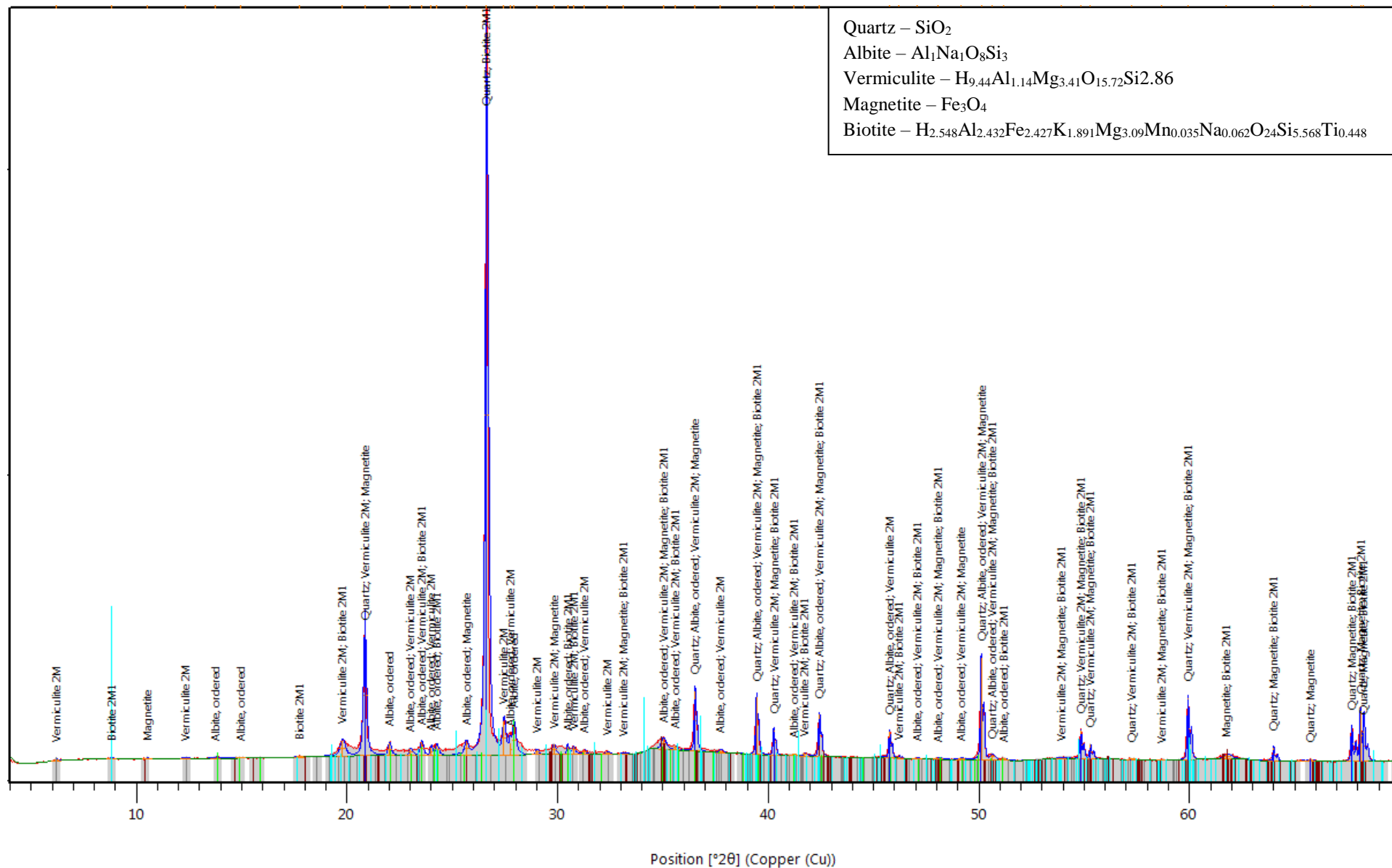
Stockdale Core SDK 2B, 28-35 cm



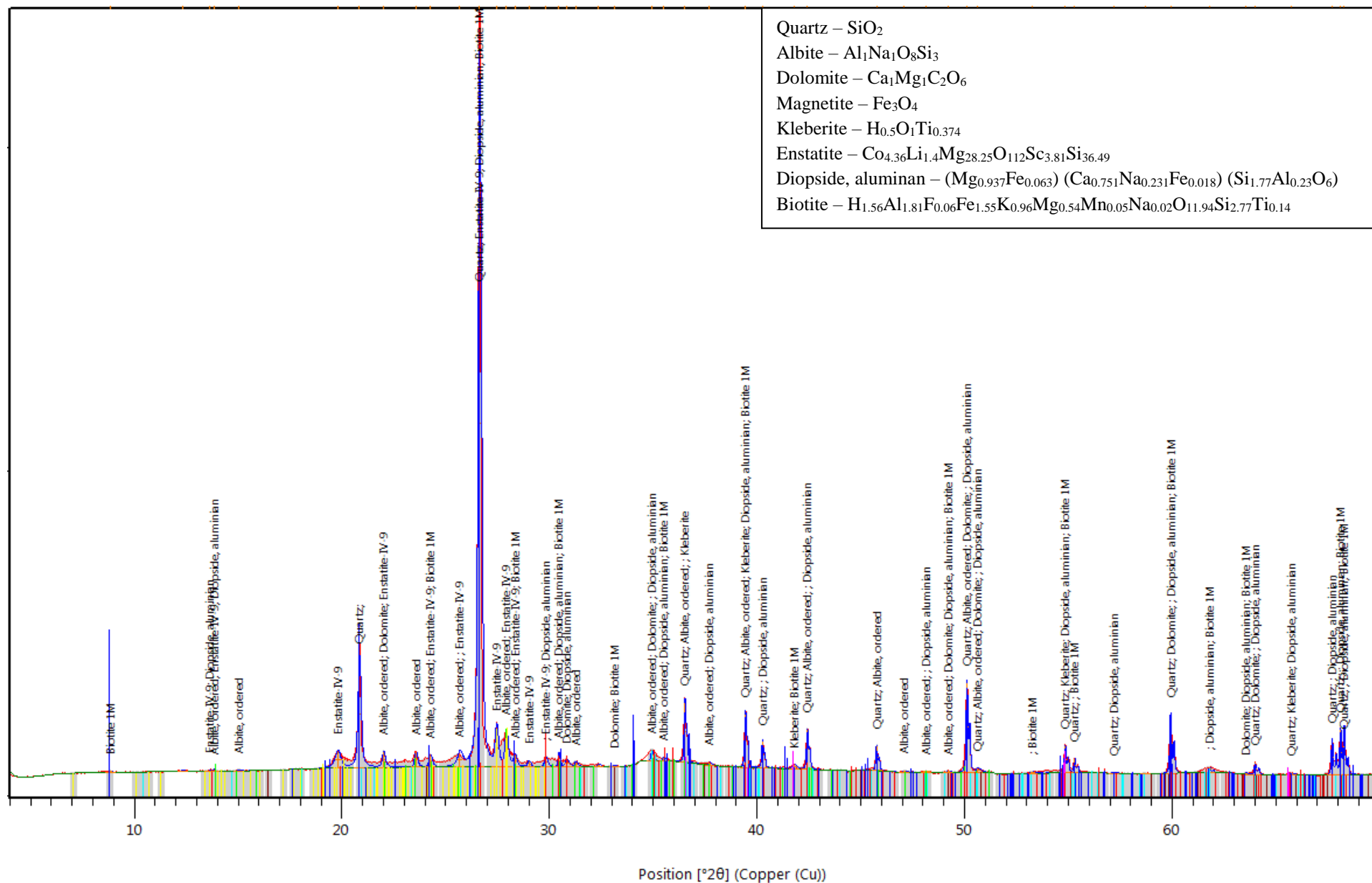
Stockdale Core SDK 2B, 42-49 cm



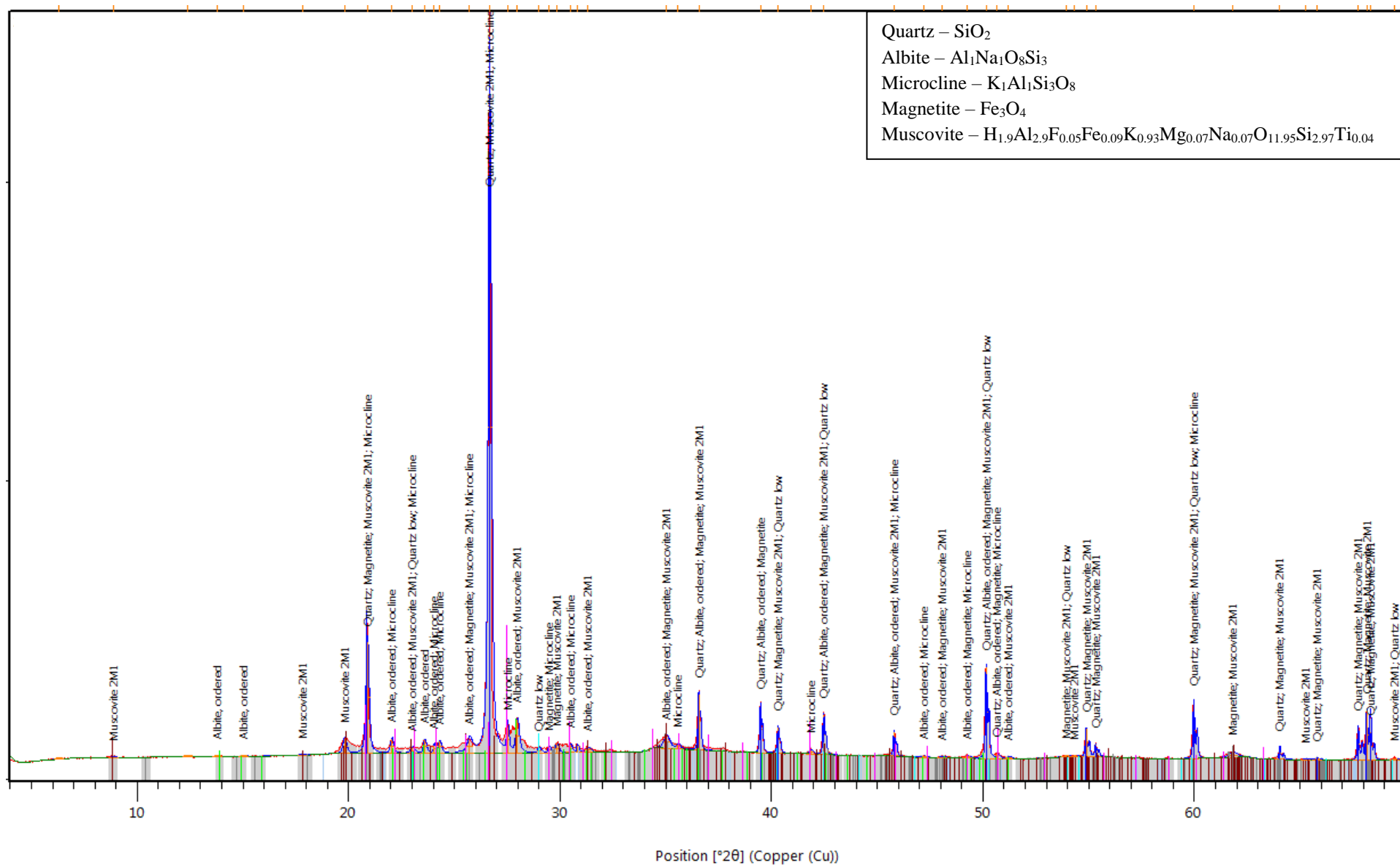
Stockdale Core SDK 2B, 54-63 cm



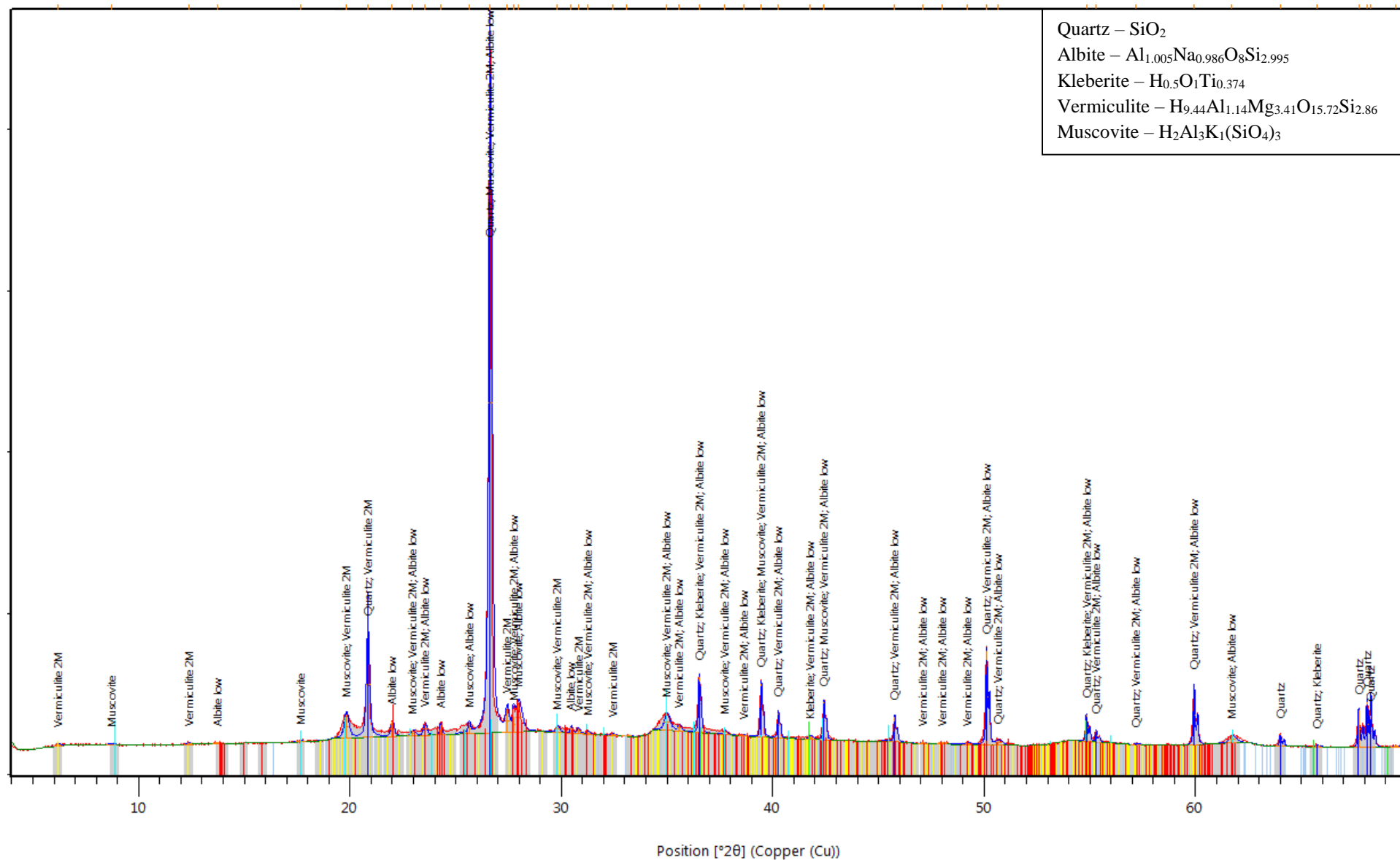
Stockdale Core SDK 2B, 71-79 cm



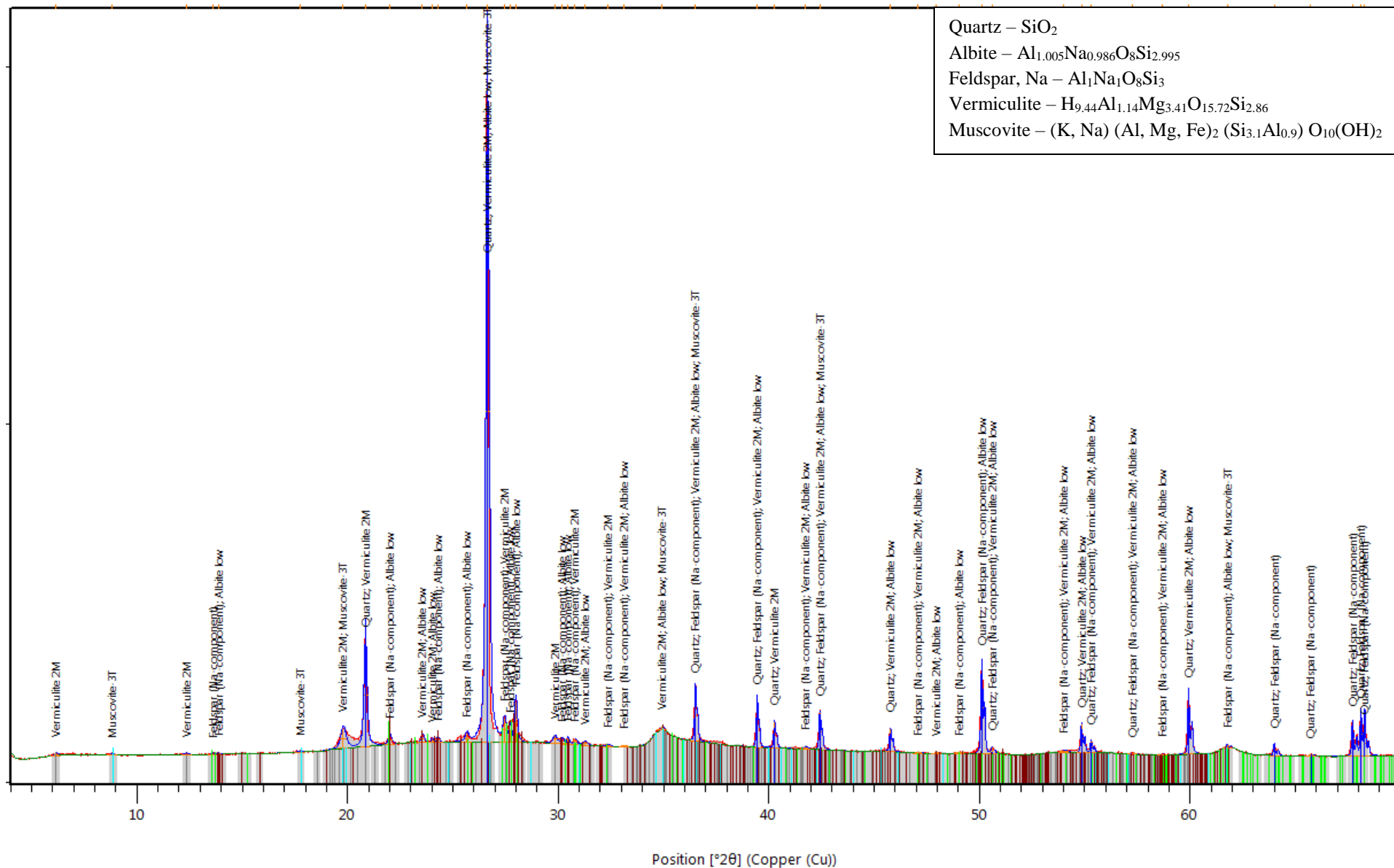
Stockdale Core SDK 3B, 0-7 cm



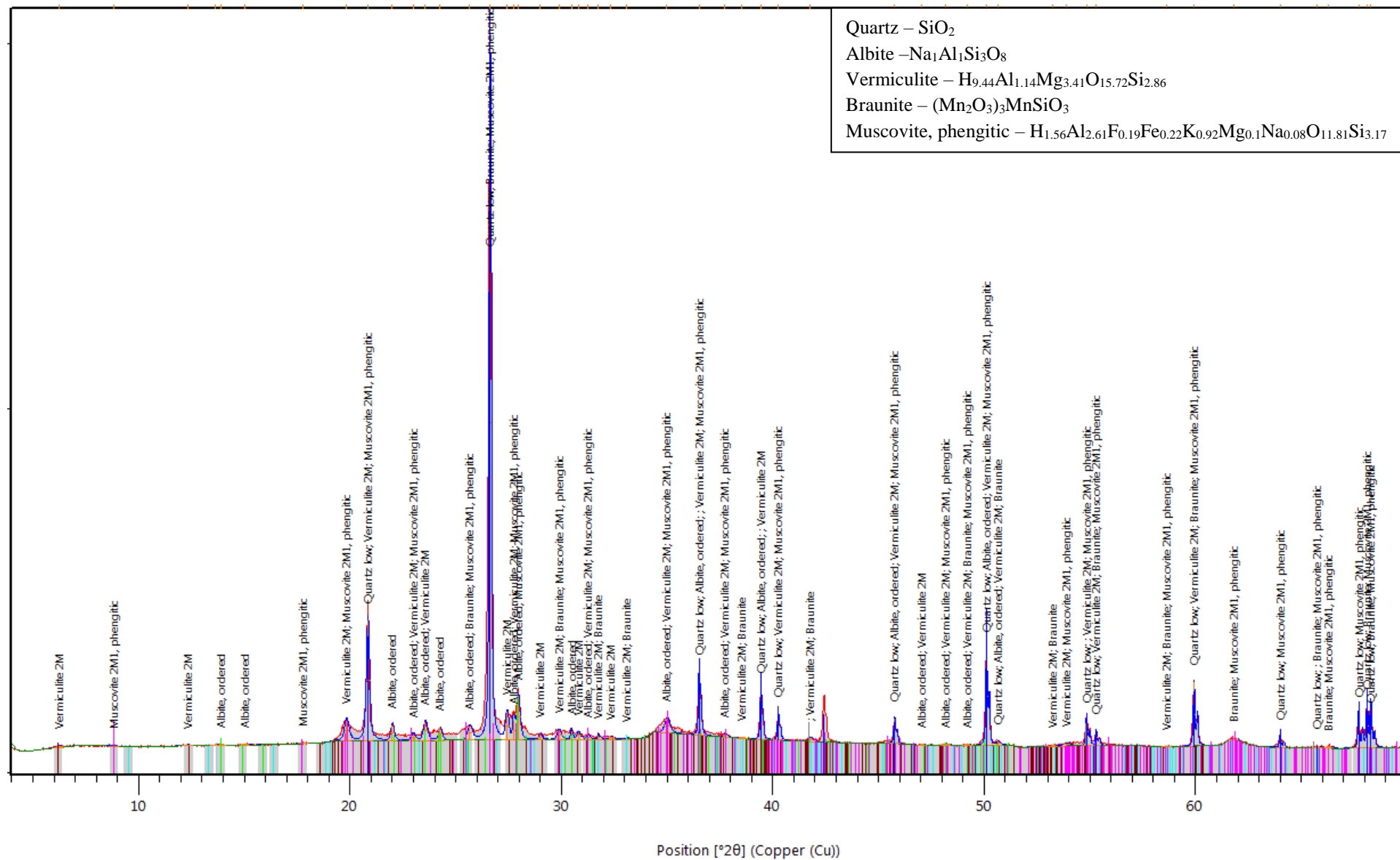
Stockdale Core SDK 3B, 7-16 cm



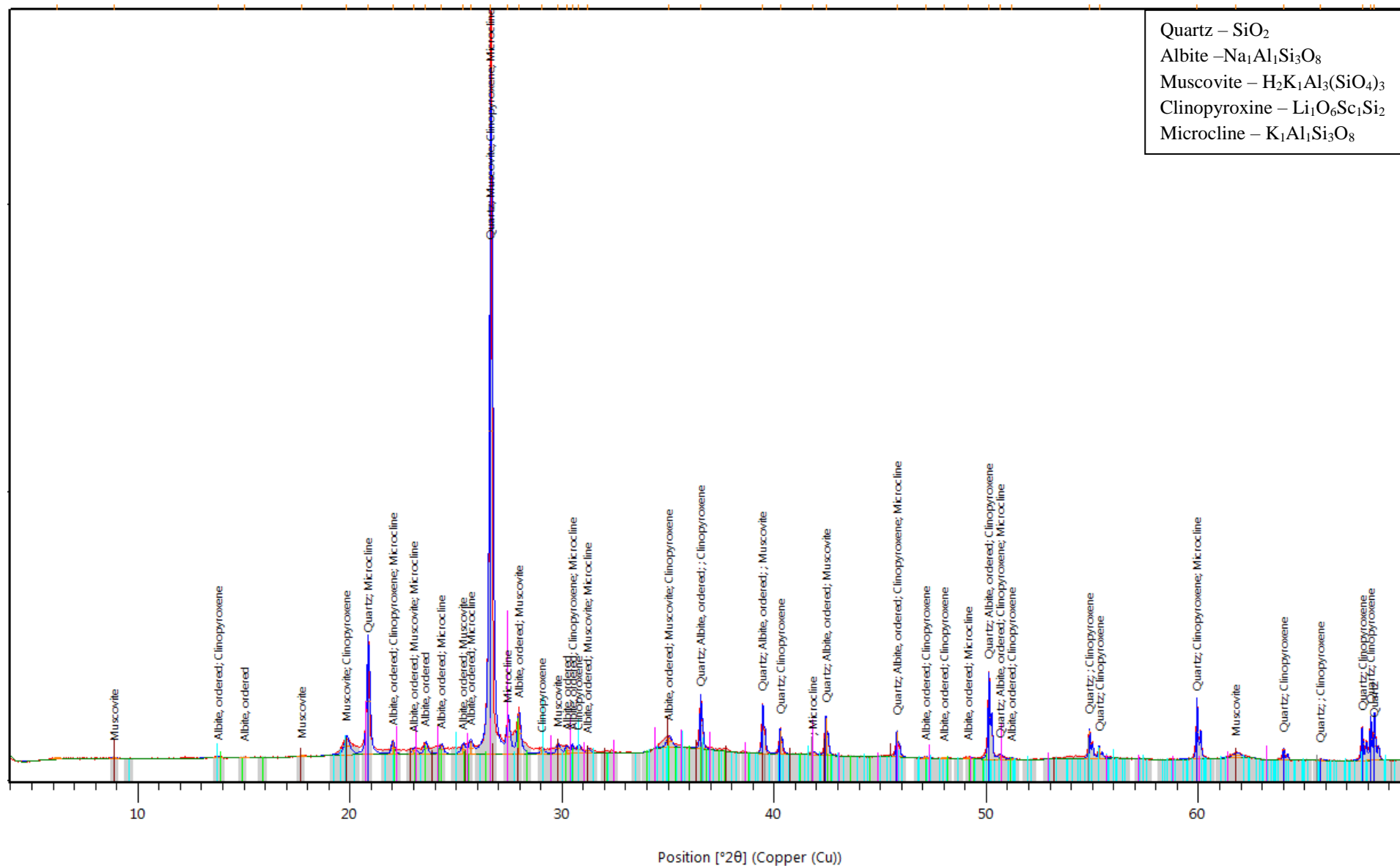
Stockdale Core SDK 3B, 20-25 cm



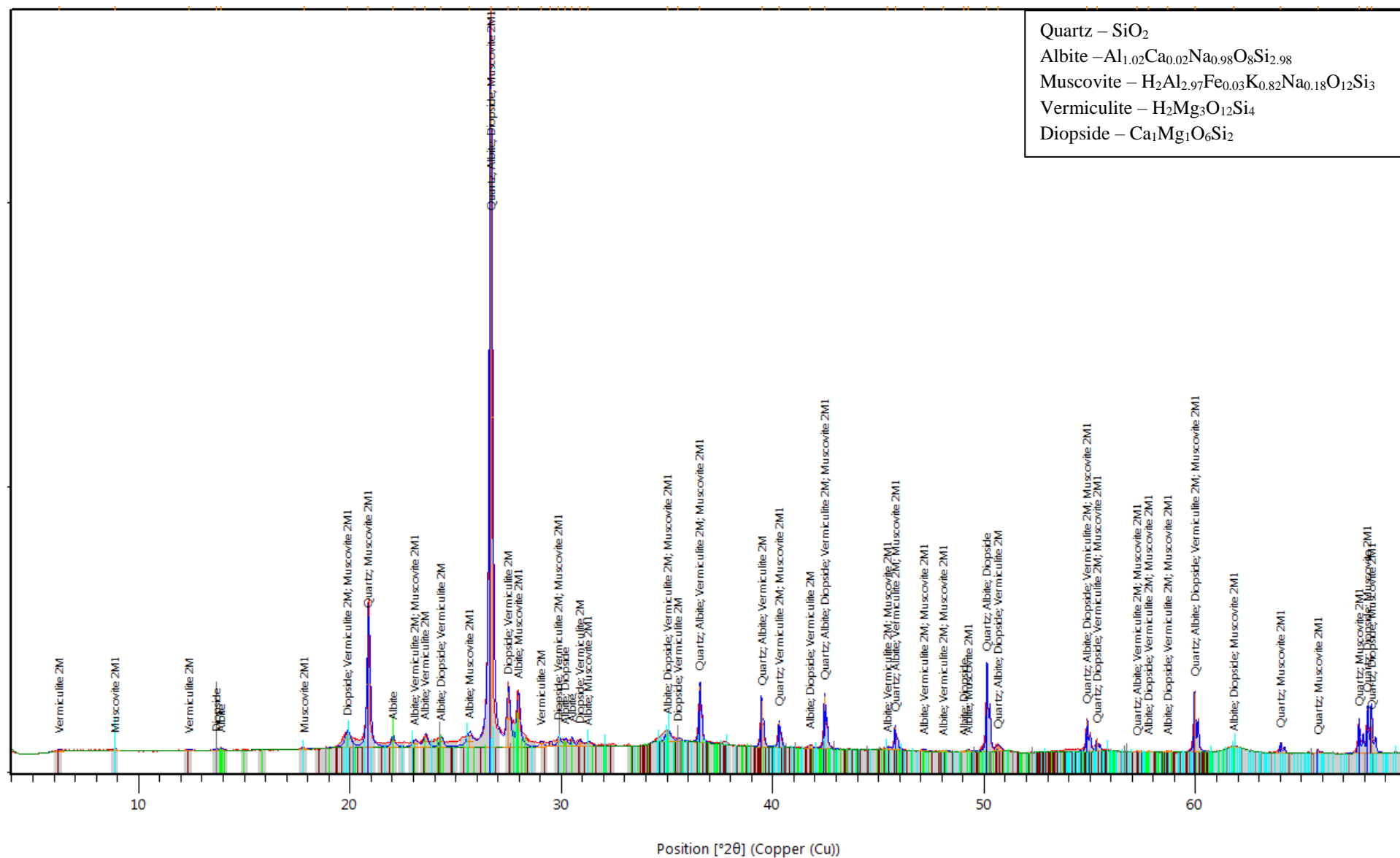
Stockdale Core SDK 3B, 30-40 cm



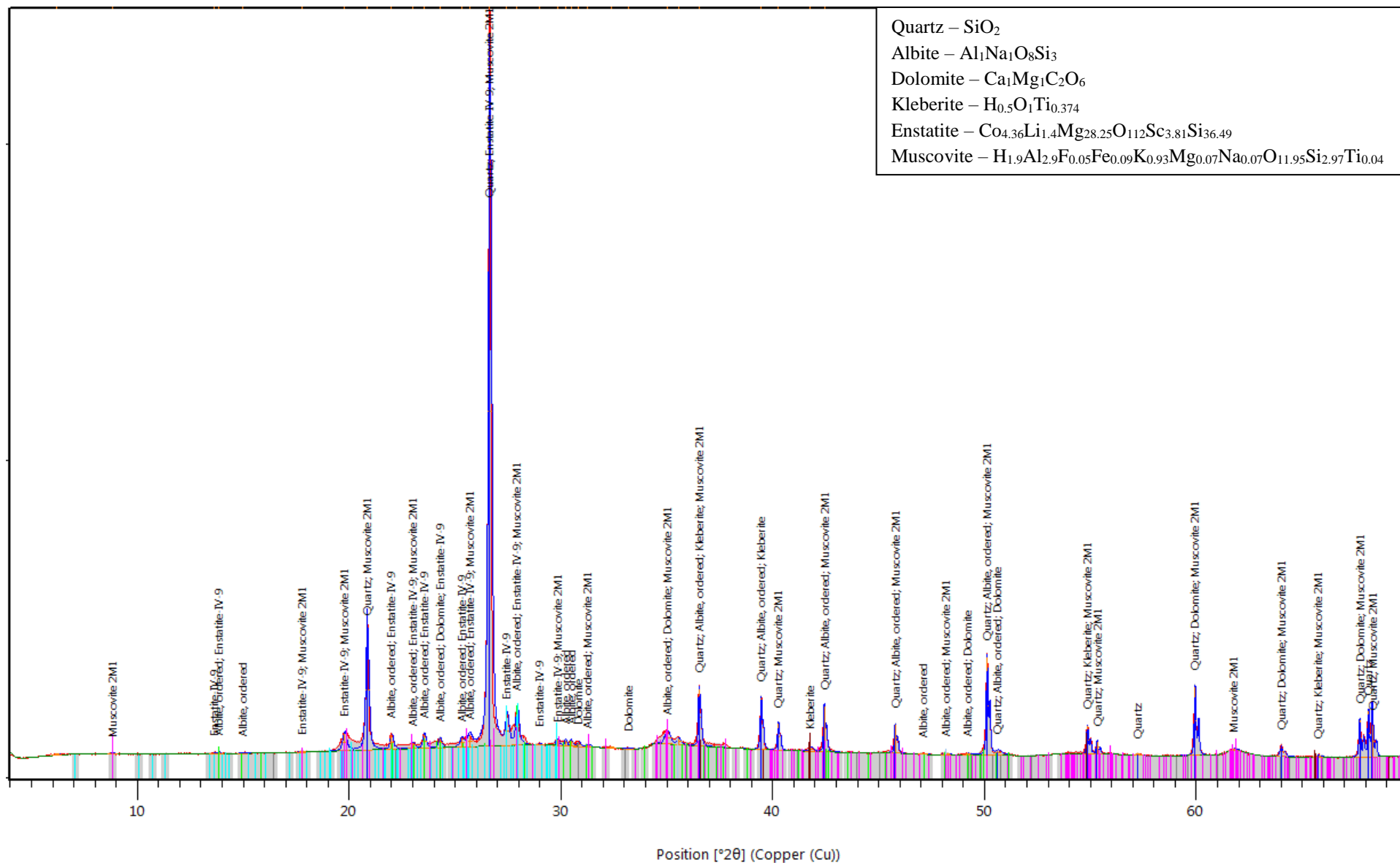
Stockdale Core SDK 3B, 41-48 cm



Stockdale Core SDK 3B, 57-61 cm



Stockdale Core SDK 3B, 61-68 cm



Stockdale Core SDK 3B, 68-76 cm

Appendix E - ICP-OES Data

Sample Labels	Depth in cm	Al	Ca	Fe	Mg	K	Na	Si	Mn	P	S	Ti	Cr	Cu	Ni	Zn
Konza 6-1T	0	4.1839	4.9807	2.9328	5.2127	6.3824	1.4321	6.4040	4.9695	3.2582	3.8091	6.7960	32.1271	11.6340	20.0778	47.6403
Konza 6-1B	30	6.8767	7.1486	4.3948	8.3846	8.6168	1.9246	7.3315	6.7314	2.2742	6.5800	5.3427	79.6581	15.9800	34.2514	125.2659
Konza 6-2	70	4.1235	175.2048	3.0505	11.5830	12.7003	3.3177	11.7138	5.5900	2.7338	25.1077	2.2987	40.0146	7.9193	25.9046	123.9423
Konza 6-3	120	3.5502	148.5161	2.9518	12.5288	13.1497	3.8505	7.2039	7.7150	2.8200	22.0796	1.6241	42.7789	9.4931	25.4687	114.2664
SDK 1 0-11	0	3.3971	11.6992	3.4831	36.2558	5.4483	1.9901	5.5863	8.0816	8.2968	5.4811	9.4711	97.7820	16.5096	165.7020	49.3468
SDK1 12-15	12	3.0453	17.4647	3.7733	65.1050	4.5006	2.1806	6.8144	9.7452	10.3070	6.8622	15.1064	148.1063	17.1922	260.8501	48.9412
SDK 2 0-13	0	3.5548	8.1993	2.6905	6.3324	6.1704	1.7419	13.2906	5.4030	6.6543	5.9532	7.4623	28.9944	12.3787	23.9562	45.9794
SDK 2 50-52	50	3.9962	13.0502	3.3053	26.4334	5.7623	2.1512	9.7173	3.6004	4.9963	4.1853	9.1587	70.2206	16.1653	107.8526	45.0940
SDK 5 0-12	0	3.9056	10.2091	3.0953	6.5115	6.3123	2.1793	17.6256	8.6078	4.8855	4.6251	6.3073	26.3160	12.6312	20.0643	44.9950
SDK 5 20-25	20	4.1421	25.2461	3.5596	9.5222	7.8689	2.8915	7.5563	14.2077	4.5161	6.1299	6.2453	29.3378	14.5631	30.9899	76.5009
SDK 2A 0-10	0	3.2845	10.9144	2.7511	7.6992	4.5683	1.7287	7.6234	7.4415	6.6212	6.0006	6.1844	31.4917	12.7491	30.9874	46.3221
SDK 2A 50-60	50	3.3940	7.7187	3.1672	22.3696	4.6773	2.5933	8.5769	8.3018	5.4696	3.2028	11.5481	67.8447	14.1363	104.9029	40.3107
SDK 3A 0-9	0	3.7226	12.6067	3.3179	20.6102	5.2562	3.5734	6.2882	10.2617	7.4952	6.8444	9.9631	76.0823	15.0522	99.6490	52.3946
SDK 3A 43-49	43	3.0370	11.5754	3.7280	42.2271	4.2439	2.9363	9.8576	12.6757	7.8030	4.4109	12.7282	146.4404	17.2097	226.7107	43.3455
SDK 1B 0-7	0	3.5106	6.7145	3.4729	31.2213	4.8174	1.8245	6.2814	6.6693	6.8608	4.1928	8.9623	118.1935	15.0748	180.6395	49.7796
SDK 1B 7-14	7	3.5868	6.7030	4.2002	45.7428	4.6369	2.0997	9.7803	8.2868	8.2114	3.5173	13.4388	185.8713	18.0353	291.0870	50.1668
SDK 1B 28-36	28	2.6986	7.6771	6.0887	119.8919	2.7211	2.5969	5.9857	13.2728	12.6255	2.9578	26.3733	384.3060	24.9723	719.9323	54.2834
SDK 1B 36-41 *	36	1.7330	11.4381	6.0880	0.0446	1.6699	2.6804	5.7850	11.2999	11.5990	3.8786	21.3942	425.7733	24.8663	784.0369	39.3415
SDK 3B 0-7	0	4.1960	5.1630	3.0437	8.0320	5.8047	1.8948	18.2782	6.0405	4.1307	3.9788	9.1289	36.9879	13.0068	30.5980	54.8967
SDK 3B 30-40	30	5.7628	4.4920	3.8964	8.0118	6.3453	2.9016	7.0005	10.9397	2.2225	2.2996	10.4385	37.9459	16.1944	29.1229	52.9979
SDK 3B 68-76	68	4.6998	3.8509	2.9863	6.9574	5.5348	3.6930	8.4729	3.7267	1.6076	1.5054	10.6341	36.4340	13.9714	21.7754	46.4744

Unit

10⁴
mg/kg

10³
mg/kg

10⁴
mg/kg

10³
mg/kg

10³
mg/kg

10²
mg/kg

10²
mg/kg

10²
mg/kg

10²
mg/kg

10²
mg/kg

10²
mg/kg

10²
mg/kg

10²
mg/kg

10²
mg/kg

10²
mg/kg

10²
mg/kg

10²
mg/kg

10²
mg/kg



These are samples from Konza's N4D watershed

These are from the creek heading downstream from the Kimberlite outcrop

These are from the creek heading upstream from the Kimberlite outcrop

These are from the transect uphill from the Kimberlite with no stream interaction

Standard Data for NIST SRM 2711a processed and analyzed with study samples

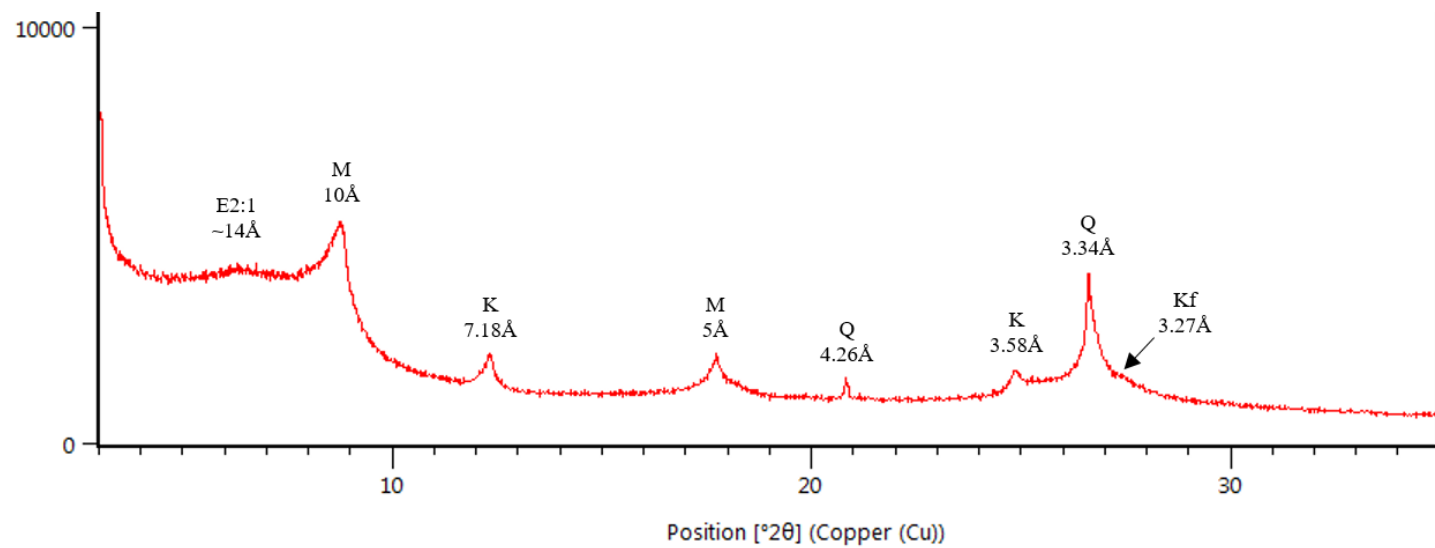
	NIST Data (Actual)(mg/kg)	Using EPA Method 3050B (Aqua Regia)			This study		
		Range (mg/kg)	Median (mg/kg)	% Recovery	Range (mg/kg)	Median (mg/kg)	% Recovery
Al	67200	9800-15000	13200	19	25678-30147	29157	42
Ca	24200	14000-17000	14000	61	16111-18713	18061	74
Cr	52.3	12-18	15	29	23-28	24	48
Cu	140	120-160	130	95	98-112	107	76
Fe	28200	14000-18000	15000	54	26301-28700	27669	98
Mg	10700	5000-6600	5700	54	7415-8312	7899	74
Mn	675	450-580	460	71	493-584	574	83
Ni	21.7	13-18	15	72	12-14	13	62
K	25300	3300-4600	3900	16	5528-6724	6122	24
Na	12000	140-210	180	1.5	339-506	414	4
Zn	414	310-380	350	85	283-324	312	75

Appendix F - Clay Fraction XRD Data

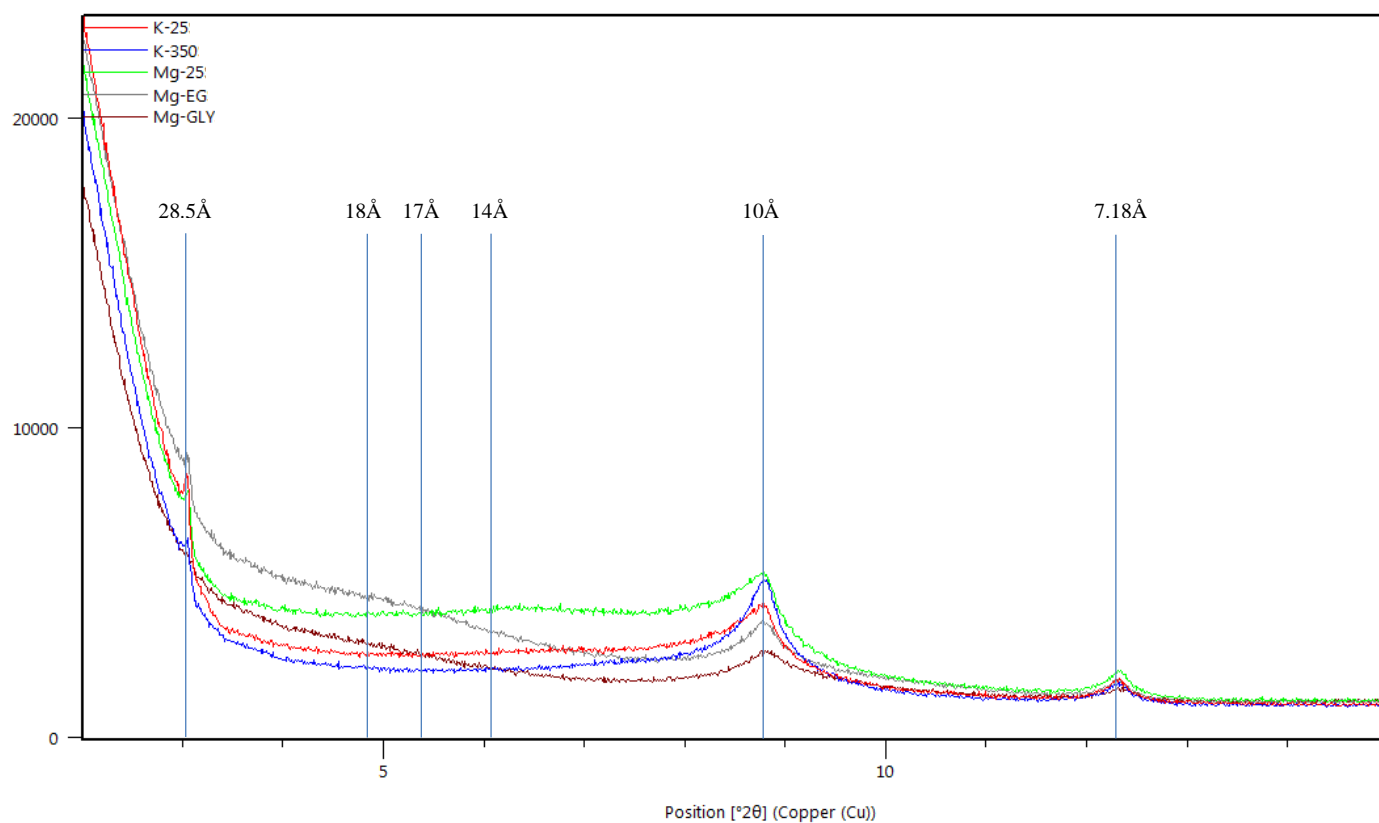
For all diffractograms in this section, identified peaks will be labeled as follows: Q = quartz, D = dolomite, Kf = K-feldspar, K = kaolinite, M = clay mica, M-S = interstratified mica-smectite, S = smectite, V = vermiculite, E2:1 = expandable 2:1 layer silicate, (G = gibbsite, possibly present in one sample but cannot be confirmed).

Konza Core 6, 0-10cm

Mg-25

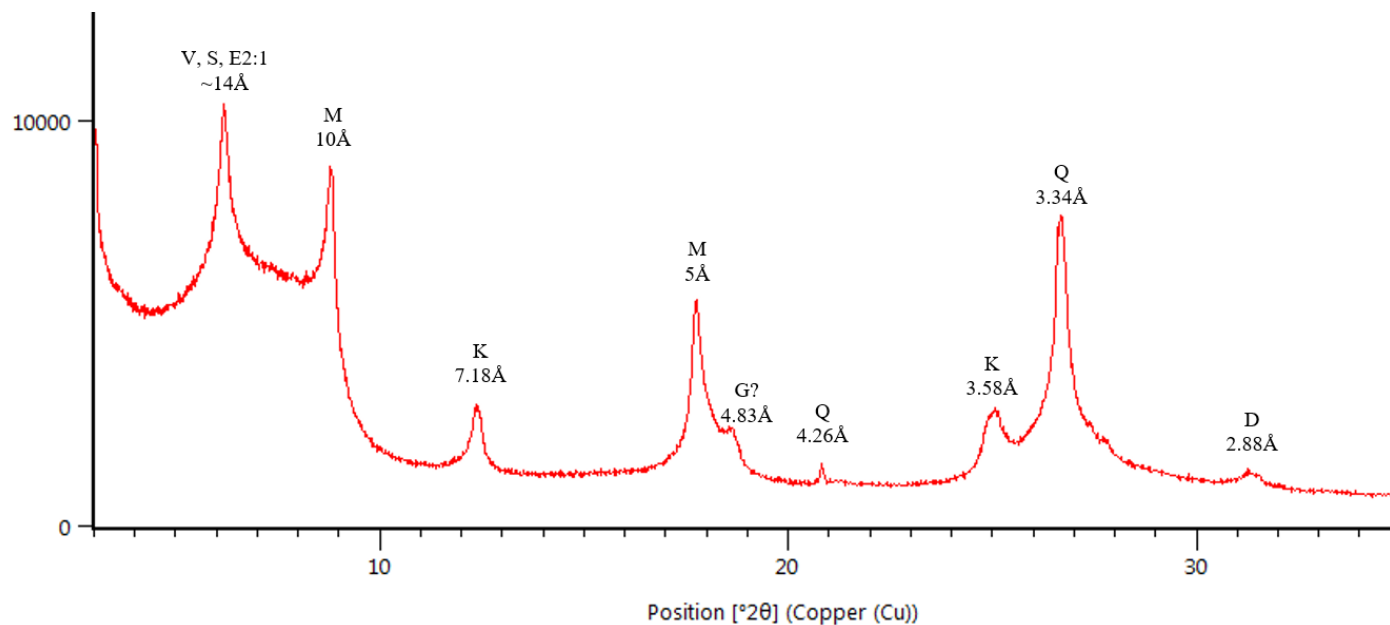


Multiple treatment overlay

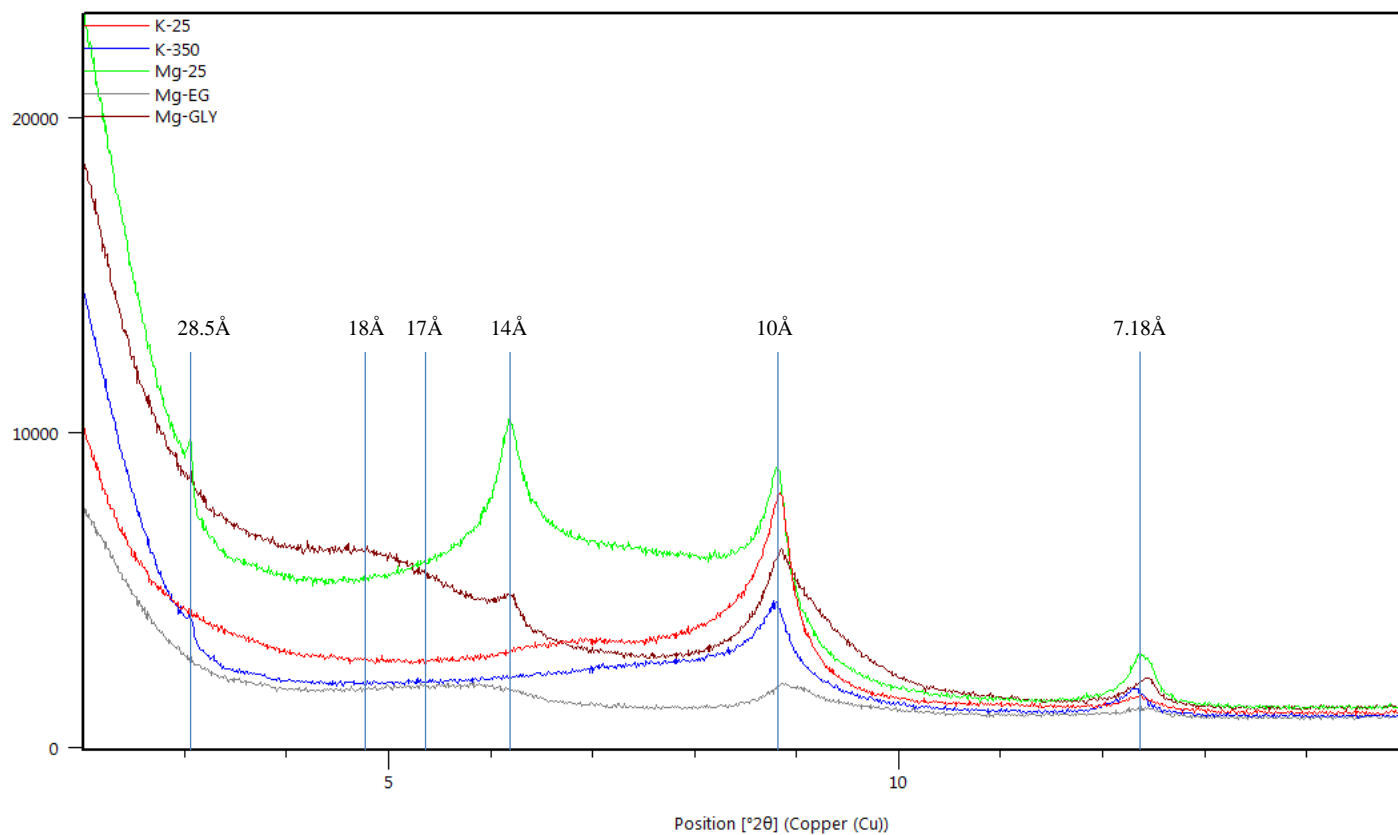


Konza Core 6, 70-80cm

Mg-25

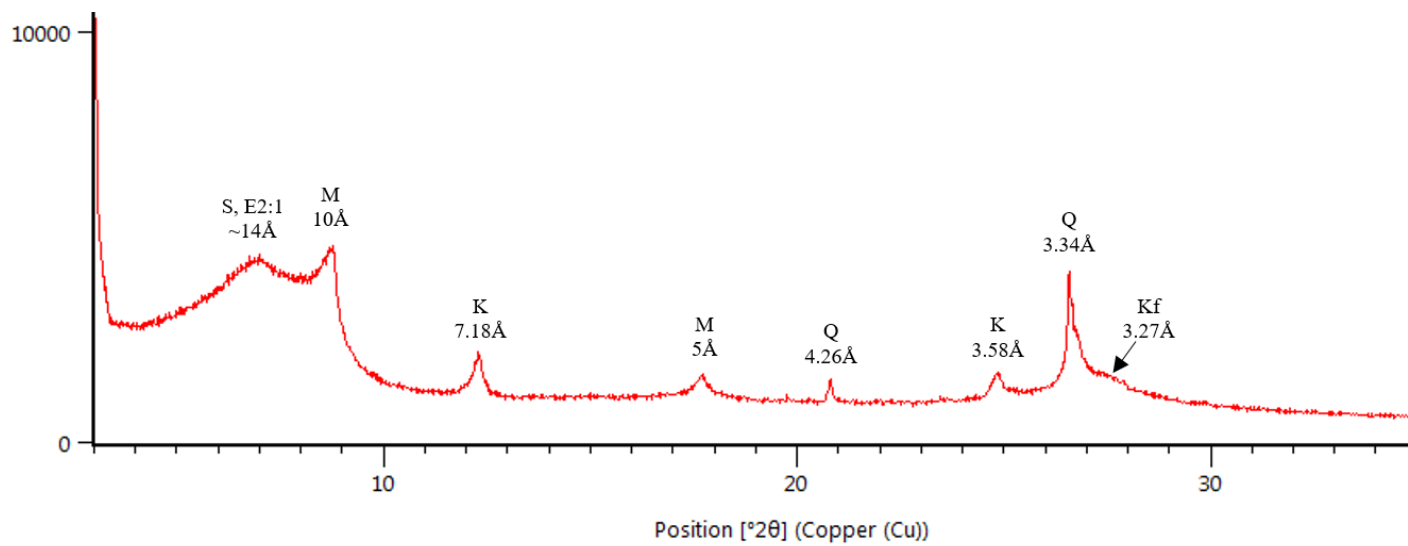


Multiple treatment overlay

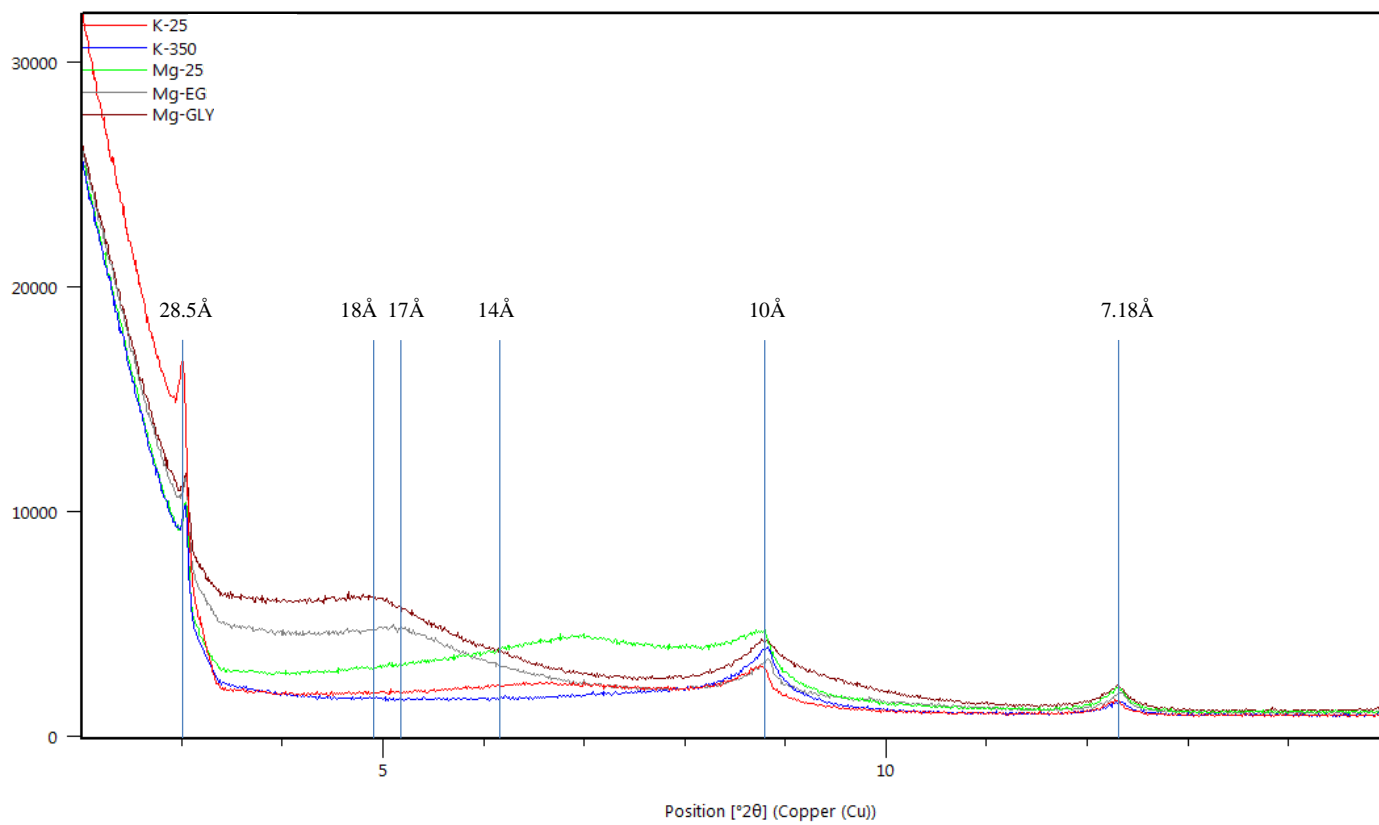


Konza Core 9, 193-203cm

Mg-25

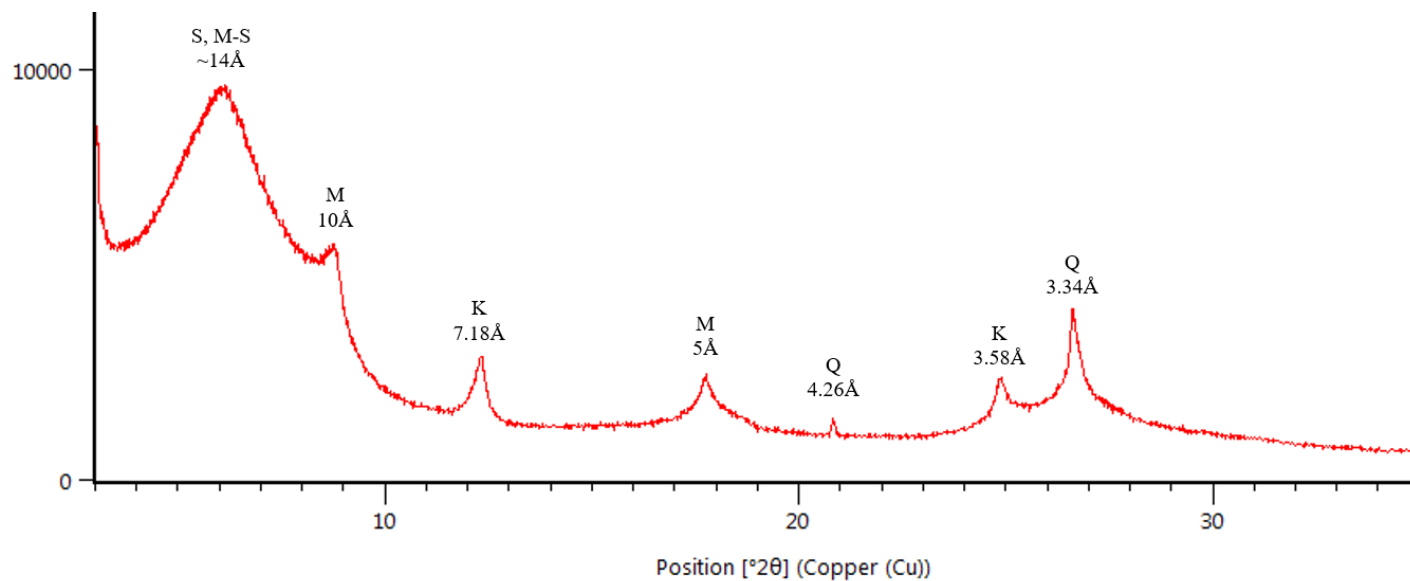


Multiple treatment overlay

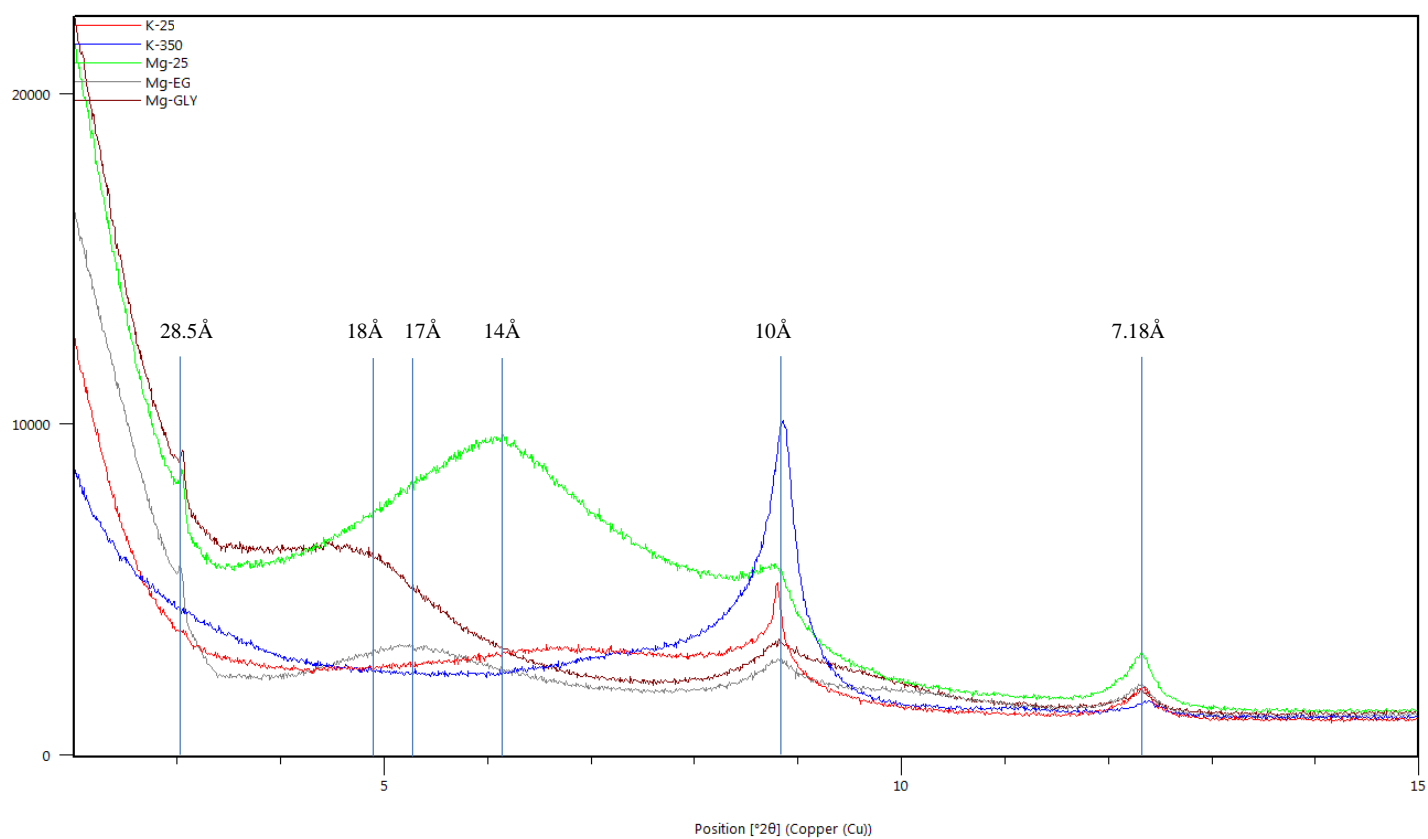


Stockdale Core SDK 1, 0-11cm

Mg-25

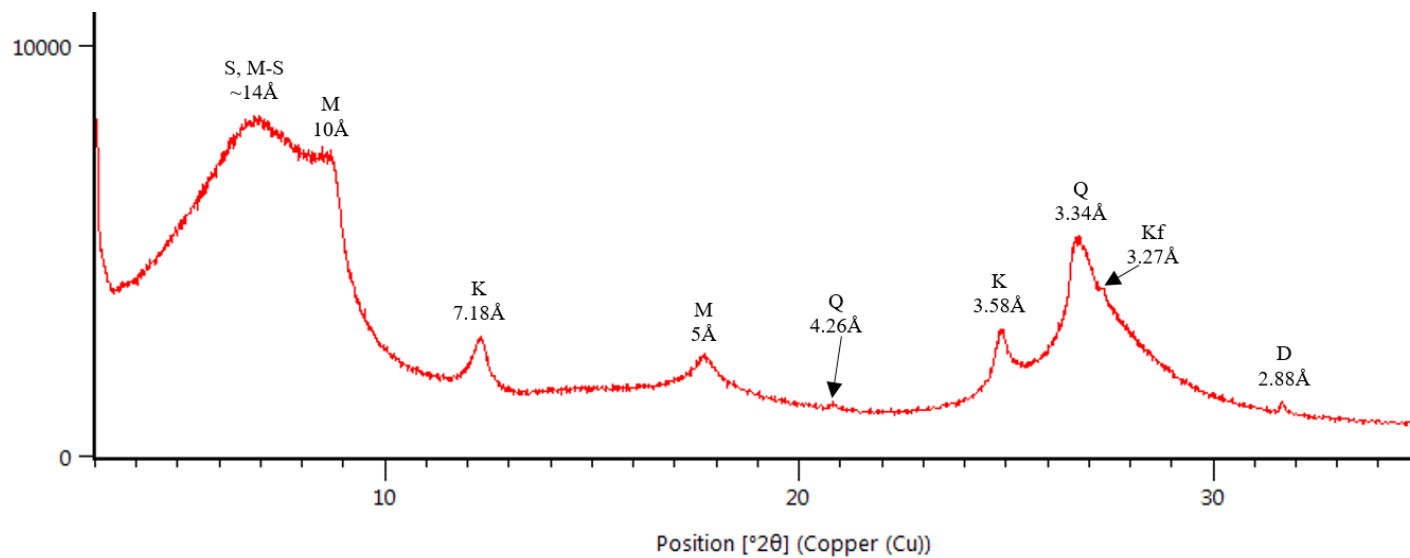


Multiple treatment overlay

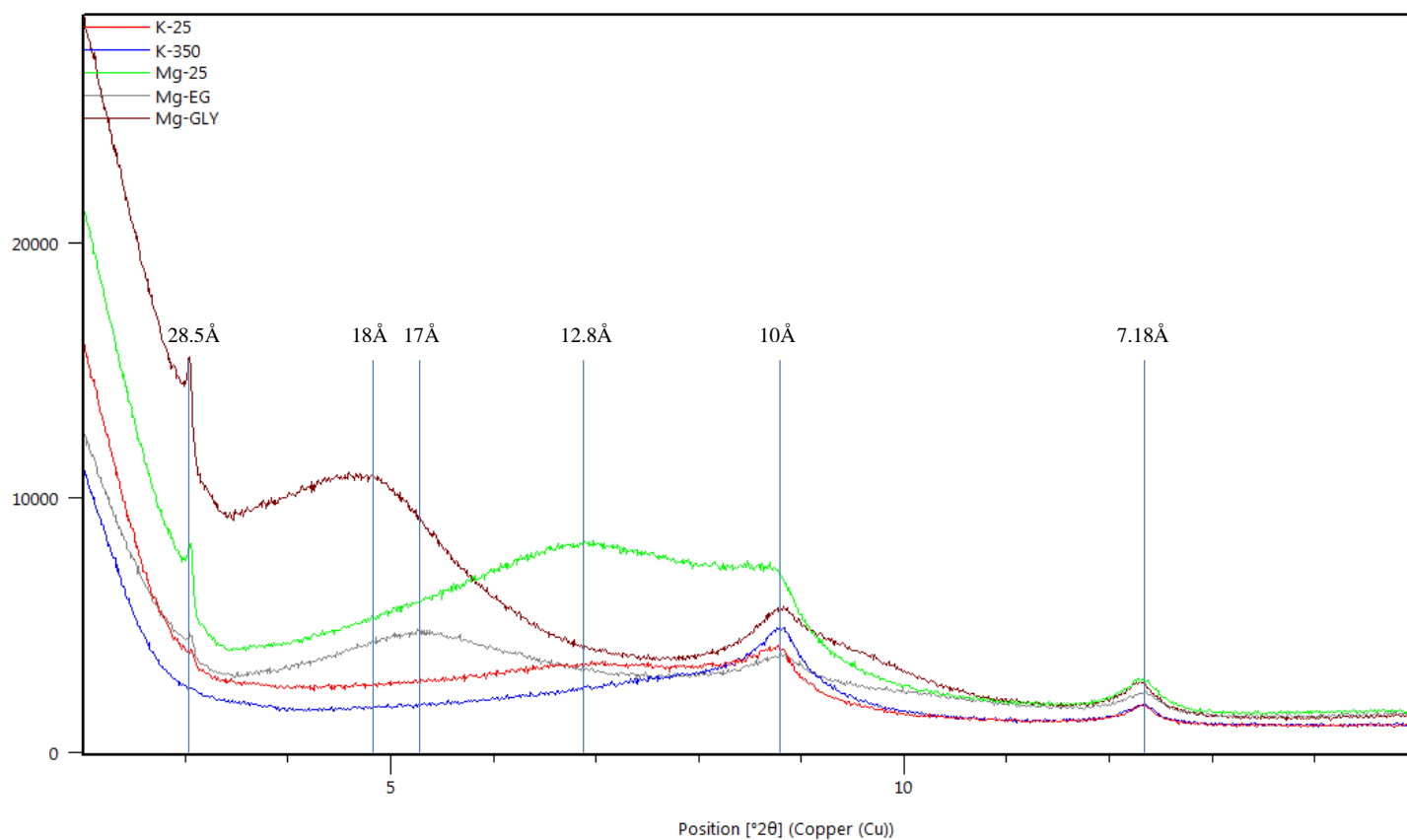


Stockdale Core SDK 2, 35-43cm

Mg-25

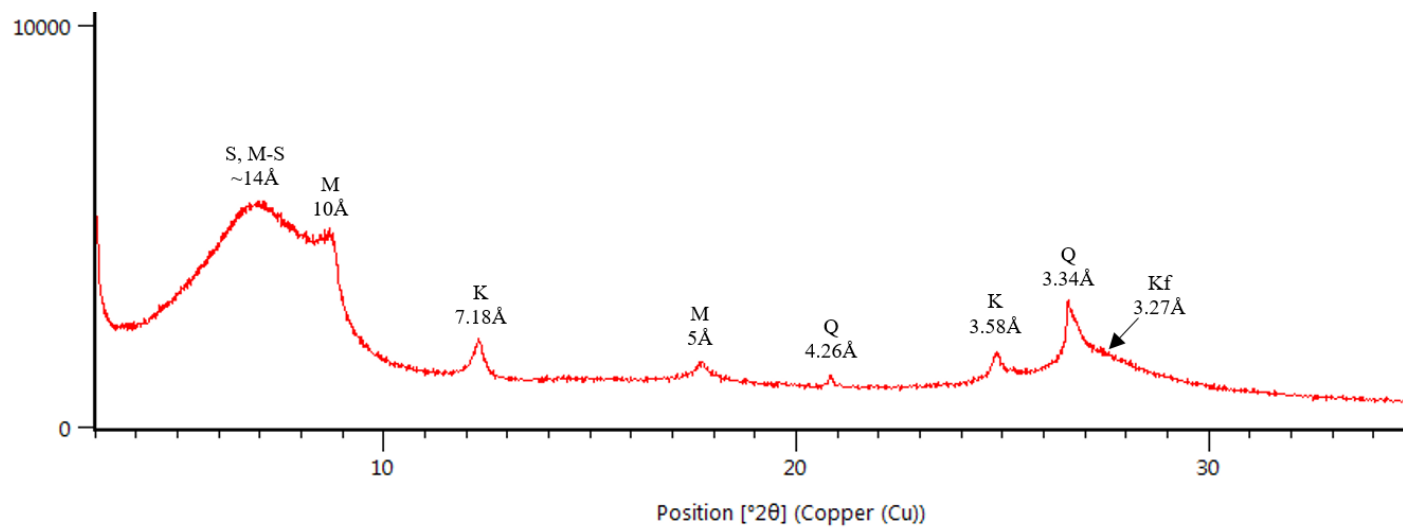


Multiple treatment overlay

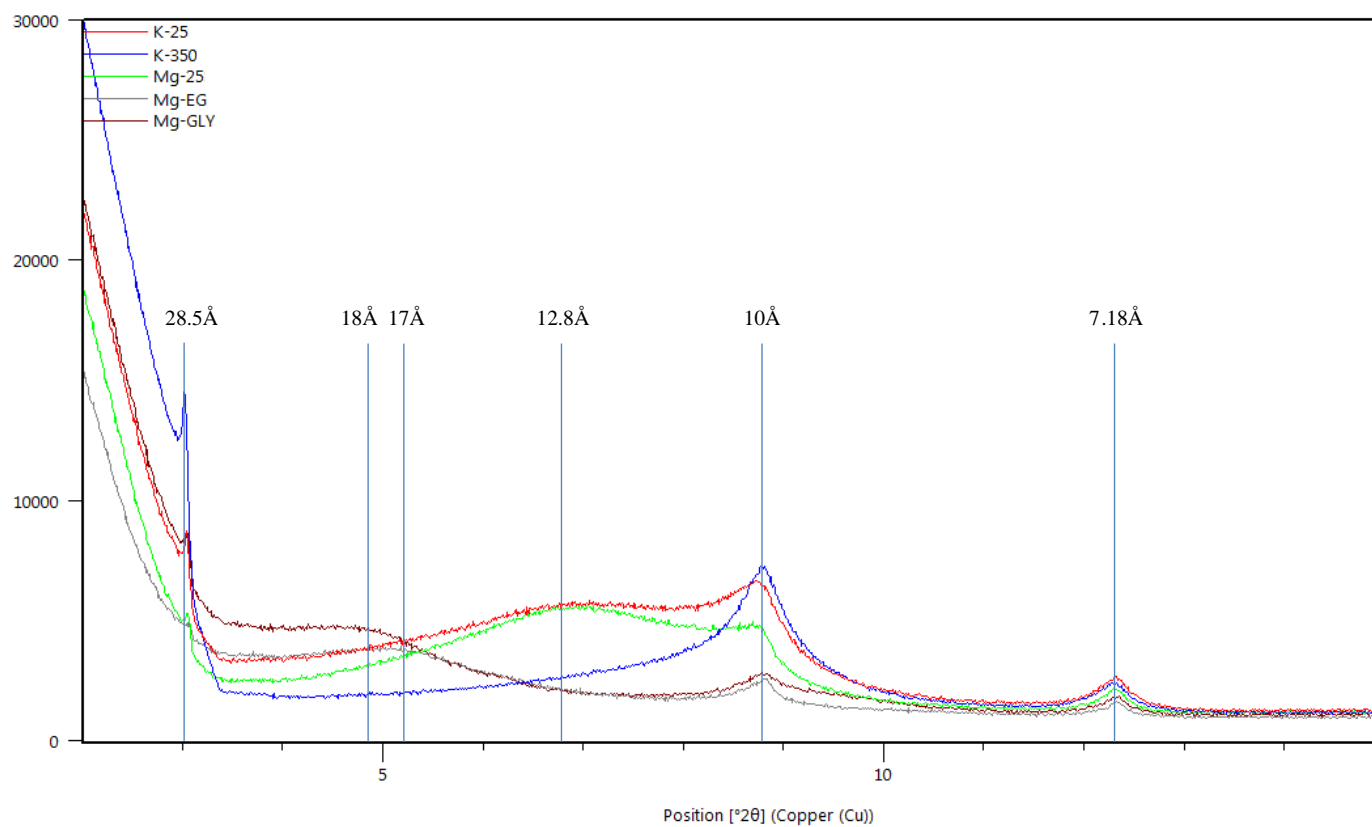


Stockdale Core SDK 2A, 32-39cm

Mg-25

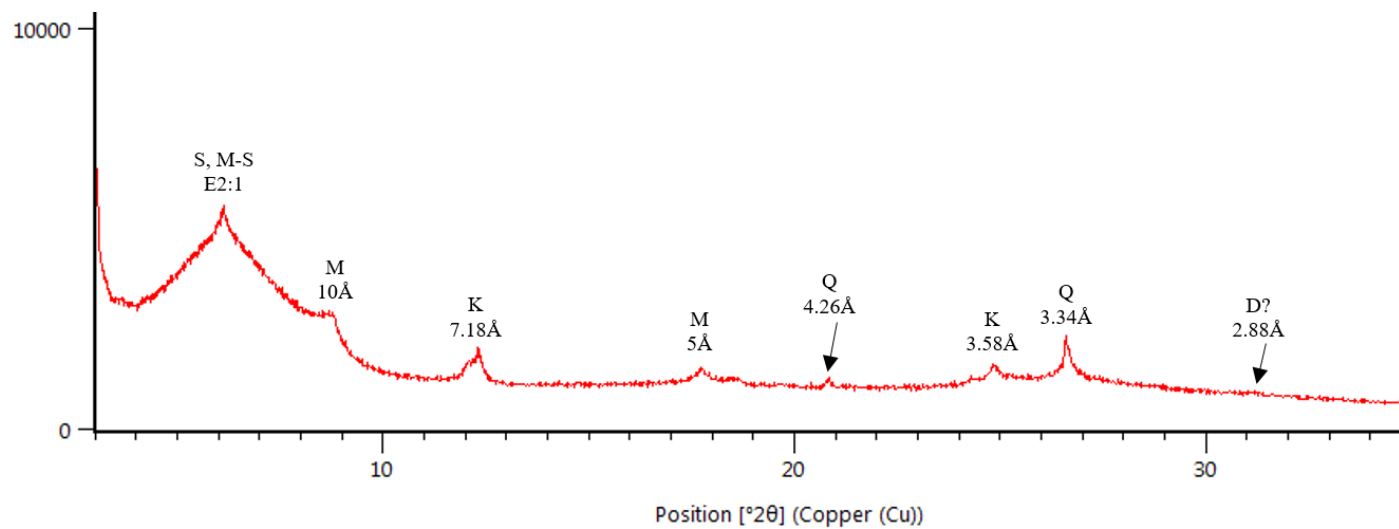


Multiple treatment overlay

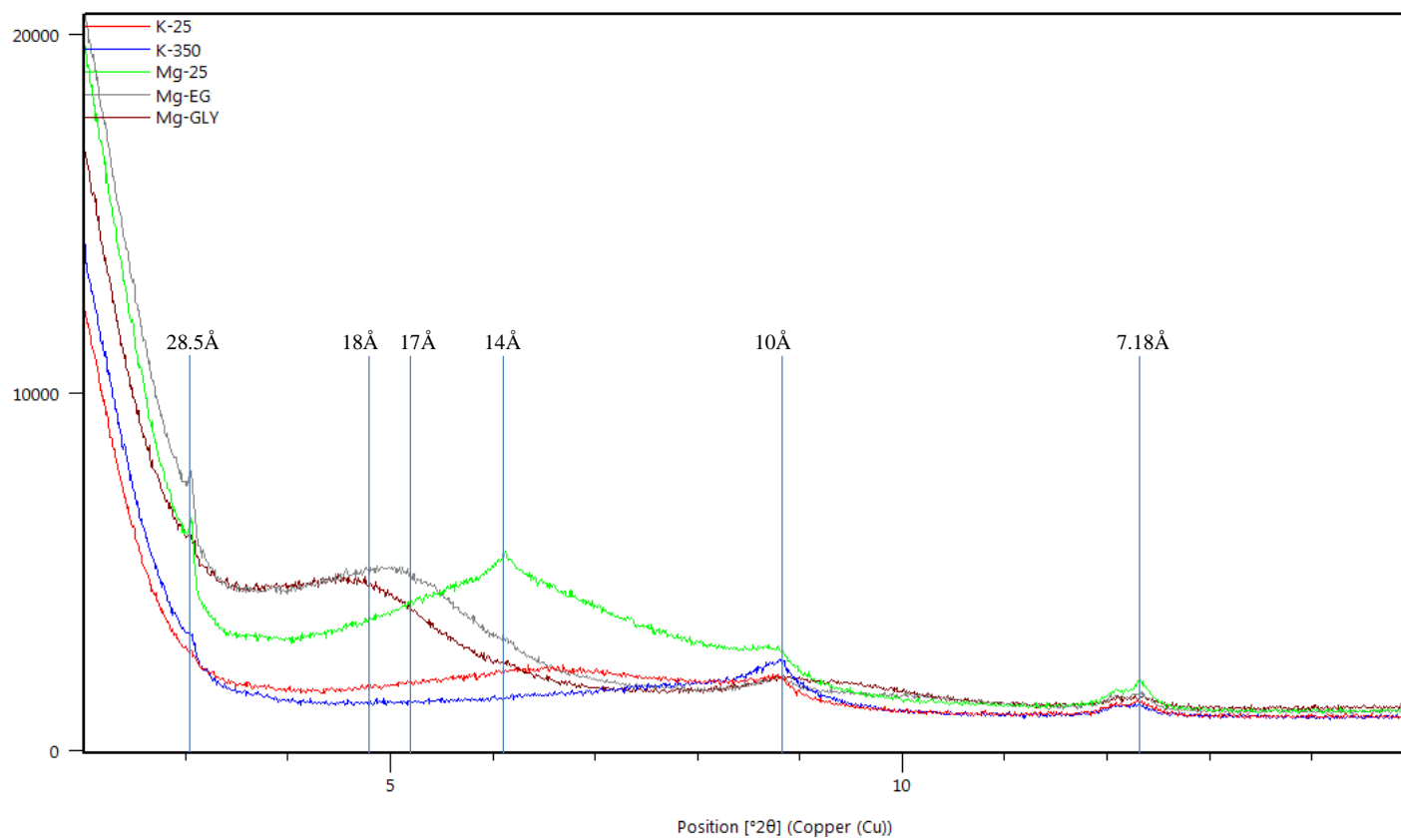


Stockdale Core SDK 1B, 28-36cm

Mg-25

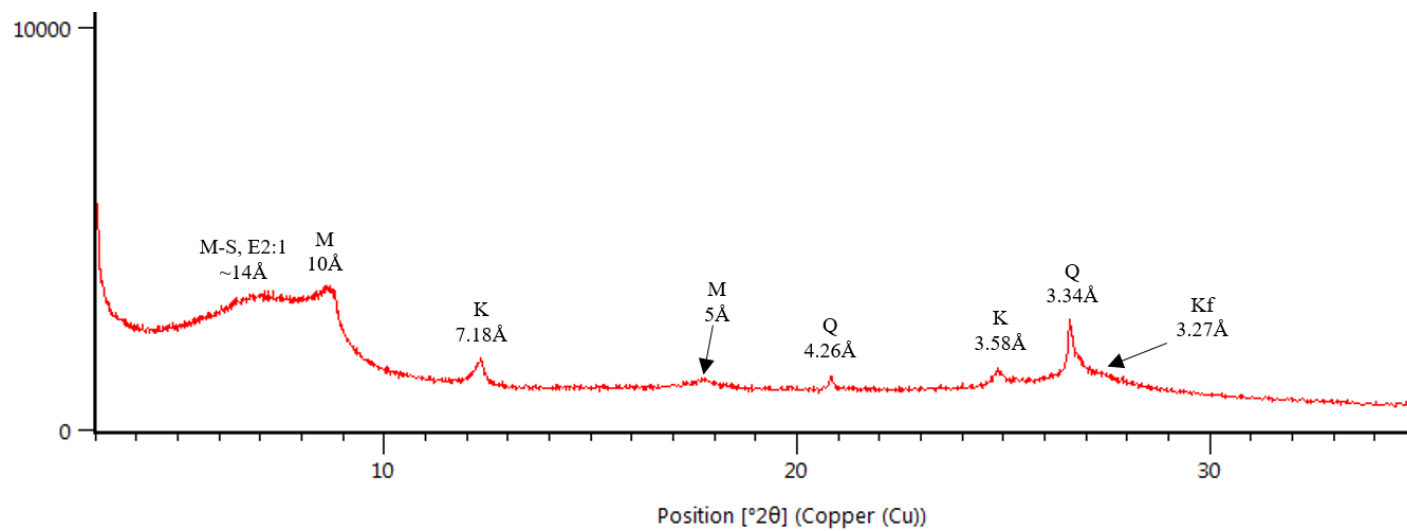


Multiple treatment overlay

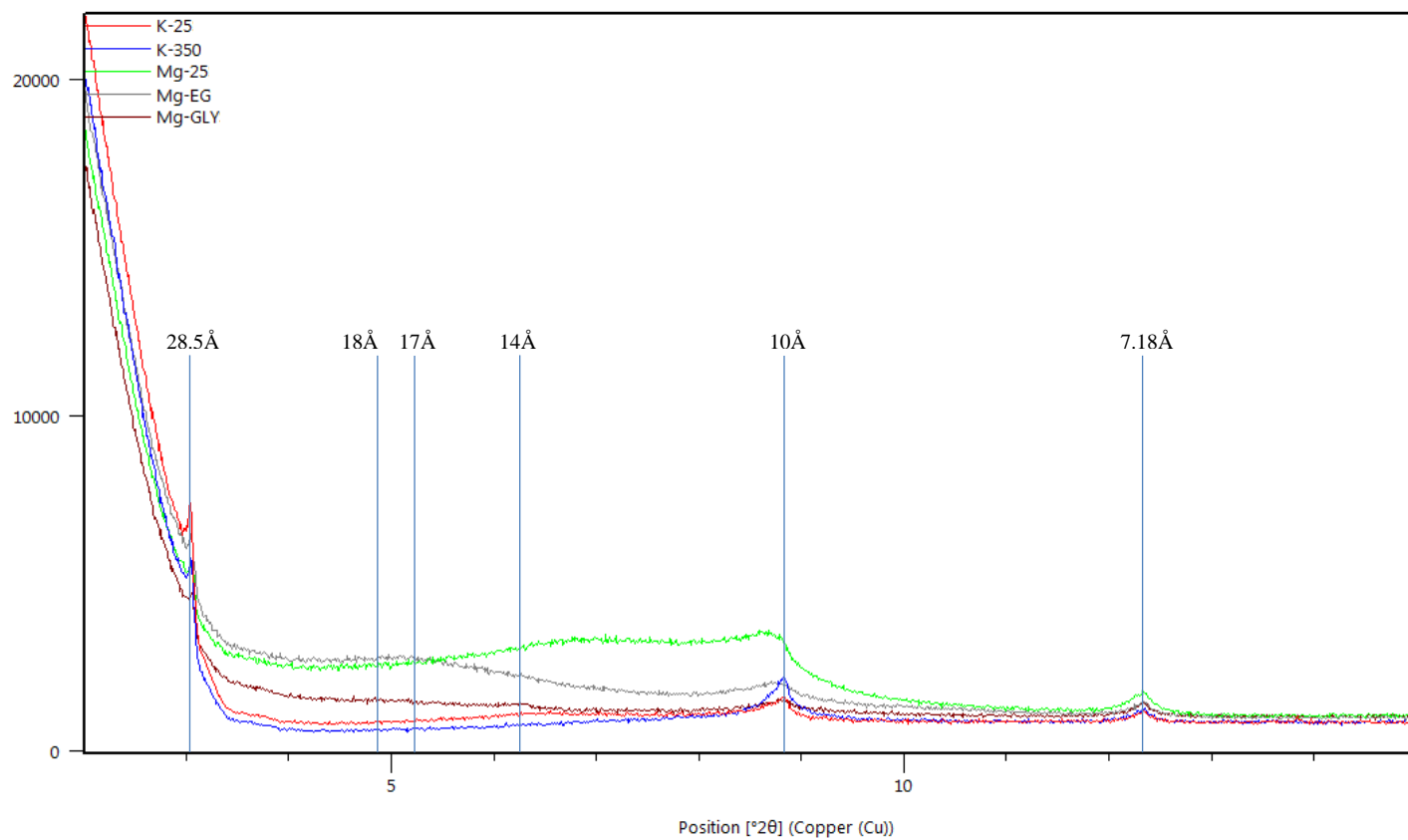


Stockdale Core SDK 2B, 71-79cm

Mg-25



Multiple treatment overlay



Appendix G - ATP Analysis Data

	Konza 3	Konza 4	Konza 5	Konza 6	SDK 1	SDK 2	SDK 5	SDK 2A	SDK 4A	SDK 1B	SDK 3B
Test 1	1872.00	1692.00	2470.00	2604.00	2479.00	2346.00	1726.00	2169.00	2656.00	2007.00	1617.00
Test 2	1790.00	1862.00	2325.00	2517.00	2579.00	2224.00	1613.00	2236.00	2411.00	2185.00	1605.00
Test 3	1853.00	1866.00	2331.00	2646.00	2483.00	2285.00	1795.00	2097.00	2716.00	2104.00	1677.00
Avg	1838.33	1806.67	2375.33	2589.00	2513.67	2285.00	1711.33	2167.33	2594.33	2098.67	1633.00
St. Dev.	42.92	99.32	82.04	65.80	56.62	61.00	91.88	69.51	161.58	89.12	38.57

Measured in relative light units (RLUs)